



**THÈSE DE DOCTORAT
DE L'UNIVERSITÉ PSL**

Préparée à l'École Normale Supérieure

**Formules asymptotiques pour le temps moyen d'arrivée
de la particule la plus rapide sous différentes
dynamiques, appliquée à la signalisation calcique et à la
transcription de l'ADN**

Soutenue par
Suney TOSTE REGALADO

Le 29 septembre 2023

École doctorale n° 386
**École Doctorale de Sciences
Mathématiques Paris Centre**

Spécialité
Mathématiques

Composition du jury :

Pr. Eva LÖCHERBACH Université de Paris1 Panthéon Sorbonne	<i>Présidente du jury</i>
Pr. Philippe ROBERT INRIA de Paris	<i>Rapporteur</i>
Pr. Grégory SCHEHR Sorbonne Université	<i>Rapporteur</i>
Dr. Miraine DÁVILA Université de Technologie de Compiègne	<i>Examinateuse</i>
Pr. Michèle THIEULLEN Sorbonne Université	<i>Examinateuse</i>
Pr. Amaury LAMBERT École Normale Supérieure, PSL	<i>Directeur de thèse</i>

Remerciements

Je tiens tout d'abord à remercier les membres du jury pour leurs révisions et leurs commentaires qui m'ont permis d'améliorer la qualité du manuscrit.

Je tiens également à remercier, à un niveau plus personnel, à mon directeur de thèse, Amaury, car sans lui, cette thèse n'aurait pas été possible. Il m'a donné des leçons très importantes non seulement en mathématiques mais aussi en matière de justice et de morale. Il a fait de mes problèmes ses propres problèmes et il s'est battu pour moi dans les moments où je ne pouvais pas le faire. Je ne pouvais donc pas avoir un meilleur mathématicien, une meilleure personne comme directeur pour m'aider dans les moments difficiles de cette thèse, et je lui en serai toujours, toujours, reconnaissant. Je remercie aussi à Didier, Stéhane, Otared, Benoît, Renauld et Elisha, pour toute l'aide, le soutien et l'écoute au moment où j'en avais le plus besoin. Et à Chloé, qui est devenue ma première amie dans ce pays et qui m'a toujours motivée et poussée à continuer.

J'ai une pensée toute particulière pour les amis qui m'ont aidé à améliorer ma culture française et ma vie en général ici: (mon tonton) Jean-Louis, (mon père français) Bernard, Isabelle, Michel, et Elisabeth sont devenus une nouvelle famille. Ils m'ont donné l'amour, l'éducation, le soutien et la force de continuer.

Je tiens à remercier mes amis, ceux que j'ai côtoyés pendant le master: Gabriel, Anh, Cyprien, Alessandro, Rutger, Roxanne, Florian et Theo, mais aussi à ceux que j'ai côtoyés dans mon précédent laboratoire et qui m'ont soutenu pendant ces 3 dernières années : Andrea, Virginie, Matteo, Kanishka, Lou, Annia, Chris, Giulia, Théo et Anna, merci beaucoup pour les moments partagés, pour la compagnie dans la tempête et pour avoir amélioré ma vie au quotidien.

Y claro está, a los amigos más cercanos, que me han acompañado y cuidado en esta etapa de mi vida: a Claudia, Richard, Yaisel, Alejandro, Nany, Emilio, Agustín, Chourouk, Josué y Anays, Míraine, Pedro, Ire y Cecy, Susely, Luis, Yoel, Willy y el resto del piquete Toulousino, muchas gracias por haber estado presentes y haberme motivado cuando pensaba que era imposible continuar.

A los amigos que están lejos, pero que se han mantenido siempre cerca: Lillian y Pache, Jessica, Lily, Lisset, Marce, Annie, Liz, Daniella, Bia y Lázaro, muchas gracias por estar pendientes.

A mi familia, que han comprendido cada una de mis decisiones y que me aman siempre.

A Nano, porque con él todo ha sido mejor, por haberme apoyado y por encontrar soluciones donde yo no podía verlas. Por haberme escuchado, levantado y por hacerme sentir siempre que era más fuerte de lo que pensaba y que podía con todo. Por haberme equipado para salir a pelear cada día sabiendo que sin importar nada, al regreso tenía una morada para refugiarme de todo. No pude tener un mejor copiloto en este viaje.

A todos, muchas gracias!

Publications

Published

- **TOSTE S.** & HOLCMAN D., “Asymptotics for the fastest among N stochastic particles: role of an extended initial distribution and an additional drift component.” *Journal of Physics A: Mathematical and Theoretical*, Volume 54, Number 28, 54 285601 (2021) | [arXiv:2010.08413](#) | [hal:04101385](#)
- **TOSTE S.** & HOLCMAN D., “Arrival time for the fastest among N switching stochastic particles.” *The European Physical Journal B*, Volume 95, Number 113 (2022) | [arXiv:2112.12760](#) | [hal:04101401](#)
- PAQUIN-LEFEBVRE F., **TOSTE S.** & HOLCMAN D., “How large the number of redundant copies should be to make a rare event probable.” *Physical Review E*, Volume 106, Number 6, 106 064402 (2022) | [arXiv:2206.12687](#) | [hal:04101404](#)
- **TOSTE S.** & HOLCMAN D., “Extreme diffusion with point-sink killing fields for fast calcium signaling at synapses.” *SIAM Journal on Applied Mathematics*, 10.1137/22M1476319 (2023) | [arXiv:2201.05915](#) | [hal:04101395](#)

In preparation

- **TOSTE S.**, PAQUIN-LEFEBVRE F. & HOLCMAN D., “Narrow escape in a 2D bounded disk with a killing field and optimal exit paths.”

*“To be kind is more important than to be right.
Many times, what people need is not a brilliant mind
that speaks but a special heart that listens.”*

F. Scott Fitzgerald

Contents

Introduction	6
0.1 General framework for the first arrival problems	7
0.1.1 Mathematical definition for the arrival times of diffusing particles	8
0.1.2 Arrival vs killing	11
0.1.3 Arrival with Switching	17
0.1.4 Preliminary results in the arrival time problem	19
0.2 Biological motivation	23
0.3 Main results of the thesis	26
I Asymptotic formulas for calcium signaling	50
1 Role of an extended initial distribution and an additional drift component	51
1.1 General framework for the first arrival time	53
1.2 Arrival times for multiple initial distributions in 1D	54
1.2.1 Arrival from a ray for multiple initial distributions	54
1.2.2 MFAT for an initial long-tail distribution touching the target site	56
1.2.3 MFAT inside the interval $[0, a]$	57
1.2.4 MFAT inside the interval $[0, c]$ when the initial distribution has a long-tail .	59
1.3 MFAT in 2D	63
1.3.1 MFAT for a uniform initial distribution	63
1.3.2 MFAT for an initial distribution with a long-tail intersecting the target site .	65
1.4 Effect of a constant drift on extreme arrival	67
1.4.1 Effect of a constant drift when the initial distribution is a Dirac delta function	67
1.4.2 Effect of a constant drift for a uniform initial distribution	68
1.4.3 Effect of a constant drift for a uniform initial distribution not intersecting the target	70
1.5 Discussion and concluding remarks	72
1.6 Appendix: Algorithm to simulate the stochastic trajectory of the fastest particles when the initial distribution can intersect with the target	73

2 Diffusion with point-sink killing fields for fast calcium signaling at synapses	75
2.1 Introduction	75
2.2 General formulas previously derived for the killing framework	78
2.3 Escape vs a killing term with a finite number of Dirac delta functions at isolated points	79
2.3.1 Survival probability with m-killing points	79
2.3.2 Survival probability with a single point-sink killing term	84
2.4 Applications: numerical simulations and quantifying calcium signaling events in synapse	88
2.4.1 Stochastic simulations for the fastest arrival with a killing term	88
2.4.2 Time scale of fast calcium signaling at synapse	89
2.5 Conclusions and perspective	95
2.6 Appendix	96
2.6.1 Escape for the fastest with a uniform killing in half-a-line	96
2.6.2 Killing in a finite interval in half a line with initial point outside the interval	98
2.6.3 Killing in a finite interval in half a line with initial point inside the interval .	99
3 Narrow escape with a uniform killing field in 2D and optimal exit paths	101
3.1 Introduction	101
3.2 Revision on the conditional first arrival time	103
3.3 Escape vs uniform killing in a 2D-disk	104
3.3.1 Fully absorbing boundary condition	104
3.3.2 Narrow absorbing boundary	108
3.4 Escape probability for a localized inner killing term	112
3.4.1 Asymptotic expression for the escape probability	112
3.5 Asymptotic formulas vs simulations	116
3.5.1 MFPT and P_e vs killing weight V	116
3.5.2 MFPT and P_e vs the killing area position	118
3.5.3 MFPT and P_e vs the killing area radius	119
3.6 Optimal path for the fastest particles	119
3.7 Killing area tangent to the narrow absorbing boundary	124
3.8 Conclusions, applications, and perspective	126

II Asymptotic formulas for transport and synthesis of proteins	128
4 Arrival time for the fastest among N switching stochastic particles	129
4.1 Introduction	129
4.2 Stochastic model	131
4.3 Explicit expressions for the MFAT when the Brownian particles start in state 1	132
4.3.1 Prototype testing case: particles start in state 1 and $D_2 = 0$	132
4.3.2 Particles start in state 1 and $D_2 \neq 0$	137
4.3.3 Particles start in state 2	140
4.4 Particles are initially uniformly distributed in an interval	142
4.4.1 Particles start in state 1	143
4.4.2 Particles start in state 2	144
4.4.3 Particles start in state 1 uniformly distributed in $[y_1, y_2]$ with $y_1 > 0$	145
4.4.4 Particles start in state 2 uniformly distributed in $[y_1, y_2]$	145
4.5 Initial distribution with a long tail	146
4.5.1 Particles start in state 1	146
4.5.2 Particles start in state 2	147
4.6 Discussion and concluding remarks	148
4.7 Appendix	150
4.7.1 Survival probability for particles starting at position $y > 0$ in state 1 with $D_1 \neq D_2$	151
4.7.2 Particles start in state 2 with $D_1 \neq D_2$	153
4.7.3 Particles start uniformly distributed in an interval	156
4.7.4 The initial distribution has a long tail and particles start in state 2	160
Discussion and perspectives	162
7.1 The fastest arrival distribution	164
7.2 Target competition	165
7.3 Tracking proteins in the ER	166

Introduction

In this PhD thesis, I study mathematically the mean first arrival time for the fastest particle among N diffusing particles, where competition, switching and killing dynamics are also considered for particles at the same time of the Brownian motion. This work is focused on the statistical properties of these arrival times defining the time scale of many biological processes including DNA transcription and calcium signaling. In this section I will briefly present the mathematical background associated with first arrival problems as well as all the biological applications that motivated this work. Finally, I will summarize the main results obtained.

0.1 General framework for the first arrival problems

In general, the first arrival problem (FAP) consists in finding the shortest time for N non-interacting independent and identically distributed (i.i.d) stochastic trajectories moving in a restricted domain Ω until they reach a specific site. The first arrival time is defined as

$$\tau^1 = \min(t_1, \dots, t_N),$$

where t_i are the i.i.d. arrival times of the N Brownian particles. From a biological point of view, these particles can be seen as ions, molecules or proteins inside the compartments of cells that need to arrive to a specific part of the cells depending on their functions. This arriving site is called the target. We are interested then in the distribution of these first arrival times (FAT) as well as their expectation. This problem is very sensitive to several conditions, such as: the geometry of the domain; the shape, size and amount of the targets; the boundary conditions; the initial distribution and the dynamics affecting the motion of the particles. Thus, all these parameters need to be taken into account in order to find the proper statistical properties of the FAT. The FAP is closely related with the narrow escape problem (NEP) [1, 2], and both are equivalent when the target is a narrow fraction of the boundary of Ω . Note that throughout all this thesis we are going to refer to arrival time or escape time depending only on the biological context, because mathematically, both terms are equivalent here as we are going only to consider the case where the target is located over the boundary of the domain and the particles move by Brownian motion. Thus, arriving to the target is the same that leaving the domain, meaning escaping. We can see the differences on Fig. 1, where the terminology of arrival time is more accurate for the time to the target N^1 (time of the red trajectory), while the terminology of escape time is more accurate for the time to the target N^2 (time of the green trajectory). Depending on the real function of the particles that we want to model, target N^1 can be seen as an obstacle to the green trajectory, meaning that for this population of particles the boundary condition associated to target N^1 is reflecting while for the red particle is absorbing. The case where it exists more than one target in the domain immediately

gains interest in order to know which task is most likely to be accomplished first. This problem is related with the derivation of the splitting probability, defined as the probability to reach a given target before the other [3].

First arrival problem vs first escape problem

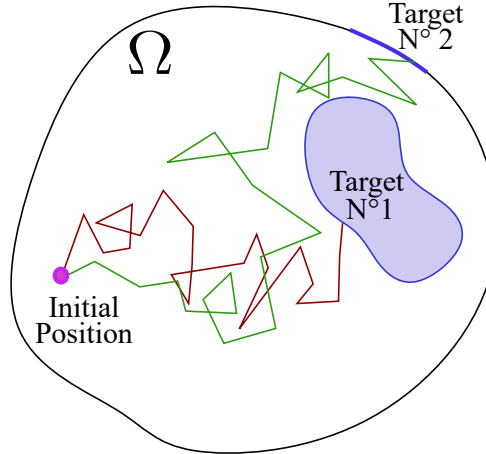


Figure 1: Schematic of a 2D-domain Ω where there exist two possible targets. Depending on the population of particles targets can be seen as obstacles. In this case the initial position of the particles is a point in correspondence with a Dirac delta initial distribution, but in general it can differ according to the biological problem that we would like to model. The FAP or the first escape problem (FEP) respectively study the statistical properties of the first among N arriving (red trajectory) or escaping particles (green trajectory).

0.1.1 Mathematical definition for the arrival times of diffusing particles

The diffusion process $\mathbf{x}(t)$ in a general domain Ω satisfies the equation

$$d\mathbf{x} = \mathbf{b}(\mathbf{x}) dt + \mathbf{B}(\mathbf{x}) d\mathbf{w}(t), \quad \text{for } \mathbf{x} \in \Omega, \quad (1)$$

where $\mathbf{b}(\mathbf{x})$ is a smooth drift vector, $\mathbf{B}(\mathbf{x})$ is a diffusion matrix, and $\mathbf{w}(t)$ is a vector of independent standard Brownian motions. A domain Ω with boundary $\partial\Omega = \partial\Omega_a \cup \partial\Omega_r$ is considered, where $\partial\Omega_a$ is an absorbing fraction of boundary (the target) and $\partial\Omega_r$ is the reflecting. When the size of $\partial\Omega_a$ is very small, we refer to the arriving problem as the narrow escape problem. The transition probability density function (pdf) of the process $\mathbf{x}(t)$ with absorption is the pdf, solution of the Fokker-Planck equation (FPE)

$$\frac{\partial p(\mathbf{x}, t | \mathbf{y})}{\partial t} = \mathcal{L}_{\mathbf{x}} p(\mathbf{x}, t | \mathbf{y}) \quad \text{for } \mathbf{x}, \mathbf{y} \in \Omega, \quad (2)$$

where $\mathcal{L}_{\mathbf{x}}$ is the forward operator

$$\mathcal{L}_{\mathbf{x}} p(\mathbf{x}, t | \mathbf{y}) = \sum_{i,j=1}^d \frac{\partial^2}{\partial x^i \partial x^j} [D^{i,j}(\mathbf{x}) p(\mathbf{x}, t | \mathbf{y})] - \sum_{i=1}^d \frac{\partial}{\partial x^i} [b^i(\mathbf{x}) p(\mathbf{x}, t | \mathbf{y})], \quad (3)$$

and $\mathbf{D}(\mathbf{x}) = \frac{1}{2} \mathbf{B}(\mathbf{x}) \mathbf{B}^T(\mathbf{x})$.

The operator $\mathcal{L}_{\mathbf{x}}$ can be equivalently written in the divergence form $\mathcal{L}_{\mathbf{x}} p(\mathbf{x}, t | \mathbf{y}) = -\nabla \cdot \mathbf{J}(\mathbf{x}, t | \mathbf{y})$,

where the components of the flux density vector $\mathbf{J}(\mathbf{x}, t | \mathbf{y})$ are

$$J^i(\mathbf{x}, t | \mathbf{y}) = - \sum_{j=1}^d \frac{\partial}{\partial x^j} [D^{i,j}(\mathbf{x}) p(\mathbf{x}, t | \mathbf{y})] + b^i(\mathbf{x}) p(\mathbf{x}, t | \mathbf{y}), \quad (i = 1, 2, \dots, d). \quad (4)$$

The initial condition for the FPE (2) associated with particles starting their motion at position $\mathbf{x} = \mathbf{y}$ is given by

$$p(\mathbf{x}, 0 | \mathbf{y}) = \delta(\mathbf{x} - \mathbf{y}) \text{ for } \mathbf{x}, \mathbf{y} \in \Omega. \quad (5)$$

The solution of the FPE (2) with initial condition (5) is given by the **Green's function** associated to the diffusive operator

$$\left(\frac{\partial}{\partial t} - \mathcal{L}_{\mathbf{x}} \right) [\cdot] = \delta(\mathbf{x}). \quad (6)$$

In general, the Green's function $G(\mathbf{x}, \mathbf{y})$ associated to the linear differential operator $\mathcal{M} = \mathcal{M}(\mathbf{x}, t)$ is the solution of the equation

$$\mathcal{M}[G(\mathbf{x}, \mathbf{y})] = \delta(\mathbf{x} - \mathbf{y}). \quad (7)$$

This property can be exploited to obtain solutions of the equation

$$\mathcal{M}[u(\mathbf{x})] = f(\mathbf{x}), \quad (8)$$

which are given by the convolution $u(\mathbf{x}) = G(\mathbf{x}, \mathbf{y}) *_y f(\mathbf{y})$. The Green's function is unique when the kernel of \mathcal{M} is trivial or after considering a combination of symmetry, boundary conditions and/or other external criteria for the problem [4, 5].

The boundary conditions for the FPE (2) associated with particles escaping only in the absorbing boundary $\partial\Omega_a$, are given by

$$\begin{aligned} p(\mathbf{x}, t | \mathbf{y}) &= 0 \text{ for } t > 0, \quad \mathbf{x} \in \partial\Omega_a, \quad \mathbf{y} \in \Omega \\ \mathbf{J}(\mathbf{x}, t | \mathbf{y}) \cdot \mathbf{n}(\mathbf{x}) &= 0 \text{ for } t > 0, \quad \mathbf{x} \in \partial\Omega_r, \quad \mathbf{y} \in \Omega, \end{aligned} \quad (9)$$

where \mathbf{n} is the external unit normal vector. If the boundary $\partial\Omega$ contains R target sites pairwise disjoint $\partial\Omega_i \subset \partial\Omega$ with $i = 1, \dots, R$, the absorbing boundary $\partial\Omega_a$ is given by

$$\partial\Omega_a = \bigcup_{i=1}^R \partial\Omega_i, \quad (10)$$

and the reflecting boundary is always given by $\partial\Omega_r = \partial\Omega - \partial\Omega_a$.

Almost everywhere when the flux through the absorbing window is needed, we could use the **Green's second identity** in order to find an approximation for the value of the solution in the absorbing boundary [6]. This identity states that for Ψ and ψ twice continuously differentiable in a domain Ω we have

$$\int_{\Omega} (\Psi(\mathbf{x}) \Delta \psi(\mathbf{x}) - \psi(\mathbf{x}) \Delta \Psi(\mathbf{x})) d\mathbf{x} = \oint_{\partial\Omega} \left(\Psi(\mathbf{x}) \frac{\partial \psi}{\partial \mathbf{n}}(\mathbf{x}) - \psi(\mathbf{x}) \frac{\partial \Psi}{\partial \mathbf{n}}(\mathbf{x}) \right) dS_{\mathbf{x}}. \quad (11)$$

Sometimes we will solve the FPE, Laplace transformed in time, given by

$$q\hat{p}(\mathbf{x}, q) - p(\mathbf{x}, 0) = L_q(\mathcal{L}_{\mathbf{x}} p(\mathbf{x}, t | \mathbf{y})) = \mathcal{L}_{\mathbf{x}} \hat{p}(\mathbf{x}, t | \mathbf{y}) \quad \text{for } \mathbf{x}, \mathbf{y} \in \Omega, \quad (12)$$

where

$$\hat{p}(\mathbf{x}, q) = L_q(p(\mathbf{x}, t)) = \int_0^\infty p(\mathbf{x}, t) e^{-qt} dt.$$

The Laplace transform allows us to solve ordinary differential equations instead of the partial differential equations, that are often very difficult to solve. In general, this transformation is well defined in $\Re(q) > \alpha$ for all functions piece-wise continuous in time and of exponential order α [7], and we denote

$$F(q) = L_q(f(t)) \quad (13)$$

to say that $F(q)$ is the Laplace transform in time t of the function $f(t)$. We have swapped in (12) the spatial forward operator $\mathcal{L}_{\mathbf{x}}$ and the Laplace transform L_q due to the continuity of the solution $p(x, t)$ in $\Omega \times [0, \infty)$ and the uniform convergence of its Laplace transform.

We could be also interested in been able to recover the function $f(t)$ once we already know its Laplace transform, this is, we would like to invert the Laplace transform. The inversion formula is given by

$$f(t) = \frac{1}{2\pi i} \int_{\chi-i\infty}^{\chi+i\infty} F(q) e^{tq} dq \quad (14)$$

with $\chi > \alpha$, and it is uniquely defined when $F(q)$ is analytic, this is for $\Re(q) > \alpha$ and $F(q)$ decays as fast as $|\frac{1}{q^p}|$ with $p \geq 0$ for q sufficiently large, or in equivalence when $|F(q)| \leq \varepsilon_q$ where $\varepsilon_q \rightarrow 0$ uniformly as $q \rightarrow \infty$. We thus denote

$$f(t) = L_t^{-1}(F(q)). \quad (15)$$

We will like then to study the distribution of the first arrival times. When all particles start at the same position, due to the independence and identical distribution of the particles, the arrival times are also independent and equally distributed, thus, the complementary cumulative distribution function of τ^1 is given by

$$\Pr\{\tau^1 > t\} = [\Pr\{t_1 > t\}]^N, \quad (16)$$

where $\Pr\{t_1 > t\} = S(t)$ is the survival probability of a single particle prior to reaching the target. This is,

$$\Pr\{t_1 > t\} = S(t) = \int_{\Omega} p(\mathbf{x}, t) d\mathbf{x}, \quad (17)$$

thus the pdf for the arrival of the first particle is given by

$$\Pr\{\tau^1 \in [t, t + dt]\} = \frac{d}{dt} \Pr\{\tau^1 \leq t\} dt = N(\Pr\{t_1 > t\})^{N-1} \Pr\{t_1 \in [t, t + dt]\}, \quad (18)$$

where the instantaneous probability is given by the flux

$$\Pr\{t_1 \in [t, t + dt]\} = \oint_{\partial\Omega_a} \frac{\partial p(\mathbf{x}, t)}{\partial \mathbf{n}} dS_{\mathbf{x}} dt. \quad (19)$$

The Mean First Arrival Time (MFAT) is defined then as the mean time for the first one among N i.i.d. Brownian particles to reach the target and it is obtained by computing the integral

$$\bar{\tau}^N = \mathbb{E}[\tau^1] = \int_0^\infty t \Pr\{\tau^1 \in [t, t + dt]\} = \int_0^\infty \Pr\{\tau^1 > t\} dt = \int_0^\infty [\Pr\{t_1 > t\}]^N dt. \quad (20)$$

Survival vs killed trajectory

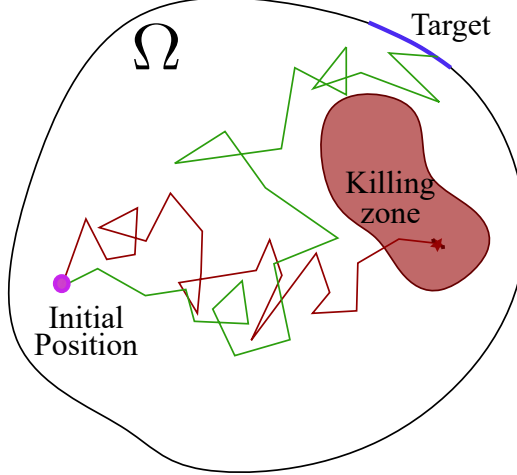


Figure 2: Schematic representation of two Brownian trajectories under a local killing field in a 2D domain Ω . The killing measure is affecting a sub-region (red zone) of the domain. The killed trajectory (red) ends its path inside the killing area while the survival trajectory (green) escapes at the boundary.

0.1.2 Arrival vs killing

When a killing rate $k(\mathbf{x})$ is added in the domain Ω , the transition probability density function of the process (1) with killing and absorption is the pdf of trajectories that have neither been killed nor absorbed in $\partial\Omega_a$ by time t [8, 9]

$$p(\mathbf{x}, t | \mathbf{y}) d\mathbf{x} = \Pr\{\mathbf{x}(t) \in \mathbf{x} + d\mathbf{x}, \tau^k > t, \tau^e > t | \mathbf{y}\}, \quad (21)$$

where τ^k is the time for a single particle to be killed and τ^e is the time to escape. This new pdf is the solution of the FPE [10]

$$\frac{\partial p(\mathbf{x}, t | \mathbf{y})}{\partial t} = \mathcal{L}_{\mathbf{x}} p(\mathbf{x}, t | \mathbf{y}) - k(\mathbf{x}) p(\mathbf{x}, t | \mathbf{y}) \quad \text{for } \mathbf{x}, \mathbf{y} \in \Omega, \quad (22)$$

where $\mathcal{L}_{\mathbf{x}}$ is the forward operator defined in (3). The probability of being killed before reaching $\partial\Omega_a$ is given by [11],

$$\Pr\{\tau^k \leq \tau^e | \mathbf{y}\} = \int_0^\infty \int_{\Omega} k(\mathbf{x}) p(\mathbf{x}, t | \mathbf{y}) d\mathbf{x} dt. \quad (23)$$

The absorption probability flux on $\partial\Omega_a$ is

$$\Pr\{\tau^e \in [t, t + dt], \tau^k > \tau^e\} = J(t | \mathbf{y}) dt = \oint_{\partial\Omega} \mathbf{J}(\mathbf{x}, t | \mathbf{y}) \cdot \mathbf{n}(\mathbf{x}) dS_{\mathbf{x}} dt, \quad (24)$$

and $\int_0^\infty J(t | \mathbf{y}) dt$ is the probability of trajectories that are absorbed. Thus the probability to escape P_e is the probability to escape before being killed, this is

$$P_e = \Pr\{\tau^e < \tau^k | \mathbf{y}\} = \int_0^\infty J(t | \mathbf{y}) dt. \quad (25)$$

When no killing rate is considered the escape probability is always 1. The pdf for the killing time τ^k is the probability of been killed at anytime t before been absorbed, this is,

$$\Pr\{\tau^k \leq t | \mathbf{y}\} = \frac{\Pr\{\tau^k \leq t, \tau^k \leq \tau^e | \mathbf{y}\}}{\Pr\{\tau^e \geq \tau^k | \mathbf{y}\}} = \frac{\int_0^t \int_{\Omega} k(\mathbf{x}) p(\mathbf{x}, s | \mathbf{y}) d\mathbf{x} ds}{\int_0^{\infty} \int_{\Omega} k(\mathbf{x}) p(\mathbf{x}, s | \mathbf{y}) d\mathbf{x} ds}. \quad (26)$$

The probability distribution of the time to absorption at $\partial\Omega_a$ is the probability of been absorbed at anytime t before been killed, this is

$$\Pr\{\tau^e \leq t | \mathbf{y}\} = \frac{\int_0^t J(s | \mathbf{y}) ds}{1 - \int_0^{\infty} \int_{\Omega} k(\mathbf{x}) p(\mathbf{x}, s | \mathbf{y}) d\mathbf{x} ds}. \quad (27)$$

The escape time of one particle is then given by the expectation of the absorption time, that is,

$$\mathbb{E}[\tau^e | \mathbf{y}] = \frac{\mathbb{E}[\tau^e \mathbf{I}_{\{\tau^e < \tau^k\}} | \mathbf{y}]}{\Pr\{\tau^e < \tau^k | \mathbf{y}\}} = \int_0^{\infty} \Pr\{\tau^e > t | \mathbf{y}\} dt = \frac{\int_0^{\infty} s J(s | \mathbf{y}) ds}{1 - \int_0^{\infty} \int_{\Omega} k(\mathbf{x}) p(\mathbf{x}, s | \mathbf{y}) d\mathbf{x} ds}. \quad (28)$$

Thus, for N independent identically distributed copies of the stochastic process (1), that can escape at time t_1, \dots, t_N , prior to get killed, without any loss of generality one can define the escape time t_i of the particle i as ∞ if the particle i is killed. The first passage time (FPT) $\tau^e(N)$ [11, 12] is the fastest time for a particle to escape through the absorbing windows given that at least one particle escapes, that is

$$\tau^e(N) = \min_N \{t_1, \dots, t_N\} = \min_n \{t_1, \dots, t_n\}, \quad (29)$$

where n is the total number of surviving particles. The cumulative distribution for the escape time of the fastest particle prior to time t when at least one particle survives is given by

$$P(t) = \Pr\{\tau^e(N) \leq t | \exists i \in \{1, \dots, N\} \text{ s.t. } \tau_i^e < \tau_i^k, p_0\}, \quad (30)$$

where τ_i^e and τ_i^k are the escape and killing time respectively for the i^{th} particle, and $p_0(x)$ is the initial distribution of particles. The mean fastest escape time (MFET) conditioned on the event that at least one particle escapes is thus defined by

$$\mathbb{E}[\tau^e(N) | n \geq 1, \mathbf{y}] = \int_0^{\infty} t \frac{dP(t)}{dt} dt = \int_0^{\infty} [P(\infty) - P(t)] dt. \quad (31)$$

By definition (30), $P(\infty) = 1$. Using Bayes' law, we obtain the decomposition

$$P(t) = \frac{\Pr\{\tau^e(N) \leq t, \exists i \in \{1, \dots, N\} \text{ s.t. } \tau_i^e < \tau_i^k | p_0\}}{\Pr\{\exists i \in \{1, \dots, N\} \text{ s.t. } \tau_i^e < \tau_i^k | p_0\}} = \frac{N(t)}{P_{\infty}}, \quad (32)$$

where P_{∞} is the probability that at least one particle escapes and the numerator $N(t)$ is defined as the probability that the fastest particle escapes before time t when at least one particle escapes.

Then, the first escape time is conditioned to the fact that at least one particle arrives at the target. The probability that at least one particle escapes is computed as follows

$$P_\infty = \Pr\{\exists i \in \{1, \dots, N\} \text{ s.t. } \tau_i^e < \tau_i^k | p_0\} = 1 - \Pr\{\forall i \in \{1, \dots, N\} : \tau_i^e \geq \tau_i^k | p_0\}. \quad (33)$$

Using that particles are independent, we obtain

$$P_\infty = 1 - \prod_{i=1}^N \Pr\{\tau_i^e \geq \tau_i^k | p_0\}, \quad (34)$$

that can be written as

$$P_\infty = 1 - (1 - \Pr\{\tau^e < \tau^k | p_0\})^N. \quad (35)$$

According to relation (25), because the probability that a single particle escapes before being killed is given by $\Pr\{\tau^e < \tau^k | p_0\} = \int_0^\infty \int_{\mathbf{y} \in \Omega} J(t | \mathbf{y}) p_0(\mathbf{y}) d\mathbf{y} dt$ then,

$$P_\infty = 1 - \left(1 - \int_0^\infty \int_{\mathbf{y} \in \Omega} J(t | \mathbf{y}) p_0(\mathbf{y}) d\mathbf{y} dt\right)^N. \quad (36)$$

For a Dirac-delta initial distribution at position \mathbf{y} , the expression obtained is

$$P_\infty = 1 - \left(1 - \int_0^\infty J(t | \mathbf{y}) dt\right)^N, \quad (37)$$

where the flux $J(s | \mathbf{y})$ is given by relation (24). Finally, the probability that $N - k$ particles are killed and only k escape alive is given by the binomial distribution

$$\Pr\{n = k\} = \binom{N}{k} \left(\int_0^\infty J(t | \mathbf{y}) dt\right)^k \left(1 - \int_0^\infty J(t | \mathbf{y}) dt\right)^{N-k}. \quad (38)$$

Working now in the numerator of (32), the joint probability that the fastest one escapes before time t when at least one particle escapes is given by

$$N(t) = \Pr\{\tau^e(N) \leq t, \exists i \in \{1, \dots, N\} \text{ s.t. } \tau_i^e < \tau_i^k | p_0\}, \quad (39)$$

that is,

$$\begin{aligned} N(t) &= 1 - \Pr\{\tau^e(N) > t \text{ or } \forall i \in \{1, \dots, N\} : \tau_i^e > \tau_i^k | p_0\} \\ &= 1 - \Pr\{\forall i \in \{1, \dots, N\} : \tau_i^e > t \text{ or } \tau_i^e > \tau_i^k | p_0\} \\ &= 1 - \prod_{i=1}^N \Pr\{\tau_i^e > t \text{ or } \tau_i^e > \tau_i^k | p_0\} \\ &= 1 - \prod_{i=1}^N (1 - \Pr\{\tau_i^e \leq t, \tau_i^e < \tau_i^k | p_0\}). \end{aligned} \quad (40)$$

The normal flux density at the boundary is the pdf of exit [10] for any particles, we thus obtain

$$\Pr\{\tau_i^e \leq t, \tau_i^e < \tau_i^k | p_0\} = \int_0^t \oint_{\partial\Omega} \mathbf{J}(\mathbf{x}, s) \cdot \mathbf{n}(\mathbf{x}) dS \mathbf{x} ds = \int_0^t J(s | \mathbf{y}) ds, \quad (41)$$

where the flux $J(s | \mathbf{y})$ is defined in relation (24). Therefore the numerator in equation (32) is

$$N(t) = 1 - \left(1 - \int_0^t J(s | \mathbf{y}) ds \right)^N.$$

To conclude, the pdf of the fastest arrival conditioned to at least one particle escapes at the absorbing boundary and given the initial density $p_0(\mathbf{x}) = \delta(\mathbf{x} - \mathbf{y})$, is

$$P(t) = \frac{N(t)}{P_\infty} = \frac{1 - \left(1 - \int_0^t J(s | \mathbf{y}) ds \right)^N}{1 - (1 - P_e)^N}, \quad (42)$$

where

$$P_e = \int_0^\infty J(s | \mathbf{y}) ds,$$

and the conditional MFPT given in equation (31) is

$$\mathbb{E}[\tau^e(N) | n \geq 1, \mathbf{y}] = \int_0^\infty \frac{\left(1 - \int_0^t J(s | \mathbf{y}) ds \right)^N - \left(1 - \int_0^\infty J(s | \mathbf{y}) ds \right)^N}{1 - \left(1 - \int_0^\infty J(s | \mathbf{y}) ds \right)^N} dt. \quad (43)$$

In [9], an expression for the MFPT was derived in 1D, but it was assumed that the survival probability decays exponentially. We believe that the previous formulation of this problem in [13] is not correct. In [13] they attempted to compute the MFPT $\mathbb{E}[\tau^e(N) | \tau^e(N) < \tau^k(N), \mathbf{y}]$, meaning that escape is always the first event. However during the computations they only conditioned that at least one particle escapes. The full expression for the $\mathbb{E}[\tau^e(N) | n(N) \geq 1, \mathbf{y}]$ with a delta-Dirac killing source without additional assumptions will be derived in this thesis, and also the formula when the killing rate is uniform in an interval. In general, the killing rate could affect any sub-region of Ω , including Ω itself when the particles can be eliminated everywhere following a probabilistic law. In 2D we will study the uniform killing in the full domain and in addition we will also study the case where the killing zone is a small disk, varying its size and position.

Similarly to the derivation above, the Mean First Killing Time (MFKT) given that at least one particle is killed [14] is given by the formula

$$\mathbb{E}[\tau^k(N) | n < N, \mathbf{y}] = \int_0^\infty t \frac{dG(t)}{dt} dt = \int_0^\infty [G(\infty) - G(t)] dt, \quad (44)$$

where,

$$G(t) = \Pr\{\tau^k(N) \leq t | \exists i \in \{1, \dots, N\} \text{ s.t. } \tau_i^k < \tau_i^e, p_0\} \quad (45)$$

is the probability of being killed before time t , conditioned on the event that at least one particle is killed. Proceeding as in formula (42), we obtain

$$G(t) = \frac{1 - \left(1 - \int_0^t \int_{\Omega} k(\mathbf{x}) p(\mathbf{x}, s) d\mathbf{x} ds \right)^N}{1 - \left(1 - \int_0^\infty \int_{\Omega} k(\mathbf{x}) p(\mathbf{x}, s) d\mathbf{x} ds \right)^N}, \quad (46)$$

leading to the formula

$$\mathbb{E}[\tau^k(N) \mid n < N, \mathbf{y}] = \int_0^\infty \frac{\left(1 - \int_0^t \int_{\Omega} k(\mathbf{x}) p(\mathbf{x}, s) d\mathbf{x} ds\right)^N - \left(1 - \int_0^\infty \int_{\Omega} k(\mathbf{x}) p(\mathbf{x}, s) d\mathbf{x} ds\right)^N}{1 - \left(1 - \int_0^\infty \int_{\Omega} k(\mathbf{x}) p(\mathbf{x}, s) d\mathbf{x} ds\right)^N} dt. \quad (47)$$

We are interested as well in the MFAT when all particles escape from the killing. We start by computing the cumulative distribution of the first arrival conditioned on the event that all particles escape, this is

$$F(t) = \frac{\Pr\{\tau^e(N) \leq t, \forall i \in \{1, \dots, N\} \text{ s.t. } \tau_i^e < \tau_i^k \mid p_0\}}{\Pr\{\forall i \in \{1, \dots, N\} \text{ s.t. } \tau_i^e < \tau_i^k \mid p_0\}} = \frac{M(t)}{P_0}. \quad (48)$$

In this case P_0 can be written as $P_0 = \Pr\{n = N \mid p_0\}$, and it can be directly obtained by formula (38). When $p_0(\mathbf{x}) = \delta(\mathbf{x} - \mathbf{y})$ we obtain

$$P_0 = P_e^N = \left[\int_0^\infty J(s \mid \mathbf{y}) ds \right]^N. \quad (49)$$

The numerator $M(t)$ in formula (48) can be obtained using that $A \cap B = A \setminus A \cap B^c$. Thus,

$$\begin{aligned} M(t) &= \Pr\{\tau^e(N) \leq t, n = N \mid \mathbf{y}\} \\ &= \Pr\{n = N\} - \Pr\{\tau^e(N) > t, n = N \mid \mathbf{y}\} \\ &= \Pr\{n = N \mid \mathbf{y}\} - \Pr\{\forall i \in \{1, \dots, N\} : \tau_i^e > t, \tau_i^e < \tau_i^k \mid \mathbf{y}\} \\ &= \Pr\{n = N \mid \mathbf{y}\} - \prod_{i=1}^N \Pr\{\tau_i^e > t, \tau_i^e < \tau_i^k \mid \mathbf{y}\}. \end{aligned} \quad (50)$$

For one particle, we can compute

$$\begin{aligned} \Pr\{\tau_i^e > t, \tau_i^e < \tau_i^k \mid \mathbf{y}\} &= \Pr\{\tau_i^e < \tau_i^k \mid \mathbf{y}\} - \Pr\{\tau_i^e \leq t, \tau_i^e < \tau_i^k \mid \mathbf{y}\} \\ &= \int_0^\infty J(s \mid \mathbf{y}) ds - \int_0^t J(s \mid \mathbf{y}) ds \\ &= \int_t^\infty J(s \mid \mathbf{y}) ds. \end{aligned} \quad (51)$$

We obtain thus,

$$M(t) = \left[\int_0^\infty J(s \mid \mathbf{y}) ds \right]^N - \left[\int_t^\infty J(s \mid \mathbf{y}) ds \right]^N, \quad (52)$$

and

$$F(t) = \frac{\left[\int_0^\infty J(s \mid \mathbf{y}) ds \right]^N - \left[\int_t^\infty J(s \mid \mathbf{y}) ds \right]^N}{\left[\int_0^\infty J(s \mid \mathbf{y}) ds \right]^N}. \quad (53)$$

Note that, $F(\infty) = 1$ as implicit supposed in the definition (48). This leads to the formula for the MFPT

$$\begin{aligned}\mathbb{E}[\tau^e(N) \mid n = N, \mathbf{y}] &= \int_0^\infty t \frac{dF(t)}{dt} dt = \int_0^\infty [F(\infty) - F(t)] dt = \int_0^\infty \left[1 - \frac{\int_0^t J(s \mid \mathbf{y}) ds}{\int_0^\infty J(s \mid \mathbf{y}) ds} \right]^N dt \\ &\approx \int_0^\delta \exp \left[-N \frac{\int_0^t J(s \mid \mathbf{y}) ds}{\int_0^\infty J(s \mid \mathbf{y}) ds} \right] dt, \text{ for } \delta \text{ small.}\end{aligned}\quad (54)$$

Similarly, when only k particles survive, we obtain

$$\begin{aligned}R(t) &= \Pr\{\tau^e(N) \leq t, n = k \mid \mathbf{y}\} \\ &= \binom{N}{k} \Pr\{\min_{\{1, \dots, k\}} \tau_i^e \leq t, \forall i \in \{1, \dots, k\} : \tau_i^e < \tau_j^k, \forall j \in \{k+1, \dots, N\} : \tau_j^e \geq \tau_j^k \mid \mathbf{y}\} \\ &= \binom{N}{k} (1 - P_e)^{N-k} \Pr\{\min_{\{1, \dots, k\}} \tau_i^e \leq t, \forall i \in \{1, \dots, k\} : \tau_i^e < \tau_i^k \mid \mathbf{y}\} \\ &= \binom{N}{k} (1 - P_e)^{N-k} \left[P_e^k - \left(\int_t^\infty J(s \mid \mathbf{y}) ds \right)^k \right].\end{aligned}\quad (55)$$

Thus, the conditional probability is given by

$$L(t) = \Pr\{\tau^e(N) \leq t \mid n = k, \mathbf{y}\} = 1 - \left[\frac{\int_t^\infty J(s \mid \mathbf{y}) ds}{\int_0^\infty J(s \mid \mathbf{y}) ds} \right]^k. \quad (56)$$

Here as well, $L(\infty) = 1$ and this leads to the formula for the MFPT

$$\begin{aligned}\mathbb{E}[\tau^e(N) \mid n = k, \mathbf{y}] &= \int_0^\infty t \frac{dF(t)}{dt} dt = \int_0^\infty [L(\infty) - L(t)] dt = \int_0^\infty \left[1 - \frac{\int_0^t J(s \mid \mathbf{y}) ds}{\int_0^\infty J(s \mid \mathbf{y}) ds} \right]^k dt \\ &\approx \int_0^\delta \exp \left[-k \frac{\int_0^t J(s \mid \mathbf{y}) ds}{\int_0^\infty J(s \mid \mathbf{y}) ds} \right] dt, \text{ for } \delta \text{ small.}\end{aligned}\quad (57)$$

We can use these formulas for the MFPT, when in the biological context that we want to model an elimination of the amount of particles can occur. And actually, depending on the context, we will choose between formulas (43), (54) and (57), to better represent the biological situation. These formulas are later used in chapters 2 and 3.

0.1.3 Arrival with Switching

When more than one type of particles is considered among the N identical and independently distributed Brownian particles, a system of partial differential equations (PDE) should be derived instead of a single PDE. This is the case for an ensemble of N Brownian particles that can switch at Poissonian random times between two states

$$1 \xrightleftharpoons[k_{12}]{k_{21}} 2, \quad (58)$$

with rates k_{12} and k_{21} . The switching times are the i.i.d inter-arrival times for the Poissonian processes (58), and thus, they are exponentially distributed with parameters k_{12} and k_{21} respectively [15].

Survival trajectory with switching

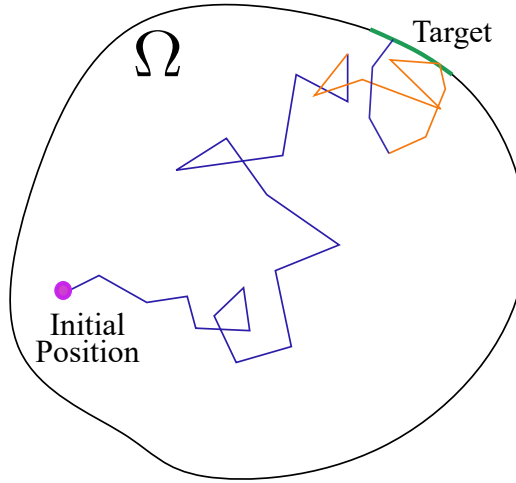


Figure 3: Schematic representation of a Brownian trajectory that switches between 2 states (blue and orange) in a 2D domain. The particle can escape at the boundary only in the blue state.

We suppose here that particles can escape only in one state, which can be without loss of generality the state 1. The Fig. 3 shows one 2D Brownian motion starting in state 1 (blue) with 2 switches. In state 2 (orange), even if the particle is at the absorbing boundary, it does not escape.

The stochastic equation for the position $\mathbf{x}(t, i)$ in state i of the particle is given for $i, j = 1, 2$ by

$$\mathbf{x}(t + \Delta t, i) = \begin{cases} \mathbf{x}(t, i) + \sqrt{2D_i} \Delta \mathbf{w}(t) & \text{w.p } 1 - k_{ij} \Delta t + o(\Delta t) \\ \mathbf{x}(t, j) & \text{w.p } k_{ij} \Delta t + o(\Delta t), i \neq j \end{cases}, \quad (59)$$

where $\mathbf{w}(t)$ is the vector of independent standard Brownian motions, $\Delta \mathbf{w}(t) = \mathbf{w}(t + \Delta t) - \mathbf{w}(t)$, k_{ij} are the transition rates from state i to j , and D_i is the diffusion coefficient in state i . This stochastic model postulates that at each time Δt a particle can either move by Brownian motion in a single state only or switch to a different state without moving. From the space representation of a simulated trajectory ($\Delta t \neq 0$ small) we will be able to see only the fraction of motion in each state as in Fig. 3, but we will not have a clue about the time that particles spend switching states before moving. These is actually very important for the simulations if the rates k_{12} and k_{21} are both large since our simulation risk of excessively increase the arrival times since the particles alternate states

many times. Another model with instantaneous switches can be built by considering 2 different systems, one for the spatial Brownian motion and other for the switchings of states, but this model will not be accurate for processes where binding or coupling takes time. The transition probability density function $p(\mathbf{x}, i, t | \mathbf{y}, j, 0)$ of the trajectory $\mathbf{x}(t, i)$ with the initial condition $\mathbf{x}(j, 0) = \mathbf{y}$, is the limit as $\Delta t \rightarrow 0$ of the integral equations

$$\begin{aligned} p(\mathbf{x}, i, t + \Delta t | \mathbf{y}, j, s) &= \frac{1 - k_{ij}\Delta t}{\sqrt{2\pi D_i \Delta t}} \int_{\Omega} p(\mathbf{z}, i, t | \mathbf{y}, j, s) \exp \left\{ -\frac{|\mathbf{x} - \mathbf{z}|^2}{2D_i \Delta t} \right\} d\mathbf{z} \\ &\quad + k_{ji}\Delta t p(\mathbf{x}, l, t | \mathbf{y}, j, s) + o(\Delta t) \quad \text{for } i, j, l = 1, 2, i \neq j. \end{aligned} \quad (60)$$

Simplifying the notation to $p(\mathbf{x}, i, t | \mathbf{y}, j, s) = p_i(\mathbf{x}, t)$, in the limit $\Delta t \rightarrow 0$, the forward system of Kolmogorov equation is given by [16]

$$\begin{aligned} \frac{\partial}{\partial t} p_1(\mathbf{x}, t) &= D_1 \Delta \mathbf{x} p_1(\mathbf{x}, t) - k_{12} p_1(\mathbf{x}, t) + k_{21} p_2(\mathbf{x}, t) \\ \frac{\partial}{\partial t} p_2(\mathbf{x}, t) &= D_2 \Delta \mathbf{x} p_2(\mathbf{x}, t) - k_{21} p_2(\mathbf{x}, t) + k_{12} p_1(\mathbf{x}, t). \end{aligned} \quad (61)$$

The boundary conditions depend on the formulation of the problem, for instance if the particles can escape only in state 1 at the absorbing boundary, the boundary conditions for both populations of particles are given by

$$\begin{aligned} p_1(\mathbf{x}, t) &= 0 \text{ for } t > 0, \mathbf{x} \in \partial\Omega_a, \\ \frac{\partial p_2}{\partial \mathbf{n}}(\mathbf{x}, t) &= 0 \text{ for } t > 0, \mathbf{x} \in \partial\Omega_a, \\ \frac{\partial p_1}{\partial \mathbf{n}}(\mathbf{x}, t) &= 0 \text{ for } t > 0, \mathbf{x} \in \partial\Omega_r, \\ \frac{\partial p_2}{\partial \mathbf{n}}(\mathbf{x}, t) &= 0 \text{ for } t > 0, \mathbf{x} \in \partial\Omega_r. \end{aligned} \quad (62)$$

If all the particles start their motion in state 1 at point $\mathbf{y} > 0$, the initial conditions are given by

$$\begin{aligned} p_1(\mathbf{x}, 0) &= \delta^d(\mathbf{x} - \mathbf{y}) \\ p_2(\mathbf{x}, 0) &= 0. \end{aligned} \quad (63)$$

Note that the general notation $\delta^d(\cdot)$ is used for the Dirac-delta function in dimension d . The normalization condition should be always satisfied

$$\int_{\Omega} (p_1(\mathbf{x}, 0) + p_2(\mathbf{x}, 0)) d\mathbf{x} = 1. \quad (64)$$

When the particle starts in state 2 at point $\mathbf{y} > 0$, the associated initial conditions are

$$\begin{aligned} p_1(\mathbf{x}, 0) &= 0 \\ p_2(\mathbf{x}, 0) &= \delta^d(\mathbf{x} - \mathbf{y}). \end{aligned} \quad (65)$$

The survival probability is then given by the survival probability of the particles in each population, this is

$$S(t) = \int_{\Omega} (p_1(\mathbf{x}, t) + p_2(\mathbf{x}, t)) d\mathbf{x}, \quad (66)$$

and the computations for the MFAT shall continue as computed in formula (20) if other dynamics are not consider.

0.1.4 Preliminary results in the arrival time problem

When the domain is the non-negative real line, $\Omega = [0, +\infty)$, with absorbing boundary only at the point $x = 0$ and with a Dirac delta function at $x = y$ as initial distribution, the well known logarithmic formula for the MFAT

$$\bar{\tau}^N \sim \frac{y^2}{4D \ln\left(\frac{N}{\sqrt{\pi}}\right)}, \quad (67)$$

is obtained for $N \gg 1$ [59]. Note that in this case, nothing is narrow, as we are working in the 1D problem. The FPE is thus the heat equation in 1D

$$\begin{aligned} \frac{\partial p(x, t)}{\partial t} &= D \frac{\partial^2 p(x, t)}{\partial x^2} \text{ for } x > 0, t > 0 \\ p(x, 0) &= \delta(x - y) \text{ for } x > 0 \\ p(0, t) &= 0 \text{ for } t > 0, \end{aligned} \quad (68)$$

where D is the diffusion coefficient. The solution to this equation is given by the Green's function

$$p(x, t) = \frac{1}{\sqrt{4Dt}} \left[\exp\left\{-\frac{(x-y)^2}{4Dt}\right\} - \exp\left\{-\frac{(x+y)^2}{4Dt}\right\} \right]. \quad (69)$$

Here, $\Pr\{t_1 > t\} = \text{erf}\left(\frac{y}{\sqrt{4Dt}}\right)$ and the key to find the formula (67) relies on the Laplace method. In this case,

$$\bar{\tau}^N = \int_0^\infty [\Pr\{t_1 > t\}]^N dt = \int_0^\infty \left[e^{\ln(\text{erf}(\frac{y}{\sqrt{4Dt}}))} \right]^N dt = \int_0^\infty e^{N \ln(\text{erf}(\frac{y}{\sqrt{4Dt}}))} dt. \quad (70)$$

This is a specific type of Laplace integrals, which are in the form

$$I(N) = \int_a^b \phi(t) e^{N\Psi(t)} dt \text{ with } N > 0. \quad (71)$$

Here $\phi(t) = 1$ and $\Psi(t) = \ln\left(\text{erf}\left(\frac{y}{\sqrt{4Dt}}\right)\right)$. Typically, N is a large parameter, and one can be interested in the **asymptotic behavior of $I(N)$ when $N \rightarrow +\infty$** . By definition, the simpler function $i(N)$ is an asymptotic of $I(N)$ when $N \rightarrow +\infty$ if

$$\lim_{N \rightarrow +\infty} \frac{I(N)}{i(N)} = 1, \quad (72)$$

written $I(N) \sim i(N)$, or $I(N) = i(N)(1 + o(1))$. The function $i(N)$ is also called the leading order term of the asymptotic expansion for $I(N)$.

Depending on specific properties of the functions $\phi(t)$ and $\Psi(t)$, and the integration domain, some Laplace integrals can be solved integrating by parts. But the most well known tool used to solve Laplace integrals is Laplace method. This method allows to find useful asymptotic representations for many functions including Gamma functions and Bessel functions.

The general idea behind the **Laplace method** [18–22] is that if $\Psi(t)$ has a (global) maximum at $t = t_0$ with $a \leq t_0 \leq b$ and if $\phi(t_0) \neq 0$ the main contribution to the full asymptotic expansion of $I(N)$ comes from a neighborhood of t_0 as $N \rightarrow +\infty$. In general, the interval of integration may be

infinite and if $\Psi(t)$ achieves its global maximum value in more than a point of the interval, we can decompose the integral in several intervals, each containing a single maximum. In the especial case where the maximum value is not achieved, meaning that $\Psi(t)$ has only a supremum when $t \rightarrow t_0$ we use the asymptotic expansion of $\Psi(t)$ around t_0 .

Integral (70) can be solved then under the short-time regime since $\Psi(t)$ is the composition of two increasing functions and thus,

$$\sup_{t \in (0, +\infty)} \Psi(t) = \sup_{t \in (0, +\infty)} \ln \left(\operatorname{erf} \left(\frac{y}{\sqrt{4Dt}} \right) \right) = \ln \left(\sup_{t \in (0, +\infty)} \operatorname{erf} \left(\frac{y}{\sqrt{4Dt}} \right) \right) = 0 = \lim_{t \rightarrow 0^+} \Psi(t) \quad (73)$$

since

$$\sup_{t \in (0, +\infty)} \operatorname{erf} \left(\frac{y}{\sqrt{4Dt}} \right) = 1. \quad (74)$$

This means that the main contribution to $I(N)$ comes from the short time expansion of $\Psi(t)$. Note then,

$$\Psi(t) = \ln \left(\operatorname{erf} \left(\frac{y}{\sqrt{4Dt}} \right) \right) = \ln \left(1 - \operatorname{erfc} \left(\frac{y}{\sqrt{4Dt}} \right) \right) \sim -\operatorname{erfc} \left(\frac{y}{\sqrt{4Dt}} \right) \text{ for } t \text{ small.} \quad (75)$$

Replacing thus the expansion of $\operatorname{erfc}(x)$ for large argument, this is

$$\operatorname{erfc}(x) = \frac{e^{-x^2}}{x\sqrt{\pi}} \left(1 - \frac{1}{2x^2} + O\left(\frac{1}{x^4}\right) \right),$$

we obtain

$$I(N) \sim \int_0^\varepsilon e^{-N\operatorname{erfc}\left(\frac{y}{\sqrt{4Dt}}\right)} dt \sim \int_0^\varepsilon e^{-N\sqrt{4Dt} \frac{e^{-\frac{y^2}{4Dt}}}{y\sqrt{\pi}}} dt \sim \frac{y^2}{4D} \int_0^{\frac{4D}{y^2}\varepsilon} e^{-N\sqrt{u} \frac{e^{-\frac{1}{u}}}{\sqrt{\pi}}} du. \quad (76)$$

The last integrand resembles to the cumulative distribution function of the **Gumbel extreme maximum value law** where

$$\Pr\{X \leq x\} = e^{-e^{-\frac{x-\mu}{\beta}}} \text{ if } X \sim \text{Gumbel}(\mu, \beta). \quad (77)$$

In fact, we have a special interest in the distributions of the forms

$$\Pr\{\tau^1 \leq t\} = 1 - e^{-Nt^k e^{-\frac{1}{t^\alpha}}} \text{ for } t > 0, N > 0, k > 0 \text{ and } \alpha > 0. \quad (78)$$

After a revision of the literature about extreme value theory [23–31] we have not found any manuscript referencing this type of distribution, so we will call it here the fastest arrival distribution (FAD(N, k, α)). Note that, the short-time approximation made in (76) for the arrival distribution of the fastest particle is an FAD with $N = \frac{N}{\pi}$, $k = \frac{1}{2}$ and $\alpha = 1$, this is, $\tau^1 \sim \text{FAD}(N, \frac{1}{2}, 1)$ for t small.

If we consider the function

$$w(u) = \sqrt{u} e^{-\frac{1}{u}}, \quad (79)$$

where $dw = \sqrt{u} e^{-\frac{1}{u}} \left(\frac{1}{2u} + \frac{1}{u^2} \right) du$, we obtain for u small the approximation $dw \approx w(\ln(w))^2$. In general, this change of variable works for the whole family of functions $w(u, k) = u^k e^{-\frac{1}{u}}$, with

$k > 0$, since $dw = u^k e^{-\frac{1}{u}} \left(\frac{k}{u} + \frac{1}{u^2} \right) du$, and for u small, one can still have the approximation $dw \approx w (\ln(w))^2$. Thus, making the change of variable (79) in (76) and integrating by parts we obtain the approximation

$$I(N) \approx \frac{y^2}{4D} N' \int_0^{\frac{4D}{y^2}\varepsilon} \frac{e^{-N'w}}{|\ln(w)|} dw, \quad (80)$$

where $N' = \frac{N}{\pi}$. This is also a Laplace integral which solution is not direct but can be found using the change of variable $z = N'w$, and it leads to the asymptotic formula (67). Note that for $z \in [0, \frac{4D}{y^2}\varepsilon N']$ we can use the approximation

$$\frac{1}{|\ln(\frac{z}{N'})|} = \frac{1}{\ln(N') \left| 1 - \frac{\ln(z)}{\ln(N')} \right|} = \frac{1}{\ln(N') \left(1 - \frac{|\ln(z)|}{\ln(N')} \right)} = \frac{1}{\ln(N')} \left(1 + \frac{|\ln(z)|}{\ln(N')} + O\left(\left(\frac{|\ln(z)|}{\ln(N')}\right)^2\right) \right) \quad (81)$$

in order to compute the integral (80). This leads to

$$\begin{aligned} I(N) &\approx \frac{y^2}{4D} \int_0^{\frac{4D}{y^2}\varepsilon N'} \frac{e^{-z}}{\ln(N')} \left(1 + \frac{|\ln(z)|}{\ln(N')} \right) dz \approx \frac{y^2}{4D \ln(N')} \int_0^\infty e^{-z} \left(1 + \frac{|\ln(z)|}{\ln(N')} \right) dz \\ &\approx \frac{y^2}{4D \ln(N')} \left(1 + \frac{\gamma_e Ei(-1)}{\ln(N')} \right) \approx \frac{y^2}{4D (\ln(N') - \gamma_e Ei(-1))}, \end{aligned} \quad (82)$$

where γ_e is the Euler–Mascheroni constant and $Ei(x)$ is the exponential integral function. Here the leading order term is

$$I(N) \sim \frac{y^2}{4D \ln(N')}, \quad (83)$$

but as during the computation we used the approximation (81), we mostly write a parameter α that helps to correct the error obtained when approximating $I(N)$ by its leading term only, this is

$$I(N) \sim \frac{y^2}{4D (\ln(N') + \alpha)}. \quad (84)$$

Here $\alpha = -\sum_{i=1}^{\infty} \int_0^\infty e^{-z} \left(\frac{|\ln(z)|}{\ln(N')} \right)^i dz$ and we see that as $N' \rightarrow +\infty$ we obtain that $\alpha \rightarrow 0$. We will use this parameter α as a fitting parameter when comparing our simulation results with the asymptotic formulas.

Laplace method is also strongly linked with **Large Deviation Theory** since it allows to show that the probability of a rare event is decaying exponentially on N for certain problems. The simplest example is the probability that a normally distributed random variable (r.v.) X takes large values, this is

$$\Pr(A) = \Pr\{X \in A\} = \frac{1}{Z} \int_A e^{-x^2} dx, \quad (85)$$

where Z is a normalizing constant. If we consider the interval A given by $A = \sqrt{N}S$ where S is a fixed interval and $N \rightarrow +\infty$, then

$$\begin{aligned} \Pr(X \in A) &= \frac{\sqrt{N}}{Z} \int_S e^{-Ns^2} ds \approx \frac{\sqrt{N}}{Z} \int_{V(s^*) \in S} e^{-N((s^*)^2 + 2s^*(s-s^*))} ds \approx \frac{\sqrt{N} e^{-N(s^*)^2}}{Z} \int_S e^{-N(2s^*(s-s^*))} ds \\ &= \frac{\sqrt{N} e^{-N(s^*)^2}}{2s^* N Z} \int_0^{2s^* N(\max S - s^*)} e^{-v} dv = \frac{e^{-N(s^*)^2}}{2s^* Z \sqrt{N}} [1 - e^{-2s^* N(\max S - s^*)}], \end{aligned} \quad (86)$$

where $s^* = \min(S) > 0$. Then,

$$\lim_{N \rightarrow +\infty} \frac{\Pr(X \in A)}{\frac{e^{-N(s^*)^2}}{2Z\sqrt{Ns^*}}} = \lim_{N \rightarrow +\infty} 1 - e^{-2s^*N(\max S - s^*)} = 1 \quad (87)$$

leading to

$$\Pr(X \in A) \sim \frac{e^{-N(s^*)^2}}{2Z\sqrt{Ns^*}}. \quad (88)$$

In this sense, Laplace method also shows that the main contribution to this probability is always coming from an optimization problem, whose complexity depends on the general problem that we want to solve.

We will focus one part of this thesis in the Freidlin-Wentzell large deviation principle and the Euler-Lagrange equation to obtain the optimal path for the motion of the fastest particles when a the killing term is included in the diffusion model.

For Brownian particles, when we have the stochastic equation (under Ito's convention)

$$d\mathbf{x}_t^\varepsilon = \mathbf{b}(\mathbf{x}_t^\varepsilon) dt + \sqrt{\varepsilon} \mathbf{B}(\mathbf{x}_t^\varepsilon) d\mathbf{w}(t), \quad \text{for } \mathbf{x} \in \Omega, \quad (89)$$

with $\mathbf{b}(x)$, $\mathbf{B}(x)$ and $\mathbf{w}(t)$ as previously defined in (1), **Freidlin-Wentzell Theory** [32, 33] proves that when the intensity of the noise vanishes ($\varepsilon \rightarrow 0$) the path of the process $(\mathbf{x}_t^\varepsilon)_{t \in [t_0, T]}$ started at \mathbf{x}_0 converges to the relaxed trajectory $(\phi_t)_{t \in [t_0, T]}$ with $T < +\infty$, solution of the Cauchy problem

$$\begin{aligned} \dot{\phi}_t &= \mathbf{b}(\phi_t) \quad \text{for } t \geq 0 \\ \phi_0 &= \mathbf{x}_0, \end{aligned} \quad (90)$$

with stationary solution $\phi_t = \mathbf{x}_0 \forall t \geq t_0$. Freidlin described the fluctuations of the diffusion process around the deterministic limit through the action functional given by

$$\mathcal{S}_{[t_0, T], \mathbf{x}_0}(\phi_t) = \frac{1}{2} \int_{t_0}^T |\sigma(\phi_t)^{-1} (\dot{\phi}_t - \mathbf{b}(\phi_t))|^2 dt, \quad (91)$$

for all $t_0 < T$ and for all absolutely continuous path $(\phi_t)_{t \in [t_0, T]}$ with $\phi_0 = \mathbf{x}_0$ and $\mathcal{S}_{[t_0, T], \mathbf{x}_0}(\phi_t) = +\infty$ otherwise. The cornerstone of the Freidlin-Wentzell theory is the large deviation principle for the general stochastic differential equation (89), which says

$$\forall \delta > 0, \forall t \in [t_0, T], \Pr \{ \max |x_t^\varepsilon - \phi_t| > \delta \} \asymp \exp \left\{ - \frac{\mathcal{S}_{[t_0, T], \mathbf{x}_0}(\phi_t)}{\varepsilon} \right\}. \quad (92)$$

Another useful link between stochastic and differential equations is the **Feynman-Kac formula** [34, 35], that helps to represent the solution of the FPE with a killing measure (22) trough the expected values of the initial condition over the paths that survive a time large enough to arrive at the absorbing boundary. Thus, given equation (22) with $p(\mathbf{x}, 0) = f(\mathbf{x})$, we can write

$$p(\mathbf{x}, t) = \mathbb{E} \left[f(\mathbf{x}_t) \exp \left(- \int_0^t k(\mathbf{x}_s) ds \right) \right], \quad (93)$$

where $\mathbf{x}_t = \mathbf{x}(t)$ is the Brownian trajectory of (1), starting at time $t = 0$ at position \mathbf{x}_0 . One of the most used consequence of the Feynman-Kac representation that we will be using here later is the formula for the survival probability, given by

$$S(t) = \int_{\Omega} p(\mathbf{x}, t) d\mathbf{x} = \mathbb{E} \left[\exp \left(- \int_0^t k(\mathbf{x}_s) ds \right) \right], \quad (94)$$

when $f(\mathbf{x}) = \delta(\mathbf{x})$.

We will use as well the **Euler-Lagrange Principle** [36,37] to find the stationary point of a certain functional $\mathcal{S}(\mathbf{q})$, related with (91), of the form

$$\mathcal{S}(\mathbf{q}) = \int_{t_1}^{t_2} L(t, \mathbf{q}(t), \dot{\mathbf{q}}(t)) dt, \quad (95)$$

such that $\mathbf{q}(t_1) = \mathbf{x}_1$ and $\mathbf{q}(t_2) = \mathbf{x}_2$, where $L(t, \mathbf{q}(t), \dot{\mathbf{q}}(t))$ is the Lagrangian of the system. There is no single expression of the Lagrangian for all possible systems but actually, any function that generates properly the motion of the system can be taken as a Lagrangian. We will not go deeply in the physics details of the function $L(t, \mathbf{q}(t), \dot{\mathbf{q}}(t))$, but we will mention here that the Euler-Lagrange equation applied to the Lagrangian gives the equation of motion for the system, which describe the behavior of the system in terms of its motion as a function of time. We consider $\mathcal{P}(t_1, t_2, x_1, x_2)$ the ensemble of all smooth paths $\mathbf{q} : [t_1, t_2] \rightarrow \mathbb{R}^n$ such that $\mathbf{q}(t_1) = \mathbf{x}_1$ and $\mathbf{q}(t_2) = \mathbf{x}_2$ and we would like to find the stationary path \mathbf{q}^* of (95). The path \mathbf{q}^* is called the optimal path or the stationary point of \mathcal{S} (with respect to any small perturbations in \mathbf{q}). Euler-Lagrange principle says that a path \mathbf{q}^* is an stationary point of \mathcal{S} if and only if it satisfies the Euler-Lagrange equation:

$$\frac{\partial L}{\partial q^i}(t, \mathbf{q}(t), \dot{\mathbf{q}}(t)) - \frac{\partial}{\partial t} \frac{\partial L}{\partial \dot{q}^i}(t, \mathbf{q}(t), \dot{\mathbf{q}}(t)) = 0, \quad \forall i = 1, \dots, n. \quad (96)$$

The resulting ordinary differential system is then the equations of motions of the system. This is also known as Hamilton's principle or the principle of least action. However, the action functional \mathcal{S} only needs to be stationary, not necessary a maximum or a minimum value, since any variation will lead to an increase in the functional integral of action.

0.2 Biological motivation

Many cellular processes are started as result of molecular activation [38]. These activation time scales, sometimes known by experimental methods, can give us an idea about the activation mechanism itself. In the case of fast calcium transient activating the Ryanodyne receptors (RyRs) in the spine apparatus (SA), the time scale of calcium diffusion transient during long-term plasticity induction is of the order of hundreds of milliseconds, fact that helped to prove that this activation was driven by the fastest ions arriving to the RyRs [39, 40]. Calcium signaling has been largely studied in the field of Neuroscience until this day [41–47], and it is one of the main biological problems inspiring this thesis.

Another process motivating this thesis is the synthesis and transport of proteins. The first step of protein synthesis is the transcription of DNA [48]. During this process active transcription factors (TFs) need to arrive to a specific part of the DNA strand called enhancer to start the recruitment of the RNA polymerase. When the mRNA is produced, this molecule needs to be transported to the ribosomes out of the nucleus. Many transcription factors help to regulate the cell cycle, controlling the rate of cellular division. Further alterations in this cycle can affect the transcriptional control of gene expression giving rise to many diseases such as cancer.

Calcium signaling

Signal transduction is the process by which a chemical signal is transmitted through a cell as a series of molecular events, which ultimately results in a cellular response [49]. The receptors for this

Scheme of a general neuron cell anatomy

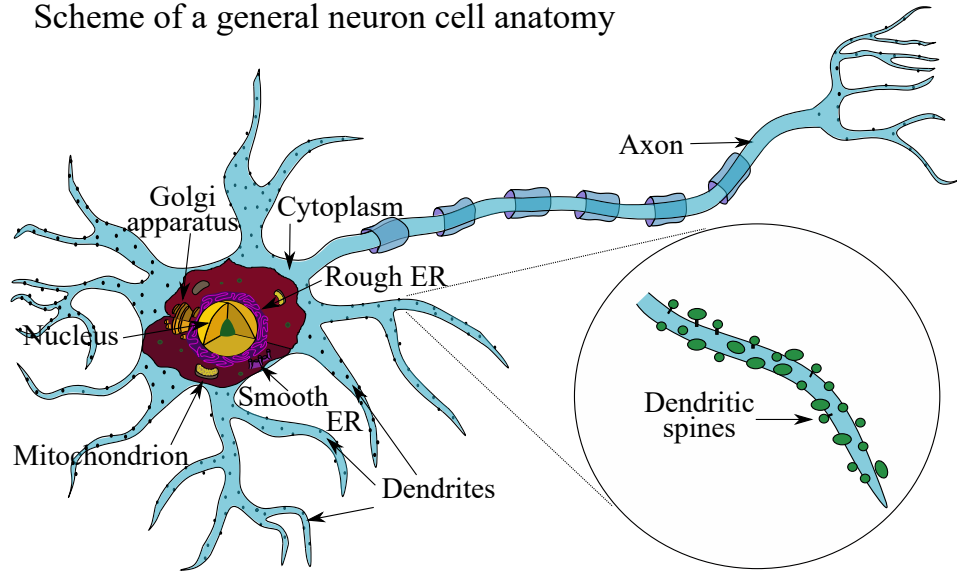


Figure 4: Schematic representation of a neuron cell anatomy and its main components.

stimulus are often specialized proteins that after the reception of the stimulus give rise to a chain of biochemical events known as a signaling pathway [50].

Calcium signaling is then the use of calcium ions (Ca^+) to communicate and drive intracellular processes. The concentration of calcium ions in the cell cytoplasm is very low compared to the typical extracellular concentration, so the regulation of the free calcium ions is essential for excitable cell like neuronal cell as they transmit neural activity. To keep this rate low, after calcium ions enter dendritic spines (see Fig 4), they are actively pumped from the cytosol to extracellular space, the Endoplasmic Reticulum (ER) and sometimes to the mitochondria by sarco/ER calcium-ATPase (SERCA) pumps. But they can also bind endogenous buffers whose target is the same, stabilize the calcium concentration in the cytoplasm. This calcium buffering can be modeled as a removal of the calcium ions in the dendritic spine compartment.

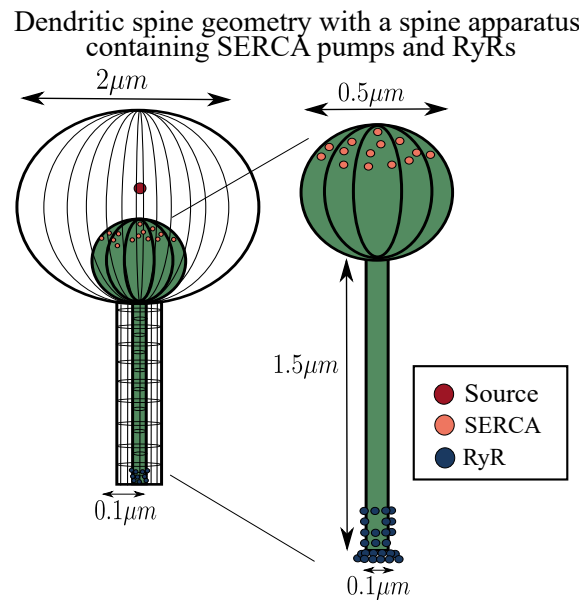


Figure 5: Idealization of a dendritic spine geometry endowed with a spine apparatus.

The spines in general are characterized by a diversity of their size, shapes and the presence or absence of structural components and organelles. Several spines may contain smooth ER, fragmented in a compartment called the spine apparatus, that regulates calcium ion concentrations by storing or releasing them and modulate synaptic inputs. We will consider here spines in general shape composed by a spherical head and a narrow cylinder as a neck as shown in Fig 5, but in general during synaptic plasticity, spine morphology can change, increasing/decreasing the head size or elongating/retracting its neck. Calcium ions can also induce calcium release (denoted calcium-induced calcium release (CICR)) from internal SA stores through the RyRs [51]. Thus, in order to know the time for CICR to happen when a large amount of calcium ions are released in the dendritic spine, we will look here for the time that it takes for free calcium ions to activate the RyR.

We will also consider the case where the ions are injected slowly on the spine, meaning that, when the injection is over, the initial distribution of ions has already spread out leading to an exponential distribution different from the Dirac-delta function. The results associated to calcium signaling are grouped in the first part of this thesis, from chapter 1 to 3.

DNA transcription and protein synthesis

Transcription is the first step of gene expression. During this process, a molecule of mRNA (messenger RNA) is produced. The RNA is called messenger RNA because it carries the message (genetic information) to the ribosomes where this information is used to assemble proteins.

The first stage of transcription is the pre-initiation. During this step, active transcription factors in

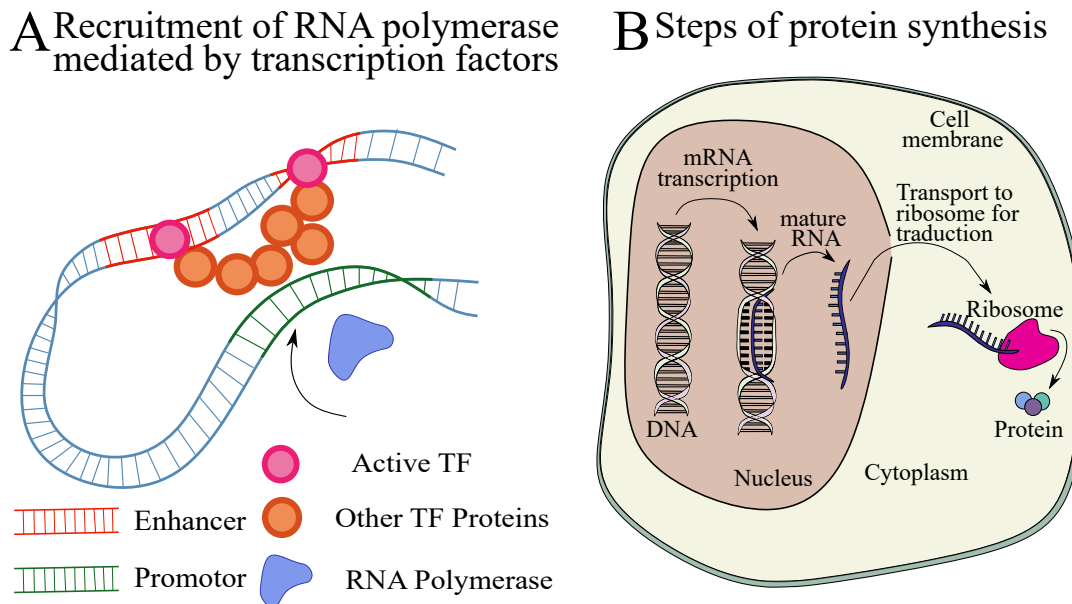


Figure 6: DNA transcription and translation of the mRNA. A. Pre-initiation step of transcription started by the binding of transcription factors to the enhancer sites. B. Schematic steps of protein synthesis with DNA transcription as a first step.

the nucleus bind the enhancer site to start the recruitment of other co-factors (other TF proteins). After all of them gated together, the DNA creates a loop between the enhancer and the promoter sites as shown in Fig. 6A. The presence of other co-factors is a signal of recruitment for the RNA

polymerase that moves then in the direction of the promoter. The second step, initiation, starts with the binding of the RNA polymerase to the promoter. Then, the elongation takes place. It is at this stage where a strand of DNA serves as the template for the mRNA molecule. The final step is the termination, resulting in the release of the newly synthesized and mature mRNA from the elongation complex. To start protein synthesis, the mRNA needs to be translated [38,52]. In eukaryotic cells, transcription and translation are compartmentalized separate processes, meaning that the mRNA molecule needs to be transported from the nucleus to the ribosomes in the cytoplasm as shown in Fig. 6B. In some cases, depending on the complexity of the cells and the proteins that are encoded by the mRNA, the molecule can be transported to very particular cellular sub-regions. Such is the case of some mRNA in neurons, which are transported from the soma (cell body of the neurons in which the dendrites branch off) to the dendrites. Transport of mature mRNA through DNA pores is accomplished by cap-binding proteins and transcription/export proteins that detect and bind to the mRNA. We are interested here in the two main aspects of protein synthesis, the first one is to study the time for active TFs to start the recruitment of RNA polymerase. The second one is to study the transport of mature mRNA once it is released. The results associated to transcription are grouped in the second part of this thesis, in chapter 4.

0.3 Main results of the thesis

Part I: Asymptotic formulas for calcium signaling

We devoted this part of the thesis to the computation of asymptotic formulas for the first arrival problem with different initial conditions and considering the elimination of particles as another dynamic in the model. We applied the obtained results to calcium dynamics in the dendritic spines.

Results section 1.2: Arrival times for multiple initial distributions in 1D. In this section we computed the MFAT for N Brownian particles with constant diffusion coefficient D inside the non-negative real line and inside a finite interval for different initial conditions as shown in the table below. Here the exit point is the origin for the infinite domain $\Omega = \mathbf{R}_+$ or in contrast, the exit points are both extreme of the interval when $\Omega = [0, a]$.

Asymptotic formulas for the MFAT of the diffusion equation			
Initial Distribution	$\Omega = \mathbf{R}_+$	Initial Distribution	$\Omega = [0, a]$
$p_0(x) = \delta(x - x_0)$	$\bar{\tau}^N \sim \frac{x_0^2}{4D \log\left(\frac{N}{\sqrt{\pi}}\right)}$	$p_0(x) = \delta(x - x_0)$	$\bar{\tau}^N \sim \frac{(\min(x_0, a - x_0))^2}{4D \log\left(\frac{N}{\sqrt{\pi}}\right)}$
$p_0(x) = \frac{1}{y_0} \mathbb{I}_{\{x \in [0, y_0]\}}$	$\bar{\tau}^N \sim \frac{y_0^2 \pi}{2DN^2}$	$p_0(x) = \frac{1}{y_0} \mathbb{I}_{\{x \in [0, y_0]\}}$	$\bar{\tau}^N \sim \frac{y_0^2 \pi}{2DN^2}$
$p_0(x) = \frac{1}{y_2 - y_1} \mathbb{I}_{\{x \in [y_1, y_2]\}}$	$\bar{\tau}^N \sim \frac{y_1^2}{4D \log\left(\frac{N}{\sqrt{\pi}}\right)}$	$p_0(x) = \frac{1}{y_2 - y_1} \mathbb{I}_{\{x \in [y_1, y_2]\}}$	$\bar{\tau}^N \sim \frac{(\min(y_1, a - y_2))^2}{4D \log\left(\frac{N}{\sqrt{\pi}}\right)}$
$p_0(x) = 2bx e^{-bx^2}$	$\bar{\tau}^N \sim \frac{1}{2DbN}$	$p_0(x) = \frac{2b}{1 - e^{-bc^2}} x e^{-bx^2} \mathbb{I}_{\{x \in [0, c]\}}$	$\bar{\tau}^N \sim \frac{1 - e^{-bc^2}}{2DbN}$
$p_0(x) = \frac{4b^{\frac{3}{2}}}{\sqrt{\pi}} x^2 e^{-bx^2}$	$\bar{\tau}^N \sim \frac{\pi^{\frac{3}{2}}}{4Db(2N)^{\frac{3}{2}}} \Gamma\left(\frac{5}{3}\right)$	-	-

We also generalized the MFAT law for the family of exponential functions (proof in page 56).

Proposition 0.1. For an initial normalized distribution $p_0(x) = Kx^\alpha e^{-bx^2}$ with $\alpha \geq 0$ and $b > 0$, where $K = \frac{2b^{\frac{\alpha+1}{2}}}{\Gamma\left(\frac{\alpha+1}{2}\right)}$, the MFAT for N particles escaping at the origin of the non-negative real line is

given by the algebraic law

$$\bar{\tau}^N \sim \left(\frac{\sqrt{\pi}(\alpha+1)\Gamma\left(\frac{\alpha+1}{2}\right)}{2N\Gamma\left(\frac{\alpha+2}{2}\right)} \right)^{\frac{2}{\alpha+1}} \frac{1}{4Db} \Gamma\left(\frac{\alpha+3}{\alpha+1}\right) \text{ when } N \gg 1. \quad (97)$$

For the validation of the asymptotic formulas we considered 3 initial distributions for the particles as in Fig. 7B, and we select the fastest one arriving at the boundary, schematically represented by the green trajectory in Fig. 7A. The simulation results for the arrival distribution and MFAT were shown in Fig. 7C, D, E and Fig. 8B respectively. We can see from Fig. 7C and E, that when particles are initially generated very close to the absorbing boundary, a good agreement is obtained between the theoretical and simulated distributions. But when particles are generated far from the absorbing boundary as in Fig. 7D, the finite N corrections seem to be rather strong and it improves when we increase the value of N . And we can see also this effect in the simulation results for the MFAT (Fig. 8B blue) where a parameter α needs to be added in the logarithmic formula to correct the asymptotic result. We can also think that for the exponential distribution in Fig. 8B (red) there is a deviation between the asymptotic formulas and the simulations results for large N , but we believe that this could be due to the Δt consider in the Euler scheme for simulations. In this case particles can be generated very close to the absorbing boundary, and we choose a Δt satisfying that

$$\Delta t \leq p \frac{\delta_N^2}{2D}, \quad (98)$$

where δ_N is the minimal distance between the particles generated and the target:

$$\delta_N = \min_N \{|\chi_1|, \dots, |\chi_N|\}. \quad (99)$$

Then, the mean square displacement, controlled by the parameter p , is smaller than the shortest distance. But, what could be happening is that we did not take p small enough, and after a few steps when N is large the fastest particles escapes over estimating the time.

Result section 1.3: MFAT in 2D.

Proposition 0.2. *For a 2D bounded domain Ω as in Fig. 9 the MFAT for N particles uniformly distributed in $\Omega^* = \{B_{r_2}(\mathbf{0}) \setminus B_{r_1}(\mathbf{0}) : \theta_1 \leq \theta \leq \theta_1 + \theta_2\}$ escaping in the boundary arc of length 2ε centered at $\mathbf{x} = (0, 0)$ is given by*

$$\bar{\tau}^N \sim \frac{r_1^2}{4D \ln\left(\frac{\sqrt{2}\pi N}{8\ln(\frac{1}{\varepsilon})}\right)}. \quad (100)$$

When particles are initially distributed in the domain Ω following $p_0(\mathbf{x}) = K|\mathbf{x}|^\alpha e^{-b|\mathbf{x}|^2}$ with $\alpha \geq 0$ and $b > 0$, we obtain

$$\bar{\tau}^N \sim \left(\frac{8\ln(\frac{1}{\varepsilon}) (\Gamma(\frac{\alpha+2}{2}) - \Gamma(\frac{\alpha+2}{2}, bR^2))}{\sqrt{2N\pi}\Gamma(\frac{\alpha}{2})} \right)^{\frac{2}{\alpha+2}} \frac{1}{4Db} \Gamma\left(\frac{\alpha+4}{\alpha+2}\right). \quad (101)$$

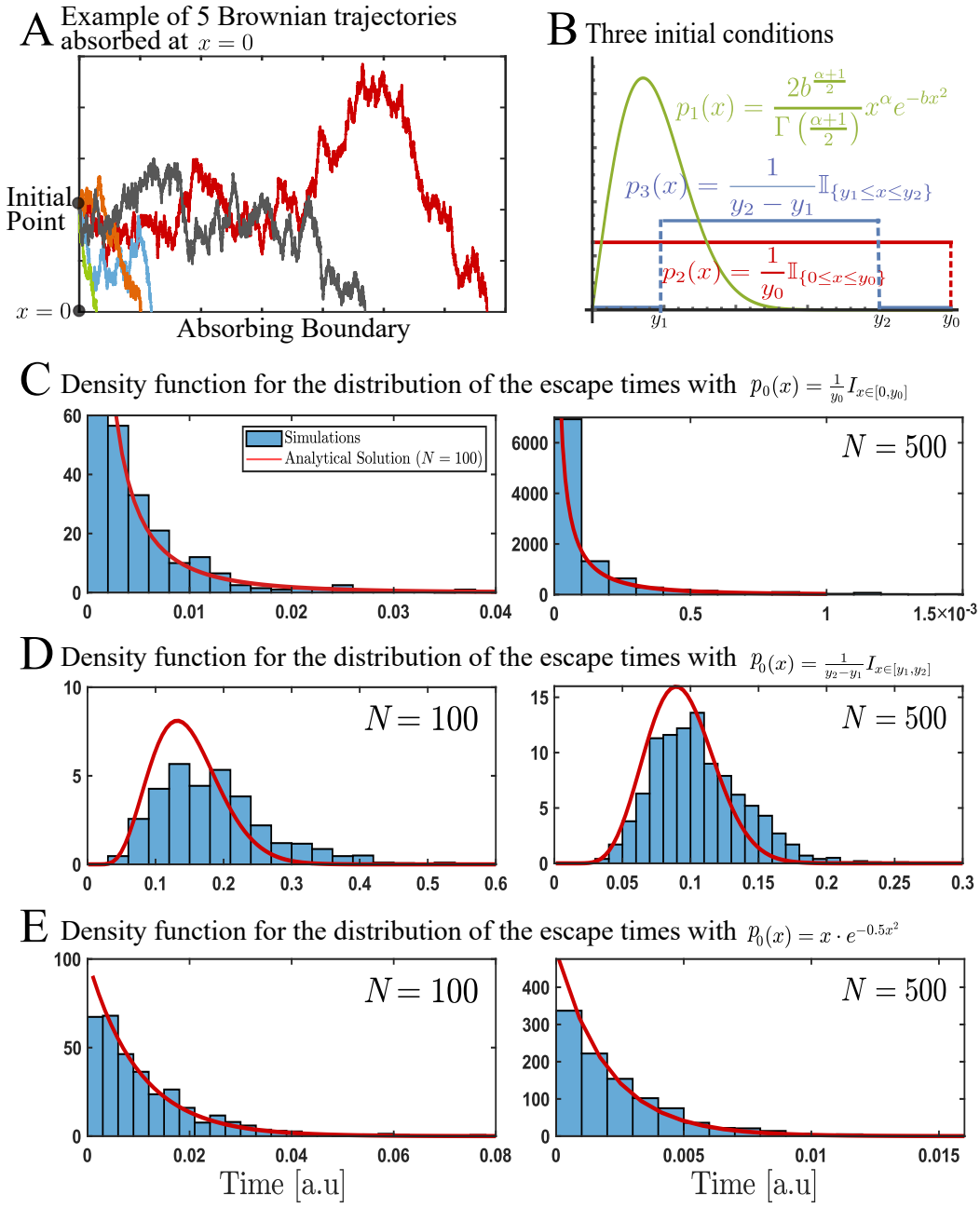


Figure 7: **Arrival times for the fastest Brownian particles for various initial distributions.** **A.** Examples of 5 independent Brownian trajectories starting at $x = 0.5$ and absorbed at $x = 0$ and the fastest is green. **B.** Three initial distributions: the exponential distribution $p_1(x) = \frac{2b^{\frac{\alpha+1}{2}}}{\Gamma(\frac{\alpha+1}{2})} x^\alpha e^{-bx^2}$ and two uniform distributions $p_2(x) = \frac{1}{y_0} \mathbb{I}_{\{0 \leq x \leq y_0\}}$ and $p_3(x) = \frac{1}{y_2 - y_1} \mathbb{I}_{\{y_1 \leq x \leq y_2\}}$. **C.** Density function for the arrival times $\bar{\tau}^N$: analytical (1.17) (red) vs stochastic simulations (blue histogram) for particles distributed with respect to $p_0(x) = \frac{1}{y_0} \mathbb{I}_{\{0 \leq x \leq y_0\}}$ for $0 < y_0 < a$ with $y_0 = 4$ and $a = 5$ for $N = 100$ (left) and $N = 500$ (right) with 1000 runs. **D.** Density function for the arrival times $\bar{\tau}^N$: analytical (1.20) (red) vs stochastic simulations (blue) for particles distributed with respect to $p_0(x) = \frac{1}{y_2 - y_1} \mathbb{I}_{\{y_1 \leq x \leq y_2\}}$ with $0 < y_1 < y_2 < a$, $y_1 = 1$ and $y_2 = 4$. **E.** Density function for the arrival time $\bar{\tau}^N$: analytical (1.24) (red) vs stochastic simulations (blue) for particles distributed with respect to $p_1(x) = \frac{2b}{1-e^{-bc^2}} xe^{-bx^2} \mathbb{I}_{\{x \in [0, c]\}}$ with $a > c > 0$ with $b = 0.5$, $\alpha = 1$ and $c = 4$.

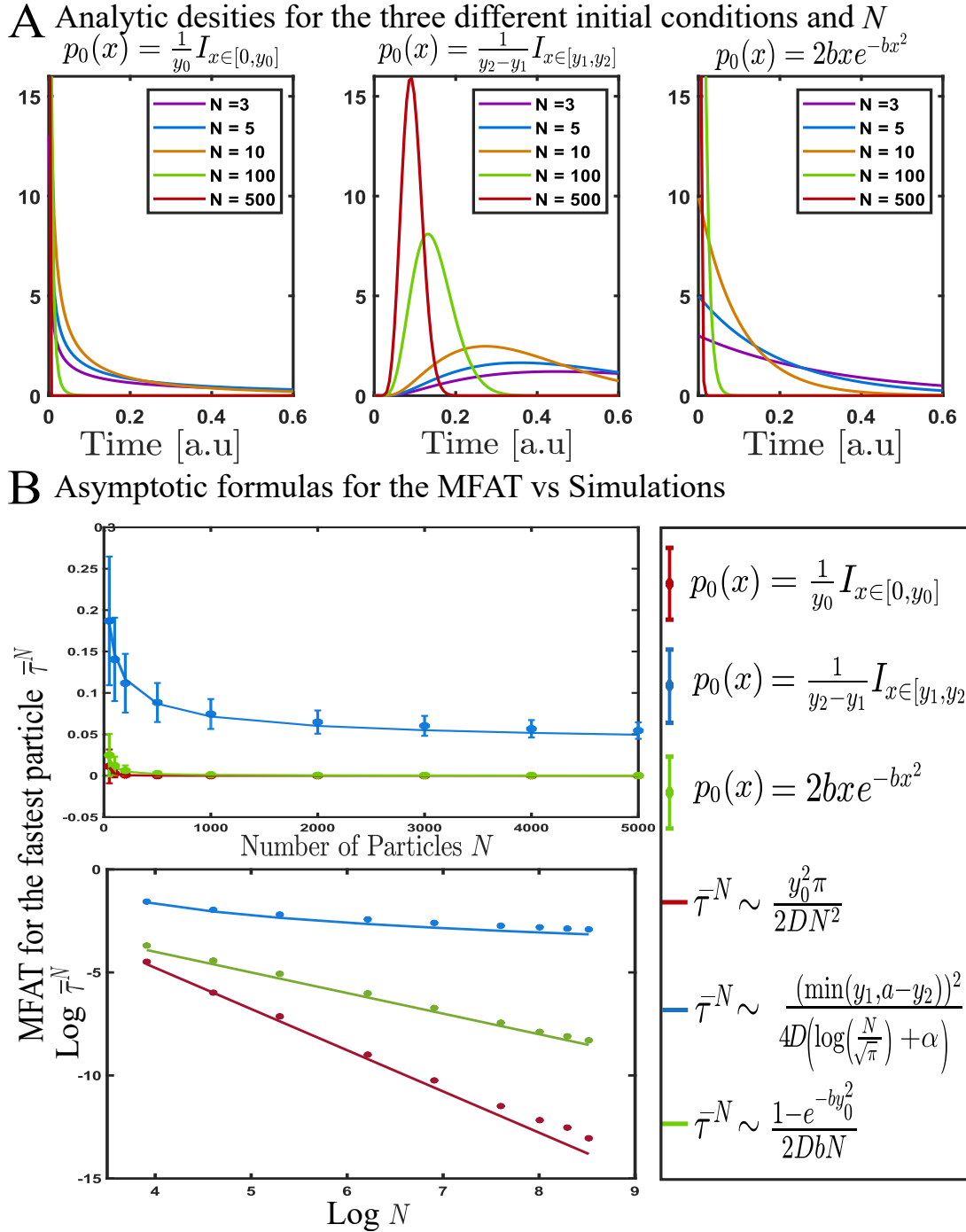


Figure 8: **Mean fastest arrival time vs the number of particles N .** **A.** Different density functions for the arrival times with total number of particles $N = [3, 5, 10, 100, 500]$ and the three initial distributions. **B.** MFAT vs N comparing stochastic simulations (colored disks) and the asymptotic formulas (continuous lines). The asymptotic expression for the MFAT when the particles are initially uniformly distributed in $[y_1, y_2]$ (blue curve given by (1.22)) is of the form $\frac{y_1^2 \pi}{4D \left(\log\left(\frac{N}{\sqrt{\pi}}\right) + \alpha \right)}$ (84) when $y_1 \ll a - y_2$. An optimal fit gives $\alpha = -2.099$. Parameters of the simulations are described in Fig. 7 with 1000 runs.

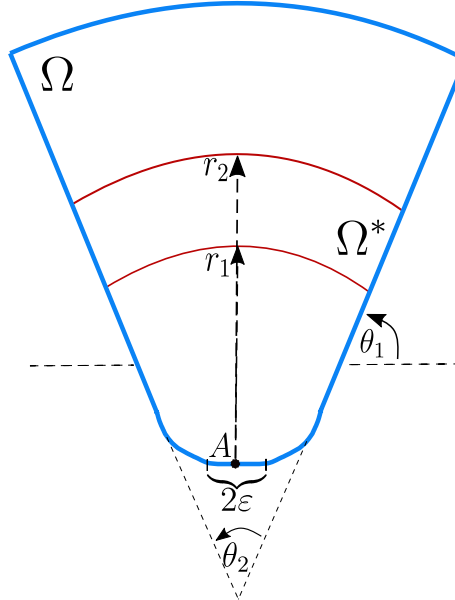


Figure 9: **Schematic of the two-dimensional domain to study the MFAT to a small arc.** The bounded domain Ω is delimited by the blue curve. The initial distribution of the Brownian particles is given by $p(x, 0) = \frac{1}{A(\Omega^*)} \mathbb{I}_{\{x \in \Omega^*\}}$, where the region $\Omega^* = \{B_{r_2}(\mathbf{A}) \setminus B_{r_1}(\mathbf{A}) : \theta_1 \leq \theta \leq \theta_1 + \theta_2\}$ is delimited by the red curves.

The proof for these propositions can be found in page 65. We can rewrite the last formula as

$$\bar{\tau}^N \sim \frac{C_\Omega}{N^{\frac{2}{\alpha+2}}}, \quad (102)$$

where

$$C_\Omega = \frac{1}{4Db} \Gamma\left(\frac{\alpha+4}{\alpha+2}\right) \left(\frac{8 \ln\left(\frac{1}{\varepsilon}\right) \left(\Gamma\left(\frac{\alpha+2}{2}\right) - \Gamma\left(\frac{\alpha+2}{2}, bR^2\right)\right)}{\sqrt{2\pi} \Gamma\left(\frac{\alpha}{2}\right)} \right)^{\frac{2}{\alpha+2}}. \quad (103)$$

Result section 1.4.1: Effect of a constant drift on the fastest arrival

Proposition 0.3. *Considering the constant drift component $\mathbf{b}(x) = a$ for the diffusion equation, the MFAT for N particles in the non-negative line starting their motion at position $x = y$ and escaping at the origin is given by the formula*

$$\bar{\tau}^N \sim \frac{y^2}{4D \ln\left(N \frac{(1+\exp\{\frac{ay}{D}\})}{2\sqrt{\pi}}\right)} \text{ when } N \text{ is large.} \quad (104)$$

(Proof in page 67.)

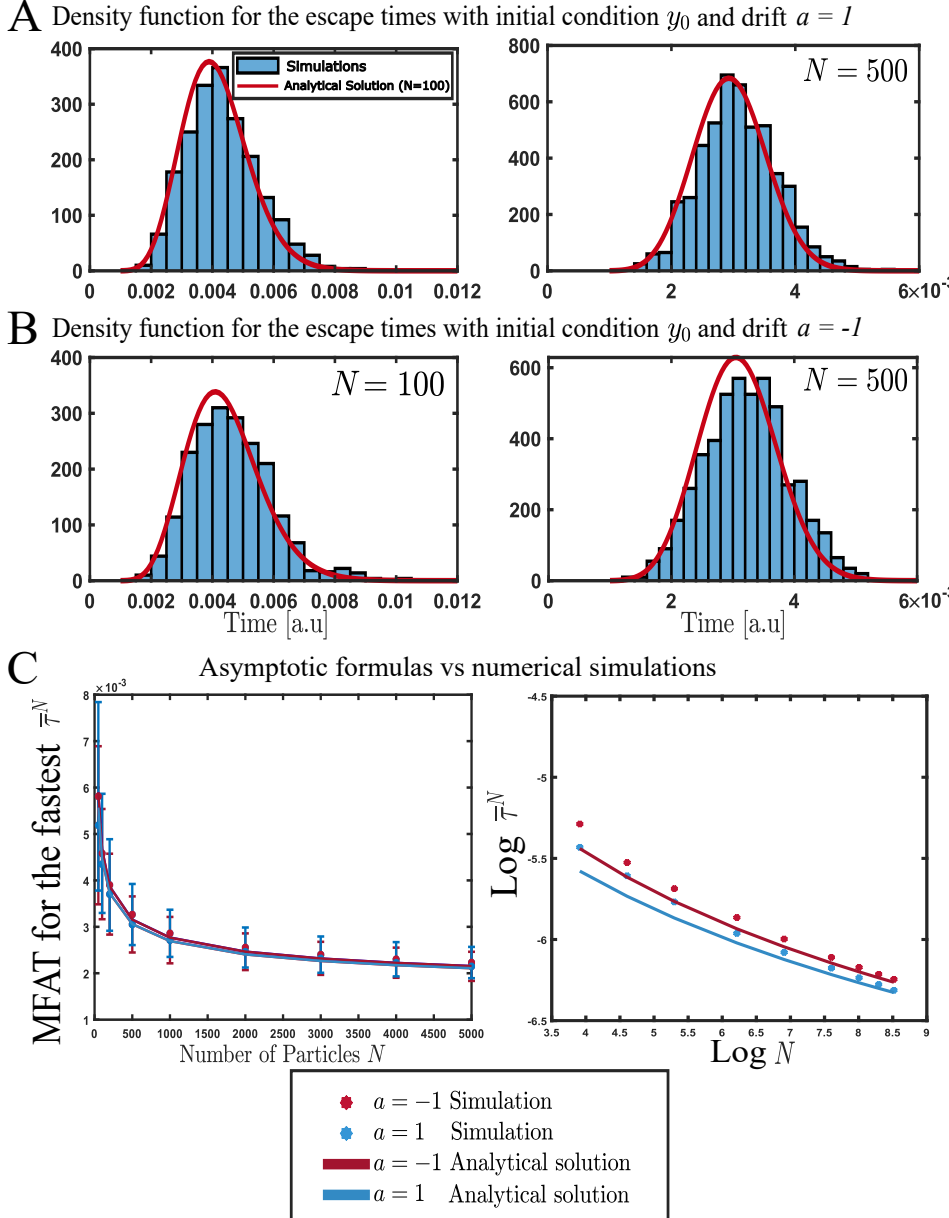


Figure 10: **Mean fastest arrival time vs the number of particles N with a drift.** **A.** Distribution of the arrival time $\bar{\tau}^N$: analytical represented by equation (1.44) (in red) vs stochastic simulations (blue histogram) for particles started at $y_0 = 0.25$ and a drift $a = 1$ for $N = 100$ (left) and $N = 500$ (right) with 1000 runs. **B.** Distribution of the arrival time $\bar{\tau}^N$: analytical expression (1.44) (in red) vs stochastic simulations (blue histogram) with drift $a = -1$. **C.** MFAT vs N obtained from stochastic simulations (colored disks) and the asymptotic formula (1.46) (continuous lines) with $y_0 = 0.25$ and 1000 runs.

Results section 2.3: Extreme escape versus killing with a finite number of delta-Dirac isolated points. We considered here the domain as the non-negative real line $\Omega = \mathbb{R}_+$ and we added to the diffusivity dynamic the elimination of particles at m isolated points $x_i \in \Omega$, with a total killing weight $V = \sum_{i=1}^m V_i$. The killing measure is thus given by

$$k(x) = \sum_{i=1}^m V_i \delta(x - x_i).$$

We denote the Laplace transform of the solution as $\hat{p}(x, q) = \mathcal{L}_q [p(x, t)]$ and the random variable denoting the final amount of survival particles is $n \in [0, N]$.

Proposition 0.4. *For N Brownian particles moving in the non-negative real line that contains m sink killing points located at position $x = x_i$ with a killing weight V_i , the conditional MFPT for escaping at the origin when at least one particle escapes is given by*

$$\mathbb{E}[\tau^e(N) | n \geq 1] \sim \frac{y^2}{4D \ln\left(\frac{N}{\sqrt{\pi}}\right)}, \quad (105)$$

when N is large. (Proof in pages 80 - 83.)

Corollary 0.1. *For one only killing point x_1 between the origin and the initial point, the conditional MFPT is given by*

$$\mathbb{E}[\tau^e(N) | n \geq 1] \sim \frac{y^2}{4D \left[\ln\left(\frac{N}{\sqrt{\pi}}\right) \right]}, \quad (106)$$

when at least one particle escapes and when there is a large number k of surviving particles, we obtain the formula

$$\mathbb{E}[\tau^e(N) | n = k] \sim \frac{y^2}{4D \left[\ln\left(\frac{k}{P_e \sqrt{\pi}}\right) \right]}. \quad (107)$$

(Proof in pages 84 - 86.)

Results section 2.4.1: Stochastic simulations of the fastest survival particles.

We performed the stochastic simulations to verify the formulas above by simulating the case where all stochastic particles survived, thus $n = N$. The simulations results for the distribution of the arrival times were shown in Fig. 11A and the MFPT was plotted in Fig. 11B and C in order to show the comparison with the asymptotic formula and the importance of a parameter β to correct the length of the trajectory made for the first escaping particle. When instead, the initial number of particles is fixed, the decay law is logarithmic with a fitting parameter α that corrects the number of killed particles as shown in the Fig. 12B.

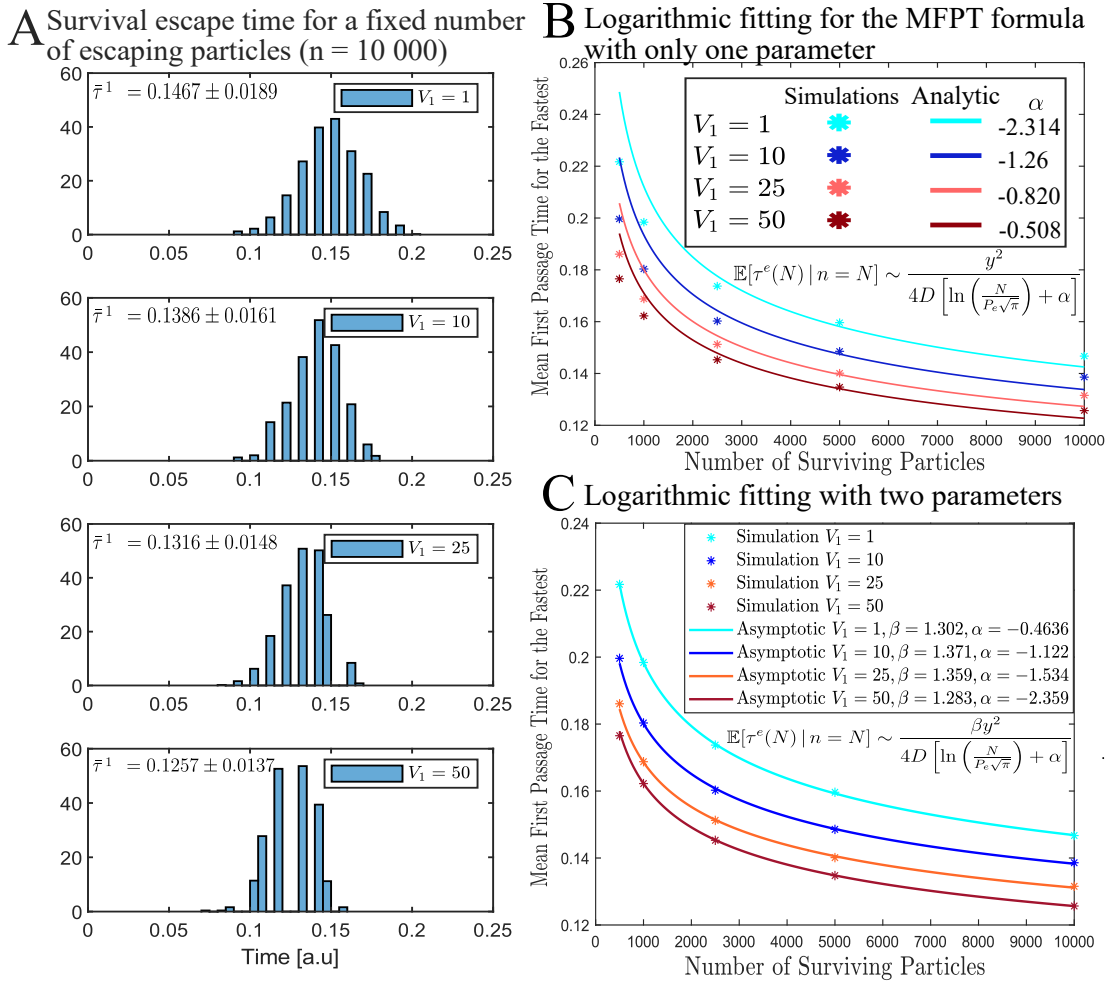


Figure 11: **Influence of the killing rate on the conditional mean escape time for the fastest particle.** **A.** Stochastic simulations for the escape time distribution of the fastest particle when particles start at $y = 2$ with a killing point in $x_1 = 1$ for $n = 10000$ and 1000 runs. **B.** MFPT vs n obtained from stochastic simulations (colored disks) and the asymptotic formula (2.29) (continuous lines) with an optimal fitting for the parameter α . **C.** MFPT vs n obtained from stochastic simulations (colored disks) and the asymptotic formula (2.29) (continuous lines) with an optimal fitting for the parameters α and β .

The proof of the following two propositions were moved to the appendix section 2.6.

Proposition 0.5. *For N Brownian particles in the non-negative real line that can escape at the origin and can be degraded everywhere in the domain at a constant killing rate V_0 the conditional MFPT when at least one particle escapes is given by*

$$\mathbb{E}[\tau^e(N) | n \geq 1] \sim \frac{y^2}{4D \ln \left(\frac{N \cosh \left(\sqrt{\frac{V_0}{D}} y \right)}{\sqrt{\pi}} \right)}. \quad (108)$$

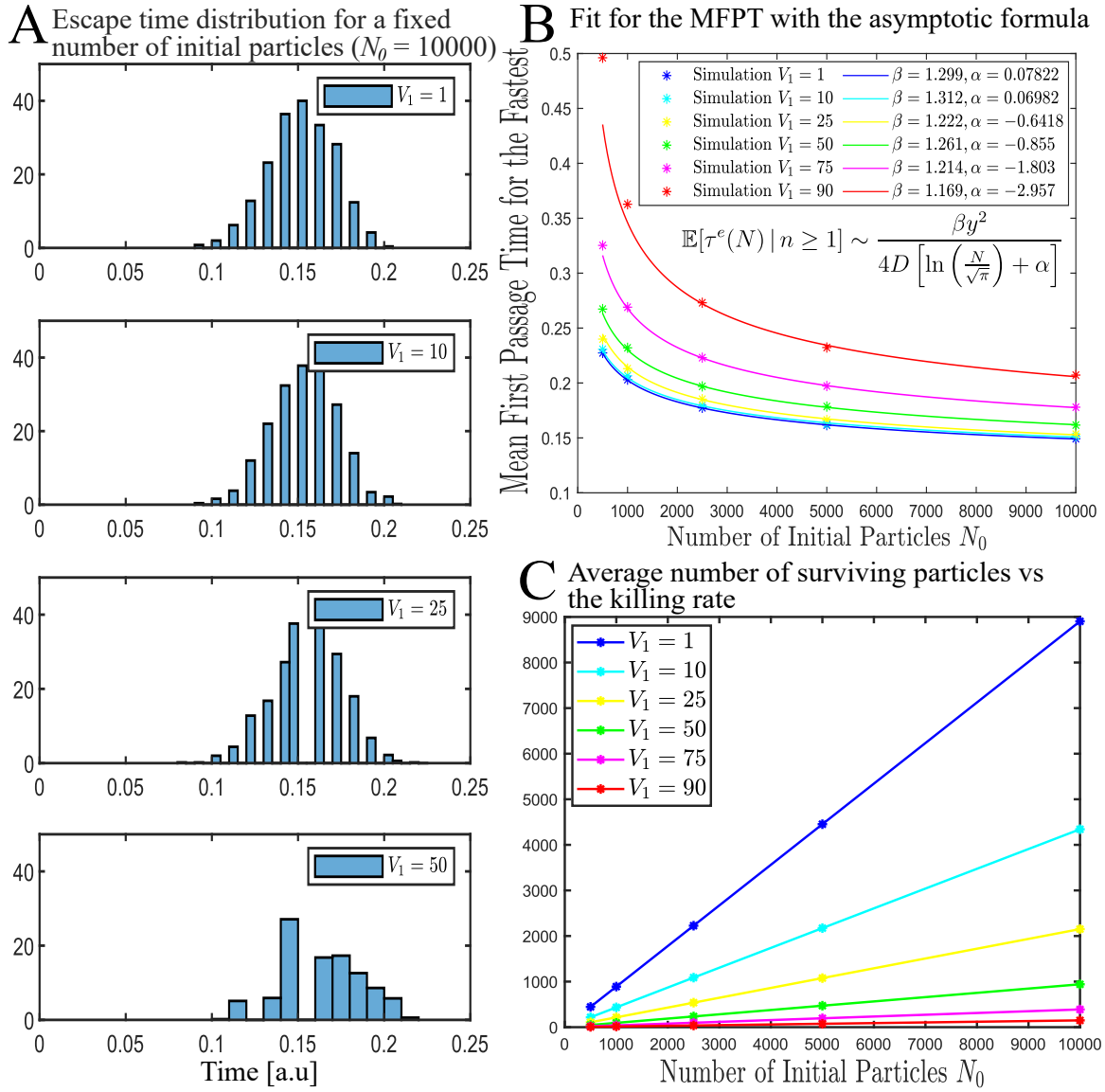


Figure 12: **Influence of the killing rate on the escape time for a large number N_0 of initial particles.** **A.** Stochastic simulations for the escape time distribution of the fastest particles starting at $y = 2$ with a killing point at $x_1 = 1$ for $N_0 = 10000$ and 1000 runs. **B.** Fit for the MFPT obtained from stochastic simulations (colored disks) and the asymptotic formula (2.25) (continuous lines). **C.** Influence of the killing weight V_1 in the number of surviving particles.

The MFPT when exactly k particles escape is given by

$$\mathbb{E}[\tau^e(N) | n = k] \sim \frac{y^2}{4D \left[\ln \left(\frac{k \left(e^{-y} \sqrt{\frac{V_0}{D}} + e^y \sqrt{\frac{V_0}{D}} \right)}{2e^{-y} \sqrt{\frac{V_0}{D}} \sqrt{\pi}} \right) \right]} \quad (109)$$

Proposition 0.6. For N Brownian particles in the non-negative real line that can escape at the origin and can be degraded everywhere in the interval $[0, L]$ at a constant killing rate V , with $y > L$,

the conditional MFPT when at least one particle escapes is given by

$$\mathbb{E}[\tau^e(N) | n \geq 1] \sim \frac{y^2}{4D \ln\left(\frac{N}{\sqrt{\pi}}\right)}, \quad (110)$$

and when exactly k particles escape is given by

$$\mathbb{E}[\tau^e(N) | n = k] \sim \frac{y^2}{4D \left[\ln\left(\frac{k \cosh\left(\sqrt{\frac{V}{D}}L\right)}{\sqrt{\pi}}\right) \right]}. \quad (111)$$

If instead, the particles start inside the killing interval ($y < L$), the conditional MFPT when at least one particle escapes is given by

$$\mathbb{E}[\tau^e(N) | n \geq 1] \sim \frac{y^2}{4D \ln\left(\frac{N \cosh\left(\sqrt{\frac{V}{D}}y\right)}{\sqrt{\pi}}\right)}, \quad (112)$$

and when exactly k particles survive is given by

$$\mathbb{E}[\tau^e(N) | n = k] \sim \frac{y^2}{4D \left[\ln\left(\frac{k \cosh\left(\sqrt{\frac{V}{D}}L\right)}{e^{-y} \sqrt{\frac{V}{D}} \sqrt{\pi}}\right) \right]}. \quad (113)$$

Results section 2.4.2: Time scale of fast calcium signaling at synapse.

In this section we apply the previous computations for the first arrival in calcium signaling, and we computed the time scale for the first killing event when we consider the killing as a binding process. This means that in our model we consider that the particles are not really eliminated but instead they bind with another molecule, removing this particle from our population of free particles.

Conclusion 1. *The time scale for calcium-induced calcium release CICR, known as the time for two free calcium ions to arrive at the Ryanodine receptor, when a degradation process such as buffering or SERCA pumps effects are considered at position $x = x_1$ with rate V_1 for N diffusive calcium ions inside a 1D approximated dendritic spine (as in Fig. 13) is given by*

$$\bar{\tau}_{CICR} \sim 2\mathbb{E}[\tau^k(N) | n = k] \sim \frac{2L^2}{4D \left[\ln\left(\frac{k}{P_e \sqrt{\pi}}\right) \right]}, \quad (114)$$

when the remainder amount of ions k is large.

Conclusion 2. *The time for the activation of a CaMKII molecule (process schematically represented in Fig. 14A) positioned at $x = x_1$ with a bounding rate V_1 that can be activated by CaM-Ca₂ complex is given by*

$$\bar{\tau}_{CaMKII} = \mathbb{E}[\tau^k(N) | n < N] \sim \frac{(y - x_1)^2}{4D \left[\ln\left(\frac{p^2 N V_1 (y - x_1)}{4D \sqrt{\pi}}\right) \right]}, \quad (115)$$

where p is the binding rate of calcium ions to the CaM molecule. We have assumed that the CaM molecules are very close to the initial source of calcium ions, and the binding between calcium ions and CaM is very fast.

Approximating spine geometry by an interval

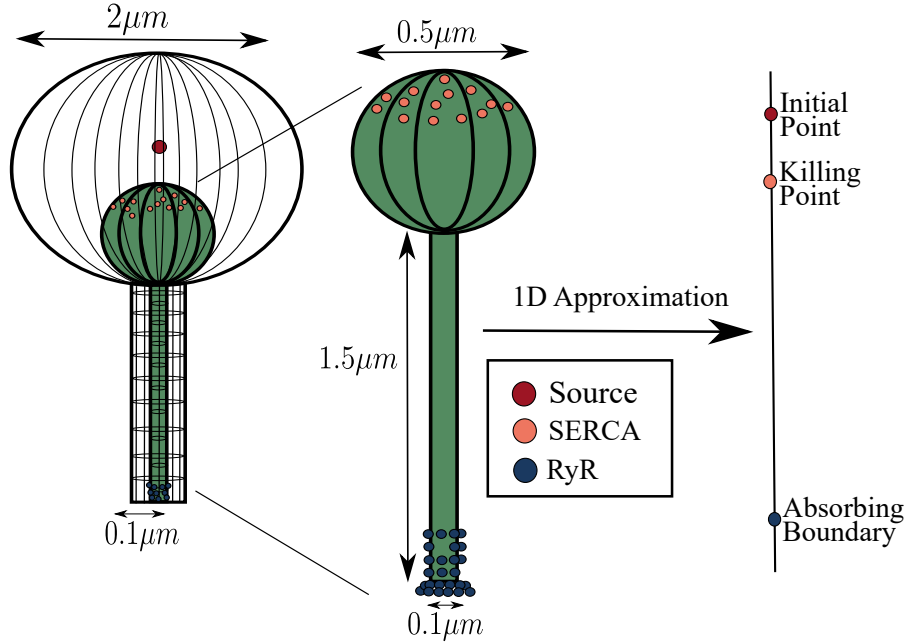


Figure 13: **Schematic representation of a dendritic spine doted with a spine apparatus and its simplification in a 1D domain.** The spine with a spine apparatus is simplified as a 1D interval with killing point $x_1 = 2\mu m$, initial point at $y = 2.5\mu m$, absorbing point $x = 0\mu m$.

Result section 3.3.1: Fully absorbing boundary condition

We considered then the effect of a uniform killing measure in a 2D disk centered at the origin with radius R , where particles start their motion at the origin and can escape everywhere in the boundary of the disk.

Proposition 0.7. *For N Brownian particles starting their motion at the origin inside the 2D disk $B_R(0)$ and escaping everywhere in $\partial B_R(0)$ the conditional MFPT when k particles survive for a uniform killing measure is given by*

$$\mathbb{E}[\tau^e(N) \mid n = k] \sim \frac{R^2}{4D \ln \left(\frac{2k}{P_e(V, D, R)} \right)}, \quad (116)$$

where V is the killing weight, D is the diffusion coefficient and the escape probability P_e is given by

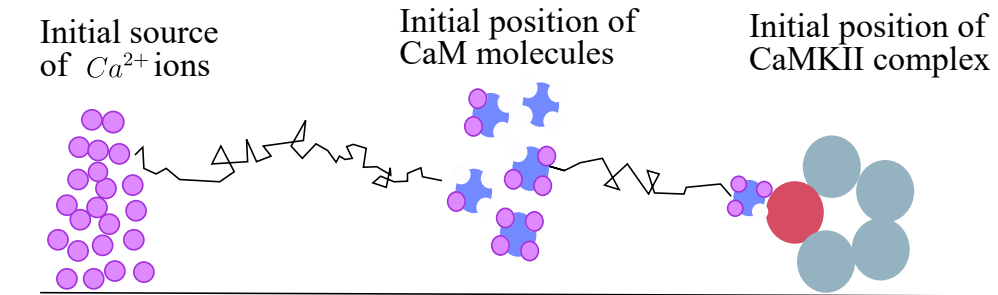
$$P_e(V, D, R) = \sqrt{\frac{V}{D}} R \left(K_1 \left(\sqrt{\frac{V}{D}} R \right) + \frac{K_0 \left(\sqrt{\frac{V}{D}} R \right)}{I_0 \left(\sqrt{\frac{V}{D}} R \right)} I_1 \left(\sqrt{\frac{V}{D}} R \right) \right). \quad (117)$$

Here $I_0(x)$ and $K_0(x)$ are the modified Bessel functions of the first and second kind and order zero. (Proof in pages 104 - 106.)

Result section 3.3.2: Narrow absorbing boundary condition

We considered as well the case where the absorbing boundary is a narrow part of $\partial B_R(0)$.

A Activation of CaMKII molecules leading to phosphorylation



B Role of CaMCa in the persistent activation of CaMKII

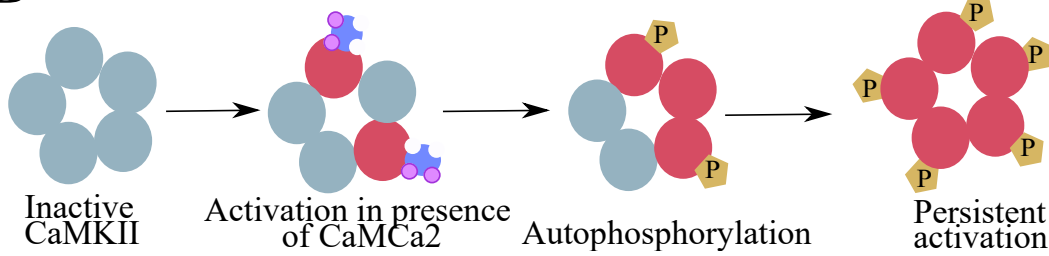


Figure 14: **Schematic representation for the long-term activation of a CaMKII complex in a 1D domain.** **A.** The calcium ions enters in the domain and activates the CaM molecules. These last ones can locally activate the CaMKII complex. **B.** When the CaMKII complex is locally activated by CaM in presence of calcium ions, the CaMKII molecule itself phosphorylates first in a neighborhood of the locally activated area, and after a few milliseconds it is fully phosphorylated. This is known as the persistent activation, which has a long-term effect in the molecule and it is associated with learning and memory loss.

Proposition 0.8. *When now the absorbing boundary is the arc of length 2ε centered at point $x = (R, 0)$ the conditional MFPT is given by*

$$\mathbb{E}[\tau^e(N) \mid n = k] \sim \frac{R^2}{4D \ln \left(\frac{k \ln \left(\frac{1}{\sqrt{\frac{V}{D}} \varepsilon} \right)}{2 \ln \left(\frac{1}{\varepsilon} \right) K_0 \left(\sqrt{\frac{V}{D}} R \right)} \right)}, \quad (118)$$

where the escape probability $P_e(V, D, R, \varepsilon)$ is given by

$$P_e(V, D, R, \varepsilon) = \int_0^\infty J(s) ds \approx \frac{K_0 \left(\sqrt{\frac{V}{D}} R \right)}{\ln \left(\frac{1}{\sqrt{\frac{V}{D}} \varepsilon} \right)}. \quad (119)$$

(Proof in pages 108 - 110.)

Result section 3.5: Asymptotic formulas vs simulations

We considered in addition a killing area well spaced from the origin and from the absorbing boundary. We performed simulations for this case and we fitted the simulations results with the logarithmic

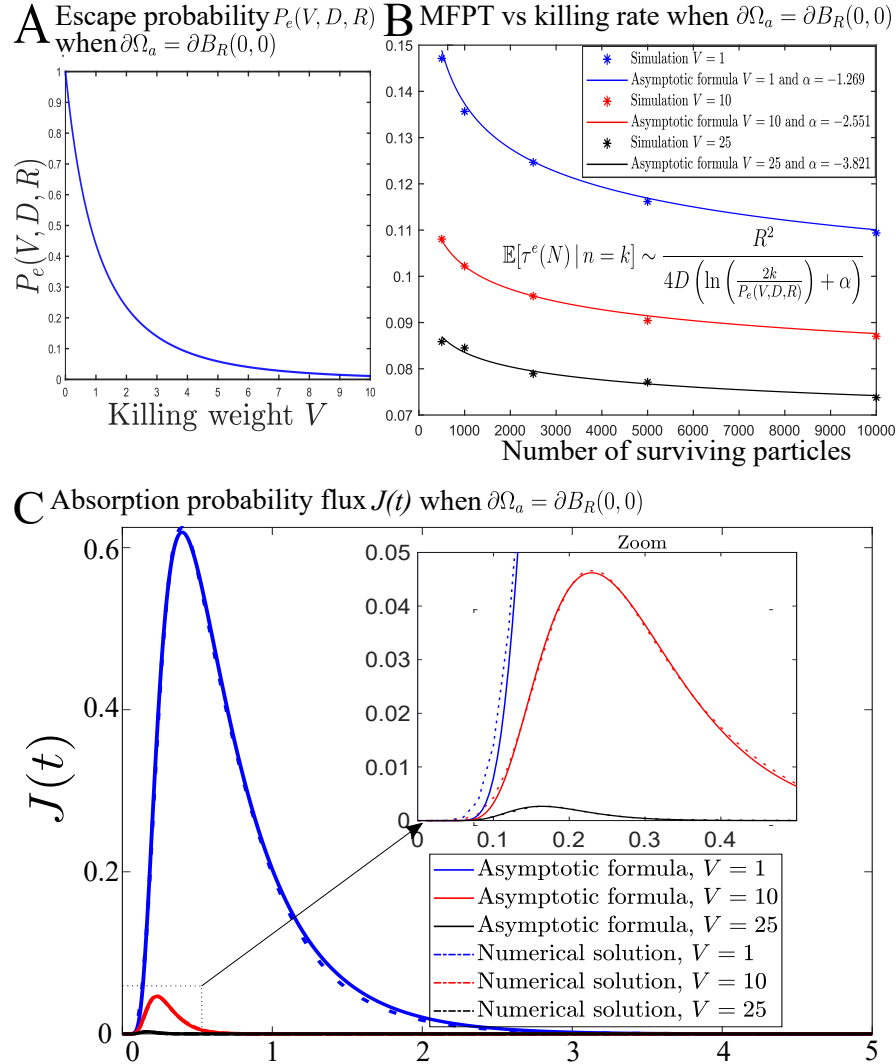


Figure 15: **Uniform killing with a fully absorbing boundary on a 2D-disk domain.** **A.** Decay of the escape probability $P_e(V, D, R)$, given by formula (3.19), as a function of the killing weight V for $D = 1$ and $R = 2$. **B.** MFPT vs k obtained from stochastic simulations (colored disks) and the asymptotic formula (3.27) (continuous lines) with $D = 1$ and $\mathbf{y} = (0, 0)$ for 1000 runs. **C.** Shrinkage of the absorption probability flux (3.23) for different values of the killing weight V .

decay indicated in Fig. 17.

We fixed then a large killing rate and we varied the position of this killing area as in Fig. 18A to obtain the distribution path of the fastest Fig. 18C.

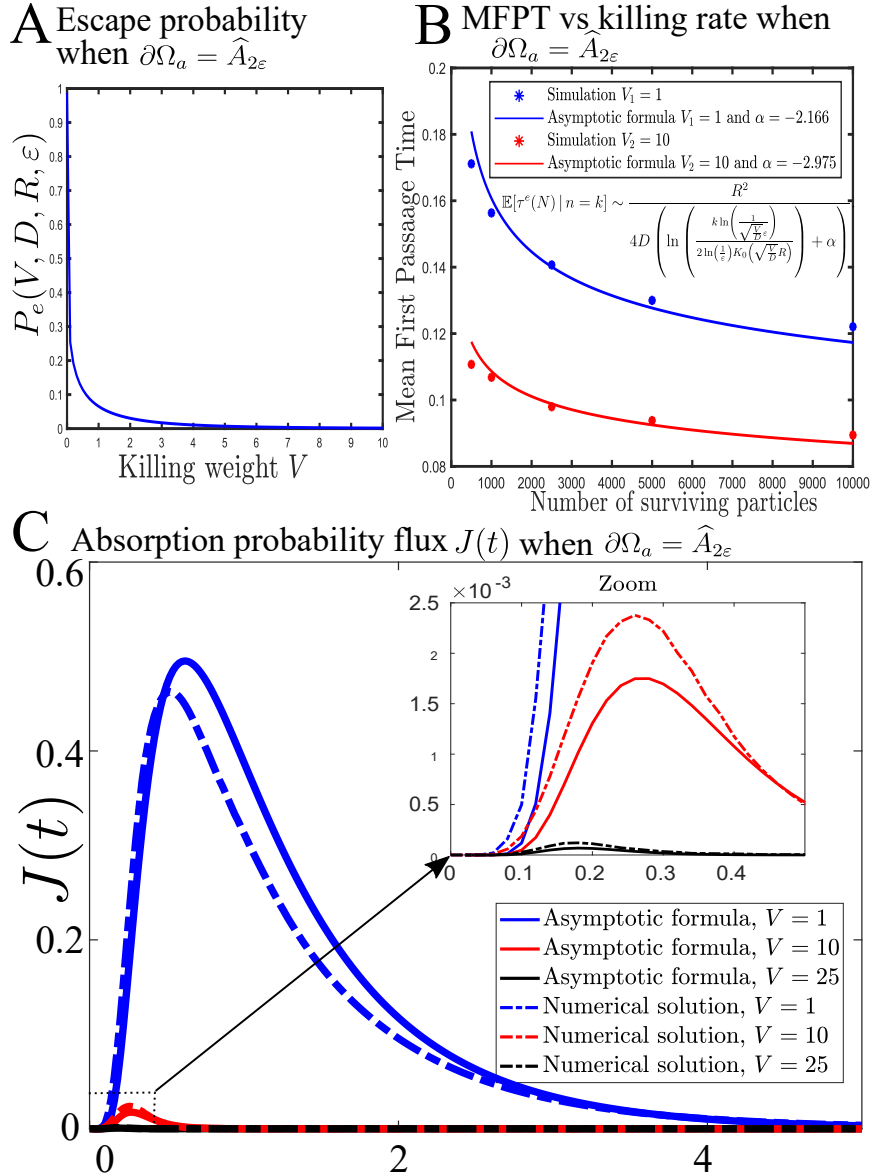


Figure 16: **Uniform killing with a narrow absorbing boundary on a 2D disk domain.** **A.** Decay of the escape probability $P_e(V, D, R, \varepsilon)$ as a function of the killing weight V for $D = 1$, $R = 2$ and $\varepsilon = 0.175$ which correspond with 10° arc of the boundary. **B.** MFPT vs number of survival particles $n = k$ obtained from stochastic simulations (colored disks) and the asymptotic formula (3.45) (continuous lines) with $D = 1$, $R = 2$, $\mathbf{y} = (0, 0)$, $\varepsilon = 0.175$ and 1000 runs. **C.** Absorption probability flux (analytical formula (3.40)) shrinks when the killing weight V increases.

We varied as well the size of this killing area as in Fig. 19A to obtain the distribution path of the fastest particle, Fig. 19C. We remark from the previous two simulations that the fastest particles avoid the killing area when the killing rate is large.

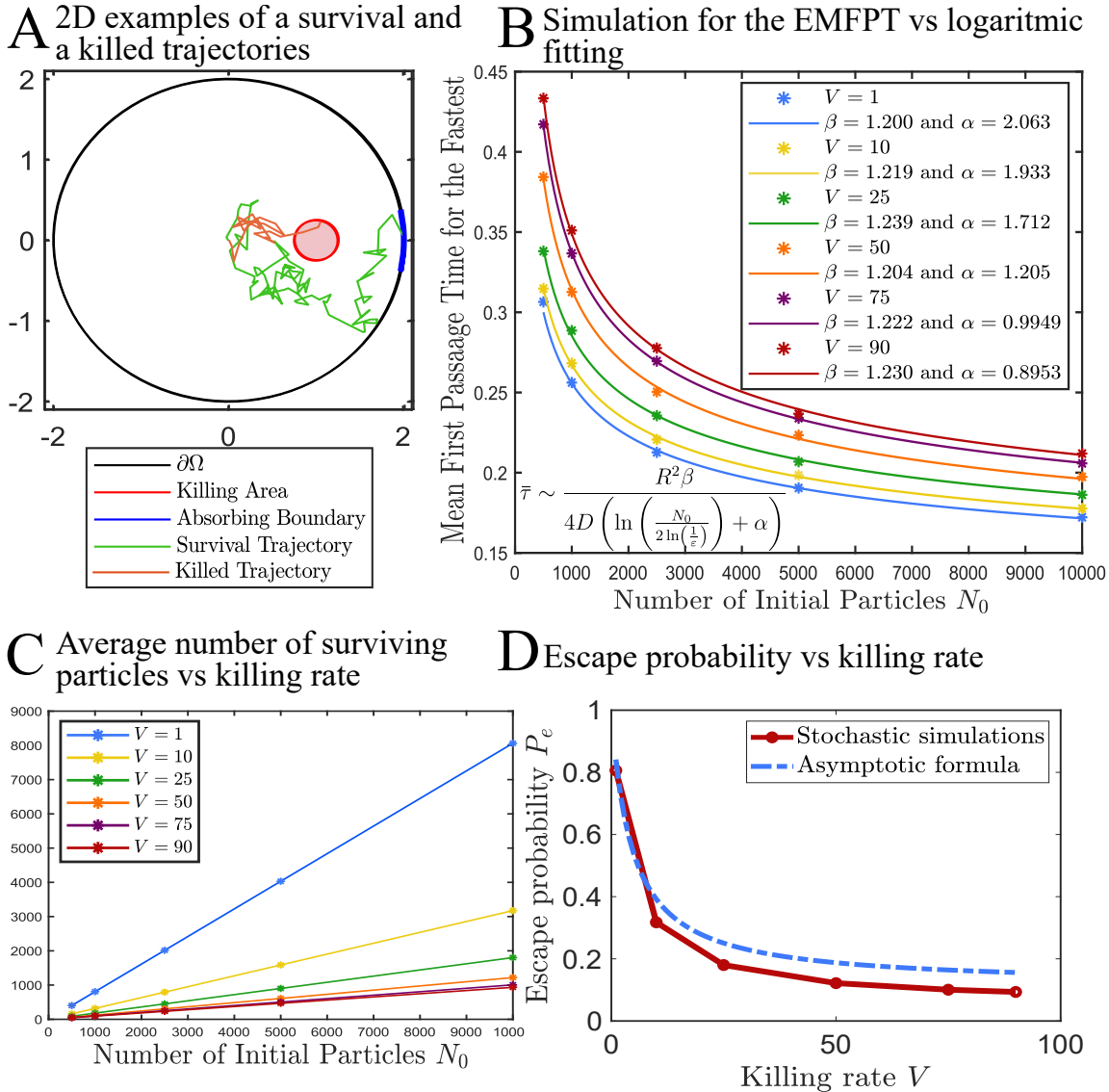


Figure 17: **Influence of the killing measure on the MFPT when the initial number of particle N_0 is large.** **A.** Two 2D examples of survival and killed particles for the problem in a disk. **B.** MFPT vs N_0 obtained from stochastic simulations (colored disks) and the fitting to the logarithmic decay (3.80) (continuous lines) for 1000 runs. **C.** Influence of the killing weight V on the number of surviving particles. **D.** Decay of the escape probability for different values of the killing weight V obtained from stochastic simulations (continuous line in red) and the asymptotic formula (3.78)(dashed lines in blue).

Proposition 0.9. *The optimal path for the fastest arriving particles can be obtained from the path representation for the Laplace integral of the conditional MFPT using the Freidlin-Wentzell large deviation principle for Brownian particles, which results in the solution of the minimization problem*

$$\min_{\substack{\phi_0=\mathbf{x}_0 \\ \phi_\tau \in \partial\Omega_a}} \left\{ \frac{1}{4D\epsilon} \int_0^\tau |\dot{\phi}_s|^2 ds + \int_0^\tau k(\phi_s) ds \right\}, \quad (120)$$

which satisfies by Euler-Lagrange's principle the ordinary differential equation

$$-\ddot{\phi}_s + 2D\epsilon \nabla k(\phi_s) = 0. \quad (121)$$

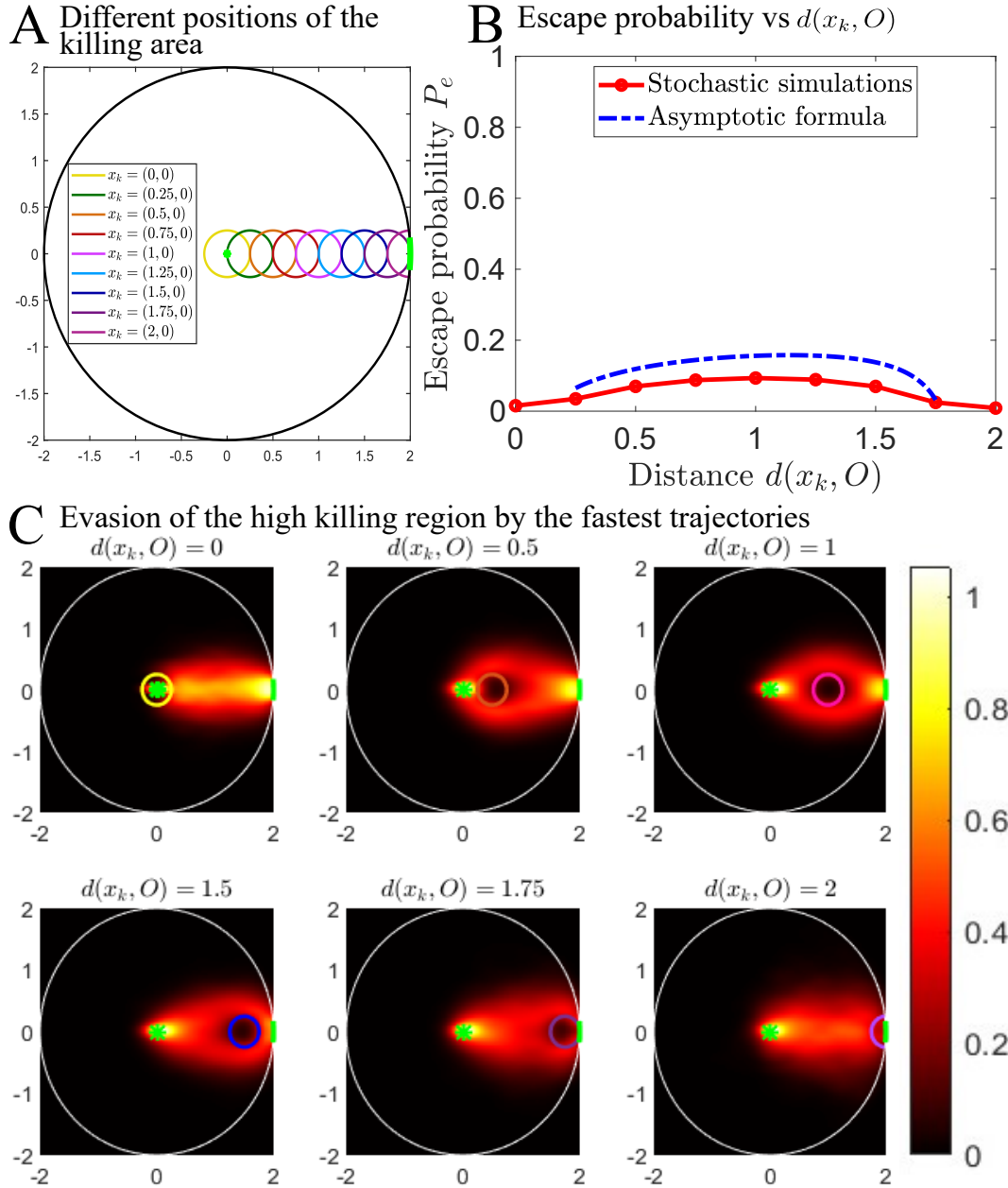


Figure 18: **Influence of the killing area position on the escape probability and fastest trajectory for $V = 90$, $D = 1$, $dt = 0.01$, $R = 2$, $r = 0.25$, $\mathbf{A} = (2, 0)$, $\varepsilon = 0.175$ and 1000 runs.** **A.** Schematic representation of different killing areas first located at the center and moving toward the narrow exit window. The initial position of the particles remains at the center if the external disk. **B.** Escape probability versus $d(x_k, O)$. **C.** Spatial distribution of the fastest trajectories for various locations of killing region.

with $\phi(0) = (0, 0)$ and $\phi(\tau) \in \partial\Omega_a$. (Derivation in pages 119 - 122.)

When the killing term is constant over the domain, we concluded that the fastest trajectories always move in the straight line between the initial point and the absorbing boundary, as shown in Fig. 20.

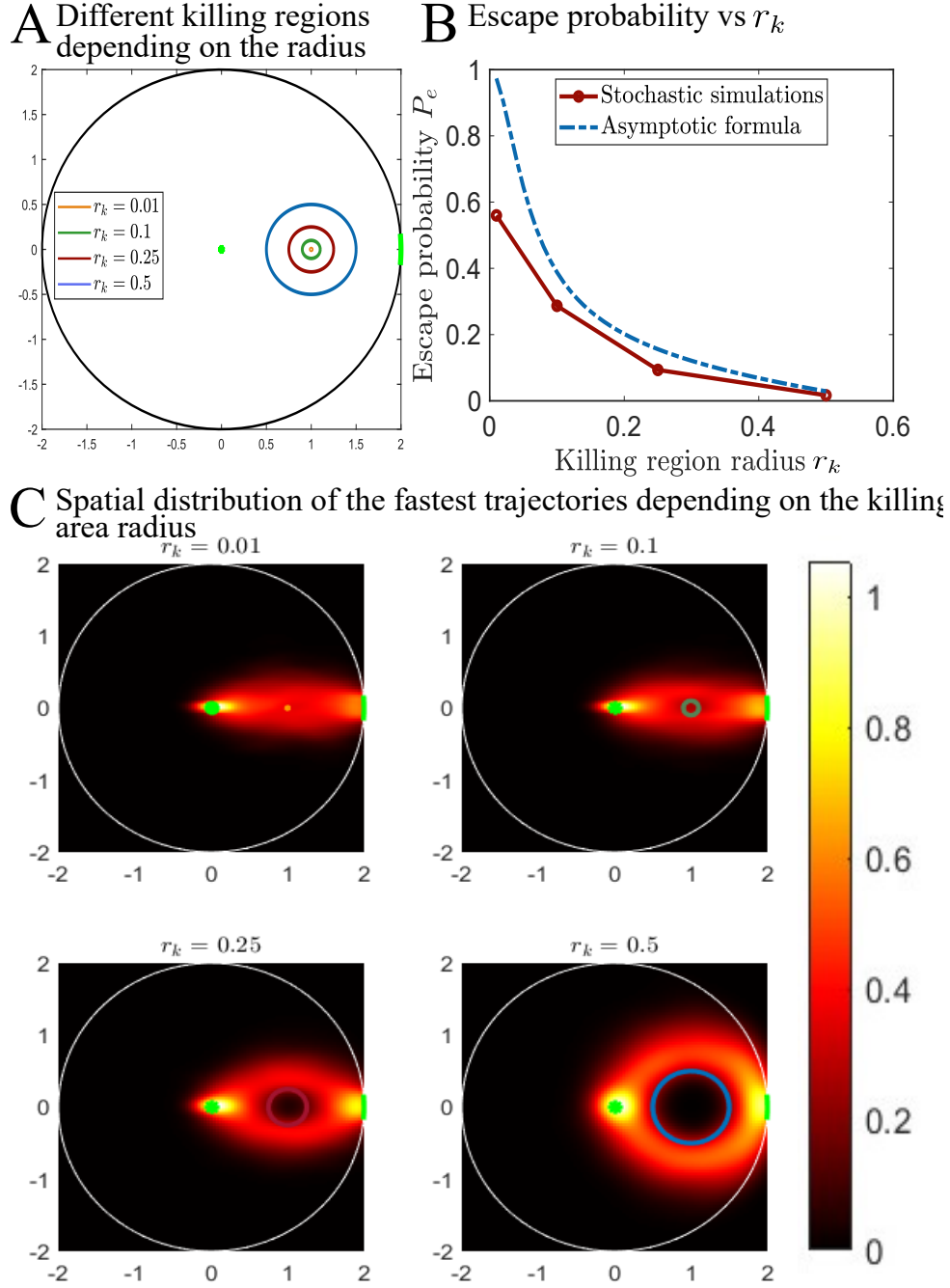


Figure 19: **Influence of the killing area radius on the escape probability and space distribution.** **A.** Schematic representation of different killing areas depending on the value of the radius with a fixed center at $\mathbf{x}_k = (1, 0)^T$. **B.** Effect of the killing radius on the escape probability for $V = 90$. **C.** Spatial distribution for the fastest trajectories for different values of the killing area radius, $D = 1$, $\varepsilon = 0.175$, $R = 2$ and $k = 1000$ runs.

We finally studied the case where the killing measure overlaps the absorbing boundary, leading to the spreading of the fastest trajectories (Fig. 22C) and a parabolic distribution of exit points (Fig. 23B).

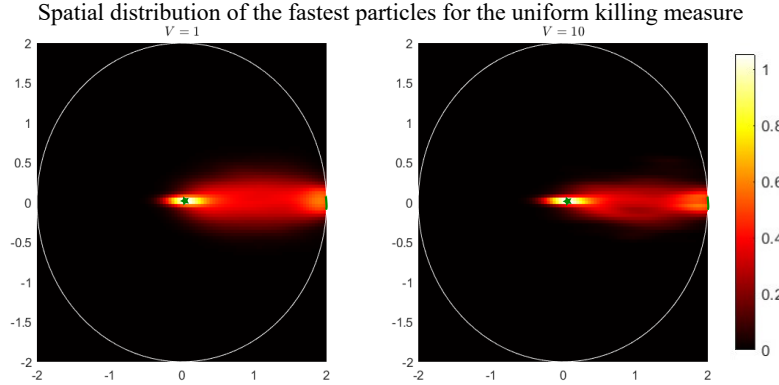
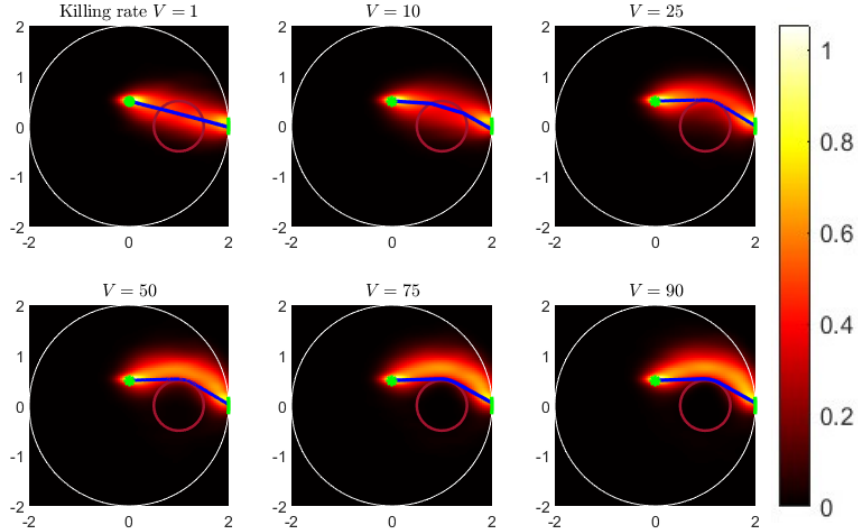


Figure 20: **Straight path for a killing measure uniform over the domain.** Spatial distribution for the fastest trajectories for different values of the killing rate V , with $D = 1$, $\varepsilon = 0.175$, $R = 2$, $\epsilon = 1$ and 1000 runs. The initial point of the particles is marked with a green start while the small absorbing boundary is the green arc around $A = (2, 0)^T$.

A Spatial distribution of the fastest particles when the killing rate increases vs optimal trajectories



B Distribution of the first arrival time when the killing rate increases

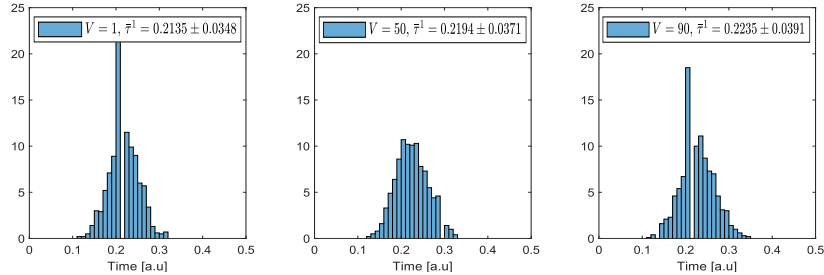


Figure 21: **Influence of the killing weight on the optimal path of the fastest particles.** **A** Deviation of the most likely path (see page 23) when the killing weight V increases for $k = 1000$ runs and $N_0 = 10000$ initial particles. **B** The mean escape time increases as the fastest particles deviate their trajectory to the absorbing windows.

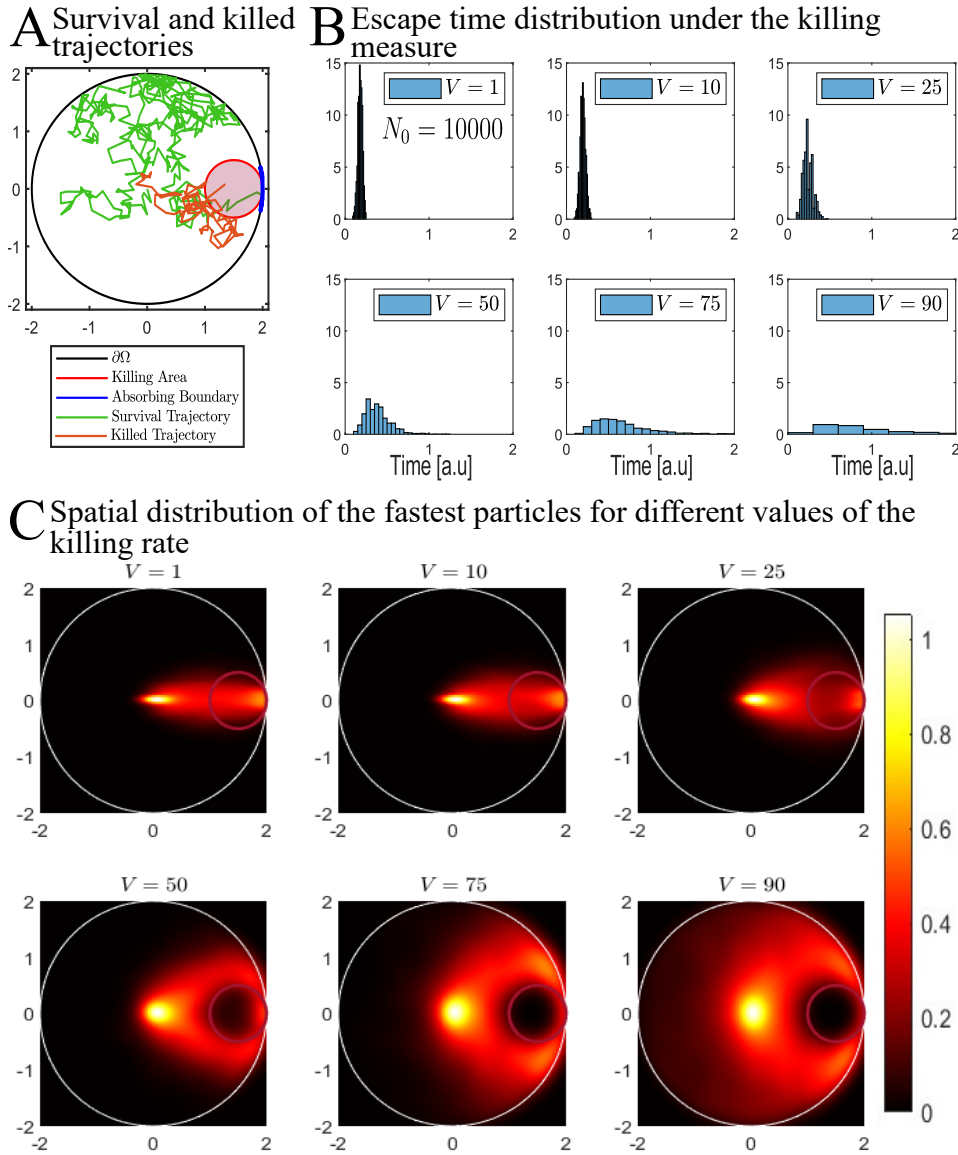


Figure 22: **Influence of the killing measure on the MFPT when the initial number of particles N_0 is large and the killing area overlaps locally with the absorbing boundary.** **A.** Two 2D examples of survival and killed particle in a disk with a tangent killing field. **B.** Escape time distribution of the fastest particle $\bar{\tau}^1$ when the killing increases in a disk tangent to the absorbing window. **C.** Effect of the killing measure on the spatial distribution of the fastest particle for considered $N_0 = 10000$ particles starting at the origin, $r_k = 0.5$, $x_k = (1.5, 0)^T$, $D = 1$, $R = 2$ and $k = 1000$ runs.

Part II: Asymptotic formulas for transport and synthesis of proteins

We devoted this part of the thesis to the computations of asymptotic formulas for the fastest arrival time of Brownian particles that can alternate between 2 states but escape only in one of them. We consider the 1D model in the non-negative real line where all particles start at position $x = y$ and escape at the boundary $x = 0$ in state 1. Here, we do not consider the elimination of particles, only switchings are possible. We applied this results to DNA transcription where transcription factors

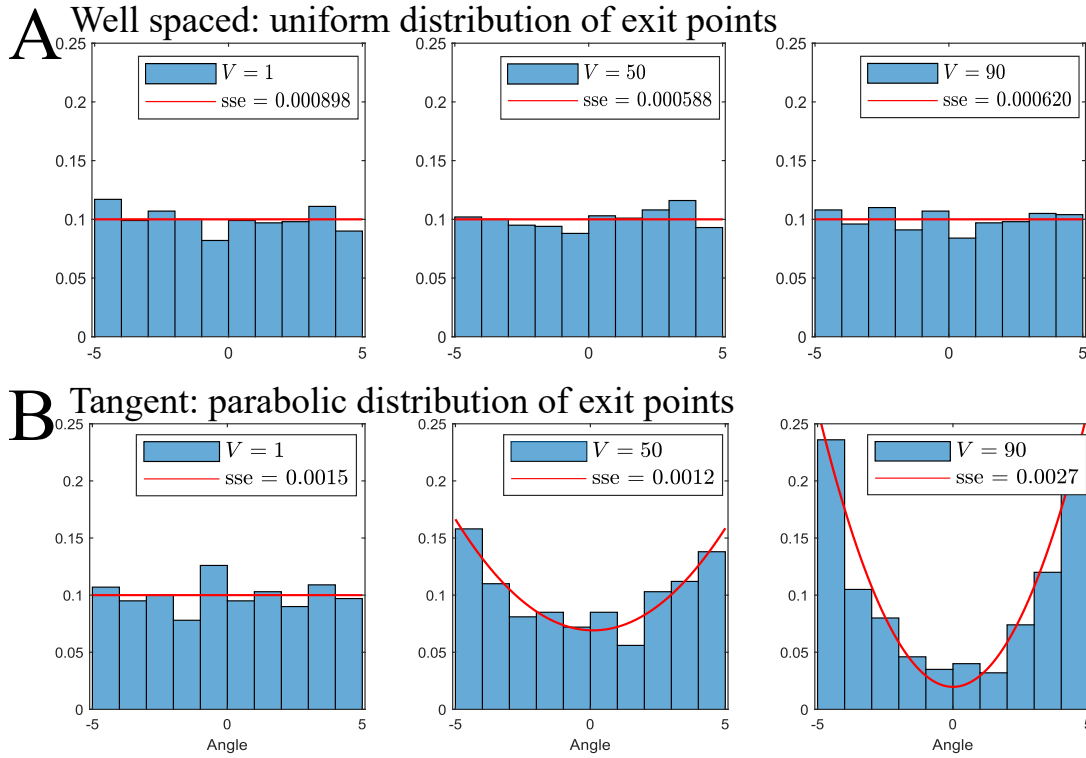


Figure 23: **Influence of the killing measure on the exit points of the boundary.** **A.** Uniform distribution of the exit points over the boundary when the killing area and the narrow escape windows are well separated for different values of the killing weight V . **B.** Parabolic effect of the killing measure in the distribution of the exit points over the absorbing window for different values of the killing weight V . Fitting with the parabolic function ($y = a(x - b)^2 + c$). First panel: $a = 0$, $b = 0$, $c = 0.1$. Second panel: $a = 0.003731$, $b = 0.1056$, $c = 0.06918$. Third panel: $a = 0.009735$, $b = -0.0006226$, $c = 0.01969$.

can alternate between active and idle inside the nucleus of the cell.

Results section 4.3: Explicit expressions for the MFAT when the Brownian particles start in state 1.

Proposition 0.10. *When particles start at position $x = y$ in state 1 and the diffusion coefficient associated to state 2 is $D_2 = 0$, the short time arrival distribution can be approximated by the distribution of the r.v. σ_s^N with density*

$$\begin{aligned} \Pr \{ \sigma_s^N \in [t + dt] \} &= -\frac{d}{dt} \left[\exp \left\{ -\frac{\sqrt{4D_1 t} N}{y \sqrt{\pi}} e^{-\frac{y^2}{4D_1 t}} \right\} \right] dt \\ &= \frac{N(\sqrt{4D_1 t})}{y \sqrt{\pi}} \exp \left\{ -\frac{y^2}{4D_1 t} \right\} \exp \left\{ -\frac{\sqrt{4D_1 t} N}{y \sqrt{\pi}} e^{-\frac{y^2}{4D_1 t}} \right\} \left[\frac{y^2}{4D_1 t^2} + \frac{1}{2t} \right] dt, \end{aligned} \quad (122)$$

leading to the asymptotic formula

$$\bar{\tau}^N \sim \frac{y^2}{4D_1 \ln \left(\frac{N}{\sqrt{\pi}} \right)}. \quad (123)$$

(Derivations from page 132 to 133.)

Proposition 0.11. When particles start in state 1 at position $x = y$ with $D_2 = 0$, the long time pdf for the first arrival is approximated by de density of the r.v. $\sigma_l^N(t)$

$$\begin{aligned} \Pr \left\{ \sigma_l^N \in [t, t + dt] \right\} &= -\frac{d}{dt} \left[\exp \left\{ -\frac{\sqrt{4D_1 t} N \mu^{\frac{3}{2}}}{y \theta^{\frac{3}{2}} \sqrt{\pi}} e^{-\frac{y^2 \theta}{4D_1 \mu t}} \right\} \right] dt \\ &= \frac{N \mu^{\frac{3}{2}} (\sqrt{4D_1 t})}{y \theta^{\frac{3}{2}} \sqrt{\pi}} \exp \left\{ -\frac{y^2 \theta}{4D_1 \mu t} \right\} \exp \left\{ -\frac{\sqrt{4D_1 t} N \mu^{\frac{3}{2}}}{y \theta^{\frac{3}{2}} \sqrt{\pi}} e^{-\frac{y^2 \theta}{4D_1 \mu t}} \right\} \left[\frac{y^2 \theta}{4D_1 \mu t^2} + \frac{1}{2t} \right] dt, \end{aligned} \quad (124)$$

where $\theta = \lambda + \mu$.

Conjecture 0.1. For a fixed N , the short asymptotic formulas are given for a specific regime depending on the Poissonian switching rates λ and μ that we generalize in the following formula

$$\bar{\tau}^S \rightarrow f \ll \bar{\tau}^{(N|I_0)} \ll \bar{\tau}^{(I_0|1)}, \quad (125)$$

where $\bar{\tau}^S \rightarrow f$ is the mean time to switch from the slower state to the fastest one, $\bar{\tau}^{(N|I_0)}$ is the asymptotic formula found through the Laplace method when particles start in state I_0 and $\bar{\tau}^{(I_0|1)}$ is the mean time to be in the state 1, where escape is possible, given the initial state.

Proposition 0.12. When particles start in state 1 where escape is possible with $D_1 > D_2$, the mean escape time is given by

$$\bar{\tau}^N \sim \frac{y^2}{4D_1 \ln \left(\frac{N}{\sqrt{\pi}} \right)}, \text{ when } \frac{1}{\mu} \ll \frac{y^2}{4D_1 \ln \left(\frac{N}{\sqrt{\pi}} \right)} \ll \frac{1}{\lambda} + \frac{1}{\mu}. \quad (126)$$

If instead, $D_2 > D_1$ the mean escape time is given by

$$\bar{\tau}^N \sim \frac{y^2}{4D_2 \ln \left(\frac{N \lambda \mu D_2}{2\sqrt{\pi}} \left(\frac{y^2}{4D_2} \right)^2 \right)}, \text{ when } \frac{1}{\lambda} \ll \frac{y^2}{4D_2 \ln \left(\frac{N \lambda \mu D_2}{2\sqrt{\pi}} \left(\frac{y^2}{4D_2} \right)^2 \right)} \ll \frac{1}{\lambda} + \frac{1}{\mu}. \quad (127)$$

See the Fig. 25 for a clear interpretation of these formulas. The derivations of results above were made from page 137 to 139.

Result section 4.3.3: Particles start in state 2.

Proposition 0.13. When particles start in state 2 with $D_1 > D_2$, the mean escape time formula is given by

$$\bar{\tau}^N \sim \frac{y^2}{4D_1 \ln \left(\frac{N}{\sqrt{\pi}} \mu \frac{y^2}{4D_1} \right)}, \text{ when } \frac{1}{\mu} \ll \frac{y^2}{4D_1 \ln \left(\frac{N}{\sqrt{\pi}} \mu \frac{y^2}{4D_1} \right)} \ll \frac{1}{\lambda}. \quad (128)$$

If instead, $D_2 > D_1$ the mean escape time is given by

$$\bar{\tau}^N \sim \frac{y^2}{4D_2 \ln \left(\frac{N}{\sqrt{\pi}} \mu \frac{y^2}{4D_2} \right)}, \text{ when } \frac{1}{\lambda} \ll \frac{y^2}{4D_2 \ln \left(\frac{N}{\sqrt{\pi}} \mu \frac{y^2}{4D_2} \right)} \ll \frac{1}{\mu}. \quad (129)$$

(Derivations from page 140 to 142.)

We summarized in Fig. 25 the strategy followed for the fastest particle under the short time regime. The results when the particles are initially uniformly and exponentially distributed are given in section 4.4 and 4.5 respectively.

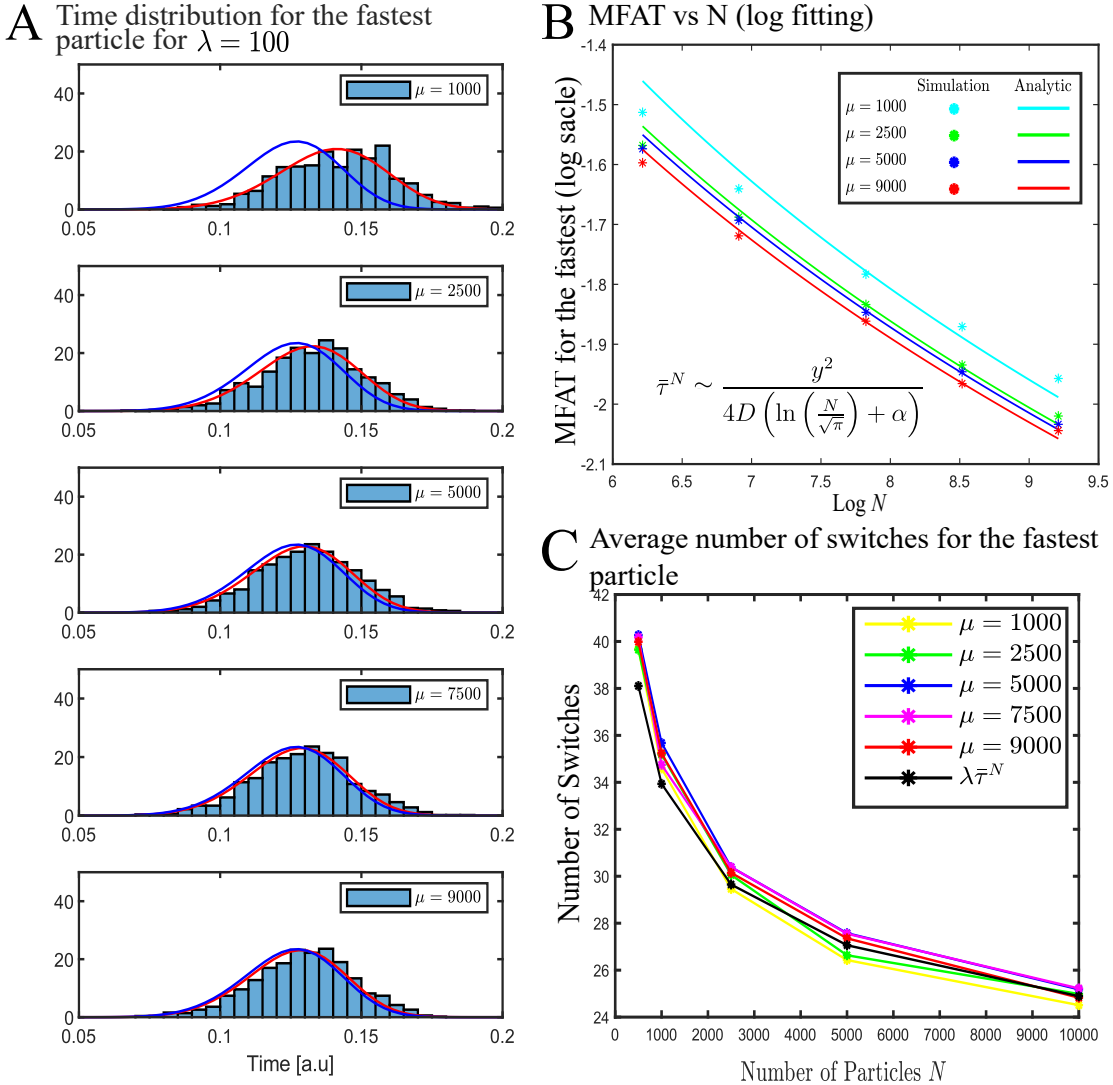


Figure 24: **Mean fastest arrival time vs the number of particles N .** **A.** Distribution of the arrival time $\bar{\tau}^N$: analytical short-time formula (4.17) (blue) and analytical long-time formula (4.20) (red) vs stochastic simulations (blue histogram) for particles starting at position $y = 2$ for $N = 10000$ with 1000 runs and $D_1 = 1$ and $D_2 = 1$ in the interval $[0, 5]$. **B.** MFAT vs N for the stochastic simulations (colored disks) and the asymptotic formulas (continuous lines) (equation 4.20) for different values of $\mu = [1000, 2500, 5000, 7500, 9000]$ and $\lambda = 100$ plotted in Log-Log scale. An optimal fit gives $\alpha = [-1.334, -0.9959, -0.9292, -0.8275, -0.8109]$. **C.** Mean number of switchings for the fastest particles (colored for each different value of μ) until its arrival to the target compared with the logarithmic law (black) proposed in formula (4.26) for $\lambda = 100$ and a factor of 1.09.

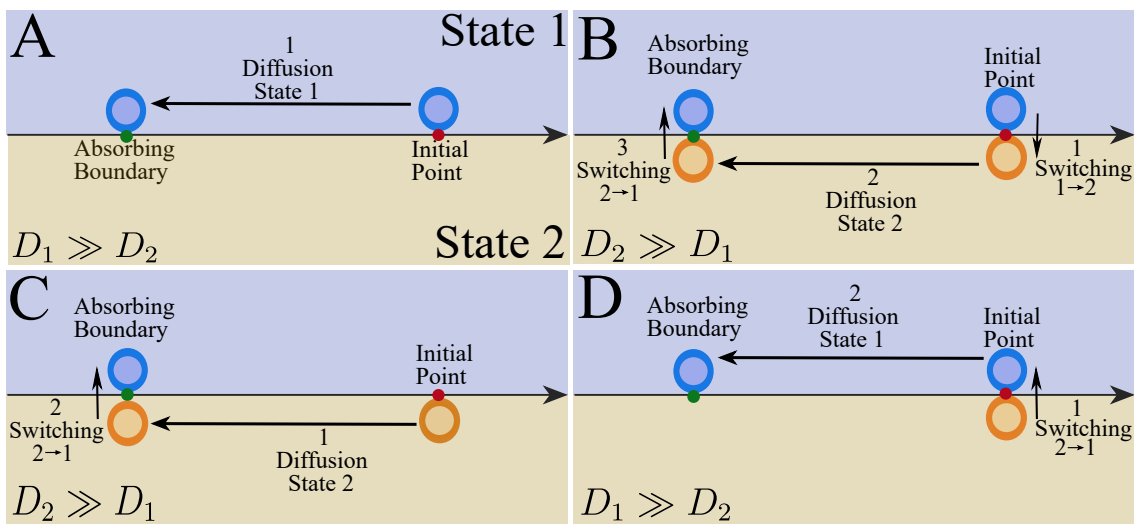


Figure 25: **Strategies followed by the fastest particle depending on the initial state and the diffusion coefficients.** **A.** Diffusion in state 1 onto the target (Initial state = 1 and $D_1 \gg D_2$). **B.** Switching from state 1 to 2. Diffusion in state 2 onto the target. Switching from state 2 to 1 (Initial state = 1 and $D_2 \gg D_1$). **C.** Diffusion in state 2 onto the target. Switching from state 2 to 1 (Initial state = 2 and $D_2 \gg D_1$). **D.** Switching from state 2 to 1. Diffusion in state 1 onto the target. (Initial state = 2 and $D_1 \gg D_2$).

Organization of the manuscript

Part I: Asymptotic formulas for calcium signaling

Chapter 1 is consecrated to the study of the role of initial distributions and drift in the mean first arrival time. In this chapter we introduce a new general exponential initial distributions for the heat equation as a direct motivation from calcium diffusion and compute how they affect the mean first arrival time. We obtain new laws decreasing algebraically in N for the 1D and 2D problem. We consider as well a drift component with constant velocity for the heat equation and we study the drift's effect on the arrival times. The solution to these problems is obtained by classical methods as the convolution with Green's function.

Chapters 2 & 3 are dedicated to the study of the effect in the mean first arrival time of a degradation term. In chapter 2 we describe the killing mechanism when point-sink killing terms are considered in 1D. We justify the 1D approximation for the killing process with the geometry of the dendrite spines and obtain the formula for the mean first activation time for transient calcium ions when at least one calcium ion escapes and when a large number of ions escape. We also compute the mean first binding time es the mean time for the first killing occurring for extruded calcium ions via CaMKII complex. We add as well the computations for uniform killing in an interval as appendix. In chapter 3 we continue the study of uniform and localized killing fields in a 2D domain. We study how the main parameters related with the killing field affect the arrival time. We show in 2D by numerical simulations that the fastest trajectories are concentrated along the geodesic path and from the large deviation principle that trajectories that contribute the most to the mean first arrival time are the trajectories along the geodesic.

Part II: Asymptotic formulas for transport and synthesis of proteins

Chapter 4 has as objective the study of the switching dynamics when two possible states are considered. In this chapter we study the mechanisms described by some transcription factors in the nucleus cell and compute the asymptotic formulas for the arrival time under different initial distributions when arrival is only possible in one of the two states. We derive short-time and long-time approximations for the arrival time distributions. We give conditions for the asymptotic formulas depending on the initial state of the particles and we find the general condition of no switchings at the fastest arrival time with a large probability. We use these asymptotic formulas to predict the time scale of the recruitment of RNA polymerase in the transcription of the DNA.

Part I

Asymptotic formulas for calcium signaling

Chapter 1

Role of an extended initial distribution and an additional drift component

*Published in TOSTE S. & HOLCMAN D., “Asymptotics for the fastest among N stochastic particles: role of an extended initial distribution and an additional drift component.” Journal of Physics A: Mathematical and Theoretical, Volume 54, Number 28, 54 285601 (2021).
arXiv:2010.08413 / hal:04101385*

Abstract

We derive asymptotic formulas for the mean exit time $\bar{\tau}^N$ of the fastest among N identical independently distributed Brownian particles to an absorbing boundary for various initial distributions (partially uniformly and exponentially distributed). Depending on the tail of the initial distribution, we report here a continuous algebraic decay for $\bar{\tau}^N$, which differs from the classical results. We derive asymptotic formulas in 1D for half-line and an interval that we compare with stochastic simulations, and we derive also the equivalent formulas in 2D. We also obtain asymptotic expression for $\bar{\tau}^N$ when an additive constant drift on the Brownian motion is added. Finally, we discuss some applications in cell biology where a molecular transduction pathway involves multiple steps and a long-tail initial distribution.

Introduction

Transient molecular activation in many cellular processes, such as gene transcription [53], calcium activity in neuronal protrusion [54] or biochemical pathways associated with a secondary messenger transduction [55] often occur in geometrical restricted micro-compartments, where the initial distribution of the source is well separated from the target site. To guarantee a reliable and fast activation, these processes are carried out by multiple redundant particles [56–60]. The multiplicity or redundancy has two effects: it increases the probability of finding a small target and, in parallel, decreases the mean activation time. Because it is usually costly to produce many copies of the same object, there is usually a compromise between the number of produced copies and the ultimate time scale of activation. In addition, for molecular processes involving multiple time steps, as we shall see here, any possible spreading of the initial distribution can affect the final activation time. For example, calcium ions enter in less than a few milliseconds inside a dendrite or neuronal synapses through few channels located on the membrane. After channels are closed, the calcium concentration has already spread, with a characteristic distribution, approximated as Gaussian in the diffusion

limit (Fig. 1.1A). But other initial distributions are possible because cellular crowding could slow down diffusion, leading to anomalous diffusion profiles [61]. Starting with such long-tail instantaneous distribution, calcium ions can fulfill several functions such as activating buffer located at a certain distances away from the calcium channels. This step is necessary for the activation of a secondary messenger that can lead to change in the physiology. Indeed, it has been known for decades that calcium concentration is a key factor for the induction of long-term synaptic changes [62], but the exact reasons are still unclear: it could be to activate enough molecules quickly. It was recently reported [54] that the initial distribution of injected calcium ions can modulate the probability of a calcium avalanche known as calcium-induced calcium release, fundamental for the induction of physiological changes underlying learning and memory. Another generic example is the secondary biochemical messenger pathway (Fig. 1.1B): molecules such as cGMP, IP_3^+ or cAMP are generated near receptors and need to travel a certain distance away to activate a second pathway. In all these cases, the initial concentration of these molecules is critical for the genesis of rhythmic oscillations or the amplification of a single molecular events. As we shall see, the initial number and their distribution can be critical for the determination of the activation time of a transduction cascade.

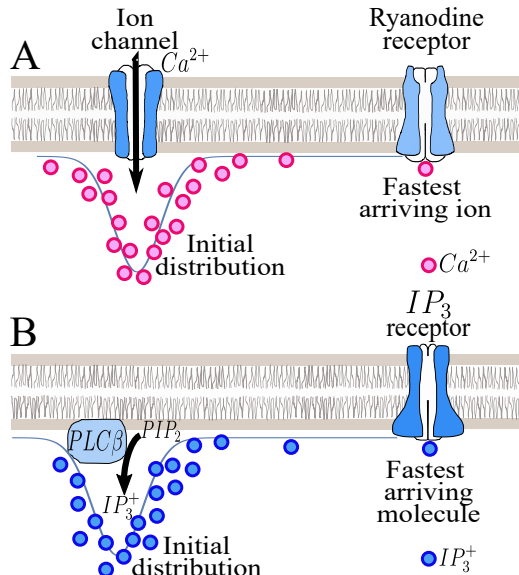


Figure 1.1: Two examples of fast molecular signalling where the initial distribution has a long-tail. **A.** Calcium ions enter very quickly through a channel or a cluster of channels. This fast entrance is associated to an initial distribution that can intersect at the tail with calcium sensitive receptors (such as Ryanodine receptors). **B.** IP_3^+ molecules, generated very quickly from PIP_2 at the cell membrane, that need to bind to IP_3 -receptor.

We recall that changing the initial number of particles on the escape time has been quantified as follows: when there are N i.i.d. particles, generated at a specific point location (entrance of a channel or a receptor), then the mean first arrival time (MFAT), which is the mean time it takes for the first particle to arrive decays with $1/\ln N$ [39, 54, 63, 64], but the decay can be much faster ($1/N^2$) when the particles are uniformly distributed [65–67].

Computing how the first arrival time depends on the initial numbers N is key to formulate biophysical laws of activation by the fastest diffusing particles to reach a target. The type of motion could matter, as revealed for spermatozoa to arrive to the ovule location, modeled as persistent motion switching direction after hitting the surface [68]. In general we are still missing the MFAT formula

for anomalous diffusion and many classical random motion such as the full Langevin equation. We compute here the mean arrival time $\bar{\tau}^N$ for the fastest among N identical Brownian particles using short-time asymptotic of the diffusion equation. In particular, we consider the case of extended initial conditions. Indeed, as mentioned above, after a molecule is generated at a specific location, additional chemical processes are involved to provide the molecular activity required to interact with a given target. Specific reactions are phosphorylations in case of transcription factor or methylations [69]. Indeed in some cases, transcription factors need to be phosphorylated or other molecules are needed, creating re-modeler complexes [70]. During these specific activation, the initial molecule can move by small drift or diffuse away allowing the initial concentration to spread a bit, a situation that we are interested in here.

This chapter is organized as follow. First, we recall the framework for the MFAT and derive explicit expressions when the initial distribution is uniform, intersecting or not with the target site for half a line \mathbf{R}_+ and for a finite interval $\Omega = [0, a]$. We study initial distributions of the form $p_1(x) = \frac{2b^{\frac{\alpha+1}{2}}}{\Gamma(\frac{\alpha+1}{2})} x^\alpha e^{-bx^2}$ with $b > 0$ and $\alpha \geq 0$ leading to the general formula (1.12)

$$\bar{\tau}^N \sim \frac{C_\alpha}{N^{\frac{2}{\alpha+1}}} \frac{1}{4Db} \text{ for } N \gg 1, \quad (1.1)$$

where

$$C_\alpha = \Gamma\left(\frac{\alpha+3}{\alpha+1}\right) \left(\frac{\sqrt{\pi}(\alpha+1)\Gamma\left(\frac{\alpha+1}{2}\right)}{2\Gamma\left(\frac{\alpha+2}{2}\right)} \right)^{\frac{2}{\alpha+1}} \quad (1.2)$$

and Γ is the Gamma function. This formula reveals a large spectrum of possible decay that depends on the analytical expression of the local overlap between the initial distribution and the target location. In addition, we provide an equivalent formula in two dimensions. Finally, we study the influence of a constant drift on the escape time $\bar{\tau}^N$.

1.1 General framework for the first arrival time

We review here the arrival time definition for a diffusion process with not other dynamics evolved as defined in section 0.1.1. The shortest arrival time for N non-interacting i.i.d. Brownian trajectories moving in a domain Ω to a small target is defined as

$$\tau^1 = \min(t_1, \dots, t_N),$$

where t_i are the i.i.d. arrival times of the N particles. The complementary cumulative distribution function of τ^1 is given by

$$\Pr\{\tau^1 > t\} = [\Pr\{t_1 > t\}]^N,$$

where $\Pr\{t_1 > t\}$ is the survival probability of a single particle prior to reaching the target. This probability can be computed from solving the diffusion equation

$$\begin{aligned} \frac{\partial p(\mathbf{x}, t)}{\partial t} &= D\Delta p(\mathbf{x}, t) \text{ for } \mathbf{x} \in \Omega, t > 0 \\ p(\mathbf{x}, 0) &= p_0(x) \text{ for } \mathbf{x} \in \Omega \\ \frac{\partial p(\mathbf{x}, t)}{\partial \mathbf{n}} &= 0 \text{ for } \mathbf{x} \in \partial\Omega_r \\ p(\mathbf{x}, t) &= 0 \text{ for } \mathbf{x} \in \partial\Omega_a \end{aligned}$$

where D is the diffusion coefficient and $\partial\Omega_r = \partial\Omega \setminus \partial\Omega_a$. The survival probability is always

$$S(t) = \Pr \{t_1 > t\} = \int_{\Omega} p(x, t) dx \quad (1.3)$$

so that the probability density function (pdf) for the arrival of the first particle is

$$\Pr \{\tau^1 \in [t, t + dt]\} = \frac{d}{dt} \Pr \{\tau^1 \leq t\} dt = N(\Pr \{t_1 > t\})^{N-1} \Pr \{t_1 \in [t, t + dt]\}, \quad (1.4)$$

where the instantaneous probability is given by the probability flux

$$\Pr \{t_1 \in [t, t + dt]\} = \oint_{\partial\Omega_a} \frac{\partial p(\mathbf{x}, t)}{\partial \mathbf{n}} dS_{\mathbf{x}} dt.$$

The MFAT is defined as the mean time for the first particle among N i.i.d. Brownian paths to reach the target and it is obtained by computing the integral

$$\bar{\tau}^N = \int_0^\infty \Pr \{\tau^1 > t\} dt = \int_0^\infty [\Pr \{t_1 > t\}]^N dt. \quad (1.5)$$

1.2 Arrival times for multiple initial distributions in 1D

1.2.1 Arrival from a ray for multiple initial distributions

We start with the case of the non-negative real line $\Omega = \mathbf{R}_+$, for which the solution of the diffusion equation

$$\begin{aligned} \frac{\partial p(x, t)}{\partial t} &= D \frac{\partial^2 p(x, t)}{\partial x^2} \text{ for } x > 0, t > 0 \\ p(x, 0) &= \delta(x - y) \text{ for } x > 0 \\ p(0, t) &= 0 \text{ for } t > 0 \end{aligned} \quad (1.6)$$

is given by

$$p(x, t) = \frac{1}{\sqrt{4Dt\pi}} \left[\exp \left\{ -\frac{(x-y)^2}{4Dt} \right\} - \exp \left\{ -\frac{(x+y)^2}{4Dt} \right\} \right]. \quad (1.7)$$

For a general initial condition, is well known that the solution of (1.6) is the convolution of the initial pdf $p(x, 0)$ with the Green's function presented in (1.7). The case of the Dirac delta function in dimension 1, 2 and 3 was previously treated in [66, 71, 72] and also the case of initial distributions spreading over a perpendicular segment in a cusp was previously studied in [73].

When the initial distribution of particles is uniform in a small portion of the non-negative real line $[0, y_0]$, the initial distribution is given by $p(x, 0) = \frac{1}{y_0} \mathbb{I}_{\{x \in [0, y_0]\}}$, and thus, the solution is

$$p(x, t) = \int_0^{y_0} \frac{1}{y_0 \sqrt{4Dt\pi}} \left[\exp \left(-\frac{(x-y)^2}{4Dt} \right) - \exp \left(-\frac{(x+y)^2}{4Dt} \right) \right] dy.$$

The survival probability given by relation (1.3) is

$$\Pr \{t_1 > t\} = \int_0^\infty p(x, t) dx = 1 - \frac{2}{\sqrt{\pi}} \int_{\frac{y_0}{\sqrt{4Dt}}}^\infty e^{-u^2} du + \frac{\sqrt{4Dt}}{y_0 \sqrt{\pi}} \left[e^{-\frac{y_0^2}{4Dt}} - 1 \right]. \quad (1.8)$$

Using the small time approximation of the complementary error function $\text{erfc}\left(\frac{y_0}{\sqrt{4Dt}}\right) = \frac{\sqrt{4Dt}}{\sqrt{\pi}y_0} e^{-\frac{y_0^2}{4Dt}}(1+O(t))$, the relation (1.8) is given for small time t by the first and last term, so that $\text{erfc}\left(\frac{y_0}{\sqrt{4Dt}}\right)$. Thus $\Pr\{t_1 > t\} \sim 1 - \frac{\sqrt{4Dt}}{y_0\sqrt{\pi}}$ and thus using relation (1.5) [17, 56], we obtain for large N the decay

$$\bar{\tau}^N \sim \int_0^\infty \exp\left\{-N \frac{\sqrt{4Dt}}{y_0\sqrt{\pi}}\right\} dt = \frac{y_0^2\pi}{2DN^2}, \quad (1.9)$$

which extends the formula for Dirac delta initial condition previously derived in [63].

This result shows that as soon as the initial condition overlaps with the target, the MFAT decay with order $1/N^2$.

We now consider a local initially uniform distribution in the shifted interval $[y_1, y_2]$ where $y_1 > 0$, not overlapping with the target site. The initial normalized distribution function is thus $p_0(x) = \frac{1}{y_2-y_1}\mathbb{I}_{\{x \in [y_1, y_2]\}}$ with $y_2 > y_1 > 0$. We now compute the survival probability, given by

$$\begin{aligned} \Pr\{t_1 > t\} &= \int_0^\infty \int_{y_1}^{y_2} \frac{1}{(y_2-y_1)\sqrt{4Dt\pi}} \left[\exp\left\{-\frac{(x-y)^2}{4Dt}\right\} - \exp\left\{-\frac{(x+y)^2}{4Dt}\right\} \right] dy dx \\ &= 1 - \frac{y_2}{y_2-y_1} \left(\frac{2}{\sqrt{\pi}} \int_{\frac{y_2}{\sqrt{4Dt}}}^\infty e^{-u^2} du \right) + \frac{y_1}{y_2-y_1} \left(\frac{2}{\sqrt{\pi}} \int_{\frac{y_1}{\sqrt{4Dt}}}^\infty e^{-u^2} du \right) \\ &\quad + \frac{\sqrt{4Dt}}{(y_2-y_1)\sqrt{\pi}} \left[e^{-\frac{y_2^2}{4Dt}} - e^{-\frac{y_1^2}{4Dt}} \right]. \end{aligned}$$

Expanding asymptotically the complementary error function, we obtain for small time t the relation

$$S(t) = \Pr\{t_1 > t\} \sim 1 - \frac{(\sqrt{4Dt})^3}{2(y_2-y_1)\sqrt{\pi}} \left[\frac{e^{-\frac{y_1^2}{4Dt}}}{y_1^2} - \frac{e^{-\frac{y_2^2}{4Dt}}}{y_2^2} \right]. \quad (1.10)$$

Note that expression (1.10) contains two exponentially small terms. It is however possible to recover the case of an initial Dirac delta function by making the expansion $y_2 = y_1(1+\varepsilon)$ and studying the limit when ε goes to zero in equation (1.10). In that case, we have

$$S_\varepsilon(t) = S(t)|_{y_2=y_1(1+\varepsilon)} \sim 1 - \frac{(\sqrt{4Dt})^3 e^{-\frac{y_1^2}{4Dt}}}{2y_1\varepsilon\sqrt{\pi}} \frac{y_1^2}{y_1^2} \left[1 - \frac{e^{-\frac{y_1^2(2\varepsilon+\varepsilon^2)}{4Dt}}}{(1+\varepsilon)^2} \right].$$

A Taylor expansion in ε leads to

$$S_\varepsilon(t) = 1 - \frac{(\sqrt{4Dt})^3 e^{-\frac{y_1^2}{4Dt}}}{\sqrt{\pi}y_1^3} \left[1 + \frac{y_1^2}{4Dt} - \varepsilon \left(1 + \frac{3y_1^2}{8Dt} + \frac{2y_1^4}{(4Dt)^2} \right) + O(\varepsilon^2) + O\left(\frac{\varepsilon}{t}\right) \right].$$

When $\varepsilon \rightarrow 0$, the survival probability $S_\varepsilon(t)$ converges to the survival probability $S_0(t)$ corresponding to an initial condition for the Dirac delta function at position y_1 , this is,

$$S_0(t) \sim 1 - \frac{(\sqrt{4Dt})^3 e^{-\frac{y_1^2}{4Dt}}}{\sqrt{\pi}y_1^3} \left[1 + \frac{y_1^2}{4Dt} \right].$$

However, the convergence is not uniform in t in the interval $[0, \infty)$, preventing to use this expansion to estimate the MFAT for the case of an interval. Thus to leading order, using that

$$\lim_{y_2 \rightarrow y_1} \Pr \{t_1 > t\} \sim 1 - \frac{\sqrt{4Dt}}{\sqrt{\pi}} \left[\frac{e^{-\frac{y_1^2}{4Dt}}}{y_1} \right],$$

we obtain to leading order the asymptotic formula for N large

$$\bar{\tau}_\varepsilon^N \approx \frac{y_1^2}{4D \ln \left(\frac{N}{\sqrt{\pi}} \right) + A_\varepsilon}, \quad (1.11)$$

where $A_\varepsilon = A_0 + \varepsilon A_1 + \dots$, where A_k are constants. Here y_1 is the shortest distance to the absorbing boundary. To conclude, to leading order, the MFAT for a small interval is the same as a Dirac delta function at the minimum point of the interval where the particles are uniformly distributed.

1.2.2 MFAT for an initial long-tail distribution touching the target site

For an initial normalized distribution $p_1(x) = Kx^\alpha e^{-bx^2}$ with $\alpha \geq 0$ and $b > 0$, and $K = \frac{2b^{\frac{\alpha+1}{2}}}{\Gamma(\frac{\alpha+1}{2})}$, the survival probability of the diffusion process is given by relation (1.3) leading to the formula

$$\begin{aligned} \Pr \{t_1 > t\} &= \frac{2b^{\frac{\alpha+1}{2}}}{\Gamma(\frac{\alpha+1}{2})} \int_0^\infty \operatorname{erf} \left(\frac{y}{\sqrt{4Dt}} \right) y^\alpha \exp \{-by^2\} dy \\ &= \frac{2}{\Gamma(\frac{\alpha+1}{2})(4Dbt)^{\frac{1}{2}}} \frac{\Gamma(\frac{\alpha+2}{2})}{\sqrt{\pi}} {}_2F_1 \left[\frac{1}{2}, \frac{\alpha+2}{2}, \frac{3}{2}, -\frac{1}{4Dbt} \right], \end{aligned}$$

where ${}_2F_1[a, b, c, z]$ is the Gauss hyper-geometric function [74]. The expansion for $z \rightarrow \infty$ (t small), gives

$${}_2F_1 \left[\frac{1}{2}, \frac{\alpha+2}{2}, \frac{3}{2}, -\frac{1}{4Dbt} \right] = \frac{\sqrt{\pi} \Gamma(\frac{\alpha+1}{2}) (4Dbt)^{\frac{1}{2}}}{2\Gamma(\frac{\alpha+2}{2})} - \frac{(4Dbt)^{\frac{\alpha+2}{2}}}{\alpha+1} + O(t^{\frac{\alpha+4}{2}}).$$

Thus for small time t , we obtain

$$\Pr \{t_1 > t\} \sim 1 - \frac{2\Gamma(\frac{\alpha+2}{2})}{(\alpha+1)\sqrt{\pi}\Gamma(\frac{\alpha+1}{2})} (4Dbt)^{\frac{\alpha+1}{2}},$$

and the MFAT is given by

$$\begin{aligned} \bar{\tau}^N &\sim \int_0^\delta \exp \left\{ -\frac{2N\Gamma(\frac{\alpha+2}{2})}{(\alpha+1)\sqrt{\pi}\Gamma(\frac{\alpha+1}{2})} (4Dbt)^{\frac{\alpha+1}{2}} \right\} dt \quad \text{for } \delta \text{ small,} \\ &\sim \left(\frac{\sqrt{\pi}(\alpha+1)\Gamma(\frac{\alpha+1}{2})}{2N\Gamma(\frac{\alpha+2}{2})} \right)^{\frac{2}{\alpha+1}} \frac{1}{4Db} \Gamma \left(\frac{\alpha+3}{\alpha+1} \right). \end{aligned} \quad (1.12)$$

When $\alpha = 0$, the initial distribution becomes $p_0 = \frac{2\sqrt{b}}{\sqrt{\pi}} \exp \{-by^2\}$, and we recover the same behavior as the case where the Brownian particles are uniformly distributed in $[0, y_0]$. For $\alpha = 1$, we obtain that the MFAT decays with $1/N$. For $\alpha = 2$, we obtain that MFAT decays like $\frac{1}{N^{2/3}}$, and so on.

1.2.3 MFAT inside the interval $[0, a]$

In this section, we present the asymptotic computation for the MFAT to one of the extremities of an interval. We start with the solution of the diffusion equation

$$\begin{aligned}\frac{\partial p(x, t)}{\partial t} &= D \frac{\partial^2 p(x, t)}{\partial x^2} \quad \text{for } x > 0, t > 0 \\ p(x, 0) &= \delta(x - y) \quad \text{for } x > 0 \\ p(0, t) &= p(a, t) = 0 \quad \text{for } t > 0,\end{aligned}\tag{1.13}$$

which is given by the infinite sum [71]

$$p(x, t) = \frac{1}{\sqrt{4Dt\pi}} \sum_{n=-\infty}^{+\infty} \left[\exp \left\{ -\frac{(x-y+2na)^2}{4Dt} \right\} - \exp \left\{ -\frac{(x+y+2na)^2}{4Dt} \right\} \right].\tag{1.14}$$

To compute the MFAT, we shall use only the first terms associated with $n = \pm 1$, since larger values of n represent exponentially small terms compared to those ones. For particles that are initially uniformly distributed in the interval $[0, a]$, this is $p_0(x) = \frac{1}{b} \mathbb{I}_{\{x \in [0, b]\}}$ with $0 < b < a$, the short-time approximation for the solution of equation (1.13) is given by

$$\begin{aligned}p(x, t) &\approx \int_0^b \frac{1}{b\sqrt{4Dt\pi}} \left[\exp \left\{ -\frac{(x-y)^2}{4Dt} \right\} - \exp \left\{ -\frac{(x+y)^2}{4Dt} \right\} + \exp \left\{ -\frac{(x-y-2a)^2}{4Dt} \right\} \right. \\ &\quad \left. - \exp \left\{ -\frac{(x+y-2a)^2}{4Dt} \right\} + \exp \left\{ -\frac{(x-y+2a)^2}{4Dt} \right\} - \exp \left\{ -\frac{(x+y+2a)^2}{4Dt} \right\} \right] dy,\end{aligned}$$

where the error made is in the order of $O\left(\frac{\exp\left\{-\frac{(x-y+3a)^2}{4Dt}\right\}}{\sqrt{t}}\right)$. The survival probability is thus approximated as

$$\begin{aligned}\Pr\{t_1 > t\} &= \int_0^a p(x, t) dx \approx \frac{1}{b} \left[\text{berf}\left(\frac{b}{\sqrt{4Dt}}\right) - (a+b)\text{erf}\left(\frac{a+b}{\sqrt{4Dt}}\right) + 2a\text{erf}\left(\frac{a}{\sqrt{4Dt}}\right) \right. \\ &\quad - (a-b)\text{erf}\left(\frac{a-b}{\sqrt{4Dt}}\right) + (2a+b)\text{erf}\left(\frac{2a+b}{\sqrt{4Dt}}\right) - 4a\text{erf}\left(\frac{2a}{\sqrt{4Dt}}\right) \\ &\quad + (2a-b)\text{erf}\left(\frac{2a-b}{\sqrt{4Dt}}\right) - \frac{(3a-b)}{2}\text{erf}\left(\frac{3a-b}{\sqrt{4Dt}}\right) - \frac{(3a+b)}{2}\text{erf}\left(\frac{3a+b}{\sqrt{4Dt}}\right) \\ &\quad + 3a\text{erf}\left(\frac{3a}{\sqrt{4Dt}}\right) + \frac{\sqrt{4Dt}}{\sqrt{\pi}} \left[e^{-\frac{b^2}{4Dt}} - 1 - e^{-\frac{(a+b)^2}{4Dt}} + 2e^{-\frac{a^2}{4Dt}} - e^{-\frac{(a-b)^2}{4Dt}} + e^{-\frac{(2a+b)^2}{4Dt}} \right. \\ &\quad \left. - 2e^{-\frac{(2a)^2}{4Dt}} + e^{-\frac{(2a-b)^2}{4Dt}} - \frac{1}{2}e^{-\frac{(3a-b)^2}{4Dt}} + e^{-\frac{(3a)^2}{4Dt}} - \frac{1}{2}e^{-\frac{(3a+b)^2}{4Dt}} \right] \left. \right].\end{aligned}$$

In the small t limit, we have the approximation

$$S(t) = \Pr\{t_1 > t\} \sim 1 - \frac{\sqrt{4Dt}}{b\sqrt{\pi}}.$$

This formula leads to the asymptotic expression for the MFAT when N is large

$$\bar{\tau}^N \sim \frac{b^2\pi}{2DN^2}.\tag{1.15}$$

To study the probability density function for the first arrival time, we are going to consider the auxiliary r.v. σ_s^N with distribution

$$\Pr\{\sigma_s^N \leq t\} = 1 - \exp\left\{-\frac{\sqrt{4Dt}N}{b\sqrt{\pi}}\right\}. \quad (1.16)$$

Note that the pdf of σ_s^N is given by

$$\Pr\{\sigma_s^N \in [t + dt]\} = -\frac{d}{dt} \left[\exp\left\{-\frac{\sqrt{4Dt}N}{b\sqrt{\pi}}\right\} \right] dt = \frac{N\sqrt{4D}}{b\sqrt{\pi t}} \exp\left\{-\frac{\sqrt{4Dt}N}{b\sqrt{\pi}}\right\} dt, \quad (1.17)$$

and note also that

$$\Pr\{\tau^1 \leq t\} = 1 - [S(t)]^N \sim \Pr\{\sigma_s^N \leq t\} \text{ when } t \text{ is small.} \quad (1.18)$$

We thus approximate the pdf for the distribution of arrival times as the pdf of the distribution σ_s^N . When the initial distribution intersect the right hand-side of the interval $p_0(x) = \frac{1}{a-b}\mathbb{I}_{\{x \in [b,a]\}}$ with $0 < b < a$, we obtain a similar expression:

$$\bar{\tau}^N \sim \frac{(a-b)^2\pi}{2DN^2}.$$

Finally, when the Brownian particles are initially uniformly distributed in an interval $[y_1, y_2]$ contained inside $[0, a]$, $p_0(x) = \frac{1}{y_2-y_1}\mathbb{I}_{\{x \in [y_1, y_2]\}}$ with $0 < y_1 < y_2 < a$, the solution of the diffusion equation (1.13) can be approximated as

$$p(x, t) \approx \int_{y_1}^{y_2} \frac{1}{(y_2 - y_1)\sqrt{4Dt\pi}} \left[\exp\left\{-\frac{(x-y)^2}{4Dt}\right\} - \exp\left\{-\frac{(x+y)^2}{4Dt}\right\} + \exp\left\{-\frac{(x-y-2a)^2}{4Dt}\right\} \right. \\ \left. - \exp\left\{-\frac{(x+y-2a)^2}{4Dt}\right\} + \exp\left\{-\frac{(x-y+2a)^2}{4Dt}\right\} - \exp\left\{-\frac{(x+y+2a)^2}{4Dt}\right\} \right] dy,$$

and the survival probability is

$$\Pr\{t_1 > t\} = \frac{1}{y_2 - y_1} \left[y_2 - y_1 + \frac{(\sqrt{4Dt})^3}{\sqrt{\pi}} \left[\frac{e^{-\frac{y_2^2}{4Dt}}}{2y_2^2} - \frac{e^{-\frac{y_1^2}{4Dt}}}{2y_1^2} - \frac{e^{-\frac{(y_2+a)^2}{4Dt}}}{2(y_2+a)^2} + \frac{e^{-\frac{(y_1+a)^2}{4Dt}}}{2(y_1+a)^2} - \frac{e^{-\frac{(a-y_2)^2}{4Dt}}}{2(a-y_2)^2} \right. \right. \\ \left. + \frac{e^{-\frac{(y_2+2a)^2}{4Dt}}}{2(y_2+2a)^2} + \frac{e^{-\frac{(a-y_1)^2}{4Dt}}}{2(a-y_1)^2} - \frac{e^{-\frac{(y_1+2a)^2}{4Dt}}}{2(y_1+2a)^2} + \frac{e^{-\frac{(2a-y_2)^2}{4Dt}}}{2(2a-y_2)^2} - \frac{e^{-\frac{(2a-y_1)^2}{4Dt}}}{2(2a-y_1)^2} - \frac{e^{-\frac{(3a-y_2)^2}{4Dt}}}{4(3a-y_2)^2} \right. \\ \left. + \frac{e^{-\frac{(3a-y_1)^2}{4Dt}}}{4(3a-y_1)^2} - \frac{e^{-\frac{(y_2+3a)^2}{4Dt}}}{4(y_2+3a)^2} + \frac{e^{-\frac{(y_1+3a)^2}{4Dt}}}{4(y_1+3a)^2} \right] \right].$$

Here again we approximate the pdf for the distribution of the arrival times as the pdf of the r.v. σ_s^N with distribution

$$\Pr\{\sigma_s^N \leq t\} = 1 - \exp\left\{-\frac{N(\sqrt{4Dt})^3 e^{-\frac{(\min(y_1, a-y_2))^2}{4Dt}}}{2(y_2 - y_1)(\min(y_1, a - y_2))^2 \sqrt{\pi}}\right\}. \quad (1.19)$$

Thus, the pdf of σ_s^N is given by

$$\begin{aligned} \Pr\{\sigma_s^N \in [t + dt]\} &= \frac{N(\sqrt{4Dt})^3}{2(y_2 - y_1)\min(y_1, a - y_2)\sqrt{\pi}} \exp\left\{-\frac{\min^2(y_1, a - y_2)}{4Dt}\right\} \\ &\quad \exp\left\{-\frac{(\sqrt{4Dt})^3 N}{2(y_2 - y_1)\sqrt{\pi}} \frac{\exp\left\{-\frac{\min^2(y_1, a - y_2)}{4Dt}\right\}}{\min^2(y_1, a - y_2)}\right\} \left[\frac{\min(y_1, a - y_2)}{4Dt^2} + \frac{3}{2t}\right] dt, \end{aligned} \quad (1.20)$$

and since

$$\Pr\{\tau^1 \leq t\} = 1 - [S(t)]^N \sim \Pr\{\sigma_s^N \leq t\} \text{ when } t \text{ is small,} \quad (1.21)$$

we approximate the pdf for distribution of arrival times as the pdf of the distribution σ_s^N .

Using a Taylor expansion when $y_2 \rightarrow y_1$ in the form $y_2 = y_1(1 + \varepsilon)$ when $\varepsilon \rightarrow 0$, the survival probability $S_\varepsilon(t)$ converges to the survival probability $S(t)$ for the case where the initial condition is a Dirac delta function. However, as shown above, the convergence is not uniform for all time $t \in [0, \infty)$, preventing to use this expansion to estimate the MFAT for the case of an interval. Thus to leading order, we have

$$\lim_{y_2 \rightarrow y_1} \Pr\{t_1 > t\} \sim 1 - \frac{\sqrt{4Dt}}{\sqrt{\pi}} \left[\frac{e^{-\frac{\min(y_1, a - y_2)^2}{4Dt}}}{\min(y_1, a - y_2)} \right],$$

leading to the asymptotic formula for large N , given by

$$\bar{\tau}_\varepsilon^N \sim \frac{\min(y_1, a - y_2)^2}{4D \ln\left(\frac{N}{\sqrt{\pi}}\right) + A_\varepsilon}, \quad (1.22)$$

where $A_\varepsilon = A_0 + \varepsilon A_1 + \dots$, where A_k are constants. Here $\min(y_1, a - y_2)$ is the shortest distance to the absorbing boundaries. To conclude, at leading order, the MFAT when the initial distribution of particles falls inside a small interval is the same as the one obtained for a Dirac delta function where the main parameter is the minimal distance from the boundaries of the interval where particles start their motion to the absorbing boundaries.

1.2.4 MFAT inside the interval $[0, c]$ when the initial distribution has a long-tail

We consider the MFAT when the initial distribution is given by $p_1(x) = \frac{2b}{1-e^{-bc^2}}xe^{-bx^2}\mathbb{I}_{\{x \in [0, c]\}}$ with $0 < c < a$. Then, the solution of the diffusion equation (1.6) is given by the following expression

$$\begin{aligned} p(x, t) &= \frac{2b}{1-e^{-bc^2}} \int_0^c \frac{1}{\sqrt{4Dt\pi}} \left[\exp\left\{-\frac{(x-y)^2}{4Dt}\right\} - \exp\left\{-\frac{(x+y)^2}{4Dt}\right\} + \exp\left\{-\frac{(x-y-2a)^2}{4Dt}\right\} \right. \\ &\quad \left. - \exp\left\{-\frac{(x+y-2a)^2}{4Dt}\right\} + \exp\left\{-\frac{(x-y+2a)^2}{4Dt}\right\} - \exp\left\{-\frac{(x+y+2a)^2}{4Dt}\right\} \right] y \exp\{-bx^2\} dy. \end{aligned}$$

For t small, the survival probability can be approximated by the formula

$$S(t) = \Pr\{t_1 > t\} \sim 1 - \frac{2Dbt}{1 - e^{-bc^2}}.$$

We approximate again the pdf for the distribution of the first arrival times as the probability of a r.v. σ_s^N with distribution

$$\Pr\{\sigma_s^N \leq t\} = 1 - \exp\left\{\frac{-2Dbt}{1 - e^{-bc^2}}\right\}. \quad (1.23)$$

Note that the pdf of σ_s^N is given by

$$\Pr\{\sigma_s^N \in [t + dt]\} = \frac{2bDN \exp\left\{-\frac{2DbtN}{1 - \exp\{-bc^2\}}\right\}}{1 - \exp\{-bc^2\}} dt, \quad (1.24)$$

and here again

$$\Pr\{\tau^1 \leq t\} = 1 - [S(t)]^N \sim \Pr\{\sigma_s^N \leq t\} \text{ when } t \text{ is small.} \quad (1.25)$$

We thus approximate the pdf for distribution of arrival times as the pdf of the distribution σ_s^N , and when N is large we have the asymptotic formula for the MFAT given by

$$\bar{\tau}^N \sim \frac{1 - e^{-bc^2}}{2DbN}. \quad (1.26)$$

We decided to compare the obtained asymptotic distributions with stochastic simulations (see Appendix for the description of the algorithm when the initial distribution touches the absorbing boundary). We generated trajectories until they reach the origin and selected the fastest one (green in Fig. 1.2A). We chose several initial distributions as in Fig. 1.2B and we compare the histogram for the arrival times of the fastest particles (in arbitrary units) with the analytical approximated expression in Fig. 1.2C, D and E when the domain of simulation is the interval $[0, a]$. We found an agreement between the analytical densities given by expressions (1.17) and (1.24), and the empirical histogram for the arrival times of the fastest particles, as shown in Fig. 1.2C and E. When particles are initially generated very close to the absorbing boundary, a good agreement is obtained between the theoretical and simulated distributions. But when particles are generated far from the absorbing boundary as in Fig. 1.2D, the finite N corrections seem to be rather strong and it improves when we increase the value of N . And we can see also this effect in the simulation results for the MFAT (Fig. 1.3B blue) where a parameter α needs to be added in the logarithmic formula to correct the asymptotic result. The MFAT decreases with the number of particles (Fig. 1.3B) as predicted by equations (1.15) red, (1.22) blue and (1.26) green. We can also think that for the exponential distribution in Fig. 1.3B (red) there is a deviation between the asymptotic formulas and the simulations results for large N , but we believe that this could be due to the Δt consider in the Euler's scheme for simulations. In this case particles can be generated very close to the absorbing boundary, and we choose a Δt satisfying that

$$\Delta t \leq p \frac{\delta_N^2}{2D}, \quad (1.27)$$

where δ_N is the minimal distance between the particles generated and the target:

$$\delta_N = \min_N \{|\chi_1|, \dots, |\chi_N|\}. \quad (1.28)$$

Then, the mean square displacement, controlled by the parameter p , is smaller than the shortest distance (see Appendix for the Euler's scheme). But, what could be happening is that we did

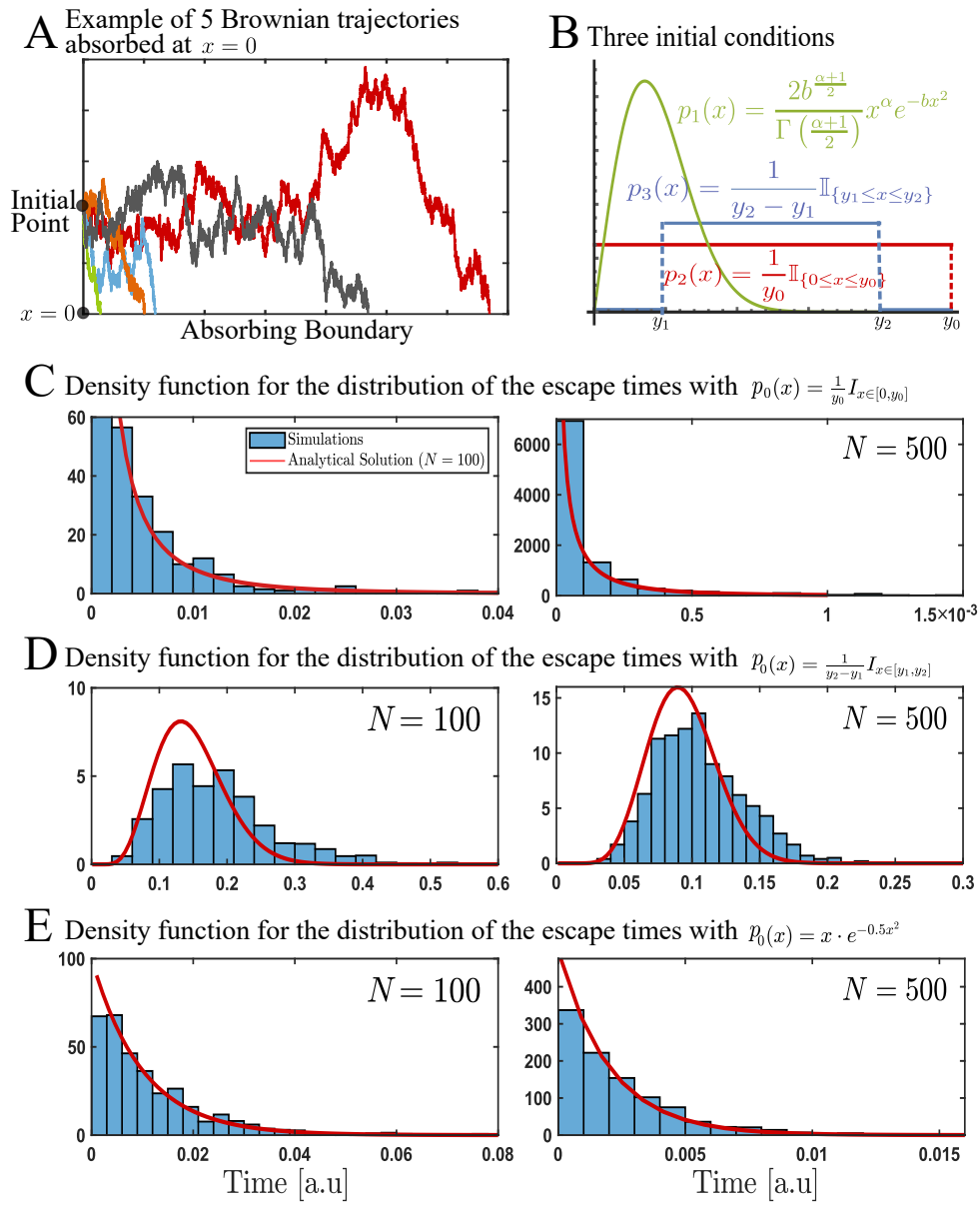


Figure 1.2: Arrival times for the fastest Brownian particles for various initial distributions.

A. Examples of 5 independent Brownian trajectories starting at $x = 0.5$ and absorbed at $x = 0$ and the fastest is green. **B.** Three initial distributions: the exponential distribution $p_1(x) = \frac{2b^{\frac{\alpha+1}{2}}}{\Gamma(\frac{\alpha+1}{2})} x^\alpha e^{-bx^2}$ and two uniform distributions $p_2(x) = \frac{1}{y_0} \mathbb{I}_{\{0 \leq x \leq y_0\}}$ and $p_3(x) = \frac{1}{y_2 - y_1} \mathbb{I}_{\{y_1 \leq x \leq y_2\}}$. **C.** Approximated pdf for the arrival time $\bar{\tau}^N$: analytical (equation (1.17)) in red vs stochastic simulations (blue histogram) for particles distributed with respect to $p_0(x) = \frac{1}{y_0} \mathbb{I}_{\{0 \leq x \leq y_0\}}$ for $0 < y_0 < a$ with $y_0 = 4$ and $a = 5$ for $N = 100$ (left) and $N = 500$ (right) with 1000 runs. **D.** Approximated pdf for the arrival time $\bar{\tau}^N$: analytical (equation (1.20)) in red vs stochastic simulations (blue) for particles distributed with respect to $p_0(x) = \frac{1}{y_2 - y_1} \mathbb{I}_{\{y_1 \leq x \leq y_2\}}$ with $0 < y_1 < y_2 < a$, $y_1 = 1$ and $y_2 = 4$. **E.** Approximated pdf for the arrival time $\bar{\tau}^N$: analytical (equation (1.24)) in red vs stochastic simulations (blue) for particles distributed with respect to $p_1(x) = \frac{2b}{1-e^{-bc^2}} x e^{-x^2} \mathbb{I}_{\{x \in [0, c]\}}$ with $a > c > 0$ with $b = 0.5$, $\alpha = 1$ and $c = 4$.

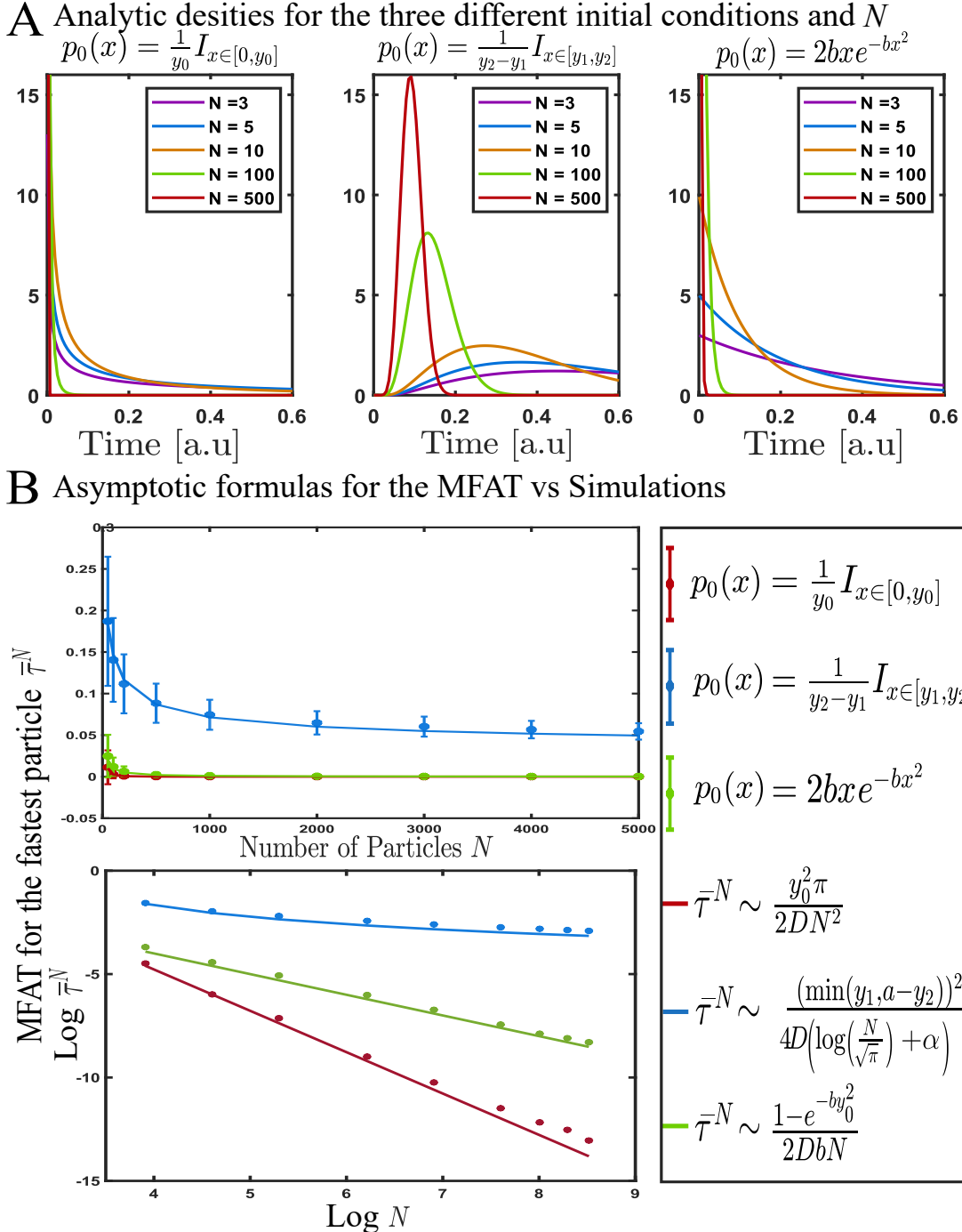


Figure 1.3: **Mean fastest arrival time vs the number of particles N .** **A.** Approximation of the probability density functions for the arrival times in an interval computed from equations (1.17), (1.20), and (1.24) for a total number of particles $N = (3, 5, 10, 100, 500)$ and the three initial distributions, presented in Fig. 1.2B. **B.** MFAT vs N comparing stochastic simulations (colored disks) and the asymptotic formulas (continuous lines). The asymptotic expression for the MFAT when the particles are initially uniformly distributed in $[y_1, y_2]$ (blue curve given by (1.22)) is of the form $\frac{y_1^2}{4D \left(\log\left(\frac{N}{\sqrt{\pi}}\right) + \alpha \right)}$ when $y_1 \ll a - y_2$. An optimal fit gives $\alpha = -2.099$. Parameters of the simulations are described in Fig. 1.2 with 1000 runs.

not take p small enough, and after a few steps when N is large the fastest particles escapes over estimating the time.

We plotted the approximated analytical pdfs for the shortest arrival time (1.17), (1.20), (1.24) and for various values of N (Fig. 1.3A).

We summarized in the next table the main asymptotic formulas associated with different initial conditions.

Asymptotic formulas for the MFAT			
Initial Distribution	$\Omega = \mathbf{R}_+$	Initial Distribution	$\Omega = [0, a]$
$p_0(x) = \delta(x - x_0)$	$\bar{\tau}^N \sim \frac{x_0^2}{4D \ln\left(\frac{N}{\sqrt{\pi}}\right)}$	$p_0(x) = \delta(x - x_0)$	$\bar{\tau}^N \sim \frac{(\min(x_0, a - x_0))^2}{4D \ln\left(\frac{N}{\sqrt{\pi}}\right)}$
$p_0(x) = \frac{1}{y_0} \mathbb{I}_{\{x \in [0, y_0]\}}$	$\bar{\tau}^N \sim \frac{y_0^2 \pi}{2DN^2}$	$p_0(x) = \frac{1}{y_0} \mathbb{I}_{\{x \in [0, y_0]\}}$	$\bar{\tau}^N \sim \frac{y_0^2 \pi}{2DN^2}$
$p_0(x) = \frac{1}{y_2 - y_1} \mathbb{I}_{\{x \in [y_1, y_2]\}}$	$\bar{\tau}^N \sim \frac{y_1^2}{4D \ln\left(\frac{N}{\sqrt{\pi}}\right)}$	$p_0(x) = \frac{1}{y_2 - y_1} \mathbb{I}_{\{x \in [y_1, y_2]\}}$	$\bar{\tau}^N \sim \frac{(\min(y_1, a - y_2))^2}{4D \ln\left(\frac{N}{\sqrt{\pi}}\right)}$
$p_0(x) = 2bx e^{-bx^2}$	$\bar{\tau}^N \sim \frac{1}{2DbN}$	$p_0(x) = \frac{2b}{1-e^{-bc^2}} xe^{-bx^2} \mathbb{I}_{\{x \in [0, c]\}}$	$\bar{\tau}^N \sim \frac{1-e^{-bc^2}}{2DbN}$
$p_0(x) = \frac{4b^{\frac{3}{2}}}{\sqrt{\pi}} x^2 e^{-bx^2}$	$\bar{\tau}^N \sim \frac{\pi^{\frac{3}{2}}}{4Db(2N)^{\frac{3}{2}}} \Gamma\left(\frac{5}{3}\right)$	-	-

To conclude, when there are N i.i.d. Brownian particles initially uniformly distributed in an interval that does not contain the escape points, either the real semi-axis or a bounded interval, then the MFAT has a similar decay with N for a Dirac delta function or a locally constant initial distribution.

1.3 MFAT in 2D

1.3.1 MFAT for a uniform initial distribution

We study here N i.i.d. Brownian particles in a confined domain in two dimensions $\Omega \subset \mathbb{R}^2$ as represented in Fig. 1.4. The particles are initially uniformly distributed in the region

$$\Omega^* = \{B_{r_2}(\mathbf{A}) \setminus B_{r_1}(\mathbf{A}) : \theta_1 \leq \theta \leq \theta_1 + \theta_2\}, \quad (1.29)$$

where $B_r(\mathbf{A})$ is a disk of radius r centered at \mathbf{A} . They can be absorbed from the domain through a single small absorbing arc of length 2ε centered at $\mathbf{x} = \mathbf{A}$ in the boundary $\partial\Omega_a$ of Ω . Here we consider the initial distribution for i.i.d Brownian particles given by

$$p(\mathbf{x}, 0) = \frac{1}{A(\Omega^*)} \mathbb{I}_{\{\mathbf{x} \in \Omega^*\}}(\mathbf{x}), \quad (1.30)$$

where the area of the region is $A(\Omega^*) = \frac{(r_2^2 - r_1^2)\theta_2}{2}$. The solution of the diffusion equation with a general initial condition is the convolution between the elementary solution $\tilde{p}(\mathbf{y}, t)$ with a Dirac delta initial distribution and the initial condition, this is

$$p(\mathbf{x}, t) = \int_{\Omega} \tilde{p}(\mathbf{y} - \mathbf{x}, t) p(\mathbf{y}, 0) d\mathbf{y}. \quad (1.31)$$

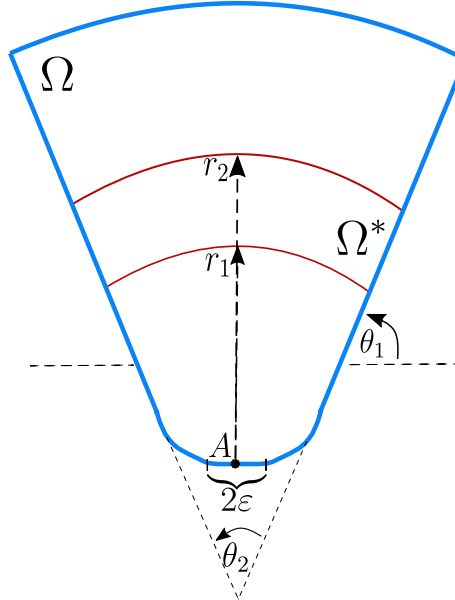


Figure 1.4: **Schematic representation of the two-dimensional domain to study the MFAT to a small arc.** The bounded domain Ω is delimited by the blue curve. The initial distribution of the Brownian particles is given by $p(\mathbf{x}, 0) = \frac{1}{A(\Omega^*)} \mathbb{I}_{\{\mathbf{x} \in \Omega^*\}}(\mathbf{x})$, where the region $\Omega^* = \{B_{r_2}(\mathbf{A}) \setminus B_{r_1}(\mathbf{A}) : \theta_1 \leq \theta \leq \theta_1 + \theta_2\}$ is delimited by the red curves.

Using the asymptotic solution computed in [71] for 2D, we obtain the approximation for the survival probability when t is small given by

$$\begin{aligned} S(t) &= \Pr\{t_1 > t\} \approx \frac{1}{A(\Omega^*)} \int_{\Omega^*} \left(1 - \frac{\sqrt{2}D\pi t}{2 \ln(\frac{1}{\varepsilon})} \frac{\exp\left\{-\frac{|\mathbf{A}-\mathbf{y}|^2}{4Dt}\right\}}{|\mathbf{A}-\mathbf{y}|^2} \right) d\mathbf{y} \\ &\approx 1 - \frac{\sqrt{2}D\pi t}{2 \ln(\frac{1}{\varepsilon}) A(\Omega^*)} \int_{\Omega^* - \mathbf{A}} \frac{\exp\left\{-\frac{|\mathbf{z}|^2}{4Dt}\right\}}{|\mathbf{z}|^2} d\mathbf{z}. \end{aligned}$$

Note now, $\Omega^* - \mathbf{A} = \{B_{r_2}(\mathbf{0}) \setminus B_{r_1}(\mathbf{0}) : \theta_1 \leq \theta \leq \theta_1 + \theta_2\}$, then $|\mathbf{z}|^2 = r^2$, where r is the distance to the point \mathbf{A} chosen as the origin of coordinates. Then we can rewrite the integral above as

$$\begin{aligned} S(t) &= 1 - \frac{\sqrt{2}D\pi t}{2 \ln(\frac{1}{\varepsilon}) A(\Omega^*)} \int_{r_1}^{r_2} \int_{\theta_1}^{\theta_1 + \theta_2} \frac{\exp\left\{-\frac{r^2}{4Dt}\right\}}{r^2} r d\theta dr \\ &= 1 - \frac{\sqrt{2}D\pi t}{2 \ln(\frac{1}{\varepsilon}) (r_2^2 - r_1^2)} \left(\text{Ei}\left(-\frac{r_2^2}{4Dt}\right) - \text{Ei}\left(-\frac{r_1^2}{4Dt}\right) \right), \end{aligned} \quad (1.32)$$

where $\text{Ei}(x) = -\int_{-x}^{\infty} \frac{e^{-t}}{t} dt$ is the exponential integral function [75]. For small t we expand this function and we obtain

$$S(t) \sim 1 - \frac{\sqrt{2}D\pi t}{2 \ln(\frac{1}{\varepsilon}) (r_2^2 - r_1^2)} \left(\frac{4Dt}{r_1^2} e^{-\frac{r_1^2}{4Dt}} - \frac{4Dt}{r_2^2} e^{-\frac{r_2^2}{4Dt}} \right). \quad (1.33)$$

Scaling $r_2 = (1 + \gamma)r_1$ and making an expansion when $\gamma \rightarrow 0$, we get

$$S(t) \sim 1 - \frac{\sqrt{2}\pi(4Dt)e^{-\frac{r_1^2}{4Dt}}}{8 \ln\left(\frac{1}{\varepsilon}\right) r_1^2} \left(1 + \frac{4Dt}{r_1^2} - 2\gamma \left(1 + \frac{r_1^2}{4Dt} \right) + O(\gamma^2) + O\left(\frac{\gamma}{t}\right) \right). \quad (1.34)$$

To conclude, when $\gamma \rightarrow 0$, the survival probability $S(t)$ is recovered for the case with the Dirac delta function at the points with $r = r_1$ as the initial condition. Thus to leading order, using that

$$\lim_{r_2 \rightarrow r_1} \Pr\{t_1 > t\} \sim 1 - \frac{\sqrt{2}\pi(4Dt)e^{-\frac{r_1^2}{4Dt}}}{8 \ln\left(\frac{1}{\varepsilon}\right) r_1^2},$$

we obtain to leading order the asymptotic formula when $\frac{N}{\ln\left(\frac{1}{\varepsilon}\right)}$ is large

$$\bar{\tau}_\varepsilon^N \approx \frac{r_1^2}{4D \ln\left(\frac{\sqrt{2}\pi N}{8 \ln\left(\frac{1}{\varepsilon}\right)}\right) + A_\varepsilon}, \quad (1.35)$$

where $A_\varepsilon = A_0 + \varepsilon A_1 + \dots$, where A_k are constants as before and r_1 is the shortest distance to the absorbing boundary. The MFAT for this case has a similar behavior as for the Dirac delta function.

1.3.2 MFAT for an initial distribution with a long-tail intersecting the target site

We study here the consequence of an initial distribution asymptotically intersecting the target site. For that goal, we consider the algebraic distribution modulated by a global exponential

$$p_1(\mathbf{x}) = K |\mathbf{x} - \mathbf{A}|^\alpha e^{-b|\mathbf{x} - \mathbf{A}|^2}. \quad (1.36)$$

The function $p_1(\mathbf{x})$ is the initial distribution for the diffusion equation (1.6), where the normalization constant is approximated on the full domain where we have added the small triangle at the summit between the dashed and the blue lines in Fig. 1.4 (the area of which is $O(\varepsilon^2)$). Thus we approximate normalization constant as

$$K^{-1} \approx \int_{\Omega} |\mathbf{x} - \mathbf{A}|^\alpha e^{-b|\mathbf{x} - \mathbf{A}|^2} dx = \int_0^R \int_{\theta_1}^{\theta_1 + \theta_2} r^\alpha e^{-br^2} r d\theta dr,$$

where R is the largest radius of the circular sector centered in \mathbf{A} that can be inscribed in Ω . This leads to the expression

$$K^{-1} = \frac{\theta_2}{2b^{\frac{2+\alpha}{2}}} \left(\Gamma\left(1 + \frac{\alpha}{2}\right) - \Gamma\left(1 + \frac{\alpha}{2}, bR^2\right) \right), \quad (1.37)$$

where $\Gamma(z)$ is the Gamma function and $\Gamma(z, t)$ is the incomplete Gamma function [76]. We can now estimate the survival probability

$$\begin{aligned}
 S(t) &= \Pr\{t_1 > t\} = \int_{\Omega} \int_{\Omega} \tilde{p}(\mathbf{x} - \mathbf{y}, t) K^{-1} |\mathbf{y} - \mathbf{A}|^{\alpha} e^{-b|\mathbf{y} - \mathbf{A}|^2} d\mathbf{y} d\mathbf{x} \\
 &\approx \int_{\Omega} K^{-1} \left(1 - \frac{\sqrt{2}D\pi t \exp\left\{-\frac{|\mathbf{A}-\mathbf{y}|^2}{4Dt}\right\}}{2 \ln\left(\frac{1}{\varepsilon}\right)} \frac{|\mathbf{A}-\mathbf{y}|^2}{|\mathbf{A}-\mathbf{y}|^2} \right) |\mathbf{y} - \mathbf{A}|^{\alpha} e^{-b|\mathbf{y} - \mathbf{A}|^2} d\mathbf{y} \\
 &\approx 1 - \frac{\sqrt{2}D\pi t}{2 \ln\left(\frac{1}{\varepsilon}\right) K} \int_{\Omega} |\mathbf{y} - \mathbf{A}|^{\alpha-2} e^{-\frac{4Dbt+1}{4Dt}|\mathbf{y}-\mathbf{A}|^2} d\mathbf{y} \\
 &\approx 1 - \frac{\sqrt{2}D\pi t \theta_2}{2 \ln\left(\frac{1}{\varepsilon}\right) K} \int_0^R r^{\alpha-1} e^{-\frac{4Dbt+1}{4Dt}r^2} dr \\
 &\approx 1 - \frac{\sqrt{2}\pi(4Dbt)^{\frac{\alpha+2}{2}} (\Gamma(\frac{\alpha}{2}) - \Gamma(\frac{\alpha}{2}, \frac{4Dbt+1}{4Dt}R^2))}{8 \ln\left(\frac{1}{\varepsilon}\right) (4Dbt+1)^{\frac{\alpha}{2}} (\Gamma(1 + \frac{\alpha}{2}) - \Gamma(1 + \frac{\alpha}{2}, bR^2))}.
 \end{aligned}$$

Thus for t small, we obtain the leading order approximation

$$S(t) \sim 1 - \frac{\sqrt{2}\pi\Gamma(\frac{\alpha}{2})}{8 \ln\left(\frac{1}{\varepsilon}\right) (\Gamma(1 + \frac{\alpha}{2}) - \Gamma(1 + \frac{\alpha}{2}, bR^2))} (4Dbt)^{\frac{\alpha+2}{2}},$$

and the formula for the MFAT given by

$$\begin{aligned}
 \bar{\tau}^N &\sim \int_0^\infty \exp\left\{-\frac{\sqrt{2}N\pi\Gamma(\frac{\alpha}{2})}{8 \ln\left(\frac{1}{\varepsilon}\right) (\Gamma(\frac{\alpha+2}{2}) - \Gamma(\frac{\alpha+2}{2}, bR^2))} (4Dbt)^{\frac{\alpha+2}{2}}\right\} dt \\
 &\sim \left(\frac{8 \ln\left(\frac{1}{\varepsilon}\right) (\Gamma(\frac{\alpha+2}{2}) - \Gamma(\frac{\alpha+2}{2}, bR^2))}{\sqrt{2}N\pi\Gamma(\frac{\alpha}{2})} \right)^{\frac{2}{\alpha+2}} \frac{1}{4Db} \Gamma\left(\frac{\alpha+4}{\alpha+2}\right).
 \end{aligned} \tag{1.38}$$

We can rewrite this formula as

$$\bar{\tau}^N \sim \frac{C_\Omega}{N^{\frac{2}{\alpha+2}}} \text{ for } \frac{N}{\ln\left(\frac{1}{\varepsilon}\right)} \gg 1, \tag{1.39}$$

where

$$C_\Omega = \frac{1}{4Db} \Gamma\left(\frac{\alpha+4}{\alpha+2}\right) \left(\frac{8 \ln\left(\frac{1}{\varepsilon}\right) (\Gamma(\frac{\alpha+2}{2}) - \Gamma(\frac{\alpha+2}{2}, bR^2))}{\sqrt{2}\pi\Gamma(\frac{\alpha}{2})} \right)^{\frac{2}{\alpha+2}}. \tag{1.40}$$

We believe that the present formula could be generalized to any dimension d , that would lead to a spectrum of possible decays of the MFAT with respect to the variable N . These decays will depend on the algebraic decay \mathbf{x}^α of the initial distribution at the target located at the origin, leading to the formulas

$$\bar{\tau}^N \sim \frac{C_\Omega}{N^{\frac{2}{\alpha+d}}} \text{ for } QN \gg 1, \tag{1.41}$$

where d is the dimension of Ω and Q is a constant related to the size of the exit window in the spatial domain. In dimension 2 we have $Q = (\ln(\frac{1}{\varepsilon}))^{-1}$.

1.4 Effect of a constant drift on extreme arrival

In half-a-line, we consider now the first arrival time of the N independent realizations of the process

$$\dot{x}_t = -a + \sqrt{2D}\dot{w}_t,$$

where a is a constant velocity and D the diffusion coefficient.

1.4.1 Effect of a constant drift when the initial distribution is a Dirac delta function

The Fokker-Planck Equation (FPE) is

$$\begin{aligned} \frac{\partial p(x,t)}{\partial t} &= D \frac{\partial^2 p(x,t)}{\partial x^2} + a \frac{\partial p(x,t)}{\partial x} \quad \text{for } x > 0, t > 0 \\ p(x,0) &= p_0(x) = \delta(x-y) \\ p(0,t) &= 0. \end{aligned} \tag{1.42}$$

To solve equation (1.42), we change the variable $p(x,t) = q(x,t) \exp\left\{\frac{-ax-a^2t/2}{2D}\right\}$, so that $q(x,t)$ satisfies the diffusion equation $\frac{\partial q(x,t)}{\partial t} = D \frac{\partial^2 q(x,t)}{\partial x^2}$. Thus the solution for $q(x,t)$ is given by equation (1.7) leading to

$$p(x,t) = \frac{\exp\left\{\frac{-a(x-y)-a^2t/2}{2D}\right\}}{\sqrt{4D\pi t}} \left[\exp\left\{-\frac{(x-y)^2}{4Dt}\right\} - \exp\left\{-\frac{(x+y)^2}{4Dt}\right\} \right].$$

The extreme escape time is given by relation (1.5)

$$\bar{\tau}^N = \int_0^\infty [S(t)]^N dt, \tag{1.43}$$

where the survival probability is

$$\begin{aligned} S(t) &= \int_0^\infty \frac{\exp\left\{\frac{-a(x-y)+a^2t/2}{2D}\right\}}{\sqrt{4D\pi t}} \left[\exp\left\{-\frac{(x-y)^2}{4Dt}\right\} - \exp\left\{-\frac{(x+y)^2}{4Dt}\right\} \right] dx \\ &= S_1(t) - S_2(t). \end{aligned}$$

with

$$S_1(t) = \frac{1}{\sqrt{\pi}} \int_{\frac{-y+at}{\sqrt{4D\pi t}}}^\infty \exp(-u^2) du \quad \text{and} \quad S_2(t) = \frac{1}{\sqrt{\pi}} \exp\left\{\frac{ay}{D}\right\} \int_{\frac{y+at}{\sqrt{4D\pi t}}}^\infty \exp(-u^2) du.$$

We rewrite the sum $S(t) = H_1(t) + H_2(t)$,

$$\begin{aligned} H_1(t) &= \frac{1}{2} \left(\operatorname{erfc}\left(\frac{-y+at}{\sqrt{4D\pi t}}\right) - \operatorname{erfc}\left(\frac{y+at}{\sqrt{4D\pi t}}\right) \right) \\ H_2(t) &= \frac{1}{2} \left(1 - \exp\left\{\frac{ay}{D}\right\} \right) \operatorname{erfc}\left(\frac{y+at}{\sqrt{4D\pi t}}\right). \end{aligned}$$

We obtain for short-time asymptotic,

$$H_1(t) \sim 1 - \sqrt{4Dt} \frac{e^{-\frac{y^2}{4Dt}}}{y\sqrt{\pi}}$$

$$H_2(t) \sim \left(1 - \exp\left\{\frac{ay}{D}\right\}\right) \sqrt{Dt} \frac{e^{-\frac{y^2}{4Dt}}}{y\sqrt{\pi}}.$$

Thus, $S(t) \approx 1 - \sqrt{Dt} \left(1 + \exp\left\{\frac{ay}{D}\right\}\right) \frac{e^{-\frac{y^2}{4Dt}}}{y\sqrt{\pi}}$ leading to an approximation for the pdf given by

$$\Pr\left\{\tau^1 \in [t+dt]\right\} \sim \frac{N\sqrt{4Dt} \frac{(1+e^{\frac{ay}{D}})}{2}}{y\sqrt{\pi}} \exp\left\{-\frac{N\sqrt{4Dt}(1+e^{\frac{ay}{D}})}{2} \frac{e^{-\frac{y^2}{(4Dt)}}}{y\sqrt{\pi}}\right\} e^{-\frac{y^2}{4Dt}} \left[\frac{1}{2t} + \frac{y^2}{4Dt^2}\right] dt. \quad (1.44)$$

and to the asymptotic approximation

$$\bar{\tau}^N = \int_0^\infty S(t)^N dt \sim \int_0^\infty \exp\left\{-N\sqrt{4Dt} \frac{(1+\exp\left\{\frac{ay}{D}\right\})}{2} \frac{e^{-\frac{y^2}{(4Dt)}}}{y\sqrt{\pi}}\right\} dt. \quad (1.45)$$

Using the Laplace method, we obtain for $N(1 + \exp\left\{\frac{ay}{D}\right\})$ large the MFAT formula

$$\bar{\tau}^N \sim \frac{y^2}{4D \ln\left(N \frac{(1+\exp\left\{\frac{ay}{D}\right\})}{2\sqrt{\pi}}\right)}. \quad (1.46)$$

To conclude, in the large N limit, adding a negative drift $a < 0$, leads to a small increase in the extreme arrival time. The formula (1.46) reveals how adding a drift can be equivalent to augmenting or reducing the number of initial particles by a factor $\exp(\frac{ay}{D})$, depending on the sign of a .

Finally, we tested the quality of the analytical approximation of the pdfs with the stochastic simulations for the shortest arrival time (1.44) with drifts $a = 1$ and $a = -1$ respectively and for different values of N (Fig. 1.5A and B). The MFAT decreases with N (Fig. 1.5C) according to equation (1.45) for $a = -1$ in red and $a = 1$ in blue. Also, notice the good agreement between the stochastic simulations and the analytical results in the log-log scale (Fig. 1.5C right) for N large.

1.4.2 Effect of a constant drift for a uniform initial distribution

When the particles are initially uniformly distributed in a small interval, $[0; y_0]$, the initial condition is given by formula $p(x, 0) = \frac{1}{y_0} \mathbb{I}_{[x \in [0, y_0]]}$, and the solution of the diffusion equation with a drift (1.42) is given by

$$p(x, t) = e^{\frac{-ax - a^2t/2}{2D}} \int_0^{y_0} \frac{\exp\left\{\frac{ay}{2D}\right\}}{\sqrt{4\pi Dt} y_0} \left[\exp\left\{-\frac{(x-y)^2}{4Dt}\right\} - \exp\left\{-\frac{(x+y)^2}{4Dt}\right\} \right] dy$$

$$= \frac{1}{2y_0} \left[\operatorname{erfc}\left(\frac{x-y_0+at}{\sqrt{4Dt}}\right) - \operatorname{erfc}\left(\frac{x+at}{\sqrt{4Dt}}\right) - e^{-\frac{ax}{D}} \left(\operatorname{erfc}\left(\frac{x-at}{\sqrt{4Dt}}\right) - \operatorname{erfc}\left(\frac{x+y_0-at}{\sqrt{4Dt}}\right) \right) \right].$$

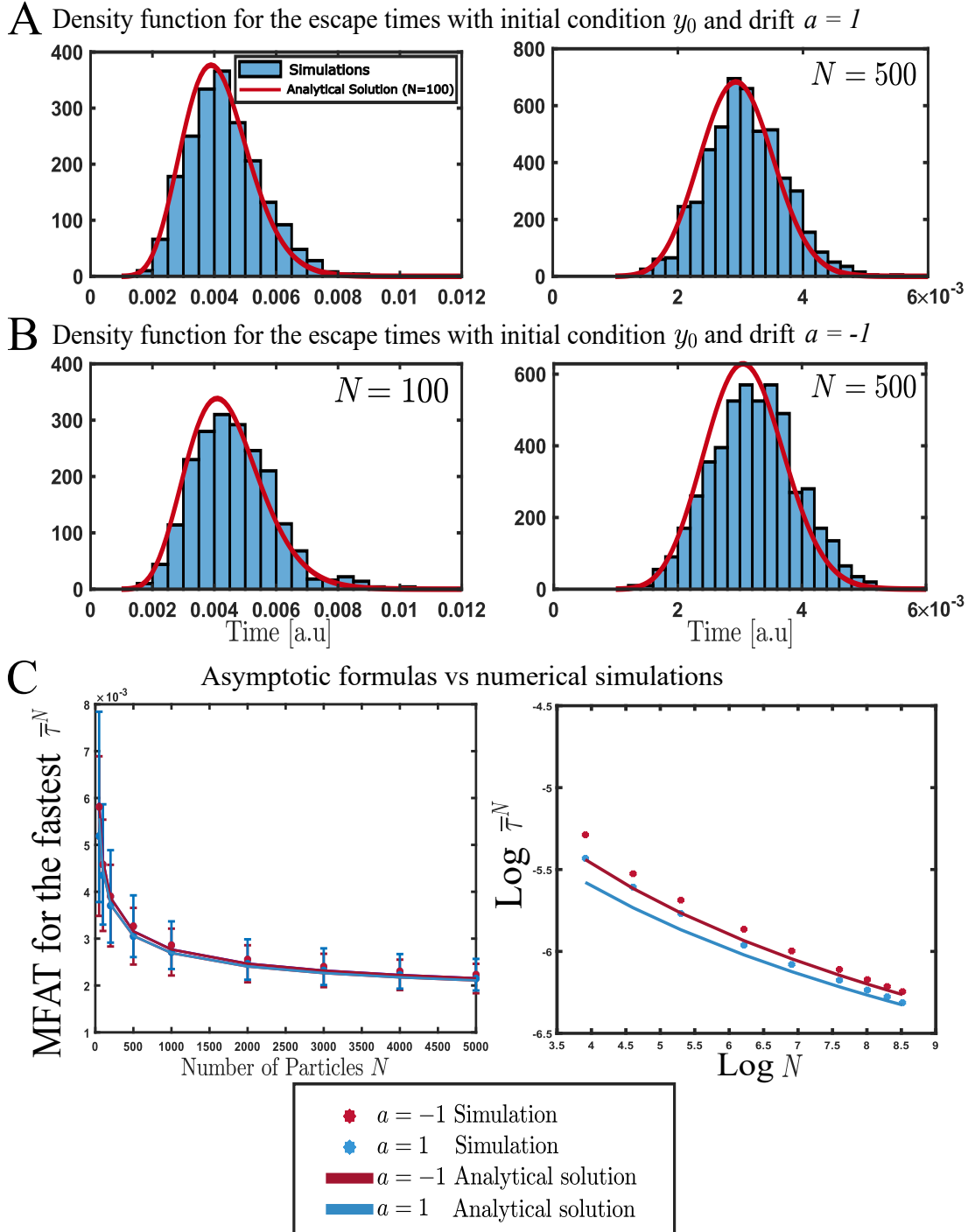


Figure 1.5: Mean fastest arrival time vs the number of particles N with a drift. **A.** Distribution of the arrival time $\bar{\tau}^N$: analytical represented by equation (1.44) (in red) vs stochastic simulations (blue histogram) for particles started at $y_0 = 0.25$ and a drift $a = 1$ for $N = 500$ (left) and $N = 500$ (right) with 1000 runs. **B.** Distribution of the arrival time $\bar{\tau}^N$: analytical expression (1.44) (in red) vs stochastic simulations (blue histogram) with drift $a = -1$. **C.** MFAT vs N obtained from stochastic simulations (colored disks) and the asymptotic formula (1.46) (continuous lines) with $y_0 = 0.25$ and 1000 runs.

Then the survival probability is

$$\begin{aligned} S(t) &= \frac{1}{2y_0} \int_0^\infty \left(\operatorname{erfc}\left(\frac{x-y_0+at}{\sqrt{4Dt}}\right) - \operatorname{erfc}\left(\frac{x+at}{\sqrt{4Dt}}\right) \right) dx \\ &- \frac{1}{2y_0} \int_0^\infty e^{-\frac{ax}{D}} \left(\operatorname{erfc}\left(\frac{x-at}{\sqrt{4Dt}}\right) - \operatorname{erfc}\left(\frac{x-at+y_0}{\sqrt{4Dt}}\right) \right) dx \\ &= S_1(t) + S_2(t). \end{aligned}$$

Using the change of variable $u = \frac{x}{\sqrt{4D\pi t}}$ we can obtain,

$$\begin{aligned} S_1(t) &= \frac{1}{2y_0} \left(-a \operatorname{terf}\left(\frac{at}{\sqrt{4Dt}}\right) + \frac{\sqrt{4Dt}}{\sqrt{\pi}} e^{-\frac{(y_0-at)^2}{4Dt}} - y_0 \operatorname{erf}\left(\frac{at-y_0}{\sqrt{4Dt}}\right) \right. \\ &\quad \left. - \frac{\sqrt{4Dt}}{\sqrt{\pi}} e^{-\frac{a^2 t^2}{4Dt}} + y_0 + a \operatorname{terf}\left(\frac{at-y_0}{\sqrt{4Dt}}\right) \right). \end{aligned}$$

Then, using the change of variable $u = \frac{x-at}{\sqrt{4Dt}}$ and integrating by parts, we obtain

$$S_2(t) = \frac{D}{2ay_0} \left(-2 \operatorname{erf}\left(\frac{at}{\sqrt{4Dt}}\right) + \operatorname{erfc}\left(\frac{y_0-at}{\sqrt{4Dt}}\right) - \operatorname{erfc}\left(\frac{y_0+at}{\sqrt{4Dt}}\right) e^{\frac{ay_0}{D}} \right).$$

Thus, making the asymptotic expansion for t small, we obtain the approximation

$$S(t) \sim 1 - \frac{\sqrt{4Dt}}{\sqrt{\pi} y_0},$$

leading to the asymptotic formula for MFAT when N is large

$$\bar{\tau}^N \sim \frac{y_0^2 \pi}{2DN^2}.$$

This result is the one obtained in the case of no drift, showing that the drift does not affect the extreme arrival time when the absorbing point overlaps with the interval where the particles are initially uniformly distributed.

1.4.3 Effect of a constant drift for a uniform initial distribution not intersecting the target

When the particles are uniformly distributed in the interval $[y_1, y_2]$ with $y_2 > y_1 > 0$, the initial distribution is of the form $p_0(x) = \frac{1}{y_2-y_1} \mathbb{I}_{\{x \in [y_1, y_2]\}}$. The solution of the diffusion equation (1.42) is given by

$$\begin{aligned} p(x, t) &= e^{\frac{-ax - a^2 t/2}{2D}} \int_{y_1}^{y_2} \frac{\exp\left\{\frac{ay}{2D}\right\}}{\sqrt{4\pi Dt}(y_2-y_1)} \left[\exp\left\{-\frac{(x-y)^2}{4Dt}\right\} - \exp\left\{-\frac{(x+y)^2}{4Dt}\right\} \right] dy \\ &= \frac{1}{2(y_2-y_1)} \left[\operatorname{erfc}\left(\frac{x-y_2+at}{\sqrt{4Dt}}\right) - \operatorname{erfc}\left(\frac{x-y_1+at}{\sqrt{4Dt}}\right) \right. \\ &\quad \left. - e^{-\frac{ax}{D}} \left(\operatorname{erfc}\left(\frac{x+y_1-at}{\sqrt{4Dt}}\right) - \operatorname{erfc}\left(\frac{x+y_2-at}{\sqrt{4Dt}}\right) \right) \right], \end{aligned}$$

and we can compute the survival probability as

$$\begin{aligned} S(t) &= \frac{1}{2(y_2 - y_1)} \int_0^\infty \left(\operatorname{erfc}\left(\frac{x - y_2 + at}{\sqrt{4Dt}}\right) - \operatorname{erfc}\left(\frac{x - y_1 + at}{\sqrt{4Dt}}\right) \right) dx \\ &\quad - \frac{1}{2(y_2 - y_1)} \int_0^\infty e^{-\frac{ax}{D}} \left(\operatorname{erfc}\left(\frac{x + y_2 - at}{\sqrt{4Dt}}\right) - \operatorname{erfc}\left(\frac{x + y_1 - at}{\sqrt{4Dt}}\right) \right) dx \\ &= S_1(t) + S_2(t). \end{aligned}$$

And, proceeding as before, we obtain

$$\begin{aligned} S_1(t) &= \frac{1}{2(y_2 - y_1)} \left(2(y_2 - y_1) - (y_2 - at)\operatorname{erfc}\left(\frac{y_2 - at}{\sqrt{4Dt}}\right) + (y_1 - at)\operatorname{erfc}\left(\frac{y_1 - at}{\sqrt{4Dt}}\right) \right. \\ &\quad \left. + \frac{\sqrt{4Dt}}{\sqrt{\pi}} \exp\left\{-\frac{(y_2 - at)^2}{4Dt}\right\} - \frac{\sqrt{4Dt}}{\sqrt{\pi}} \exp\left\{-\frac{(y_1 - at)^2}{4Dt}\right\} \right) \end{aligned}$$

and

$$\begin{aligned} S_2(t) &= \frac{-D}{2a(y_2 - y_1)} \left(\operatorname{erfc}\left(\frac{y_1 - at}{\sqrt{4Dt}}\right) - \operatorname{erfc}\left(\frac{y_2 - at}{\sqrt{4Dt}}\right) \right. \\ &\quad \left. - e^{\frac{ay_1}{D}} \operatorname{erfc}\left(\frac{y_1 + at}{\sqrt{4Dt}}\right) + e^{\frac{ay_2}{D}} \operatorname{erfc}\left(\frac{y_2 + at}{\sqrt{4Dt}}\right) \right). \end{aligned}$$

The asymptotic short-time expansion leads to the approximation

$$\begin{aligned} S(t) &\approx 1 - \frac{D\sqrt{Dt}}{a(y_2 - y_1)\sqrt{\pi}} \left[\frac{\exp\left\{-\frac{(y_1 - at)^2}{4Dt}\right\}}{y_1 - at} - \frac{\exp\left\{-\frac{(y_2 - at)^2}{4Dt}\right\}}{y_2 - at} \right. \\ &\quad \left. + \exp\left\{\frac{ay_2}{D}\right\} \frac{\exp\left\{-\frac{(y_2 + at)^2}{4Dt}\right\}}{y_2 + at} - \exp\left\{\frac{ay_1}{D}\right\} \frac{\exp\left\{-\frac{(y_1 + at)^2}{4Dt}\right\}}{y_1 + at} \right]. \end{aligned} \quad (1.47)$$

We shall consider the case where $y_2 = y_1(1 + \varepsilon)$ in formula (1.47), and ε tends to zero, thus

$$S(t) \sim S_0(t) + S_1(t)\varepsilon + S_2(t)\frac{\varepsilon^2}{2} + \dots \quad (1.48)$$

where

$$\begin{aligned} S_0(t) &= 1 - \frac{\sqrt{Dt}\exp\left\{-\frac{y_1^2}{(4Dt)}\right\}}{y_1\sqrt{\pi}} \left(1 + e^{\frac{ay_1}{4Dt}} \right) \\ S_1(t) &= \frac{3}{\sqrt{4D\pi t}} \exp\left\{-\frac{(y_1 - at)^2}{(4Dt)}\right\} - \frac{a}{2D} e^{\frac{ay_1}{4Dt}} \operatorname{erfc}\left(\frac{y_1 + at}{\sqrt{4Dt}}\right) \\ &\quad + \frac{D(y_1 - at)}{2aDt\sqrt{4Dt}} \exp\left\{-\frac{(y_1 - at)^2}{(4Dt)}\right\} \left(1 - e^{\frac{ay_1}{4Dt}} \right) \end{aligned}$$

When $\varepsilon \rightarrow 0$ (that is $y_2 \rightarrow y_1$), we recover in equation (1.48), the survival probability for the Dirac delta function $\delta(x - y_1)$, but we cannot obtain the MFAT due to the exponentially small terms that appear canceling with each other when ε and $\frac{\varepsilon}{t}$ are small. Thus, to leading order, we have for $N \left(1 + \exp\left\{\frac{ay}{D}\right\}\right)$ large

$$\bar{\tau}^N \sim \frac{y_1^2}{4D \ln\left(\frac{N\left(1 + \exp\left\{\frac{ay}{D}\right\}\right)}{2\sqrt{\pi}}\right)}. \quad (1.49)$$

1.5 Discussion and concluding remarks

In summary, we have obtained several asymptotic formulas for the mean time of the fastest Brownian particles to reach a target. These formulas crucially depend on the initial distribution toward the isolate target: we found algebraic vs $1/\ln N$ decays depending on the different initial density profile. In the context of extreme value statistics, the first arrival time τ^1 is the minimum among the random arrival times

$$\tau^1 = \min(t_1, t_2, \dots, t_N) \geq 0, \quad (1.50)$$

and thus the limiting distribution is given by the Weibull law. This is the case when the target site located at the origin is included in the support of the initial distribution of the particles. Indeed, in that case, the pdf of the first arrival times behaves as a power law near zero. The Weibull expression implies the algebraic dependence of τ^1 with N . However, if the origin is not part of the initial density profile, the pdf of the first arrival times has an essential singularity at small argument (see above equation (1.11)). Consequently, the limiting form is not a Weibull distribution but instead it resembles a Gumbel distribution, which in turn implies a decay in the form of $\frac{1}{\ln N}$, as discussed in the review [64] (below equation (1.33) therein).

In general, the renewal interest of extreme statistics [39, 63, 77] is due to recent direct applications in cell biology [57, 78–80] which appears as a frame to explain fast molecular activation. The frame of extreme statistics can be used to compute how the molecular activation time depends on the main parameters, involving the geometrical organization and the dynamics (diffusion or other stochastic processes). The fastest molecules to activate a target site uses the shortest path, thus showing that the redundancy property can overcome the hindrance of a crowded environment.

This redundancy principle is ubiquitous in cell biology: One class of example is calcium signaling that can be amplified by activating the calcium-induced calcium released pathway [55]. This amplification does not require the transport of all ions but only the first ones to arrive to a specific targets made of few clustered receptors. The amplification occurs in few milliseconds instead of hundreds of milliseconds as would be predicted by the time scale of the classical diffusion and the narrow escape theory [11] at synapse of neuronal cells [81–84]. Interestingly the arrival time of the fastest among N decays with $\frac{\delta^2}{\ln N}$, when the source and the target are well separated by a distance δ . However, there are several situations where choosing the Dirac delta function might not be the best model, as we discussed here. For example, when the particle injection could take a certain time, an extended initial distribution can build up, that could be approximated by a Gaussian or any other related distribution with an algebraic decay, especially when the motion can be modeled as anomalous diffusion (see relation (1.12)).

Another transduction applications concerns the activation of secondary messengers such as IP_3^+ receptors involved in the genesis of calcium wave in astrocytes [85] or the fast activation of TRP channels in fly photo-receptor, which are located very close to the source of the photo-conversion. In addition, we obtained here a novel formula when the dynamics contains a local constant flow added to the Brownian component. A local flow could accelerate the transport of the fastest molecules, which could be the case for the delivery occurring inside the endoplasmic reticulum network [86]. This network is indeed composed of thin tubules well approximated as dimension one segment intersecting at nodes.

Finally, it would be interesting to extend the present analysis to the case of exiting from a basin of attraction and study the mean arrival time of the fastest particle. The case of an Ornstein-Uhlenbeck (OU) process is already delicate as there is no exact closed formula for the survival probability with a zero absorbing boundary condition at a given threshold. Indeed for an OU pro-

cess $dx = -\theta xdt + \sqrt{2D}dw$ centered at the origin with an absorbing boundary at $x = 0$, initial point at $x = y$ and $\theta \geq 0$, the arrival time for the fastest is given at leading order by the same formula as if there was only diffusion and no drift. In this very particular case, the solution has the form

$$p(x, t) = \sqrt{\frac{\theta}{2\pi D(1 - e^{-2\theta t})}} \left[\exp \left\{ -\frac{\theta}{2D} \frac{(x - ye^{-\theta t})^2}{(1 - e^{-2\theta t})} \right\} - \exp \left\{ -\frac{\theta}{2D} \frac{(x + ye^{-\theta t})^2}{(1 - e^{-2\theta t})} \right\} \right] \quad (1.51)$$

and the survival probability is

$$\Pr \{t_1 > t\} = 1 - \operatorname{erfc} \left(\frac{\sqrt{\theta}ye^{-\theta t}}{\sqrt{2D(1 - e^{-2\theta t})}} \right). \quad (1.52)$$

Then, for t small, we have

$$\bar{\tau}^N \sim \frac{y^2}{4D \ln \left(\frac{N}{\sqrt{\pi}} \right)}. \quad (1.53)$$

However for other cases in which the absorbing boundary is not at the maximum point of the parabola, a general approximated formula [87] has been proposed, correcting erroneous expression found in the literature. At this stage, we could not use their complex formula to estimate the time of the fastest. We speculate that the formula for the mean arrival time for the fastest should be associated not with the Euclidean distance but with the control problem for the Freidlin-Wentzell functional in the Large-Deviation theory, a project for a future investigation.

1.6 Appendix: Algorithm to simulate the stochastic trajectory of the fastest particles when the initial distribution can intersect with the target

To simulate the arrival of the fastest particle to an absorbing boundary, we use the classical Euler's scheme [88]. When the source is well separated from the absorbing boundary, we follow each Brownian particle and estimated the time for the first one to arrive.

When particles are initially positioned with a distribution that could intersect with the absorbing boundary, the simulation scheme requires more attention, because in principle, particles can be found as close as we wish to the absorbing boundary, and thus the discretization time step could influence the time of the fastest. We thus design the following algorithm:

1. We generated N initial positions uniformly distributed: $\chi_1, \dots, \chi_N \in [0, y_0]$, where 0 and a are the absorbing boundaries and $y_0 \ll a$.
2. The time step Δt of the Euler's scheme depends on the shortest distance

$$\delta_N = \min_N \{|\chi_1|, \dots, |\chi_N|\}, \quad (1.54)$$

so that the mean square jump is smaller than the shortest distance:

$$\Delta t \leq p \frac{\delta_N^2}{2D}, \quad (1.55)$$

where D is the diffusion coefficient, $p < 1$ is a security parameter. In practice, we choose $p = 0.2$.

3. For each realization ω , we generated a simulation following step 1 and 2 and computed the first arrival time of the fastest:

$$\tau_{\omega_j}^N = \inf_{i=1..N} t_{i,j}, \quad (1.56)$$

where $j = \inf_k \{X(k\Delta t) \leq 0 | X((k-1)\Delta t) > 0 \text{ or } X(k\Delta t) \geq a | X((k-1)\Delta t) < a\}$.

4. We approximate the mean fastest arrival time by the empirical sums:

$$\bar{\tau}_m^N = \frac{1}{m} \sum_1^m \tau_{\omega_j}^N, \text{ with } \bar{\tau}^N = \lim_{m \rightarrow +\infty} \bar{\tau}_m^N. \quad (1.57)$$

Chapter 2

Diffusion with point-sink killing fields for fast calcium signaling at synapses

Published in *TOSTE S. & HOLCMAN D.*, “Extreme diffusion with point-sink killing fields for fast calcium signaling at synapses” *SIAM Journal on Applied Mathematics*, 10.1137/22M1476319 (2023).

arXiv:2201.05915 / hal:04101395

Abstract

We study here the time for the fastest diffusing particle to escape from the boundary of an interval with point-sink killing sources. The killing represents a degradation that leads to the probabilistic removal of the moving Brownian particles. We compute asymptotically the mean time it takes for the fastest particle escaping alive and obtain the statistic distribution. These computations relies on an explicit expression for the time dependent flux of the Fokker-Planck equation using the time dependent Green’s function and Duhamel’s formula. We obtain a general formula for several point-sink killing, showing how they directly interact. The range of validity of the present formula for the mean times of the fastest is evaluated with Brownian simulations. Finally, we discuss some applications to the early calcium signaling at neuronal synapses.

2.1 Introduction

For more than a century, the time scale of molecular activation has relied on the Smoluchowski’s computation for the flux of a single particle reaching an absorbing sphere, a process modeled by the associated diffusion equation [10, 89–91]. This flux defines the reciprocal of the forward binding rate and also the time scale of cellular activation with a single molecular event. However, recently the time scale of activation for signaling event associated with calcium transients at neuronal synapses was found to be much faster than the one predicted by Smoluchowski’s rate. This paradox about the fast time scale can be explained by the extreme statistical events [39] for the arrival time of the fastest particles among many [40, 66, 92]. Briefly, there is no need of transporting a distribution of particles from one region to another to generate a response: the fastest arriving particles are sufficient to trigger the needed events after finding and binding to the key narrow targets. This event can for example open a channel that can trigger the release of the same species. This is well

known in the case of calcium, known as calcium-induced calcium release [51]. The time of the fastest particle to arrive to a small target is in fact modulated by the initial copy number of identically distributed random particles. Recently, we hypothesize that this number sets the time to activation in most signaling molecular events, reproduction, gene expression and it is thus, a fundamental achievement of life evolution at mostly all levels [57, 58, 79, 80, 93–97]. Such large number guarantees that a rare event that would be impossible to trigger in a reasonable time scale, will actually take place by the fastest particles in a reasonable time. This large number compensates for the unknown position of the small targets and the hidden geometry to be explored. The initial distribution of particles is often well separated from these target. This large number has been well calibrated for each applications, summarized as the redundancy principle [93].

The extreme statistics theory allows to compute the mean time of the fastest with respect to the parameters of the problem such as the diffusion coefficient for a diffusion process, the distance to the source and the initial number of particle [63, 98, 99]. These computations have been extended to sub- and super- diffusion, but also when the initial distribution can extend close to the target window [67, 100–103].

In the present manuscript, we study the role of a killing source that can terminate the trajectory of a random particle before it can reach a target. The killing rate is the probability per unit time and unit length to terminate a trajectory. However, a moving particle can pass through a killing site many times without being terminated, in contrast to an absorbing boundary, where the trajectory is terminated with probability 1. Such a killing event can modify the escape time, due to the probability to be killed before escape [8]. The probability of reaching small target and the conditional mean times are relevant to quantify the success of viral infection in cells [9] or spermatozoa in the uterus [68, 104, 105]. We are interested here, in computing the mean time it takes for the fastest among many independent and equally distributed Brownian particles to reach a target when the killing term is a sum of Dirac delta functions located in an interval. To illustrate the present approach and the relevance of dimension reduction, we shall use two examples from neuroscience: the first one concerns the spillover of neurotransmitters such glutamate after synaptic activation. The neurotransmitters diffuse near glial cells that contains transporters (Fig. 2.1A), the role of which is to remove these neurotransmitters from the extra-cellular space. This extrusion mechanism can be modeled as a one dimensional diffusion process with killing in an interval due the small space separation along the thin axon or dendrite. The second example concerns calcium dynamics in dendritic spines: the fastest calcium ions that enter following synaptic activation can trigger fast calcium release. However the fastest calcium ions should be interrupted by long-time binding buffers or extruded by pumps on their way to the base of the spine (Fig. 2.1B). This interruption mechanism can be modeled as well by a killing term. We will also discuss below the case of calcium bound to calmodulin that can activate the CaMKII kinase. We propose to compute the probability and the mean time to activate a CaMKII [106]. This activation is relevant for the induction of long-term memory at a synaptic level. Here the relevant time is the first time that one CaM containing two calcium ions will arrive at a CAMKII before it exits. This process is computed as the first bound to CaMKII, modeled by a removal.

In these examples, the role of the killing term is to terminate the particle trajectories at random times. The effect of the killing term is accounted by an additive term in the Fokker-Planck equation, that describes the probability density function of the survival process before escape occurs [8, 107–110].

This chapter is organized as follows: in section 2.2, we summarize the background: stochastic formulation and Fokker-Planck equation relevant to compute the mean first escape time under a killing field [111]. In section 2.3, using a short-time asymptotic expansion for the solution of the

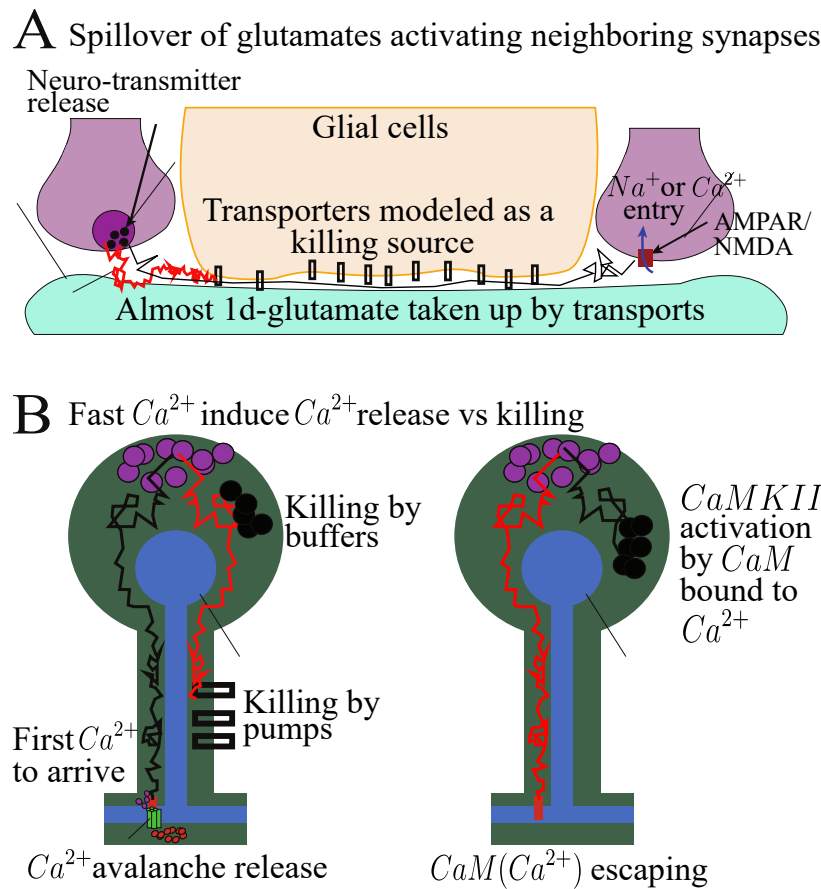


Figure 2.1: **Escape versus killing in the regulation of molecular neuronal signaling.** **A.** Spillover of neurotransmitters after synaptic activation between glial cells (yellow), that contain transporters (modeled as killing term) to remove them from the extra-cellular space. Each trajectory can be terminated (red) or can arrive to receptors to activate the influx of ion in the neighboring synaptic terminal (purple). **B.** Left: Calcium dynamics in a dendritic spine: the fastest calcium ions can trigger a process called calcium-induce calcium-release, if the ions are not stopped by a long-time binding buffer or extruded by pumps. Right: CaMKII kinase activation by calcium bound to calmodulin molecules. The probability and the mean time to activate the kinase CaMKII by the first calmodulin bound to calcium is one of the application explained here.

diffusion equation with a single and multiples Dirac delta killing terms, we derive the formulas for the mean first escape time among many trajectories that escape before being killed in the non-negative real line. In section 2.4, we compare the asymptotic result with respect to the stochastic simulations. In section 2.4.2, we apply the present concept to model and determine the time of key calcium activation processes that can trigger long-term memory in dendritic spines.

2.2 General formulas previously derived for the killing framework

We review here the arrival time definition for a stochastic process with a killing term as defined in section 0.1.2. We consider a stochastic process $\mathbf{x}(t)$ in the domain Ω satisfying the equation

$$d\mathbf{x} = \mathbf{b}(\mathbf{x}) dt + \sqrt{2}\mathbf{B}(\mathbf{x}) d\mathbf{w}(t) , \text{ for } \mathbf{x} \in \Omega, \quad (2.1)$$

where $\mathbf{b}(\mathbf{x})$ is a smooth drift vector, $\mathbf{B}(\mathbf{x})$ is a diffusion matrix, and $\mathbf{w}(t)$ is a vector of independent standard Brownian motions. A killing rate $k(\mathbf{x})$ is added in the domain Ω with boundary $\partial\Omega = \partial\Omega_a \cup \partial\Omega_r$, where $\partial\Omega_a$ is a small absorbing part and $\partial\Omega_r$ is the reflecting boundary. The transition probability density function (pdf) of the process $\mathbf{x}(t)$ with killing and absorption is the pdf of trajectories that have neither been killed nor absorbed in $\partial\Omega_a$ by time t ,

$$p(\mathbf{x}, t | \mathbf{y}) d\mathbf{x} = \Pr\{\mathbf{x}(t) \in \mathbf{x} + d\mathbf{x}, \tau^k > t, \tau^e > t | \mathbf{y}\},$$

where τ^k is the time for the particle to be killed and τ^e is the time of absorption. This pdf is the solution of the Fokker-Planck equation (FPE) [10]

$$\frac{\partial p(\mathbf{x}, t | \mathbf{y})}{\partial t} = \mathcal{L}_{\mathbf{x}} p(\mathbf{x}, t | \mathbf{y}) - k(\mathbf{x}) p(\mathbf{x}, t | \mathbf{y}) \quad \text{for } \mathbf{x}, \mathbf{y} \in \Omega, \quad (2.2)$$

where $\mathcal{L}_{\mathbf{x}}$ is the forward operator

$$\mathcal{L}_{\mathbf{x}} p(\mathbf{x}, t | \mathbf{y}) = \sum_{i,j=1}^d \frac{\partial^2 D^{i,j}(\mathbf{x}) p(\mathbf{x}, t | \mathbf{y})}{\partial x^i \partial x^j} - \sum_{i=1}^d \frac{\partial b^i(\mathbf{x}) p(\mathbf{x}, t | \mathbf{y})}{\partial x^i}, \quad (2.3)$$

and $\mathbf{D}(\mathbf{x}) = \frac{1}{2}\mathbf{B}(\mathbf{x})\mathbf{B}^T(\mathbf{x})$. The operator $\mathcal{L}_{\mathbf{x}}$ can be written in the divergence form $\mathcal{L}_{\mathbf{x}} p(\mathbf{x}, t | \mathbf{y}) = -\nabla \cdot \mathbf{J}(\mathbf{x}, t | \mathbf{y})$, where the components of the flux density vector $\mathbf{J}(\mathbf{x}, t | \mathbf{y})$ are

$$J^i(\mathbf{x}, t | \mathbf{y}) = - \sum_{j=1}^d \frac{\partial D^{i,j}(\mathbf{x}) p(\mathbf{x}, t | \mathbf{y})}{\partial x^j} + b^i(\mathbf{x}) p(\mathbf{x}, t | \mathbf{y}), \quad (i = 1, 2, \dots, d).$$

The initial and boundary conditions for the FPE (2.2) are

$$\begin{aligned} p(\mathbf{x}, 0 | \mathbf{y}) &= \delta(\mathbf{x} - \mathbf{y}) \text{ for } \mathbf{x}, \mathbf{y} \in \Omega \\ p(\mathbf{x}, t | \mathbf{y}) &= 0 \text{ for } t > 0, \mathbf{x} \in \partial\Omega_a, \mathbf{y} \in \Omega \\ \mathbf{J}(\mathbf{x}, t | \mathbf{y}) \cdot \mathbf{n}(\mathbf{x}) &= 0 \text{ for } t > 0, \mathbf{x} \in \partial\Omega - \partial\Omega_a, \mathbf{y} \in \Omega. \end{aligned}$$

The particular case where there is no drift vector, this is $\mathbf{b}(\mathbf{x}) = 0$, the FPE with the initial and boundary conditions written as above, models the Brownian motion of particles that start at point \mathbf{y} . These particles are absorbed at point $x = 0$ or degraded by the effect of the killing term $k(\mathbf{x})$. The absorption probability flux on $\partial\Omega_a$ is

$$J(t | \mathbf{y}) = \oint_{\partial\Omega} \mathbf{J}(\mathbf{x}, t | \mathbf{y}) \cdot \mathbf{n}(\mathbf{x}) dS_{\mathbf{x}}, \quad (2.4)$$

and $\int_0^\infty J(t | \mathbf{y}) dt$ is the probability of trajectories that have been absorbed at $\partial\Omega_a$.

For N independent identically distributed copies of the stochastic process (2.1), that can escape at

time t_1, \dots, t_N , prior to get killed, we consider the escape time of the fastest one and we shall derive here a formula for the probability and mean escape time of the fastest Brownian motion. Note that $t_i = +\infty$ if the i -th particle was killed. The mean first passage time (MFPT) is the fastest time for a particle to escape through the narrow window located on the surface of the domain Ω , that is

$$\tau^e(N) = \min_N \{t_1, \dots, t_N\}.$$

All these times are conditioned to the fact that at least one particle survived. Then, $\tau^e(N)$ is always a finite quantity. We denote here by n the random variable for the amount of surviving particles. The conditional MFPT, when at least one particle survives, can be expressed in terms of the absorption probability flux as

$$\mathbb{E}[\tau^e(N) | n \geq 1, \mathbf{y}] = \int_0^\infty \frac{\left(1 - \int_0^t J(s | \mathbf{y}) ds\right)^N - \left(1 - \int_0^\infty J(s | \mathbf{y}) ds\right)^N}{1 - \left(1 - \int_0^\infty J(s | \mathbf{y}) ds\right)^N} dt. \quad (2.5)$$

When all particles survive, this is $n = N$ the conditional MFPT can be written as

$$\mathbb{E}[\tau^e(N) | n = N, \mathbf{y}] = \int_0^\infty \left[1 - \frac{\int_0^t J(s | \mathbf{y}) ds}{\int_0^\infty J(s | \mathbf{y}) ds} \right]^N dt. \quad (2.6)$$

If instead, only a fixed (but large) number k of particles survive, the conditional MFPT is given by

$$\mathbb{E}[\tau^e(N) | n = k, \mathbf{y}] = \int_0^\infty \left[1 - \frac{\int_0^t J(s | \mathbf{y}) ds}{\int_0^\infty J(s | \mathbf{y}) ds} \right]^k dt. \quad (2.7)$$

Similarly, we can compute the mean first killing time, given by the formula

$$\mathbb{E}[\tau^k(N) | n < N, \mathbf{y}] = \int_0^\infty \frac{\left(1 - \int_0^t \int_\Omega k(x) p(x, s) dx ds\right)^N - \left(1 - \int_0^\infty \int_\Omega k(x) p(x, s) dx ds\right)^N}{\left(\int_0^\infty \int_\Omega k(x) p(x, s) dx ds\right)^N} dt. \quad (2.8)$$

The derivation of these formulas can be found in section 0.1.2 of the Introduction.

2.3 Escape vs a killing term with a finite number of Dirac delta functions at isolated points

2.3.1 Survival probability with m-killing points

We consider here m isolated points in the non-negative real line $\Omega = \mathbf{R}_+$ where diffusing particle can be degraded with a total weight $V = \sum_{i=1}^m V_i$. The killing term is given by

$$k(x) = \sum_{i=1}^m V_i \delta(x - x_i).$$

Brownian particles with diffusion coefficient D can escape at the boundary $x = 0$. To determine the formula for the MFPT of the fastest particle escaping alive, we solve the diffusion equation with the m Dirac delta killing terms by using the Green's function [8] for this domain. This method allows us to obtain an integral representation for the survival probability. The FPE is given by

$$\begin{aligned}\frac{\partial p(x, t | y)}{\partial t} &= D \frac{\partial^2 p(x, t | y)}{\partial x^2} - \sum_{i=1}^m V_i \delta(x - x_i) p(x, t | y) \\ p(x, 0 | y) &= \delta(x - y) \\ p(0, t | y) &= 0.\end{aligned}\tag{2.9}$$

This equation can be decomposed into:

$$\begin{aligned}\frac{\partial p(x, t | y)}{\partial t} - D \frac{\partial^2 p(x, t | y)}{\partial x^2} &= F(x, t) \\ p(x, 0 | y) &= 0,\end{aligned}\tag{2.10}$$

where $F(x, t) = \sum_{i=1}^m V_i \delta(x - x_i) p(x, t | y)$, and

$$\begin{aligned}\frac{\partial p(x, t | y)}{\partial t} - D \frac{\partial^2 p(x, t | y)}{\partial x^2} &= 0 \\ p(x, 0 | y) &= \delta(x - y) \\ p(0, t | y) &= 0.\end{aligned}\tag{2.11}$$

The fundamental solution of equation (2.11) is the Green's function

$$G(x, t | y) = \frac{1}{2\sqrt{\pi Dt}} \left(\exp \left\{ -\frac{(x-y)^2}{4Dt} \right\} - \exp \left\{ -\frac{(x+y)^2}{4Dt} \right\} \right),$$

while the solution of equation (2.10) is given by Duhamel's formula by the convolution

$$P(x, t | y) = \int_0^t \int_{\mathbb{R}} F(y, s) G(x, t-s | y) dy ds.$$

Thus the general solution of equation (2.9) is

$$p(x, t | y) = G(x, t) - \sum_{i=1}^m \int_0^t \frac{V_i p(x_i, s | y)}{\sqrt{4\pi D(t-s)}} \left(\exp \left\{ \frac{-(x-x_i)^2}{4D(t-s)} \right\} - \exp \left\{ \frac{-(x+x_i)^2}{4D(t-s)} \right\} \right) ds. \tag{2.12}$$

The pdf $p(x, t | y)$ is known once the probability density functions $p(x_1, t | y), \dots, p(x_m, t | y)$ are determined. Setting $x = x_1, x = x_2, \dots, x = x_m$ in equation (2.12) we obtain a system of integral equation in the single variable t for the unknown functions

$$\phi_j(t) = p(x_j, t | y) \text{ for } j = 1, \dots, m.$$

We thus obtain

$$\phi_j(t) = G_j(t) - \sum_{i=1}^m \int_0^t \frac{V_i \phi_i(s)}{\sqrt{4D\pi(t-s)}} \left(\exp \left\{ -\frac{(x_j - x_i)^2}{4D(t-s)} \right\} - \exp \left\{ -\frac{(x_j + x_i)^2}{4D(t-s)} \right\} \right) ds,$$

where $G_j(t) = G(x_j, t)$. The solution $p(x, t | y)$ will be determined once all the functions $\phi_i(t)$ are known. To compute this, we use the Laplace transform in time and we shall derive a system of linear equations

$$\hat{\phi}_j(q) = \hat{G}_j(q) - \sum_{i=1}^m \frac{V_i \hat{\phi}_i(q)}{\sqrt{4D\pi q}} \left(\exp \left\{ -\frac{|x_j - x_i| \sqrt{q}}{\sqrt{D}} \right\} - \exp \left\{ -\frac{|x_j + x_i| \sqrt{q}}{\sqrt{D}} \right\} \right). \quad (2.13)$$

Using the parameters $d_{ij} = \frac{|x_j - x_i|}{\sqrt{D}}$, $m_{ij} = \frac{|x_j + x_i|}{\sqrt{D}}$, $W_i = \frac{V_i}{\sqrt{4D\pi}}$, we rewrite the system (2.13) in the matrix form

$$\mathbf{M}(x_1, \dots, x_m) \hat{\Phi} = \hat{\mathbf{G}},$$

where

$$\mathbf{M}(x_1, \dots, x_m) = \begin{pmatrix} 1 + W_1 \frac{e^{-d_{11}\sqrt{q}} - e^{-m_{11}\sqrt{q}}}{\sqrt{q}} & \dots & W_m \frac{e^{-d_{1m}\sqrt{q}} - e^{-m_{1m}\sqrt{q}}}{\sqrt{q}} \\ \vdots & \ddots & \vdots \\ W_1 \frac{e^{-d_{1m}\sqrt{q}} - e^{-m_{1m}\sqrt{q}}}{\sqrt{q}} & \dots & 1 + W_m \frac{e^{-d_{mm}\sqrt{q}} - e^{-m_{mm}\sqrt{q}}}{\sqrt{q}} \end{pmatrix} \quad (2.14)$$

and

$$\hat{\Phi} = \begin{pmatrix} \hat{\phi}_1 \\ \vdots \\ \hat{\phi}_m \end{pmatrix}, \hat{\mathbf{G}} = \begin{pmatrix} \hat{G}_1 \\ \vdots \\ \hat{G}_m \end{pmatrix}. \quad (2.15)$$

We can write the matrix equation above as

$$\mathbf{M}(x_1, \dots, x_m) = I_m + \frac{\mathbf{N}(x_1, \dots, x_m)}{\sqrt{q}},$$

where

$$\mathbf{N}(x_1, \dots, x_m) = [W_j (e^{-d_{ij}\sqrt{q}} - e^{-m_{ij}\sqrt{q}})]_{ij} \quad (2.16)$$

for $i, j = 1, \dots, m$ and the coefficients of $\mathbf{N}(x_1, \dots, x_m)$ are algebraic functions of d_{ij} and m_{ij} depending on the Laplace variable q . The matrix $\mathbf{M}(x_1, \dots, x_m)$ is the sum of the identity with an $O\left(\frac{1}{\sqrt{q}}\right)$ perturbation, thus it is invertible and for large q , we have the formal expansion

$$\mathbf{M}^{-1}(x_1, \dots, x_m) = \left(I_m + \frac{\mathbf{N}(x_1, \dots, x_m)}{\sqrt{q}} \right)^{-1} = \sum_{k=0}^{\infty} \left(-\frac{\mathbf{N}(x_1, \dots, x_m)}{\sqrt{q}} \right)^k \approx I_m - \frac{\mathbf{N}(x_1, \dots, x_m)}{\sqrt{q}}.$$

The solution can be written thus as $\hat{\Phi} = \mathbf{M}^{-1}(x_1, \dots, x_m) \hat{\mathbf{G}}$. We will use below the first order approximation $\left(O\left(\frac{1}{\sqrt{q}}\right)\right)$ to estimate the leading order term of the mean escape time.

We shall now compute the probability that the first particle escapes alive. From the model we have

$$\int_0^\infty J(s) ds = D \int_0^\infty \frac{\partial p}{\partial x}(x=0, t | y) dt.$$

Differentiating relation (2.12) and evaluating the Laplace transform in $q = 0$, we get

$$D \int_0^\infty \frac{\partial p}{\partial x}(x=0, t|y) dt = 1 - \sum_{i=1}^m V_i \hat{\phi}_i(0).$$

Finally, we obtain the probability that at least one particle escapes is given by

$$P_\infty = 1 - \left(\sum_{i=1}^m V_i \hat{\phi}_i(0) \right)^N.$$

We shall now compute the MFPT for the fastest Brownian particle. From formula (2.5), we use a short-time expansion of

$$s(t) = \left(1 - \int_0^t J(s) ds \right)^N - \left(1 - \int_0^\infty J(s) ds \right)^N.$$

We then compute

$$\begin{aligned} \int_0^t J(s) ds &= D \int_0^t \frac{\partial p}{\partial x}(x=0, s|y) ds \\ &= D \int_0^t \frac{\partial G}{\partial x}(x=0, s|y) ds - D \sum_{i=1}^m V_i \int_0^t \int_0^s \phi_i(u) \frac{\partial G}{\partial x}(x=0, s-u|x_i) du ds \\ &= \operatorname{erfc}\left(\frac{y}{\sqrt{4Dt}}\right) - D \sum_{i=1}^m V_i \int_0^t \phi_i(u) \operatorname{erfc}\left(\frac{x_i}{\sqrt{4D(t-u)}}\right) du. \end{aligned}$$

For t small, the order of the integral

$$F_i(t) = DV_i \int_0^t \phi_i(u) \operatorname{erfc}\left(\frac{x_i}{\sqrt{4D(t-u)}}\right) du,$$

depends on the order of the functions $\phi_i(u)$ and $\operatorname{erfc}\left(\frac{x_i}{\sqrt{4D(t-u)}}\right)$, that are continuous and differentiable functions in $[0, t]$ and $(0, t)$ respectively. Then, there exists a constant $c_i(t) \in [0, t]$ such that

$$F_i(t) = DV_i \phi_i(c_i(t)) \operatorname{erfc}\left(\frac{x_i}{\sqrt{4D(t-c_i(t))}}\right) t,$$

and thus, for t small, $c_i(t)$ is small, and using the expansion for large argument of the $\operatorname{erfc}(x)$, we have the approximation,

$$F_i(t) = O\left(\exp\left\{-\frac{x_i^2}{4D(t-c_i(t))}\right\} \sqrt{(t-c_i(t))t^{1+k}}\right),$$

where k is the order of $\phi_i(c_i(t))$. We have $\phi_i(0) = 0$ for $x_i \neq y$. When $x_i = y$, we have $\phi_i(0) = 1$ and

$$F_i(t) = O\left(\exp\left\{-\frac{x_i^2}{4Dt}\right\} t^{\frac{3}{2}+k}\right) > O\left(\exp\left\{-\frac{x_i^2}{4Dt}\right\} t^{\frac{1}{2}}\right).$$

Then, for t small, the short-time asymptotic of $s(t)$ is dominated by the short-time asymptotic of

$$D \int_0^t \frac{\partial G}{\partial x} (x = 0, s | y) = \operatorname{erfc} \left(\frac{y}{\sqrt{4Dt}} \right).$$

Finally, we obtain from relation (2.5) the MFPT formula

$$\mathbb{E}[\tau^e(N) | n \geq 1] \approx \int_0^\delta \frac{\left(1 - \frac{\sqrt{4Dt} \exp \left\{ -\frac{y^2}{4Dt} \right\}}{y\sqrt{\pi}} \right)^N - \left(\sum_{i=1}^m V_i \hat{\phi}_i(0) \right)^N}{1 - \left(\sum_{i=1}^m V_i \hat{\phi}_i(0) \right)^N} dt,$$

for $0 < \delta < 1$. Here we have approximated the value of the integral over $[0, +\infty)$ by the value of the integral in a neighborhood of $t = 0$, following the Laplace method. Thus for N large as $\left(\sum_{i=1}^m V_i \hat{\phi}_i(0) \right) \in (0, 1)$, we obtain

$$\mathbb{E}[\tau^e(N) | n \geq 1] \approx \int_0^\delta \left[1 - N \frac{\sqrt{4Dt} \exp \left\{ -\frac{y^2}{4Dt} \right\}}{y\sqrt{\pi}} \right] dt \approx \int_0^\delta \exp \left\{ -N \frac{\sqrt{4Dt} \exp \left\{ -\frac{y^2}{4Dt} \right\}}{y\sqrt{\pi}} \right\} dt, \quad (2.17)$$

leading to

$$\mathbb{E}[\tau^e(N) | n \geq 1] \sim \frac{y^2}{4D \ln \left(\frac{N}{\sqrt{\pi}} \right)}. \quad (2.18)$$

The formula (2.18) does not reveal how the mean first escape time for the fastest particle depends on the parameters associated with the killing term. We compute to leading order the killing probability

$$P_k = 1 - P_e = \sum_{i=1}^m V_i \hat{\phi}_i(0),$$

with respect to the physical parameters. Using the inverse matrix (2.17), the first approximation gives

$$\hat{\phi}_i = \sum_j \left(I_m - \frac{\mathbf{N}(x_1, \dots, x_m)}{\sqrt{q}} \right)_{ij} \hat{G}_j,$$

then,

$$\sum_{i=1}^m V_i \hat{\phi}_i(q) = \sum_{i,j} \left(V_i \hat{G}_i(q) - \frac{V_i V_j \alpha_{ij}(q)}{2\sqrt{Dq}} \hat{G}_j(q) \right),$$

where $\alpha_{ij}(q) = e^{-d_{ij}\sqrt{q/D}} - e^{-m_{ij}\sqrt{q/D}}$. The Laplace transform of the Green's function is given by

$$\hat{G}(x_i, q | \mathbf{y}) = \frac{1}{2\sqrt{Dq}} \left(\exp \left\{ -|y - x_i| \sqrt{\frac{q}{D}} \right\} - \exp \left\{ -|y + x_i| \sqrt{\frac{q}{D}} \right\} \right),$$

and for $q = 0$ we obtain

$$P_k = \sum_{i=1}^m \frac{V_i}{2D} (|y - x_i| - |y + x_i|) - \sum_{i,j=1}^m \frac{V_j V_i}{2D^2} (|y - x_i| - |y + x_i|)(d_{ij} - m_{ij}). \quad (2.19)$$

Formula (2.19) reveals the nonlinear dependency between the Dirac delta functions located at position x_i and the initial position y , the killing weights V_i and the diffusion coefficient D . The term P_k is always less than 1. Consequently, for large N , it does not influence formula (2.18). We will exemplify this point more clearly in the next subsection where we only have one killing point.

2.3.2 Survival probability with a single point-sink killing term

We compute here the time-dependent survival probability and the MFPT for first among N survival particles in the presence of a single Dirac delta killing term at position x_1 located on the half-line $x > 0$. We recall that the FPE is given by

$$\begin{aligned} \frac{\partial p(x, t | y)}{\partial t} &= D \frac{\partial^2 p(x, t | y)}{\partial x^2} - V_1 \delta(x - x_1) p(x, t | y) \\ p(x, 0 | y) &= \delta(x - y) \\ p(0, t | y) &= 0. \end{aligned} \quad (2.20)$$

The general solution of equation (2.20) is the integral equation

$$p(x, t | y) = G(x, t | y) - \int_0^t \frac{V_1 p(x_1, s | y)}{2\sqrt{\pi D(t-s)}} \left(\exp \left\{ \frac{-(x-x_1)^2}{4D(t-s)} \right\} - \exp \left\{ -\frac{(x+x_1)^2}{4D(t-s)} \right\} \right) ds. \quad (2.21)$$

Setting $x = x_1$ in equation (2.21), it reduces to an integral equation in the single variable t for the unknown function $\phi(t) = p(x_1, t | y)$. The solution $p(x, t | y)$ is completely determined once $\phi(t)$ is known. To compute this term, we use the Laplace transform in time. The integral equation (2.21) becomes

$$\hat{\phi}(q) = -V_1 \frac{\hat{\phi}(q)}{2\sqrt{Dq}} \left(1 - \exp \left\{ -|x_1| \sqrt{\frac{2q}{D}} \right\} \right) + \hat{G}(x_1, q | y),$$

where

$$\hat{G}(x_1, q | y) = \frac{1}{2\sqrt{Dq}} \left(\exp \left\{ -|y - x_1| \sqrt{\frac{q}{D}} \right\} - \exp \left\{ -|y + x_1| \sqrt{\frac{q}{D}} \right\} \right).$$

The solution is

$$\hat{\phi}(q) = \frac{\hat{G}(x_1, q | y)}{1 + \frac{V_1}{2\sqrt{Dq}} \left(1 - \exp \left\{ -|x_1| \sqrt{\frac{2q}{D}} \right\} \right)} = \frac{\left(\exp \left\{ -|y - x_1| \sqrt{\frac{q}{D}} \right\} - \exp \left\{ -|y + x_1| \sqrt{\frac{q}{D}} \right\} \right)}{V_1 \left(1 - \exp \left\{ -x_1 \sqrt{\frac{2q}{D}} \right\} \right) + 2\sqrt{Dq}},$$

and at $q = 0$ we obtain

$$\hat{\phi}(0) = \frac{|y + x_1| - |y - x_1|}{V_1 2x_1 + 2D}. \quad (2.22)$$

When $\hat{\phi}(q)$ is known, we obtain the general solution of (2.21) as

$$\hat{p}(x, q | y) = \hat{G}(x, q | y) - V_1 \frac{\hat{\phi}(q)}{2\sqrt{Dq}} \left(\exp \left\{ -|x - x_1| \sqrt{\frac{q}{D}} \right\} - \exp \left\{ -|x + x_1| \sqrt{\frac{q}{D}} \right\} \right),$$

and thus,

$$\begin{aligned} \hat{p}(x, q | y) &= -\frac{V_1}{4Dq + V_1\sqrt{4Dq} (1 - \exp \{-2|x_1|\sqrt{\frac{q}{D}}\})} \left(\exp \left\{ -(|y - x_1| + |x - x_1|) \sqrt{\frac{q}{D}} \right\} \right. \\ &\quad - \exp \left\{ -(|y + x_1| + |x - x_1|) \sqrt{\frac{q}{D}} \right\} + \exp \left\{ -(|y + x_1| + |x + x_1|) \sqrt{\frac{q}{D}} \right\} \quad (2.23) \\ &\quad \left. - \exp \left\{ -(|y - x_1| + |x + x_1|) \sqrt{\frac{q}{D}} \right\} \right) + \hat{G}(x, q | y). \end{aligned}$$

We rewrite expression (2.23) as a sum of the five terms, that we shall compute separately:

$$\hat{p}(x, q | y) = \hat{p}_1(x, q | y) + \hat{p}_2(x, q | y) + \hat{p}_3(x, q | y) + \hat{p}_4(x, q | y) + \hat{G}(x, q | y). \quad (2.24)$$

The first term is defined by

$$\hat{p}_1(x, q | y) = -\frac{V_1}{4D} \frac{\exp \left\{ -(|y - x_1| + |x - x_1|) \sqrt{\frac{q}{D}} \right\}}{q + \frac{V_1}{2\sqrt{D}} \sqrt{q}},$$

We apply the inverse Laplace transform for each solution using the generic expression for $\alpha > 0$,

$$L^{-1} \left(\frac{e^{-\alpha\sqrt{q}}}{q + \sqrt{q} \frac{V_1}{2\sqrt{D}}} \right) = \exp \left\{ \frac{\alpha V_1}{2\sqrt{D}} + \frac{V_1^2}{4D} t \right\} \operatorname{erfc} \left(\frac{\alpha}{2t^{1/2}} + \frac{V_1}{2\sqrt{D}} t^{1/2} \right).$$

We obtain

$$p_1(x, t | y) = -\frac{V_1}{4D} \exp \left\{ \frac{(|y - x_1| + |x - x_1|)V_1}{2D} + \frac{V_1^2}{4D} t \right\} \operatorname{erfc} \left(\frac{(|y - x_1| + |x - x_1|)}{\sqrt{4Dt}} + \frac{V_1}{2\sqrt{D}} t^{1/2} \right).$$

For small time t , we have the approximations

$$p_1(x, t | y) \approx -\frac{V_1}{4D} \exp \left\{ \frac{(|y - x_1| + |x - x_1|)V_1}{2D} \right\} \operatorname{erfc} \left(\frac{(|y - x_1| + |x - x_1|)}{\sqrt{4Dt}} \right),$$

and similarly for the other terms in relation (2.23):

$$p_2(x, t | y) \approx \frac{V_1}{4D} \exp \left(\frac{(|y + x_1| + |x - x_1|)V_1}{2D} \right) \operatorname{erfc} \left(\frac{(|y + x_1| + |x - x_1|)}{\sqrt{4Dt}} \right),$$

$$p_3(x, t | y) \approx -\frac{V_1}{4D} \exp \left\{ \frac{(|y + x_1| + |x + x_1|)V_1}{2D} \right\} \operatorname{erfc} \left(\frac{(|y + x_1| + |x + x_1|)}{\sqrt{4Dt}} \right),$$

$$p_4(x, t | y) \approx \frac{V_1}{4D} \exp \left\{ \frac{(|y - x_1| + |x + x_1|)V_1}{2D} \right\} \operatorname{erfc} \left(\frac{(|y - x_1| + |x + x_1|)}{\sqrt{4Dt}} \right).$$

The escape probability is given by

$$\int_0^\infty J(t)dt = D \int_0^\infty \frac{\partial p}{\partial x}(x=0, t|y) dt,$$

and differentiating relation (2.23) and evaluating in $q = 0$, we obtain

$$D \int_0^\infty \frac{\partial p}{\partial x}(x=0, t|y) dt = 1 - V_1 \hat{\phi}(0).$$

Finally, using relation (2.22), we obtain the probability that at least one particle escapes given by

$$P_\infty = 1 - (V_1 \hat{\phi}(0))^N = 1 - \left(V_1 \frac{|y+x_1| - |y-x_1|}{V_1 2|x_1| + 2D} \right)^N.$$

We shall now compute the MFPT for the fastest particle. Using formula (2.5), we can obtain the short-time approximation for

$$s(t) = \left(1 - \int_0^t J(s) ds \right)^N - \left(1 - \int_0^\infty J(s) ds \right)^N.$$

Indeed, using the expansion of the complementary error function for large argument (t small), we get from relation (2.5) that the MFPT when N is large is given by

$$\mathbb{E}[\tau^e(N) | n \geq 1] \approx \int_0^\delta \frac{\left(1 - \frac{\sqrt{4Dt} \exp\left\{-\frac{y^2}{4Dt}\right\}}{y\sqrt{\pi}} \right)^N - (V_1 \hat{\phi}(0))^N}{1 - (V_1 \hat{\phi}(0))^N} dt,$$

for $0 < \delta < 1$. This integral can be estimated for N large as

$$\begin{aligned} \mathbb{E}[\tau^e(N) | n \geq 1] &\approx \int_0^\delta \left[1 - N \frac{\sqrt{4Dt} \exp\left\{-\frac{y^2}{4Dt}\right\}}{y\sqrt{\pi} \left(1 - (V_1 \hat{\phi}(0))^N \right)} \right] dt \approx \int_0^\delta \left[1 - N \frac{\sqrt{4Dt} \exp\left\{-\frac{y^2}{4Dt}\right\}}{y\sqrt{\pi}} \right] dt \\ &\approx \int_0^\delta \exp\left\{ -N \frac{\sqrt{4Dt} \exp\left\{-\frac{y^2}{4Dt}\right\}}{y\sqrt{\pi}} \right\} dt, \end{aligned}$$

leading to the formula

$$\mathbb{E}[\tau^e(N) | n \geq 1] \sim \frac{y^2}{4D \ln\left(\frac{N}{\sqrt{\pi}}\right)}. \quad (2.25)$$

In the simulations, we will be working with a finite amount of particles, thus a parameter α to correct the number of surviving particles, and a parameter β that corrects the distance made for the fastest particles are probably to be needed. This last one could correct the fact that the fastest particle could be eliminated by the killing term and the one arriving now has done a larger trajectory, leading to a formula in the form

$$\mathbb{E}[\tau^e(N) | n \geq 1] \sim \frac{\beta y^2}{4D \left[\ln\left(\frac{N}{\sqrt{\pi}}\right) + \alpha \right]}. \quad (2.26)$$

These kind of parameters was already used in [71], to obtain a better adjustment with the model. We can also approximate the density function for the distribution of the first escape times as the density of the r.v. σ_s^N with distribution

$$\Pr\{\sigma_s^N \leq t\} = 1 - \exp\left\{\frac{-N\sqrt{4Dt}e^{-\frac{y^2}{(4Dt)}}}{y\sqrt{\pi}}\right\}. \quad (2.27)$$

In this case the pdf of σ_s^N is given by

$$\Pr\{\sigma_s^N \in [t + dt]\} = \frac{N\sqrt{4Dt}e^{-\frac{y^2}{(4Dt)}}}{y\sqrt{\pi}} \exp\left\{\frac{-N\sqrt{4Dt}e^{-\frac{y^2}{(4Dt)}}}{y\sqrt{\pi}}\right\} \left[\frac{1}{2t} + \frac{y^2}{4Dt^2}\right] dt,$$

and note also that

$$\Pr\{\tau^e(N) \leq t\} = 1 - [S(t)]^N \sim \Pr\{\sigma_s^N \leq t\} \text{ when } t \text{ is small.} \quad (2.28)$$

For the case when a fixed and large number k of particles escape, we obtain the MFPT formula given by

$$\begin{aligned} \mathbb{E}[\tau^e(N) \mid n = k] &\sim \int_0^\delta \exp\left[-k \frac{\int_0^t J(s \mid y) ds}{\int_0^\infty J(s \mid y) ds}\right] dt \sim \int_0^\delta \exp\left[-\frac{k}{P_e} \operatorname{erfc}\left(\frac{y}{\sqrt{4Dt}}\right)\right] dt \\ &\sim \frac{y^2}{4D \ln\left(\frac{k}{P_e \sqrt{\pi}}\right)}. \end{aligned} \quad (2.29)$$

The formula (2.29) is revealing that the asymptotic for the fastest escape time with k surviving particles, where the escape probability for each of them is P_e , is the same formula that considering only diffusion (without killing) with an initial amount of $\frac{k}{P_e}$ particles. Note as well that when the killing rate V_1 is increasing, $P_e = 1 - V_1 \hat{\phi}(0)$ is decreasing and thus the mean escape time $\mathbb{E}[\tau^e(N) \mid n = k, \mathbf{y}]$ is decreasing.

Equivalently, we can have the formula for the mean first killing time given by (2.8), where

$$\int_0^\infty \int_\Omega k(x)p(x, s) dx ds = V_1 \hat{\phi}_1(0) \text{ and } \int_0^t \int_\Omega k(x)p(x, s) dx ds \approx \frac{V_1}{4D} \frac{\exp\left\{-\frac{(x_1-y)^2}{4Dt}\right\} (4Dt)^{\frac{3}{2}}}{\sqrt{\pi}(x_1-y)^2}.$$

Thus, we obtain

$$\mathbb{E}[\tau^k(N) \mid n < N] \approx \int_0^\infty \frac{\left(1 - \frac{V_1(4Dt)^{\frac{3}{2}} \exp\left\{-\frac{(x_1-y)^2}{4Dt}\right\}}{4D(y-x_1)^2 \sqrt{\pi}}\right)^N - \left(1 - V_1 \hat{\phi}(0)\right)^N}{1 - \left(1 - V_1 \hat{\phi}(0)\right)^N} dt. \quad (2.30)$$

Computing asymptotically the integral above, we obtain the formula for the mean first killing time

$$\mathbb{E}[\tau^k(N) \mid n < N] \sim \frac{(y-x_1)^2}{4D \left[\ln\left(\frac{NV_1(y-x_1)}{4D\sqrt{\pi}}\right) \right]}. \quad (2.31)$$

2.4 Applications: numerical simulations and quantifying calcium signaling events in synapse

In this section, we study the range of validity of the asymptotic formula derived above. We also show how the diffusion with killing can be used to quantify calcium dynamics in a sub-cellular compartment called the spine neck [112].

2.4.1 Stochastic simulations for the fastest arrival with a killing term

We discuss here several applications of the MFPT computations presented above. First, to test the range of accuracy of the asymptotic formulas, we run stochastic simulations for the first escape time with a killing term as a Dirac delta function at point x_1 when all particles are initially distributed at position y for different initial numbers of particles N_0 and killing weights V_1 . The stochastic simulation follows Euler's scheme (Fig. 2.2A): for a particle crossing the point x_1 in any sense during the time step Δt , that is $x(t) \leq x_1 \leq x(t + \Delta t)$ or the other side, we have

$$x(t + \Delta t) = \begin{cases} x(t) + \sqrt{2D}\Delta w(t) & \text{w.p } 1 - V_1 I_{\{x(t) \leq x_1 \leq x(t + \Delta t)\}} \text{ or } \{x(t + \Delta t) \leq x_1 \leq x(t)\} \Delta t \\ \text{TERMINATED}, & \text{w.p } V_1 I_{\{x(t) \leq x_1 \leq x(t + \Delta t)\}} \text{ or } \{x(t + \Delta t) \leq x_1 \leq x(t)\} \Delta t \end{cases}$$

Live particles can be destroyed at Poissonian rate V_1 with probability $V_1 \Delta t$, when passing over the point x_1 . We are interested in the statistical properties of the fastest particle reaching the absorbing boundary prior to be killed (Fig. 2.2B). Outside the crossing point x_1 , the Euler's scheme

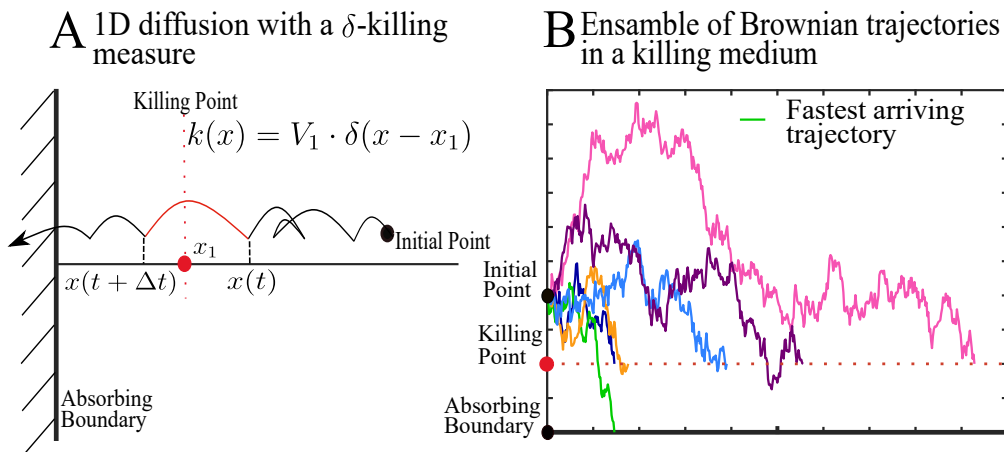


Figure 2.2: **Escape versus killing for the fastest particles.** **A.** 1D Brownian motion passing through the Dirac delta killing field at point x_1 . The particle is absorbed when reaching the boundary on the left. **B.** Five among six random walks are terminated while the survival trajectory (green) reaches the boundary.

is the classical Brownian jump at scale Δt . We started the simulation at point $y = 2$ with diffusion coefficient $D = 1$ with the killing point at $x_1 = 1$, with a time step $\Delta t = 0.01$. Note that we do not fix the initial number of particles N_0 , but we run simulations until we reach a given amount n of survival particles with $n = (500, 1000, 2500, 5000, 10000)$. As shown in Fig. 2.3A the simulated

mean escape time decays with the killing weight V_1 in agreement with formula (2.29). We tried to fit the simulations results with the asymptotic formula (2.29), this is with

$$\mathbb{E}[\tau^e(N) | n = k] \sim \frac{y^2}{4D \left[\ln \left(\frac{k}{P_e \sqrt{\pi}} \right) + \alpha \right]}, \quad (2.32)$$

where the parameter α was supposed to correct the effect of the killing term, but the results were no so good as shown in Fig. 2.3B. This is due to the fact that the killing could remove the fastest trajectories, and the one that is arriving as the first one could have done a very large trajectory before escaping. This removal, will affect thus the smaller distance to the target, and then, a parameter β is also needed to correct the smaller distance, previously given by y . In the case of an infinite number of particles, this parameter will not be necessary since the fastest particle will follow indeed the direct line [113, 114]. We fitted thus the simulation results with the formula

$$\mathbb{E}[\tau^e(N) | n = k] \sim \frac{\beta y^2}{4D \left[\ln \left(\frac{k}{P_e \sqrt{\pi}} \right) + \alpha \right]}. \quad (2.33)$$

What we could expect from the fitting is that this parameter β does not vary to much, even for different values of the killing rate V_1 . The fitting was made using the *fit* function from Matlab, where we can choose the model with which we want to fit our data and it returns the 95% interval of confidence and the optimal value in that interval which minimize the sum of square errors. We show the results in Fig. 2.3C. The MFPT decreases with the number of surviving particles. The parameter β has a variance $\text{var}(\beta) = 0.0013771875$ and the parameter α increases its absolute value when the killing rate V_1 increases. This behavior of the parameter α is not very surprising since the short-time approximation made for the flux is an increasing function of V_1 .

We decided to explore as well the case where the initial number of particles $N_0 = (500, 1000, 2500, 5000, 10000)$ is fixed and at least one particle escapes. The initial number of particles does not necessarily correspond to the number of surviving particles that will escape. In practice, a very small number of particles will escape for a large value of the killing rate V_1 . To illustrate this difference, we plotted the distribution of the escape times (Fig. 2.4A) and the MFPT (Fig. 2.4B) vs the killing rate V_1 respectively. The main difference with the results shown in Fig. 2.3 is that now, the MFPT is increasing as the killing rate V_1 increases. This is due to the decreasing amount of surviving particles n (Fig. 2.4C), a direct consequence of the killing term.

2.4.2 Time scale of fast calcium signaling at synapse

Calcium dynamics at synapses is a fundamental step to transform neuronal spike coding, propagated across neurons into long-term molecular changes at a sub-cellular level, called synaptic plasticity, at the bases of learning and memory [106]. Interestingly, following a transient in the spine head (Fig. 2.5), fast calcium increase in dendrite is much faster than predicted by the classical transport resulting from the theory of diffusion [92]. This observation was interpreted as a consequence of the arrival of the fastest calcium ions that trigger calcium by a mechanism called calcium-induced calcium release through a class of receptor called Ryanodine receptor (RyR) located at the base of spine (Fig. 2.5). While the mean time of calcium-induced calcium release (CICR) was previously computed as the arrival of the first two calcium ions to a RyR, this computed neglected the influence of calcium buffers that can capture, for a long-time, calcium ions on their way to the receptors, thus preventing a fast CICR. The main calcium buffers in the cytoplasm includes Trophin C, Calmodulin,

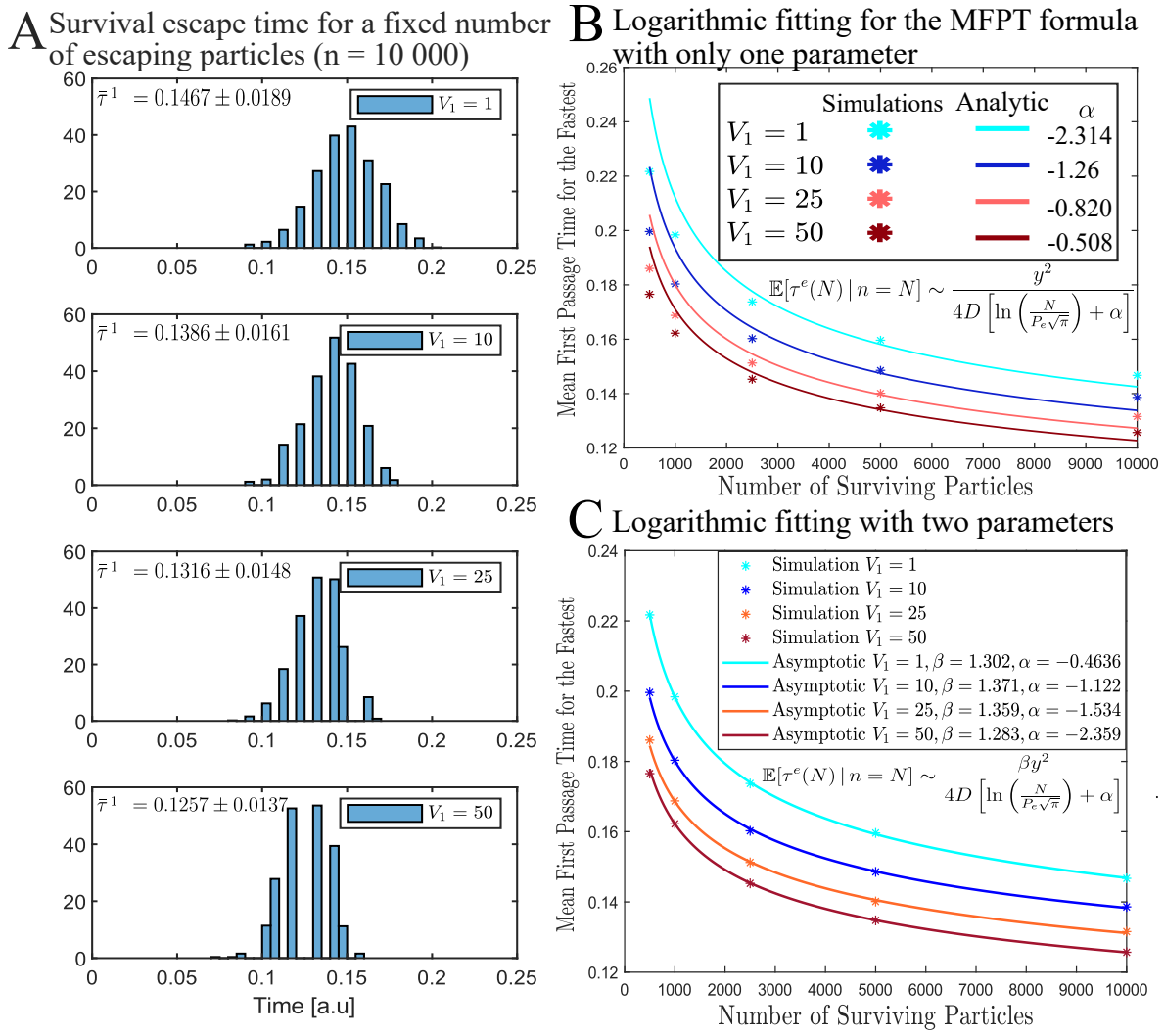


Figure 2.3: **Influence of the killing rate on the conditional mean escape time for the fastest particle.** **A.** Stochastic simulations for the escape time distribution of the fastest particle when particles start at $y = 2$ with a killing point in $x_1 = 1$ for $n = 10000$ and 1000 runs. **B.** MFPT vs n obtained from stochastic simulations (colored disks) and the asymptotic formula (2.29) (continuous lines) with an optimal fitting for the parameter α . **C.** MFPT vs n obtained from stochastic simulations (colored disks) and the asymptotic formula (2.29) (continuous lines) with an optimal fitting for the parameters α and β .

Calcineurin and Myosin. If the concentration of buffer is high, the calcium trajectory that will arrive to a target will be significantly reduced when a large number of ions are not captured. Calcium buffers could thus prevent the fast activation of CICR or even a second messenger pathway such as IP3 receptors, located at the base of a spine [115–118] if the concentration of ions is low.

Effect of calcium buffers modeled as a killing point source on Calcium-Induced Calcium Release

We propose now to model calcium dynamics in spine head as a diffusion in narrow cylinder, approximated as an interval in 1D. Indeed, due to the small size of the narrow cylinder and head of the dendritic spine, we could approximate the motion of calcium particles inside the narrow cylinder

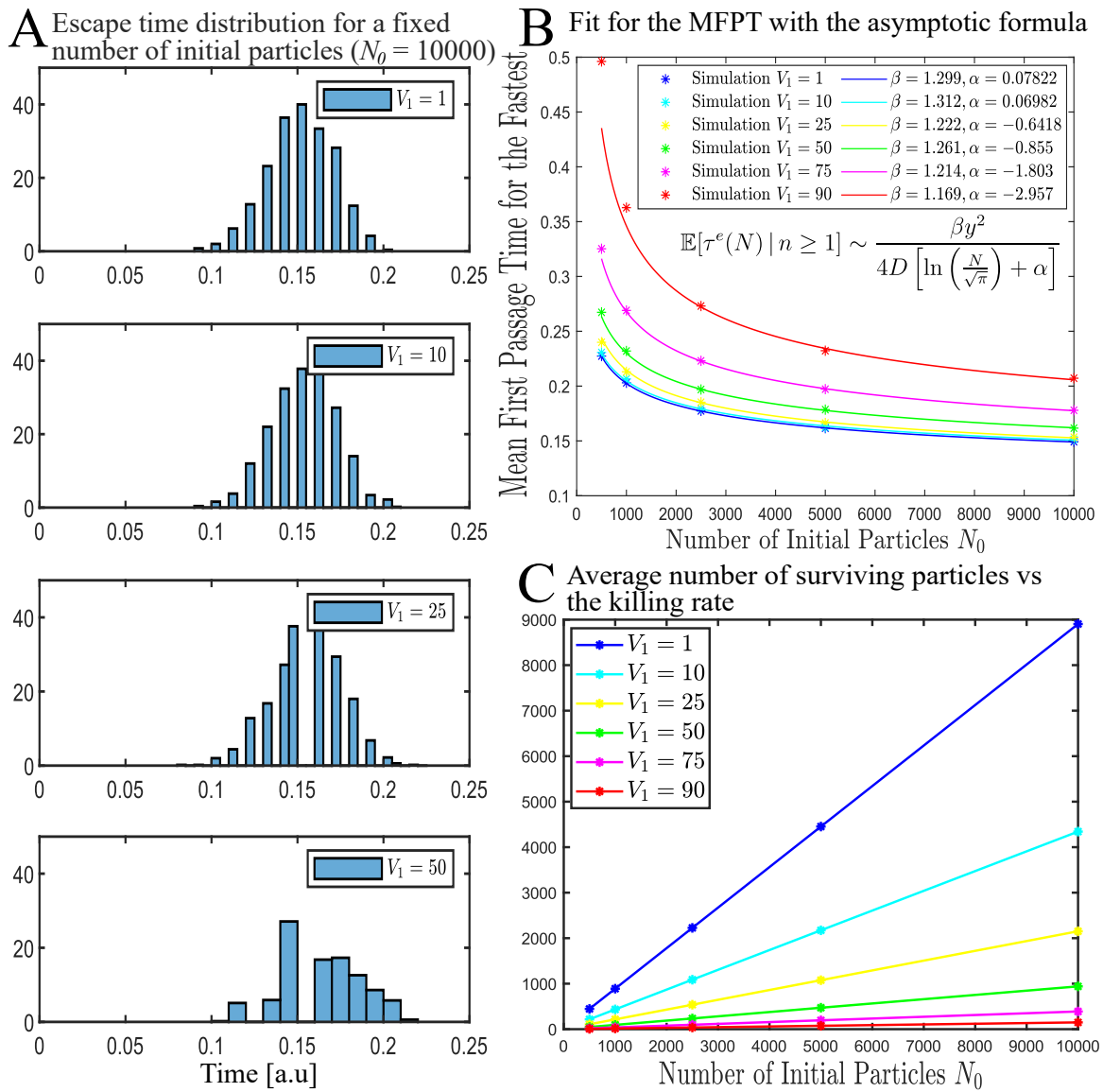


Figure 2.4: **Influence of the killing rate on the escape time for a large number N_0 of initial particles.** **A.** Stochastic simulations for the escape time distribution of the fastest particles starting at $y = 2$ with a killing point at $x_1 = 1$ for $N_0 = 10000$ and 1000 runs. **B.** Fit for the MFPT obtained from stochastic simulations (colored disks) and the asymptotic formula (2.25) (continuous lines). **C.** Influence of the killing weight V_1 in the number of surviving particles.

by a one dimensional Brownian motion in an interval. The fast ions binding to a buffer molecule will be account by the killing term in the diffusion equation, and since the unbinding process is often much longer than the binding time (hundreds vs few milliseconds), we can neglect here the unbinding time. The cases where the killing occurs uniformly on a interval is discussed in appendix section 2.6. The effect of calcium removal by SERCA pumps can also be represented by a single or many killing points inside the interval $[0, L]$. The process of CICR induced by the binding of calcium ions to RyR is modeled as an absorbing boundary, where escape occurs.

We start the model, after there are a total of $N Ca^{2+}$ ions that have entered the dendritic spine through the receptors (dark red point) located in the spine head (Fig. 2.5). The time of CICR is

Approximating spine geometry by an interval

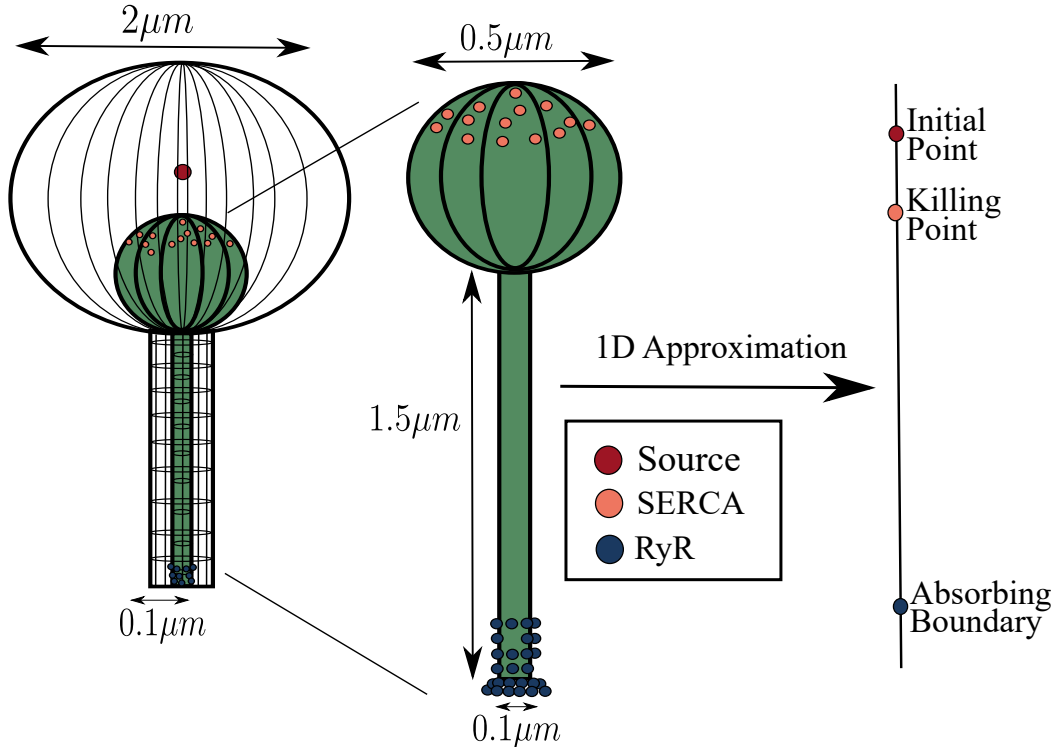


Figure 2.5: **Schematic representation of a dendritic spine doted with a spine apparatus and its simplification in a 1D domain.** The spine with a spine apparatus is simplified as a 1D interval with killing point $x_1 = 2\mu m$, initial point at $y = 2.5\mu m$, absorbing point $x = 0\mu m$.

computed after the arrival of two fastest Ca^{2+} ions at the RyR (blue dots) at the bottom of the spine (absorbing boundary condition). After the RyR is activated, an avalanche through a CIRC from the spine apparatus (SA) is generated. This leads to an amplification of the calcium signal. The CICR process can be computed from the escape time distribution of the second fastest particle arriving to the absorbing end point of the interval, that model the spine neck. The pdf for the time the first ion arrives to the boundary allows to compute the pdf for second one to arrive by conditioning on the arrival of the first one at time s , while there are still $N - 1$ ions very close to the initial point. Thus we obtain the relation:

$$\begin{aligned} \Pr \{ \tau^2 \in [t, t + dt] \} &= \int_0^t \Pr \{ \tau^2 \in [t, t + dt] | \tau^1 \in [s, s + ds] \} S^{N-1}(s) \Pr \{ \tau^1 \in [s, s + ds] \} \\ &\approx \int_0^t \Pr \{ \tau^2 \in [t, t + dt] | \tau^1 \in [s, s + ds] \} \Pr \{ \tau^1 \in [s, s + ds] \}, \end{aligned} \quad (2.34)$$

where we consider that the remaining $N - 1$ particles are still alive close to the initial position when the killing weight V_1 is not too large, thus we use the approximation [92]

$$S^{N-1}(t) = \left(\int_0^L \Pr \{ x(t) \in [x, x + dx] \} dx \right)^{N-1} \approx 1.$$

We approximate the motion inside the narrow cylinder by a one dimensional Brownian motion in an interval $[0, L]$, with $y < L$, where y is the initial position of the source, as shown in Fig. 2.5A.

In practice $y = L$. The buffers or SERCA pumps are represented by a single killing point. Using the approximation summarized by equation (2.25), the escape time for the two fastest particles [92] is computed directly, leading to

$$\mathbb{E}[\tau^e(N) | n \geq 2] \approx 2\mathbb{E}[\tau^e(N) | n \geq 1] \sim \frac{2L^2}{4D \left[\ln \left(\frac{N}{\sqrt{\pi}} \right) \right]}. \quad (2.35)$$

To conclude, the relation (2.35) does not show the direct consequence of the killing buffer provided that at least one particle survive. But instead, when we perform the analysis knowing that a fixed and large number of ions are not captured by the buffers, we obtain

$$\mathbb{E}[\tau^e(N) | n = k] \approx 2\mathbb{E}[\tau^e(N) | n = k] \sim \frac{2L^2}{4D \left[\ln \left(\frac{k}{P_e \sqrt{\pi}} \right) \right]} \quad (2.36)$$

and the buffer effect is to decrease the binding time. Implicitly, the escape probability P_e is depending on the position of the killing source and the killing weight V_1 . We recall that

$$P_e = 1 - V_1 \int_0^\infty p(x_1, t) dt. \quad (2.37)$$

For several killing points given by Dirac delta functions, the mean first passage time is given by formula (2.18). When buffer molecules are uniformly distributed, formula (2.48) should be used instead.

Time to induce long-term change at a molecular level

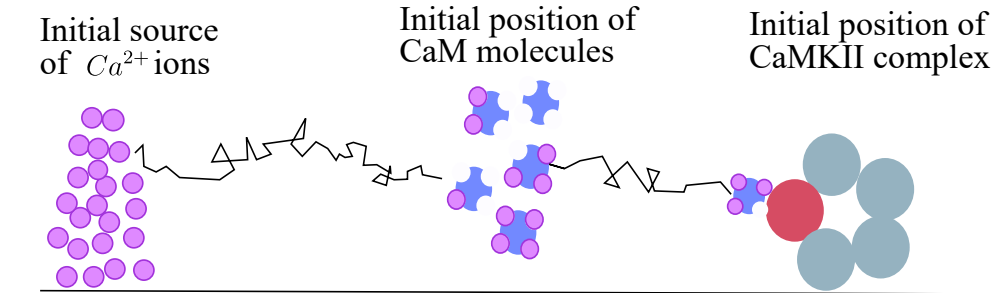
The second example we shall discuss consists in the induction of plastic changes at a molecular level following high calcium concentration level entering into the neuronal synapse. The first step of the signaling consists in calcium ions binding to calmodulin and then the complex calcium-calmodulin needs to bind to a kinase third partner CaMKII [106]. We propose to estimate the probability to activate a given number N_{CaMKII} of CaMKII kinases inside a spine and how long does it take for such activation.

We first consider that calcium bind quickly to calmodulin (CaM) at the time scale given by the first ions to arrival to the CaM sites, of the order of less than 1 millisecond [119]. We also consider that the unbinding time is very long (hundreds compared to few milliseconds). The binding of a molecule of CaM containing a calcium ion to the kinase CaMKII can be achieved by the four components: $CaMCa_1$, $CaMCa_2$, $CaMCa_3$ and $CaMCa_4$. This can be summarized by the following chemical rate equations:



We consider the approximation that the number of molecules in each category is given by $N_i = p^i N$, with $i = 1, \dots, 4$, and $p < 1$. Thus the number of calcium ions bound to the molecule CaM decays exponentially with the initial number of calcium ions. The complex $CaMCa_i$ can dissociate with a

A Activation of CaMKII molecules leading to phosphorylation



B Role of CaMCa in the persistent activation of CaMKII

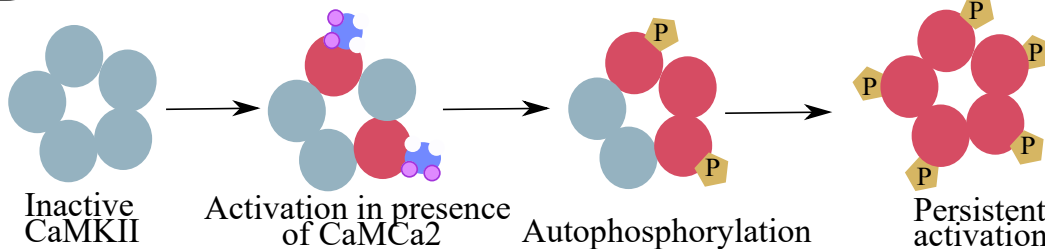


Figure 2.6: **Schematic representation for the long-term activation of a CaMKII complex in a 1D domain.** **A.** The calcium ions enters in the domain and activates the CaM molecules. These last ones can locally activate the CaMKII complex. **B.** When the CaMKII complex is locally activated by CaM in presence of calcium ions, the CaMKII molecule itself phosphorylates first in a neighborhood of the locally activated area, and after a few milliseconds it is fully phosphorylated. This is known as a persistent activation, which has the long-term effect in the molecule and it is associated with learning and memory loss.

rate κ which is much shorter than the binding rate.

We apply now the result developed in the previous section to $CaMCA_i^{2+}$ $i = 1, \dots, 4$, that can diffuse and thus escape the spine at the absorbing boundary. In that case, using relation (2.22), the probability that there are N_{CaMKII} molecules of CaMKII bound to the population $CaMCA_i$ is given by the killing probability

$$P_i = \left(\frac{x_1 V_1}{V_1 x_1 + D} \right)^{N_i}. \quad (2.42)$$

Here we considered that the $CaMKII$ molecules are located at position x_1 and V_1 represent the binding rate. When there are more CaMKII molecules activated than CaM bound to calcium, we approximate $V_1 \approx k_1 N_{CaMKII}$, where k_1 is the forward binding rate. In general, the mean number of bound CaMKII can be computed using a binomial law associated to P_i . Thus

$$\langle CaMKII - CaMCA_i \rangle = P_i N_{CaMKII} \quad (2.43)$$

and the variance is $P_i(1 - P_i)N_{CaMKII}$. Finally, the total number of bound CaMKII is obtained by summing over $i = 1, \dots, 4$ as follows

$$\langle CaMKII_{\text{bound}} \rangle = \sum_i \langle CaMKII - CaMCA_i \rangle = \sum_i N_{CaMKII} \left(\frac{V_1 x_1}{V_1 x_1 + D} \right)^{N_p^i}. \quad (2.44)$$

The time of activation of the CaMKII molecules by the population of *CaM**Ca*₂, which is the one that can lead to phosphorylation [106], keeping the kinase CaMKII active, is given in our model by the time for the first killing to occur, as it represents the binding of *CaM**Ca*₂ to CaMKII. We have assumed as well that the CaM molecules are very close to the initial source of calcium ions, and as the binding between calcium ions and CaM is very fast, the activation time for CaMKII can be computed from formula (2.31) leading to

$$\mathbb{E}[\tau^k(N) | n < N, y] \sim \frac{(y - x_1)^2}{4D \left[\ln \left(\frac{p^2 N V_1 (y - x_1)}{4D\sqrt{\pi}} \right) \right]}, \quad (2.45)$$

where $D = 100 \mu m^2/s$, $N = 500$, $y = 1 \mu m$, $x_1 = 0.1 \mu m$, $p = 0.2$ [119], V_1 is not known but it could be found from experiments. For instance if $V_1 = 50 \mu m/s$, we can find the mean time for activate the CaMKII by replacing all values in the formula, and thus we obtain $\bar{\tau}^k(N) \approx 0.0085 s$, meaning that the activation of these molecules is in the order of a few milliseconds.

2.5 Conclusions and perspective

We reported here various escape asymptotic formulas for the fastest particles to reach the boundary of an interval when there are multiple Dirac delta killing sources. We obtain the asymptotic formulas when the initial and surviving number of particles is large. These formulas revealed the mixed role of dynamics and killing that influences the fastest particle to escape. In general we have obtained, using Laplace's method, the decay in $1/\ln(N)$ but from the simulations results we notice that for a fixed number N the fastest particle is not following the direct path, as a parameter β is needed to correct the smallest distance.

We used this framework to estimate how buffers can influence calcium dynamics at synapses in the process of Calcium-Induced Calcium Release and we also estimate the time of CaMKII activation. In general, the present approach can be used to derive the time scale of biochemical processes, where signaling occurs through the fastest particles. This framework can also account for the time to activate an ensemble of chemical processes [120] or the time for a chemical message to be delivered when it is carried by few particles among many [57, 78, 79]. Finding a target is key to activate sub-cellular process [93]. However, during this event, the diffusing messenger can bind to molecules that can trap or destroy them, thus affecting the path of the fastest particles to their final target. These binding molecules can diminish the arrival probability, but interestingly, they reduce the arrival time when a large number of particle survive, as shown by formulas 2.29, 2.48, 2.51 and 2.53: indeed, the fastest particles should avoid staying in the domain where they can terminated, either while crossing a point or uniform killing zone. These formulas further reveal that the distribution of killing sources influences on the fastest escape time.

There are other examples where the present theory could be relevant: in the cell nucleus [121], transcription factors (TFs) are switching between different states before escaping to a small target site: the TFs are moving as a Brownian particles and can bind to various ligands to change state (acetylation or sumolysation) [38]. The TFs can be degraded, preventing the fastest to reach the target, while gene activation can only occur in one of the appropriate state. This example shows that the number of TFs can accelerate the production of mARN, but the escape time could be limited by killing processes. Finally, it would be interesting to extend the present study in higher dimensions emphasizing the case where the fastest particles can avoid entering in the killing region.

2.6 Appendix

We presented in this appendix the computations for the mean first escape time when the killing term is uniform over the full domain and over an interval that may or may not contain the initial point.

2.6.1 Escape for the fastest with a uniform killing in half-a-line

We now consider the escape time for the fastest particle when the killing rate $k(x, t) = V_0$ is constant over the non-negative real line $x \geq 0$. The diffusion coefficient is D and the pdf follows the FPE given by

$$\begin{aligned}\frac{\partial p(x, t | y)}{\partial t} &= D \frac{\partial^2 p(x, t | y)}{\partial x^2} - V_0 p(x, t | y), \quad \text{for } x \in \mathbb{R}_+, t > 0 \\ p(x, 0 | y) &= \delta(x - y) \\ p(0, t | y) &= 0.\end{aligned}$$

The solution for this equation is given by

$$p(x, t | y) = \exp\{-V_0 t\} \frac{1}{2\sqrt{\pi Dt}} \left(\exp\left\{-\frac{(x-y)^2}{4Dt}\right\} - \exp\left\{-\frac{(x+y)^2}{4Dt}\right\} \right)$$

and the flux is

$$J(t | y) = D \frac{\partial p}{\partial x}(x=0, t | y) = \exp\{-V_0 t\} \frac{y}{t\sqrt{4\pi Dt}} \left(\exp\left\{-\frac{y^2}{4Dt}\right\} \right).$$

Thus using the inverse Laplace transform

$$\int_0^\infty \frac{1}{\sqrt{\pi t^{3/2}}} e^{-at-b/t} dt = \frac{1}{2\sqrt{b}} \exp\left\{-2\sqrt{ab}\right\},$$

we find the expression for the escape probability given by

$$\int_0^\infty J(t | y) dt = \exp\left\{-y\sqrt{\frac{V_0}{D}}\right\}.$$

Thus, the probability that at least one escapes alive in an ensemble of N is

$$P_\infty = 1 - \left(1 - \int_0^\infty J(t | y) dt \right)^N = 1 - \left(1 - \exp\left\{-y\sqrt{\frac{V_0}{D}}\right\} \right)^N.$$

Similarly, we obtain the expression for the total flux for a single particle

$$\begin{aligned}\int_0^t J(s | y) ds &= \int_0^t \frac{y \exp\{-V_0 s\} \exp\left\{-\frac{y^2}{4Ds}\right\}}{\sqrt{4D\pi s}} ds \\ &= \frac{1}{2} \left(\exp\left\{-y\sqrt{\frac{V_0}{D}}\right\} \operatorname{erfc}\left(\frac{y}{\sqrt{4Dt}} - \sqrt{V_0 t}\right) + \exp\left\{y\sqrt{\frac{V_0}{D}}\right\} \operatorname{erfc}\left(\frac{y}{\sqrt{4Dt}} + \sqrt{V_0 t}\right) \right).\end{aligned}$$

For t small, using the expansion for the complementary error function for large arguments we compute the numerator of the MFPT (relation 2.17) as

$$\begin{aligned} s(t) &\approx \left(1 - \frac{e^{-\frac{y^2}{4Dt}} \sqrt{4Dt}}{y\sqrt{\pi}} \frac{\left(e^{-y\sqrt{\frac{V_0}{D}}} + e^{y\sqrt{\frac{V_0}{D}}} \right)}{2} \right)^N - \left(1 - e^{-y\sqrt{\frac{V_0}{D}}} \right)^N \\ &\approx 1 - \left(1 - e^{-y\sqrt{\frac{V_0}{D}}} \right)^N + \sum_{k=1}^N \binom{N}{k} \left(\frac{e^{-\frac{y^2}{4Dt}} \sqrt{4Dt}}{y\sqrt{\pi}} \frac{\left(e^{-y\sqrt{\frac{V_0}{D}}} + e^{y\sqrt{\frac{V_0}{D}}} \right)}{2} \right)^k. \end{aligned}$$

This, leads to the following integral dominated for t small when N large,

$$\begin{aligned} \mathbb{E}[\tau^e(N) | n \geq 1, y] &\approx \int_0^\delta \left[1 - N \frac{\sqrt{4Dt} \exp\left\{-\frac{y^2}{4Dt}\right\} \left(e^{-y\sqrt{\frac{V_0}{D}}} + e^{y\sqrt{\frac{V_0}{D}}} \right)}{2y\sqrt{\pi} \left(1 - \left(1 - e^{-y\sqrt{\frac{V_0}{D}}} \right)^N \right)} \right] dt \quad (2.46) \\ &\approx \int_0^\delta \exp \left\{ -N \frac{\sqrt{4Dt} \exp\left\{-\frac{y^2}{4Dt}\right\} \left(e^{-y\sqrt{\frac{V_0}{D}}} + e^{y\sqrt{\frac{V_0}{D}}} \right)}{2y\sqrt{\pi} \left(1 - \left(1 - e^{-y\sqrt{\frac{V_0}{D}}} \right)^N \right)} \right\} dt, \end{aligned}$$

leading to the asymptotic formula

$$\mathbb{E}[\tau^e(N) | n \geq 1, y] \sim \frac{y^2}{4D \ln \left(\frac{N \left(e^{-y\sqrt{\frac{V_0}{D}}} + e^{y\sqrt{\frac{V_0}{D}}} \right)}{2\sqrt{\pi}} \right)}. \quad (2.47)$$

We can also obtain from formula (2.7)

$$\mathbb{E}[\tau^e(N) | n = k, y] \sim \frac{y^2}{4D \left[\ln \left(\frac{k \left(e^{-y\sqrt{\frac{V_0}{D}}} + e^{y\sqrt{\frac{V_0}{D}}} \right)}{2e^{-y\sqrt{\frac{V_0}{D}}} \sqrt{\pi}} \right) \right]}. \quad (2.48)$$

Note that, when $V_0 = 0$, we recover in both expressions the asymptotic formula for the case without killing and a Dirac delta function as initial condition.

2.6.2 Killing in a finite interval in half a line with initial point outside the interval

We consider the diffusion of a particle that starts at a point y outside the interval $[0, L]$. The pdf of that particle's trajectory satisfies the equation

$$\begin{aligned}\frac{\partial p(x, t | y)}{\partial t} &= D \frac{\partial^2 p(x, t | y)}{\partial x^2} - V \chi_{[0, L]}(x) p(x, t | y) \quad \text{on } \mathbf{R}_+ \\ p(x, 0 | y) &= \delta(x - y) \\ p(0, t | y) &= 0.\end{aligned}\tag{2.49}$$

To compute the explicit solution, $p(x, t | y)$, we Laplace transform the equation with respect to the time variable t and we obtain the equation

$$\begin{aligned}\frac{\partial^2 u}{\partial x^2}(x, q) - \left(\frac{q + V}{D}\right) u(x, q) &= 0 \quad \text{for } x \in [0, L] \\ \frac{\partial^2 u}{\partial x^2}(x, q) - \left(\frac{q}{D}\right) u(x, q) &= -\frac{1}{D} \delta(x - y) \quad \text{for } x \in (L, +\infty),\end{aligned}$$

where $u(x, q) = L_q(p(x, t | y))$, and the bounded solutions in \mathbf{R}_+ are in the form

$$\begin{aligned}u(x, q) &= A \exp\left\{-\sqrt{\frac{q+V}{D}}x\right\} - A \exp\left\{\sqrt{\frac{q+V}{D}}x\right\} \quad \text{for } x \in [0, L] \\ u(x, q) &= \frac{1}{\sqrt{4Dq}} \exp\left\{-\sqrt{\frac{q}{D}}|x - y|\right\} + B \exp\left\{-\sqrt{\frac{q}{D}}|x + y|\right\} \quad \text{for } x \in (L, +\infty).\end{aligned}$$

We are looking for the solutions that are continuous at $x = L$ and whose first derivative is also continuous at $x = L$. Then solving the corresponding system we get

$$\begin{aligned}A &= -\frac{e^{\sqrt{\frac{q}{D}}(L-y)}}{D \left(\left(\sqrt{\frac{q+V}{D}} - \sqrt{\frac{q}{D}} \right) e^{-\sqrt{\frac{q+V}{D}}L} + \left(\sqrt{\frac{q+V}{D}} + \sqrt{\frac{q}{D}} \right) e^{\sqrt{\frac{q+V}{D}}L} \right)}, \\ B &= \frac{\left(\sqrt{\frac{q+V}{D}} - \sqrt{\frac{q}{D}} \right) e^{-\left(\sqrt{\frac{q+V}{D}} - 2\sqrt{\frac{q}{D}} \right)L} - \left(\sqrt{\frac{q+V}{D}} - \sqrt{\frac{q}{D}} \right) e^{\left(\sqrt{\frac{q+V}{D}} + 2\sqrt{\frac{q}{D}} \right)L}}{\sqrt{4Dq} \left(\left(\sqrt{\frac{q+V}{D}} - \sqrt{\frac{q}{D}} \right) e^{-\sqrt{\frac{q+V}{D}}L} + \left(\sqrt{\frac{q+V}{D}} + \sqrt{\frac{q}{D}} \right) e^{\sqrt{\frac{q+V}{D}}L} \right)}.\end{aligned}$$

The escape probability is given by

$$\int_0^\infty J(t) dt = D \int_0^t \frac{\partial p}{\partial x}(x = 0, t | y) dt = D \frac{\partial u}{\partial x}(0, 0) = \frac{1}{\cosh\left(\sqrt{\frac{V}{D}}L\right)}.$$

For t small, we have

$$\begin{aligned}\int_0^t J(s) ds &= D \int_0^t \frac{\partial p}{\partial x}(x = 0, s | y) ds \sim \int_0^t \left[L_s^{-1} \left(e^{-y\sqrt{\frac{q}{D}}} \right) - VLL_s^{-1} \left(\frac{e^{-y\sqrt{\frac{q}{D}}}}{\sqrt{4Dq}} \right) \right] ds \\ &\sim \operatorname{erfc}\left(\frac{y}{\sqrt{4Dt}}\right).\end{aligned}$$

Then, we have

$$P_\infty = 1 - \left(1 - \int_0^\infty J(t | y) dt \right)^N = 1 - \left(1 - \frac{1}{\cosh(\sqrt{\frac{V}{D}}L)} \right)^N,$$

and

$$\begin{aligned} s(t) &\approx \left(1 - \frac{e^{-\frac{y^2}{4Ds}} \sqrt{4Dt}}{y\sqrt{\pi}} \right)^N - \left(1 - \frac{1}{\cosh(\sqrt{\frac{V}{D}}L)} \right)^N \\ &\approx 1 - \left(1 - \frac{1}{\cosh(\sqrt{\frac{V}{D}}L)} \right)^N + \sum_{k=1}^N \binom{N}{k} \left(\frac{e^{-\frac{y^2}{4Ds}} \sqrt{4Dt}}{y\sqrt{\pi}} \right)^k. \end{aligned}$$

This leads to the following integral dominated for t small when N is large

$$\begin{aligned} \mathbb{E}[\tau^e(N) | n \geq 1, y] &\approx \int_0^\delta \left[1 - N \frac{\sqrt{4Dt} \exp\left\{-\frac{y^2}{4Dt}\right\}}{y\sqrt{\pi} \left(1 - \left(1 - \frac{1}{\cosh(\sqrt{\frac{V}{D}}L)} \right)^N \right)} \right] dt \\ &\approx \int_0^\infty \exp\left\{ -N \frac{\sqrt{4Dt} \exp\left\{-\frac{y^2}{4Dt}\right\}}{y\sqrt{\pi}} \right\} dt, \end{aligned}$$

we obtain thus the asymptotic formula

$$\mathbb{E}[\tau^e(N) | n \geq 1, y] \sim \frac{y^2}{4D \ln\left(\frac{N}{\sqrt{\pi}}\right)}. \quad (2.50)$$

From formula (2.7) we obtain the MFPT when exactly k particles escapes, given by

$$\mathbb{E}[\tau^e(N) | n = k, y] \sim \frac{y^2}{4D \left[\ln\left(\frac{k \cosh(\sqrt{\frac{V}{D}}L)}{\sqrt{\pi}}\right) \right]}. \quad (2.51)$$

Note that, when $V = 0$, we recover the asymptotic formula for the case without a killing term and a Dirac delta function as initial condition.

2.6.3 Killing in a finite interval in half a line with initial point inside the interval

In this case, we consider the diffusion of a particle that starts at point y inside the interval $[0, L]$, then the pdf for the particle's trajectory satisfies the equation (2.49). Applying the Laplace transform

to this equation, we obtain

$$\begin{aligned}\frac{\partial^2 u}{\partial x^2}(x, q) - \left(\frac{q+V}{D}\right)u(x) &= -\frac{1}{D}\delta(x-y) && \text{for } x \in [0, L] \\ \frac{\partial^2 u}{\partial x^2}(x, q) - \left(\frac{q}{D}\right)u(x) &= 0 && \text{for } x \in (L, +\infty),\end{aligned}$$

where $u(x, q) = L_q(p(x, t|y))$. Here, the bounded solutions in \mathbf{R}_+ are in the form

$$\begin{aligned}u(x, q) &= A \left(\exp \left\{ -\sqrt{\frac{q+V}{D}}|x-y| \right\} - \exp \left\{ -\sqrt{\frac{q+V}{D}}|x+y| \right\} \right) \\ &+ \left(A - \frac{1}{\sqrt{4D(q+V)}} \right) \left(\exp \left\{ \sqrt{\frac{q+V}{D}}|x-y| \right\} - \exp \left\{ \sqrt{\frac{q+V}{D}}|x+y| \right\} \right) \quad \text{for } x \in [0, L] \\ u(x, q) &= B \exp \left\{ -\sqrt{\frac{q}{D}}x \right\} \quad \text{for } x \in (L, +\infty).\end{aligned}$$

Because we are looking for the continuous solutions at $x = L$ with first derivative continuous at $x = L$, we can solve the corresponding system and we obtain

$$\begin{aligned}A &= \frac{-\left(\sqrt{\frac{q+V}{D}}+\sqrt{\frac{q}{D}}\right)\left(e^{\sqrt{\frac{q+V}{D}}(L-y)}-e^{\sqrt{\frac{q+V}{D}}(L+y)}\right)\frac{1}{\sqrt{4D(q+V)}}}{\left(\left(\sqrt{\frac{q+V}{D}}-\sqrt{\frac{q}{D}}\right)\left(e^{-\sqrt{\frac{q+V}{D}}(L-y)}-e^{-\sqrt{\frac{q+V}{D}}(L+y)}\right)-\left(\sqrt{\frac{q+V}{D}}+\sqrt{\frac{q}{D}}\right)\left(e^{\sqrt{\frac{q+V}{D}}(L-y)}-e^{\sqrt{\frac{q+V}{D}}(L+y)}\right)\right)}, \\ B &= \frac{e^{-\sqrt{\frac{q}{D}}L}}{D\left(\left(\sqrt{\frac{q+V}{D}}-\sqrt{\frac{q}{D}}\right)\left(e^{-\sqrt{\frac{q+V}{D}}(L-y)}-e^{-\sqrt{\frac{q+V}{D}}(L+y)}\right)-\left(\sqrt{\frac{q+V}{D}}+\sqrt{\frac{q}{D}}\right)\left(e^{\sqrt{\frac{q+V}{D}}(L-y)}-e^{\sqrt{\frac{q+V}{D}}(L+y)}\right)\right)}.\end{aligned}$$

The escape probability is given by

$$\int_0^\infty J(t)dt = D \int_0^t \frac{\partial p}{\partial x}(x=0, t|y) dt = D \frac{\partial u}{\partial x}(0, 0) = \exp \left\{ -y\sqrt{\frac{V}{D}} \right\},$$

and for small t , we obtain the approximation

$$\int_0^t J(s)ds = D \int_0^t \frac{\partial p}{\partial x}(x=0, s|y) ds \approx \int_0^t L_s^{-1} \left(e^{-y\sqrt{\frac{q}{D}}} \right) ds \approx \text{erfc} \left(\frac{y}{\sqrt{4Dt}} \right).$$

Then, as in the case for the uniform killing, we get the asymptotic formula

$$\mathbb{E}[\tau^e(N) | n \geq 1, y] \sim \frac{y^2}{4D \ln \left(\frac{N \left(e^{-y\sqrt{\frac{V}{D}}} + e^{y\sqrt{\frac{V}{D}}} \right)}{2\sqrt{\pi}} \right)}. \quad (2.52)$$

From formula (2.7) we obtain the MFPT when exactly k particles escapes. This formula is given by

$$\mathbb{E}[\tau^e(N) | n = k, y] \sim \frac{y^2}{4D \left[\ln \left(\frac{k \cosh(\sqrt{\frac{V}{D}}L)}{2e^{-y\sqrt{\frac{V}{D}}}\sqrt{\pi}} \right) \right]}. \quad (2.53)$$

Chapter 3

Narrow escape with a uniform killing field in 2D and optimal exit paths

Chapter in preparation by TOSTE S., PAQUIN-LEFEBVRE F. & HOLCMAN D.

Abstract

Narrow escape theory studies the time distribution of the fastest among many identical stochastic particles to escape from a narrow window. In this manuscript, we study how a killing measure that can terminate diffusing particles influencing the statistics for the fastest particle. We first compute asymptotically the mean time for the fastest to escape alive when there is a uniform killing measure in the entire domain. This computation uses the time-dependent flux across the absorbing section that can either be the entire boundary or a small portion of it. We also present asymptotic computations and stochastic simulations of the escape probability when the killing is restricted to a small region of the domain. Finally, we find that the optimal paths followed by the fastest particle avoiding the killing zone is the solution of a variational problem.

3.1 Introduction

Narrow escape describes the statistical properties of the fastest among many identical and independent stochastic particles, with the same initial distribution, escaping through a narrow window [93, 100, 101, 122]. The fastest particle to reach a small target often defines the time scales of activation in molecular biology. There are numerous examples in cell physiology, such as membrane channel activation triggered by the arrival of the first molecules to a key site. Other examples are transcription factors within the nucleus, calcium ions that induce calcium release to amplify the signal inside a dendrite [102] or particles that can alternate between motion along the boundary and inside of a domain, such as bacteria or spermatozoa [68, 104, 105, 123]. In the context of fertility, spermatozoa could be degraded, thus affecting the probability of finding the egg in a reasonable time. A similar situation can be found during the early step of viral infection in a cell, where viral particles must enter through a small pore of the nucleus [12], before being degraded by the defense mechanism of the cell [38]. Degradation is also a key response to unfolded proteins correcting the stress in the endoplasmic reticulum (ER), event that could lead to cellular death and afterwards to many human diseases [124, 125]. In the particular case of Ca^{2+} ions inside the *ER*, the killing

measure could be used to model calcium buffers, such as SERCA pumps and calmodulin.

Here, we study the arrival to an absorbing boundary of the fastest particle that has survived to

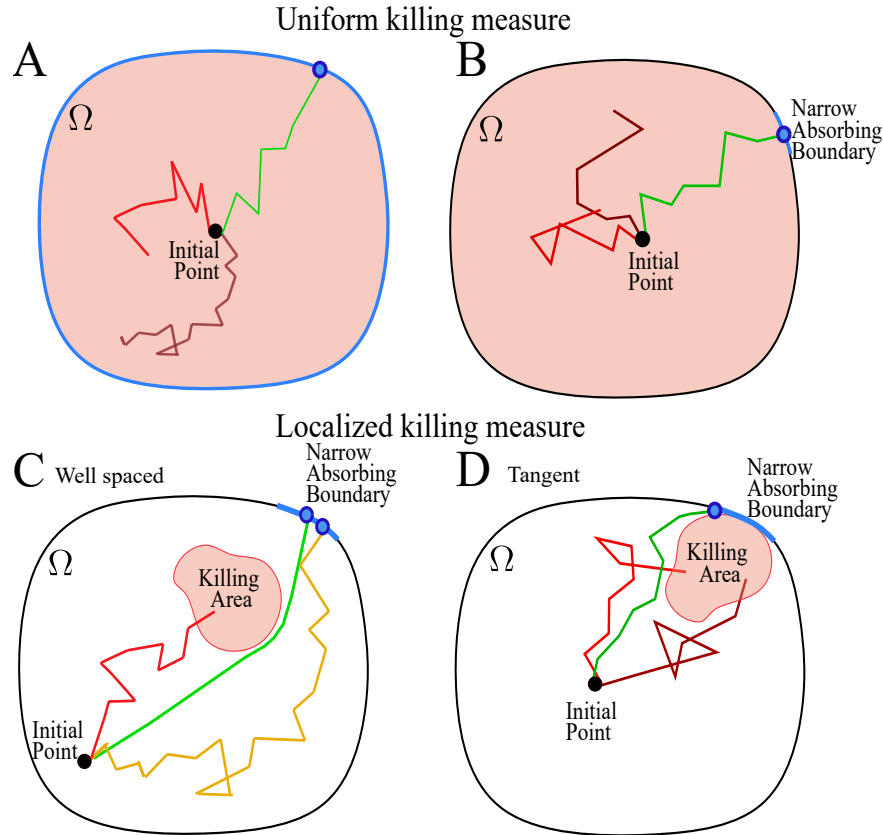


Figure 3.1: **Escape vs Killing for different scenarios.** **A.** Survival trajectory (green) vs killed (red) trajectories in a 2D-domain with uniform killing and fully absorbing boundary condition. **B.** The absorbing boundary is a small portion of the boundary. **C.** The killing area is confined (pink region), while trajectory can escape at the small absorbing window (blue). The fastest trajectory is plotted in green. **D.** The killing area is tangent to the small absorbing window (blue) making difficult the escape.

a killing field in a disk domain. The killing term models the termination of trajectories at any position where it is present. Under this condition, particles can terminate their motion inside the killing area, as shown in Fig. 3.1 (red trajectories). This killing measure modifies thus the amount of survival particles, therefore the escape probability and also the possible trajectory of the fastest. In one dimension, the optimal trajectory for the fastest cannot avoid the killing region [126], leading to specific laws for the mean time of the fastest particles depending on the killing measure. In two dimensions, depending on the location of the killing area, the fastest trajectories could avoid the killing measure as is shown by the trajectories yellow and green in Fig 3.1C.

We consider a two-dimensional diffusion model, where particles can terminate their motion inside the killing area, while others can escape from the domain through the absorbing boundary. When the absorbing boundary is a small section this problem relies on the narrow escape theory [8, 11]. The killing measure $k(\mathbf{x}, t)$ is the rate per unit time and unit measure at which a trajectory is terminated at a given location. A particle can pass through the killing area many times without being eliminated, in contrast to an absorbing boundary, where the trajectory is terminated with probability 1.

We compute here asymptotic formulas for the mean escape time of the fastest particle with uni-

form killing inside the 2D-disk domain where the absorbing boundary is either the full boundary (Fig 3.1A) or a narrow part of it (Fig 3.1B). We present also some simulation results for the case where the killing area is a subdomain of the 2D-disk with a narrow absorbing boundary as shown in Fig 3.1C. The manuscript is organized as follows: in section 2, we present the narrow escape theory with a killing measure. In section 3, we consider the Euclidean 2D-disk and the uniform killing measure, with a fully and narrow absorbing boundary (Fig 3.1A-B). In section 4, we compute the probability to escape through a narrow absorbing window when the killing area is either well separated or tangent to the absorbing window (Fig 3.1C-D). In section 5, we show the stochastic simulations results made in order to analyze the influence of the most important parameters on the mean first passage time (MFPT) and on the escape probability (P_e). In section 6 we employ the large deviation principle to obtain the optimal paths associated with the fastest particles when the killing area is well separated from the absorbing window. Finally, in section 7, we show results that illustrate how a killing region tangent to the absorbing boundary (Fig 3.1D) affects the arrival time.

3.2 Revision on the conditional first arrival time

We consider a stochastic process $\mathbf{x}(t)$ evolving in a domain Ω , which satisfying the stochastic dynamics

$$d\mathbf{x} = \mathbf{b}(\mathbf{x}) dt + \sqrt{2}\mathbf{B}(\mathbf{x}) d\mathbf{w}(t) \quad \text{for } \mathbf{x} \in \Omega, \quad (3.1)$$

where $\mathbf{b}(\mathbf{x})$ is a smooth drift vector, $\mathbf{B}(\mathbf{x})$ is a diffusion matrix, and $\mathbf{w}(t)$ is a vector of independent standard Brownian motions. The domain boundary is decomposed as $\partial\Omega = \partial\Omega_a \cup \partial\Omega_r$, where $\partial\Omega_r$ is reflecting while $\partial\Omega_a$ consists of a small absorbing part. A killing measure $k(x, t)$ is added to the process (2.1) to model the removal of particles inside the domain as already introduced in section 0.1.2. The transition probability density function (pdf) of the process $\mathbf{x}(t)$ with killing and absorption is the pdf of trajectories that have neither been killed nor been absorbed in $\partial\Omega_a$ by time t , this is

$$p(\mathbf{x}, t | \mathbf{y}) d\mathbf{x} = \Pr\{\mathbf{x}(t) \in \mathbf{x} + d\mathbf{x}, \tau^k > t, \tau^e > t | \mathbf{y}\}, \quad (3.2)$$

where τ^k and τ^e are the random times at which one particle is either killed or absorbed. This pdf is solution of the Fokker-Planck equation (FPE) [127]

$$\frac{\partial p(\mathbf{x}, t | \mathbf{y})}{\partial t} = \mathcal{L}_{\mathbf{x}} p(\mathbf{x}, t | \mathbf{y}) - k(\mathbf{x})p(\mathbf{x}, t | \mathbf{y}) \quad \text{for } \mathbf{x}, \mathbf{y} \in \Omega, \quad (3.3)$$

where $\mathcal{L}_{\mathbf{x}}$ is the forward operator

$$\mathcal{L}_{\mathbf{x}} p(\mathbf{x}, t | \mathbf{y}) = \sum_{i,j=1}^d \frac{\partial^2 D^{i,j}(\mathbf{x})p(\mathbf{x}, t | \mathbf{y})}{\partial x^i \partial x^j} - \sum_{i=1}^d \frac{\partial b^i(\mathbf{x})p(\mathbf{x}, t | \mathbf{y})}{\partial x^i}, \quad (3.4)$$

and $\mathbf{D}(\mathbf{x}) = \frac{1}{2}\mathbf{B}(\mathbf{x})\mathbf{B}^T(\mathbf{x})$. Using the divergence operator, $\mathcal{L}_{\mathbf{x}}$ can be written in the form $\mathcal{L}_{\mathbf{x}} p(\mathbf{x}, t | \mathbf{y}) = -\nabla \cdot \mathbf{J}(\mathbf{x}, t | \mathbf{y})$, where the components of the flux density vector $\mathbf{J}(\mathbf{x}, t | \mathbf{y})$ are

$$J^i(\mathbf{x}, t | \mathbf{y}) = - \sum_{j=1}^d \frac{\partial D^{i,j}(\mathbf{x})p(\mathbf{x}, t | \mathbf{y})}{\partial x^j} + b^i(\mathbf{x})p(\mathbf{x}, t | \mathbf{y}), \quad (i = 1, 2, \dots, d). \quad (3.5)$$

Initial and boundary conditions for the FPE (3.3) are

$$p(\mathbf{x}, 0 | \mathbf{y}) = \delta(\mathbf{x} - \mathbf{y}) \text{ for } \mathbf{x}, \mathbf{y} \in \Omega \quad (3.6)$$

$$p(\mathbf{x}, t | \mathbf{y}) = 0 \text{ for } t > 0, \mathbf{x} \in \partial\Omega_a, \mathbf{y} \in \Omega \quad (3.7)$$

$$\mathbf{J}(\mathbf{x}, t | \mathbf{y}) \cdot \mathbf{n}(\mathbf{x}) = 0 \text{ for } t > 0, \mathbf{x} \in \partial\Omega_r = \partial\Omega \setminus \partial\Omega_a, \mathbf{y} \in \Omega. \quad (3.8)$$

The absorption probability flux on $\partial\Omega_a$ is

$$\Pr\{\tau^e \in [t, t + dt], \tau^k > \tau^e\} = J(t | \mathbf{y}) = \oint_{\partial\Omega} \mathbf{J}(\mathbf{x}, t | \mathbf{y}) \cdot \mathbf{n}(\mathbf{x}) dS_{\mathbf{x}}, \quad (3.9)$$

thus the probability to escape before being killed is

$$\Pr\{\tau^e < \tau^k | \mathbf{y}\} = \int_0^\infty J(t | \mathbf{y}) dt. \quad (3.10)$$

For N independent identically distributed copies driven by the stochastic process (3.1), we define the arrival times as t_1, \dots, t_N where $t_i = \infty$ if the i -th particle is killed before escaping and we propose to derive here a formula for the probability and the conditional mean time when a large number of particles escape. The conditional mean first passage time (MFPT) is the first time for a Brownian particle to escape through a narrow window located on the boundary and it is defined as

$$\tau^e(N) = \min\{t_1, \dots, t_N\},$$

where N is the initial number of particles. The conditional mean first passage time can be expressed in terms of the absorption probability flux (3.9) as obtained in section 0.1.2, leading to the general expression

$$\mathbb{E}[\tau^e(N) | n = k] = \int_0^\infty \left[1 - \frac{\int_0^t J(s | \mathbf{y}) ds}{\int_0^\infty J(s | \mathbf{y}) ds} \right]^k dt. \quad (3.11)$$

We derive in the manuscript different expressions for the MFPT depending on the killing measure and the geometry of the killing area when no drift is consider and the diffusion coefficient is constant.

3.3 Escape vs uniform killing in a 2D-disk

The mean first passage time for the fastest among N_0 Brownian particles starting at the origin, moving inside the disk $\Omega = B_R(0, 0)$, with a fully absorbing boundary and without a killing measure $\bar{\tau}^1(N_0) = \mathbb{E}[\min(t_1, \dots, t_{N_0})]$ is given by the logarithmic formula $\bar{\tau}^1(N_0) \sim \frac{R^2}{4D \ln(2N_0)}$, where D is the diffusion coefficient. This result is obtained by reducing the FPE to a 1D equation using the radial symmetry of the domain and the absorbing boundary.

3.3.1 Fully absorbing boundary condition

By adding an uniform killing measure $k(x, t) = V \mathbf{I}_{x \in \Omega}(x)$ with a killing weight V in the domain and keeping the fully absorbing boundary, as shown in the schematic Fig. 3.1A, we obtain the FPE

$$\frac{\partial p(\mathbf{x}, t)}{\partial t} = D \Delta_{2d} p(\mathbf{x}, t) - V p(\mathbf{x}, t) \quad \text{on } B_R(0, 0) \quad \text{for } t > 0, \quad (3.12)$$

$$p(\mathbf{x}, 0) = \delta(\mathbf{x}) \quad \text{on } B_R(0, 0),$$

$$p(\mathbf{x}, t) = 0 \quad \text{on } \partial B_R(0, 0) \quad \text{for } t > 0.$$

The Laplace's transform in time $\hat{p}(\mathbf{x}, q) = L_q(p(\mathbf{x}, t)) = \int_0^\infty p(\mathbf{x}, t)e^{-qt}dt$ satisfies the ordinary equation

$$\Delta_{2D}\hat{p}(\mathbf{x}, q) - \left(\frac{q+V}{D}\right)\hat{p}(\mathbf{x}, q) = -\frac{\delta(\mathbf{x})}{D}, \quad (3.13)$$

where q is the frequency variable, and \mathbf{x} is the "untransformed" variable. We have swapped here the integral from the Laplace's transform and the derivatives in the spatial variable since $p(\mathbf{x}, t) \in C^1[\Omega]$. Using polar coordinates $\hat{p}(\mathbf{x}, q) = u(r, q)$ we obtain

$$\frac{\partial^2 u(r, q)}{\partial r^2} + \frac{1}{r} \frac{\partial u(r, q)}{\partial r} - \left(\frac{q+V}{D}\right) u(r, q) = -\frac{\delta(r)}{2\pi D r}, \quad (3.14)$$

where r is the radius. This is a modified Bessel's differential equation [128] in the form

$$x^2 \frac{d^2 y}{dx^2} + x \frac{dy}{dx} - (x^2 + \alpha^2)y = 0, \quad (3.15)$$

where $x = \sqrt{\frac{q+V}{D}}r$ and $\alpha = 0$. The Laplace transform of the boundary condition becomes now $u(R, q) = 0$, leading to the solution given by

$$u(r, q) = \frac{1}{2\pi D} \left(K_0 \left(\sqrt{\frac{q+V}{D}}r \right) - \frac{K_0 \left(\sqrt{\frac{q+V}{D}}R \right)}{I_0 \left(\sqrt{\frac{q+V}{D}}R \right)} I_0 \left(\sqrt{\frac{q+V}{D}}r \right) \right), \quad (3.16)$$

where $I_0(x)$ and $K_0(x)$ are the modified Bessel functions of the first and second kind and order zero. We remark here that the second term in (3.16) is correcting the solution at the boundary. We can compute the flux $J(s)$ defined in formula (3.9) as

$$J(s) = -2\pi R D L_s^{-1} \left(\frac{du(r, q)}{dr} \right) |_{r=R}, \quad (3.17)$$

where $L_s^{-1}(F(x, q))$ is the inverse Laplace transform of the function $F(x, q)$. We define now, the escape probability $P_e(V, D, R)$ using the Laplace's transform as follows

$$P_e(V, D, R) = \int_0^\infty J(s) ds = L_q(J(s))|_{q=0}, \quad (3.18)$$

and then, setting $q = 0$ in the Laplace transform of equation (3.17) we obtain

$$P_e(V, D, R) = \sqrt{\frac{V}{D}} R \left(K_1 \left(\sqrt{\frac{V}{D}} R \right) + \frac{K_0 \left(\sqrt{\frac{V}{D}} R \right)}{I_0 \left(\sqrt{\frac{V}{D}} R \right)} I_1 \left(\sqrt{\frac{V}{D}} R \right) \right), \quad (3.19)$$

where $I_1(x)$ and $K_1(x)$ are modified Bessel functions of order one. The escape probability $L(V, D, R)$ decreases as a function V when the killing weight V increases as shown in Fig. 3.2A.

For small time t or equivalently q large in the Laplace's domain, we can approximate the solution by

$$u(r, q) \approx \frac{1}{2\pi D} \left(K_0 \left(\sqrt{\frac{q+V}{D}}r \right) - \frac{(2R-r)^{\frac{1}{2}}}{r^{\frac{1}{2}}} K_0 \left(\sqrt{\frac{q+V}{D}}(2R-r) \right) \right), \quad (3.20)$$

using the asymptotic approximations for large arguments of the modified Bessel functions $K_\alpha(x) = \sqrt{\frac{\pi}{2x}} e^{-x} (1 + O(\frac{1}{x}))$ and $I_\alpha(x) = \frac{e^x}{\sqrt{2\pi x}} (1 + O(\frac{1}{x}))$. This is,

$$\begin{aligned} u(r, q) &\approx \frac{1}{2\pi D} \left(K_0 \left(\sqrt{\frac{q+V}{D}} r \right) - \frac{\sqrt{\frac{\pi}{2\sqrt{\frac{q+V}{D}} R}} e^{-\sqrt{\frac{q+V}{D}} R}}{\sqrt{\frac{e\sqrt{\frac{q+V}{D}} R}{2\pi\sqrt{\frac{q+V}{D}} R}}} \frac{e^{\sqrt{\frac{q+V}{D}} r}}{\sqrt{2\pi\sqrt{\frac{q+V}{D}} r}} \right) \\ &\approx \frac{1}{2\pi D} \left(K_0 \left(\sqrt{\frac{q+V}{D}} r \right) - \frac{\sqrt{\frac{\pi}{2\sqrt{\frac{q+V}{D}}}} e^{-\sqrt{\frac{q+V}{D}}(2R-r)}}{\sqrt{r}} \right) \\ &\approx \frac{1}{2\pi D} \left(K_0 \left(\sqrt{\frac{q+V}{D}} r \right) - \frac{\sqrt{2R-r}}{\sqrt{r}} K_0 \left(\sqrt{\frac{q+V}{D}} (2R-r) \right) \right). \end{aligned} \quad (3.21)$$

Now, we can find the inverse Laplace transform of the solution as the combination of inverse Laplace transform of Bessel functions K_0 , given by the formula

$$u(r, s) \approx \frac{e^{-Vs}}{4\pi D s} \left(e^{-\frac{r^2}{4Ds}} - \frac{(2R-r)^{\frac{1}{2}}}{r^{\frac{1}{2}}} e^{-\frac{(2R-r)^2}{4Ds}} \right), \quad (3.22)$$

when s is small. Following formula (3.17) we obtain an approximate expression for the flux when t is small given by

$$J(s) \approx e^{-Vs} e^{-\frac{R^2}{4Ds}} \left(\frac{R^2}{2Ds^2} - \frac{1}{s} \right). \quad (3.23)$$

For small time t , we can have an expression for the integral of the flux using the Taylor expansion $e^{-Vs} = 1 - Vs + O(s^2)$. This is

$$\begin{aligned} \int_0^t J(s) ds &\approx \int_0^t \frac{(1 - Vs + \frac{V^2 s^2}{2}) e^{-\frac{R^2}{4Dt}}}{2D} \left(\frac{R^2}{s^2} - \frac{1}{s} \right) ds \\ &\approx \left(2 + Vt + \frac{R^2 V^2 t}{4D} \right) e^{-\frac{R^2}{4Dt}} - \left(1 + \frac{3VR^2}{4D} + \frac{V^2 R^4}{16D^2} \right) \Gamma \left(0, \frac{R^2}{4Dt} \right), \end{aligned} \quad (3.24)$$

where $\Gamma(a, x)$ is the upper incomplete Gamma function [129]. Under the small t regime we have the approximation

$$\int_0^t J(s) ds = 2e^{-\frac{R^2}{4Dt}} + O \left(t e^{-\frac{R^2}{4Dt}} \right), \quad (3.25)$$

whose leading order term is $2e^{-\frac{R^2}{4Dt}}$, as in the case without killing. Thus, following formula (3.11), we have the asymptotic formula

$$\mathbb{E}[\tau^e(N) | n = k] = \int_0^\infty \left[1 - \frac{\int_0^t J(s | \mathbf{y}) ds}{\int_0^\infty J(s | \mathbf{y}) ds} \right]^k dt \approx \int_0^\delta \left(1 - \frac{2e^{-\frac{R^2}{4Dt}}}{P_e(V, D, R)} \right)^k dt \sim \frac{R^2}{4D \ln \left(\frac{2k}{P_e(V, D, R)} \right)}. \quad (3.26)$$

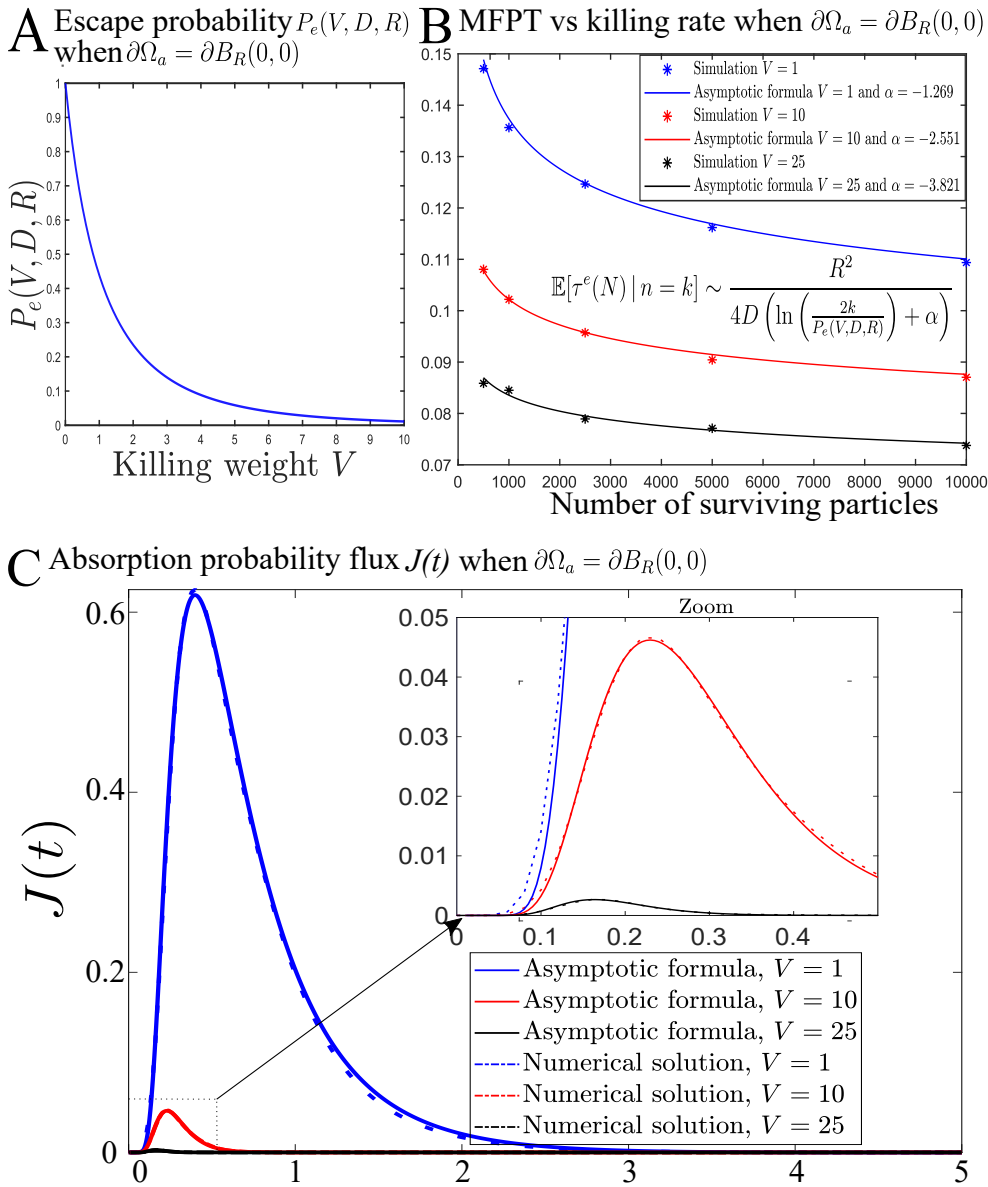


Figure 3.2: **Uniform killing with a fully absorbing boundary on a 2D-disk domain.** **A.** Decay of the escape probability $P_e(V, D, R)$, given by formula (3.19), as a function of the killing weight V for $D = 1$ and $R = 2$. **B.** MFPT vs k obtained from stochastic simulations (colored disks) and the asymptotic formula (3.27) (continuous lines) with $D = 1$ and $\mathbf{y} = (0, 0)$ for 1000 runs. **C.** Shrinkage of the absorption probability flux (3.23) for different values of the killing weight V .

The first approximation was made using Laplace method, where we have approximated the full integral by the integral around the point $t = 0$. The second approximation can be obtained following the same exact steps given in section 0.1.4 at page 20.

Fig. 3.2B shows the good agreement between the asymptotic formula for the flux given in the formula (3.23) and the numerical solution found using COMSOL for $D = 1$, $R = 2$, and $V = (1, 10, 25)$.

We are interested in the time necessary for the fastest particle to escape over a collection of k survival particles, and thus we simulate only the scenario where all the particles survive, for $k \in$

(500, 1000, 2500, 5000, 10000). We then compute the average of the fastest particles over 1000 simulations. Here all the particles started at the origin, and the discrete time-step is $dt = 0.01$, the diffusion coefficient is $D = 1$, the domain radius is $R = 2$. Finally, the values for the killing weight V were taken in (1, 10, 25), and our simulation results are shown in Fig. 3.2B. This figure shows the fitting made between the stochastic simulations and the asymptotic formula

$$\mathbb{E}[\tau^e(N) | n = k] \sim \frac{R^2}{4D \left(\ln \left(\frac{2k}{P_e(V,D,R)} \right) + \alpha \right)} \quad (3.27)$$

for the different values of the killing weight presented before. The parameter α is correcting the approximations up to leading order that we have made. The fact that from the simulations results we see that when V increases, α increases as well in its absolute value is telling us that the sum of the remainder terms in approximation (3.25) is an increasing function of V . The quantity in the right hand side in formula (3.26) decreases when the killing weight V increases as well as the results obtained from the simulations. This means that, when the probability to be killed increases, the time for the fastest arriving particle is decreasing when conditioning on the survival number of particles is fixed and large. This result can be seen as an extension of the 1D associated problem that was already studied in [126]. Note also that when $V \rightarrow 0$ we obtain that $P_e(V,D,R) \rightarrow 1$ and thus, $\mathbb{E}[\tau^e(N) | n = k] \rightarrow \bar{\tau}^1(k)$.

3.3.2 Narrow absorbing boundary

We now consider the escape for the fastest particle when the absorbing boundary consists of a narrow arc of length 2ε centered around the point $\mathbf{A} = (R, 0)$ on the boundary of the disk, as shown in the schematic Fig. 3.1B. The FPE becomes then

$$\begin{aligned} \frac{\partial p(\mathbf{x}, t)}{\partial t} &= \Delta_{2D} p(\mathbf{x}, t) - V p(\mathbf{x}, t) \quad \text{on } \Omega \quad \text{for } t > 0, \\ p(\mathbf{x}, 0) &= \delta(\mathbf{x}) \quad \text{on } \Omega, \\ p(\mathbf{x}, t) &= 0 \quad \text{on } \partial\Omega_a \quad \text{for } t > 0, \\ \frac{\partial p(\mathbf{x}, t)}{\partial \mathbf{n}} &= 0 \quad \text{on } \partial\Omega_r \quad \text{for } t > 0, \end{aligned} \quad (3.28)$$

where $\partial\Omega_a$ and $\partial\Omega_r$ are the absorbing and reflecting boundaries respectively, and thus $\partial\Omega = \partial\Omega_a \cup \partial\Omega_r$.

Upon applying the Laplace's Transform in time $\hat{p}(\mathbf{x}, q) = L_q(p(\mathbf{x}, t)) = \int_0^\infty p(\mathbf{x}, t) e^{-qt} dt$ to equation (3.28), we get

$$\Delta_{2D} \hat{p}(\mathbf{x}, q) - \left(\frac{q + V}{D} \right) \hat{p}(\mathbf{x}, q) = -\frac{\delta(\mathbf{x})}{D}, \quad (3.29)$$

subject to the boundary conditions

$$\hat{p}(\mathbf{x}, q) = 0 \quad \text{on } \partial\Omega_a \quad \text{for } q \geq 0 \quad (3.30)$$

$$\frac{\partial \hat{p}(\mathbf{x}, q)}{\partial \mathbf{n}} = 0 \quad \text{on } \partial\Omega_r \quad \text{for } q \geq 0. \quad (3.31)$$

To solve this equation, we use the Helmholtz-Green's function $\hat{G}(x, q)$ solution of

$$\begin{aligned}\Delta_{\mathbf{x}} \hat{G}(\mathbf{x}, q) - \left(\frac{q+V}{D} \right) \hat{G}(\mathbf{x}, q) &= -\frac{\delta(\mathbf{x})}{D} \\ \frac{\partial G(\mathbf{x}, q)}{\partial \mathbf{n}_x} &= 0 \quad \text{on } \partial\Omega \quad \text{for } q \geq 0,\end{aligned}\tag{3.32}$$

with Neumann boundary conditions. The solution for the origin centered disk is given by

$$\hat{G}(\mathbf{x}, q | \mathbf{y}) = \frac{1}{2\pi D} K_0 \left(\sqrt{\frac{q+V}{D}} |\mathbf{x} - \mathbf{y}| \right) + U(\mathbf{x}, \mathbf{y}),\tag{3.33}$$

for $\mathbf{x}, \mathbf{y} \in \partial\Omega$ where $|\cdot|$ is the Euclidean distance and $U(\mathbf{x}, \mathbf{y})$ given in [130] page 59 as an infinity sum representing the effect of the boundary condition. Using Green's second identity, we obtain the integral representation of the solution (3.28)

$$\hat{p}(\mathbf{x}, q) = \hat{G}(\mathbf{x}, q) + D \oint_{\partial\Omega_a} \hat{G}(\mathbf{x}, q | \mathbf{y}') \frac{\partial \hat{p}(\mathbf{x}, q | \mathbf{y}')}{\partial \mathbf{n}_x} dS_{\mathbf{y}'}\tag{3.34}$$

with $\mathbf{y}' \in \partial\Omega_a$. Setting $x = \mathbf{A} \in \partial\Omega_a$ where \mathbf{A} is the center of the absorbing boundary $\partial\Omega_a$ we obtain, using (3.30), the identity

$$0 = \hat{G}(\mathbf{A}, q) + D \oint_{\partial\Omega_a} \hat{G}(\mathbf{A}, q | \mathbf{y}') \frac{\partial \hat{p}(\mathbf{A}, q | \mathbf{y}')}{\partial \mathbf{n}_{\mathbf{A}}} dS_{\mathbf{y}'}.\tag{3.35}$$

We use here the leading order approximation to the boundary flux density which results in a constant solution of Helmholtz equation [11] in the form

$$\frac{\partial \hat{p}(\mathbf{x}, q | \mathbf{y}')}{\partial \mathbf{n}_x} = -C_{\mathbf{x}}(q) \quad \text{for all } \mathbf{x} \in \partial\Omega_a,\tag{3.36}$$

and we set $\mathbf{x} = \mathbf{A}$. Thus, at leading order we obtain

$$\hat{G}(\mathbf{A}, q) \approx \frac{C_A(q)}{2\pi} \oint_{\partial\Omega_a} K_0 \left(\sqrt{\frac{q+V}{D}} |\mathbf{A} - \mathbf{y}'| \right) dS_{\mathbf{y}'},\tag{3.37}$$

where $dS_{\mathbf{y}'}$ is the arc length of $\partial\Omega_a$. Because $\varepsilon \ll 1$, the expansion of the Green's function for small arguments when $|\mathbf{A} - \mathbf{y}'| \leq \varepsilon$ leads to

$$\begin{aligned}\hat{G}(\mathbf{A}, q) &\approx \frac{C_A(q)}{2\pi} \oint_{\partial\Omega_a} -\ln \left(\sqrt{\frac{q+V}{D}} |\mathbf{A} - \mathbf{y}'| \right) dS_{\mathbf{y}'} \approx \frac{C_A(q)}{\pi} \int_0^\varepsilon -\ln \left(\sqrt{\frac{q+V}{D}} r \right) dr \\ &\approx -\frac{C_A(q)}{\pi} \varepsilon \ln \left(\sqrt{\frac{q+V}{D}} \varepsilon \right).\end{aligned}\tag{3.38}$$

Thus, we can approximate $C_A(q)$ by

$$C_A(q) \approx \frac{\pi \hat{G}(\mathbf{A}, q)}{-\varepsilon \ln \left(\sqrt{\frac{q+V}{D}} \varepsilon \right)}.\tag{3.39}$$

Finally, to leading order, when $\sqrt{\frac{q+V}{D}}\varepsilon \ll 1$ and q is large, the flux in equation (3.9) can be approximated as

$$\begin{aligned} J(t) &\approx -D|\partial\Omega_a|\mathcal{L}_t^{-1}(-C_A(q)) \approx 2D\varepsilon L_t^{-1}\left(\frac{\pi\hat{G}(\mathbf{A}, q)}{-\varepsilon \ln\left(\sqrt{\frac{q+V}{D}}\varepsilon\right)}\right) \\ &\approx \frac{1}{\ln\left(\frac{1}{\varepsilon}\right)}L_t^{-1}\left(K_0\left(\sqrt{\frac{q+V}{D}}R\right)\right) \approx \frac{e^{-Vt}e^{-\frac{R^2}{4Dt}}}{2\ln\left(\frac{1}{\varepsilon}\right)t}. \end{aligned} \quad (3.40)$$

Thus, proceeding as in the section before when t is small we obtain

$$\int_0^t J(s)ds \approx \frac{e^{-\frac{R^2}{4Dt}}(1-Vt)4Dt}{2R^2\ln\left(\frac{1}{\varepsilon}\right)} \approx \frac{1}{8\ln\left(\frac{1}{\varepsilon}\right)}\left(-4Vte^{-\frac{R^2}{4Dt}} + \left(4 + \frac{R^2V}{D}\right)\Gamma\left(0, \frac{R^2}{4Dt}\right)\right), \quad (3.41)$$

which can approximated to leading order when t small by

$$\int_0^t J(s)ds \sim \frac{e^{-\frac{R^2}{4Dt}}4Dt}{2R^2\ln\left(\frac{1}{\varepsilon}\right)}. \quad (3.42)$$

We can compute the full integral of the flux as the Laplace transform of $J(t)$ at $q = 0$, leading to the escape probability

$$P_e(V, D, R, \varepsilon) = \int_0^\infty J(s)ds \approx \frac{K_0\left(\sqrt{\frac{V}{D}}R\right)}{\ln\left(\frac{1}{\sqrt{\frac{V}{D}}\varepsilon}\right)}. \quad (3.43)$$

Note that $\lim_{V \rightarrow 0} P_e(V, D, R, \varepsilon) = 1 \forall \varepsilon > 0$. This means that, when there is not killing, the particle might escape after a long time, but it escapes with probability 1. Also, for a fixed killing weight V , we obtain that

$$\lim_{\varepsilon \rightarrow 0} P_e(V, D, R, \varepsilon) = 0 \quad (3.44)$$

saying that when the size of the narrow windows goes to 0 no particle escapes. Thus, following formula (3.11), the asymptotic formula for large k is given by

$$\begin{aligned} \mathbb{E}[\tau^e(N) | n = k] &\approx \int_0^\delta \left(1 - \frac{e^{-\frac{R^2}{4Dt}}4Dt \ln\left(\frac{1}{\sqrt{\frac{V}{D}}\varepsilon}\right)}{2R^2\ln\left(\frac{1}{\varepsilon}\right)K_0\left(\sqrt{\frac{V}{D}}R\right)}\right)^k dt \\ &\approx \int_0^\delta e^{-\frac{4Dt \ln\left(\frac{1}{\sqrt{\frac{V}{D}}\varepsilon}\right)ke^{-\frac{R^2}{4Dt}}}{2R^2\ln\left(\frac{1}{\varepsilon}\right)K_0\left(\sqrt{\frac{V}{D}}R\right)}} dt \sim \frac{R^2}{4D \ln\left(\frac{k \ln\left(\frac{1}{\sqrt{\frac{V}{D}}\varepsilon}\right)}{2\ln\left(\frac{1}{\varepsilon}\right)K_0\left(\sqrt{\frac{V}{D}}R\right)}}\right)}. \end{aligned} \quad (3.45)$$

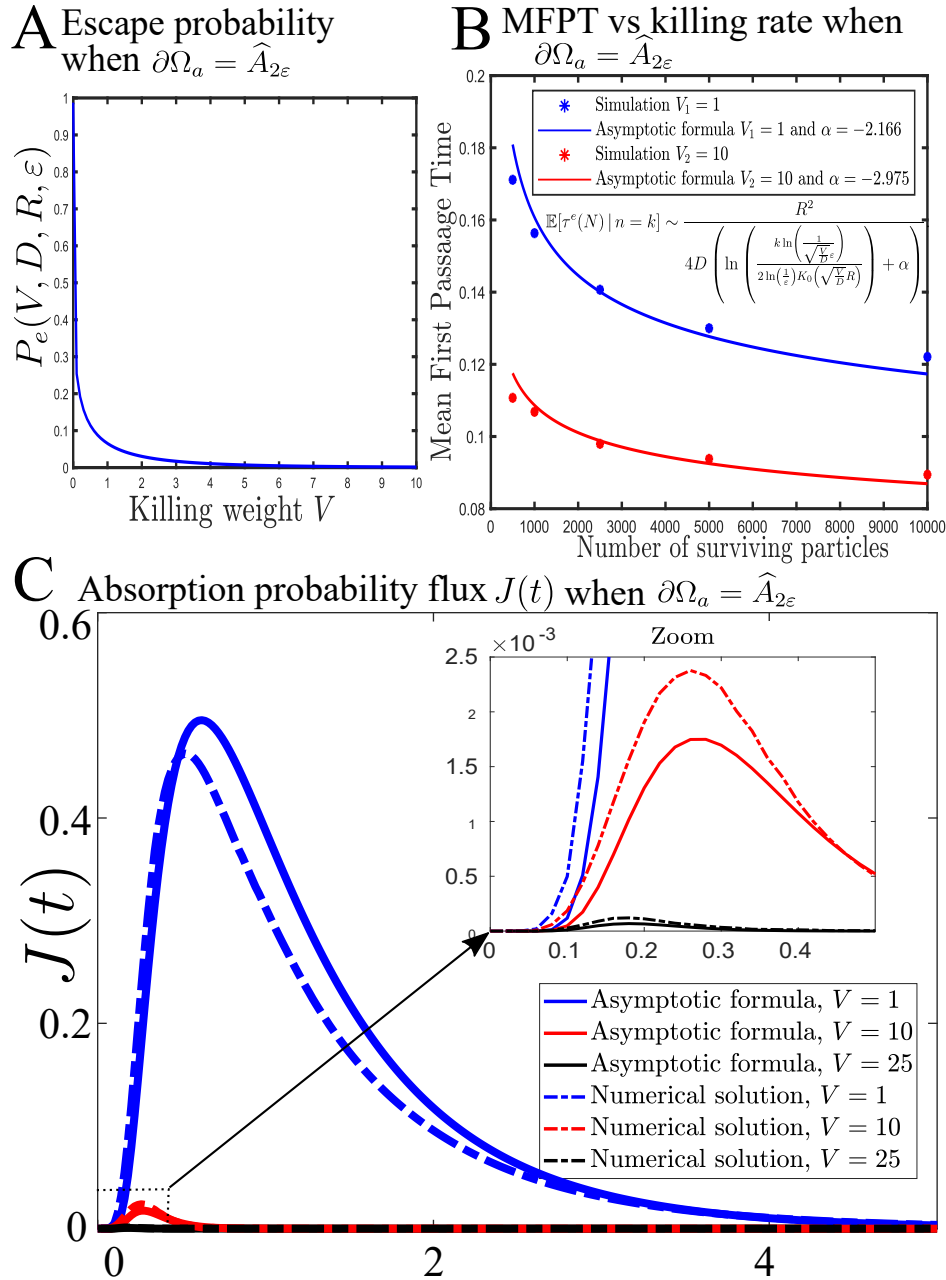


Figure 3.3: **Uniform killing with a narrow absorbing boundary on a 2D disk domain.** **A.** Decay of the escape probability $P_e(V, D, R, \varepsilon)$ as a function of the killing weight V for $D = 1$, $R = 2$ and $\varepsilon = 0.175$ which correspond with 10° arc of the boundary. **B.** MFPT vs number of survival particles $n = k$ obtained from stochastic simulations (colored disks) and the asymptotic formula (3.45) (continuous lines) with $D = 1$, $R = 2$, $\mathbf{y} = (0, 0)$, $\varepsilon = 0.175$ and 1000 runs. **C.** Absorption probability flux (analytical formula (3.40)) shrinks when the killing weight V increases.

We remark from the result that the leading order term of formula (3.45) converges to

$$\mathbb{E}[\tau^e(N) | n = k] \rightarrow \frac{R^2}{4D \ln \left(\frac{k}{2 \ln(\frac{1}{\varepsilon})} \right)} = \bar{\tau}^1 \left(\frac{k}{4 \ln(\frac{1}{\varepsilon})} \right) \quad (3.46)$$

when $V \rightarrow 0$. This dependency in $\ln(\frac{1}{\varepsilon})$ was already observed in [71]. On the other hand, when $\varepsilon \rightarrow 0$ we do not recover that $\mathbb{E}[\tau^e(N) | n = k] \rightarrow \infty$ but this could be due to the short time approximations made, as we already saw in (3.44) that the escape probability $P_e(V, D, R, \varepsilon)$ is properly going to 0. We show in Fig. 3.3A, the escape probability $P_e(V, D, R, \varepsilon)$ as a function of the killing weight V . The comparison between the approximation (3.40) obtained for the flux $J(t)$ and the numerical solution founded by COMSOL are shown in Fig. 3.3B. As in section 3.1, we perform simulations where all the particles started at the origin, the discrete time-step is $dt = 0.01$, the diffusion coefficient is $D = 1$, the domain radius is $R = 2$, and the absorbing window corresponds to a 10 degrees arc of the origin centered circle around $\mathbf{A} = (2, 0)$ ($\varepsilon = 0.175$). The values for the killing weight V were taken to be $V = 1$ and $V = 10$. The simulation results are shown in Fig. 3.3C revealing that the mean first passage time for the fastest decreases as the killing weight increases, a behavior expected from the asymptotic formula (3.45). This behavior agrees with the previous simulation result shown in Fig. 3.2C for the fully absorbing boundary case. Simulations with large killing rate are computationally expensive, thus, we only explore here regimes with small killing rates.

3.4 Escape probability for a localized inner killing term

In this section, we derive an expression for the escape probability (functions P_e in the previous sections) when the killing field is localized within a sub-region of the domain, where Brownian particles are free to move. This computation will help us to characterize the influence of the main parameters on the model such as the killing region center x_k , the killing radius r_k and the radius of the absorbing circular arc ε .

3.4.1 Asymptotic expression for the escape probability

We consider that the region Ω is a disk of radius R whose boundary is everywhere reflective except for a narrow absorbing circular arc $\partial\Omega_a$ of radius $\varepsilon \ll R$ and centered in $\mathbf{A} = (R, 0)$. We integrate in time the solution $p(\mathbf{x}, t)$ of the FPE equation (3.28), this is

$$\tilde{p}(\mathbf{x}) = \int_0^\infty p(\mathbf{x}, t) dt, \quad (3.47)$$

where the initial distribution is $p_0(\mathbf{x})$, and we focus here on solving the spatial PDE satisfied by $\tilde{p}(\mathbf{x})$:

$$\begin{aligned} D\Delta\tilde{p}(\mathbf{x}) - k(\mathbf{x})\tilde{p}(\mathbf{x}) &= -p_0(\mathbf{x}), \quad \mathbf{x} \in \Omega, \\ \tilde{p}(\mathbf{x}) &= 0, \quad \mathbf{x} \in \partial\Omega_a, \quad \frac{\partial\tilde{p}}{\partial\mathbf{n}}(\mathbf{x}) = 0, \quad \mathbf{x} \in \partial\Omega \setminus \partial\Omega_a. \end{aligned} \quad (3.48)$$

We consider the case where $p_0(\mathbf{x}) = \delta(\mathbf{x})$, D is the diffusion coefficient and $k(\mathbf{x})$ is the spatial killing measure. The killing occurs within the sub-region $\Omega_k \subset \Omega$. We consider that the killing field $k(\mathbf{x})$ is uniform inside Ω_k and vanishes outside. The killing region Ω_k corresponds to a smaller disk of radius $r_k \ll R$ and center in \mathbf{x}_k . To avoid discontinuities we regularize (3.48) by approximating the killing measure as a smooth function

$$k(\mathbf{x}) \equiv \frac{V}{2} \left(1 + \tanh \left(\frac{r_k - |\mathbf{x} - \mathbf{x}_k|}{\Gamma} \right) \right), \quad (3.49)$$

where $|\cdot|$ is the Euclidean distance and Γ is the thickness of the transition layer near the killing region boundary $\partial\Omega_k$, satisfying $\Gamma \ll r_k$. Within Ω_k the killing measure is therefore equal to V while it vanishes outside the killing region and its smooth transition layer.

To derive the asymptotic approximation for the probability of a Brownian particle reaching the narrow absorbing window $\partial\Omega_a$ before being killed within the killing region Ω_k , we remain that

$$\Pr\{\mathbf{x}_t \in [\mathbf{x}, \mathbf{x} + d\mathbf{x}], \tau^k \in [t, dt]\} = k(\mathbf{x})p(\mathbf{x}, t)d\mathbf{x} dt, \quad (3.50)$$

then, integrating over space and time we obtain

$$\Pr\{\tau^k < \tau^e\} = \int_{\Omega} k(\mathbf{x})\tilde{p}(\mathbf{x})d\mathbf{x} \quad (3.51)$$

and thus, the escape probability is

$$P_e = 1 - \int_{\Omega} k(\mathbf{x})\tilde{p}(\mathbf{x})d\mathbf{x}, \quad \mathbf{x} \in \Omega. \quad (3.52)$$

We make here the approximation that $\tilde{p}(\mathbf{x})$ is constant within Ω_k and we obtain

$$P_e \approx 1 - V\pi r_k^2 \tilde{p}(\mathbf{x}_k). \quad (3.53)$$

To perform the asymptotic analysis, we exploit the two small geometrical parameters

$$r_k \ll R, \quad \text{and} \quad \varepsilon \ll R, \quad (3.54)$$

while the distances from the center of the killing region to the origin, or to the boundary,

$$|\mathbf{x}_k - \mathbf{A}| \sim O(R), \quad \text{and} \quad |\mathbf{x}_k| \sim O(R), \quad (3.55)$$

are well-spaced.

Applying the divergence theorem to (3.48) yields a constraint on the total exit flux across $\partial\Omega_a$:

$$\int_{\partial\Omega_a} D \frac{\partial \tilde{p}}{\partial \mathbf{n}} d\mathbf{x} = \int_{\Omega} k(\mathbf{x})\tilde{p}(\mathbf{x})d\mathbf{x} - 1. \quad (3.56)$$

To compute the flux

$$g(\mathbf{x}) \equiv D \frac{\partial \tilde{p}(\mathbf{x})}{\partial \mathbf{n}}, \quad \mathbf{x} \in \partial\Omega_a, \quad (3.57)$$

we use a regular Taylor expansion

$$g(\mathbf{x}) \approx g(\mathbf{A}) + (\nabla g(\mathbf{x})|_{\mathbf{x}=\mathbf{A}})^T (\mathbf{x} - \mathbf{A}) + \dots, \quad (3.58)$$

and thus at first order, the constraint (3.56) becomes

$$g(\mathbf{A}) = -\frac{1}{2\varepsilon} + \frac{V\pi r_k^2}{2\varepsilon} \tilde{p}(\mathbf{x}_k). \quad (3.59)$$

To obtain a general expression for $\tilde{p}(\mathbf{x})$, we use the Neumann Green's function $G(\mathbf{x}; \mathbf{y})$, solution of

$$\begin{aligned} D\Delta \mathbf{x} G(\mathbf{x}; \mathbf{y}) &= \frac{1}{|\Omega|} - \delta(\mathbf{x} - \mathbf{y}), \quad \mathbf{x}, \mathbf{y} \in \Omega; \\ D \frac{\partial G(\mathbf{x}, \mathbf{y})}{\partial \mathbf{n}} &= 0, \quad \mathbf{x} \in \partial\Omega, \mathbf{y} \in \Omega; \quad \int_{\Omega} G(\mathbf{x}; \mathbf{y}) d\mathbf{x} = 0, \end{aligned} \quad (3.60)$$

the solution of which in a disk of radius R [131] is

$$\begin{aligned} G(\mathbf{x}; \mathbf{y}) &= \frac{1}{2\pi D} \left(-\ln \left(\frac{1}{R} |\mathbf{x} - \mathbf{y}| \right) - \ln \left(\left| \frac{1}{R^2} \mathbf{x} |\mathbf{y}| - \frac{\mathbf{y}}{|\mathbf{y}|} \right| \right) \right. \\ &\quad \left. + \frac{1}{2R^2} (|\mathbf{x}|^2 + |\mathbf{y}|^2) - \frac{3}{4} \right). \end{aligned} \quad (3.61)$$

The structure of the expansion near the singularity \mathbf{y} differs whether it belongs to the boundary or not. When $|\mathbf{y}| < R$ we have the general expression

$$G(\mathbf{x}; \mathbf{y}) \sim -\frac{1}{2\pi D} \ln \left(\frac{1}{R} |\mathbf{x} - \mathbf{y}| \right) + U(\mathbf{y}; \mathbf{y}), \quad \mathbf{y} \in \Omega \setminus \partial\Omega, \quad (3.62)$$

for \mathbf{x} near \mathbf{y} , and where $U(\mathbf{y}; \mathbf{y})$ corrects the boundary condition, thus

$$U(\mathbf{y}; \mathbf{y}) = -\frac{1}{2\pi D} \left(\ln \left(1 - \frac{|\mathbf{y}|^2}{R^2} \right) - \frac{1}{R^2} |\mathbf{y}|^2 + \frac{3}{4} \right), \quad \mathbf{y} \in \Omega \setminus \partial\Omega, \quad (3.63)$$

while for $|\mathbf{y}| = R$, we get

$$G(\mathbf{x}; \mathbf{y}) \sim -\frac{1}{\pi D} \ln \left(\frac{1}{R} |\mathbf{x} - \mathbf{y}| \right) + U(\mathbf{y}; \mathbf{y}), \quad \mathbf{y} \in \partial\Omega, \quad (3.64)$$

for \mathbf{x} near \mathbf{y} , with

$$U(\mathbf{y}; \mathbf{y}) = \frac{1}{8\pi D}, \quad \mathbf{y} \in \partial\Omega. \quad (3.65)$$

Applying Green's second identity to (3.48) and (3.60), we obtain the exact expression

$$\begin{aligned} \tilde{p}(\mathbf{y}) &= \frac{1}{|\Omega|} \int_{\Omega} \tilde{p}(\mathbf{x}) d\mathbf{x} + G(0; \mathbf{y}) - \int_{\Omega} k(\mathbf{x}) G(\mathbf{x}; \mathbf{y}) \tilde{p}(\mathbf{x}) d\mathbf{x} \\ &\quad + \int_{\partial\Omega_a} G(\mathbf{x}; \mathbf{y}) g(\mathbf{x}) d\mathbf{x}, \end{aligned} \quad (3.66)$$

from which we derive an approximation for $\tilde{p}(\mathbf{x}_\epsilon)$. Setting $\mathbf{y} = \mathbf{A}$ within (3.66), we obtain

$$\begin{aligned} \frac{1}{|\Omega|} \int_{\Omega} \tilde{p}(\mathbf{x}) d\mathbf{x} &= -G(0; \mathbf{A}) + \int_{\Omega} k(\mathbf{x}) G(\mathbf{x}; \mathbf{A}) \tilde{p}(\mathbf{x}) d\mathbf{x} \\ &\quad - \int_{\partial\Omega_a} G(\mathbf{x}; \mathbf{A}) g(\mathbf{x}) d\mathbf{x}, \end{aligned} \quad (3.67)$$

upon using the absorbing boundary condition. Because the exit window and the killing region are well-spaced the integral term involving the killing measure can readily be approximated by

$$\int_{\Omega} k(\mathbf{x}) G(\mathbf{x}; \mathbf{A}) \tilde{p}(\mathbf{x}) d\mathbf{x} \approx V\pi r_k^2 G(\mathbf{x}_k; \mathbf{A}) \tilde{p}(\mathbf{x}_k) \quad (3.68)$$

when r_k is small. For the second integral term within (3.67) we employ the expansion of the Green's function near a singularity located on the boundary, thus yielding

$$\int_{\partial\Omega_a} G(\mathbf{x}, \mathbf{A}) g(\mathbf{x}) d\mathbf{x} \approx 2g(\mathbf{A}) \int_0^a \left(-\frac{1}{\pi D} \ln \left(\frac{\rho}{R} \right) + U(\mathbf{A}; \mathbf{A}) \right) d\rho \quad (3.69)$$

and then upon integrating and substituting the value for $U(\mathbf{A}; \mathbf{A})$ given in (3.65) we obtain

$$\int_{\partial\Omega_a} G(\mathbf{x}, \mathbf{A})g(\mathbf{x})d\mathbf{x} \approx \frac{2\varepsilon g(\mathbf{A})}{\pi D} \left(\ln\left(\frac{R}{\varepsilon}\right) + \frac{9}{8} \right). \quad (3.70)$$

By substituting the constraint (3.59) and adding (3.68) to (3.70), we find that the average density value over Ω satisfies

$$\begin{aligned} \frac{1}{|\Omega|} \int_{\Omega} \tilde{p}(\mathbf{x})d\mathbf{x} &\approx -G(0; \mathbf{A}) + V\pi r_k^2 G(\mathbf{x}_k, \mathbf{A})\tilde{p}(\mathbf{x}_k) \\ &+ \frac{1}{\pi D}(1 - V\pi r_k^2 \tilde{p}(\mathbf{x}_k)) \left(\ln\left(\frac{R}{\varepsilon}\right) + \frac{9}{8} \right). \end{aligned} \quad (3.71)$$

Then we set $\mathbf{y} = \mathbf{x}_k$ within (3.66) to obtain

$$\begin{aligned} \tilde{p}(\mathbf{x}_k) &= \frac{1}{|\Omega|} \int_{\Omega} \tilde{p}(\mathbf{x})d\mathbf{x} + G(0; \mathbf{x}_k) - \int_{\Omega} k(\mathbf{x})G(\mathbf{x}; \mathbf{x}_k)\tilde{p}(\mathbf{x})d\mathbf{x} \\ &+ \int_{\partial\Omega_a} G(\mathbf{x}; \mathbf{x}_k)g(\mathbf{x})d\mathbf{x}, \end{aligned} \quad (3.72)$$

and once again because the killing region and the absorbing window are well-spaced, we get when ε is small, the following approximation

$$\int_{\partial\Omega_a} G(\mathbf{x}; \mathbf{x}_k)g(\mathbf{x})d\mathbf{x} \approx 2\varepsilon g(\mathbf{A})G(\mathbf{A}; \mathbf{x}_k), \quad (3.73)$$

for the last integral term. Near the singularity we compute

$$\int_{\Omega} k(\mathbf{x})G(\mathbf{x}; \mathbf{x}_k)\tilde{p}(\mathbf{x})d\mathbf{x} \approx V\tilde{p}(\mathbf{x}_k)2\pi \int_0^{r_k} \left(-\frac{1}{2\pi D} \ln\left(\frac{\rho}{R}\right) + U(\mathbf{x}_k; \mathbf{x}_k) \right) \rho d\rho, \quad (3.74)$$

which reduces to

$$\int_{\Omega} k(\mathbf{x})G(\mathbf{x}; \mathbf{x}_k)\tilde{p}(\mathbf{x})d\mathbf{x} \approx \frac{Vr_k^2}{D}\tilde{p}(\mathbf{x}_k) \left(\frac{1}{2} \ln\left(\frac{R}{r_k}\right) + \frac{1}{4} + \pi DU(\mathbf{x}_k; \mathbf{x}_k) \right), \quad (3.75)$$

and finally we obtain that

$$\begin{aligned} \tilde{p}(\mathbf{x}_k) &\approx -G(0; \mathbf{A}) + V\pi r_k^2 G(\mathbf{x}_k, \mathbf{A})\tilde{p}(\mathbf{x}_k) + \frac{1}{\pi D}(1 - V\pi r_k^2 \tilde{p}(\mathbf{x}_k)) \left(\ln\left(\frac{R}{\varepsilon}\right) + \frac{9}{8} \right) \\ &+ G(0; \mathbf{x}_k) - \frac{Vr_k^2}{D}\tilde{p}(\mathbf{x}_k) \left(\frac{1}{2} \ln\left(\frac{R}{r_k}\right) + \frac{1}{4} + \pi DU(\mathbf{x}_k; \mathbf{x}_k) \right) \\ &+ (V\pi r_k^2 \tilde{p}(\mathbf{x}_k) - 1)G(\mathbf{A}; \mathbf{x}_k). \end{aligned} \quad (3.76)$$

By solving for $\tilde{p}(\mathbf{x}_k)$ this equation, we get the following expression

$$\tilde{p}(\mathbf{x}_k) \approx \frac{\frac{1}{V\pi r_k^2} \left(\ln\left(\frac{R}{\varepsilon}\right) + \frac{9}{8} + \pi D(G(0; \mathbf{x}_k) - G(0; \mathbf{A}) - G(\mathbf{A}; \mathbf{x}_k)) \right)}{\frac{D}{Vr_k^2} + \frac{1}{2} \ln\left(\frac{R}{r_k}\right) + \ln\left(\frac{R}{\varepsilon}\right) + \frac{11}{8} + \pi D(U(\mathbf{x}_k; \mathbf{x}_k) - 2G(\mathbf{A}; \mathbf{x}_k))}, \quad (3.77)$$

and from the approximation $P_e \approx 1 - \pi r_k^2 k \tilde{p}(\mathbf{x}_k)$, we derive the following asymptotic formula for the escape probability with respect to the various parameter and the Green's function:

$$P_e \approx \frac{\frac{D}{Vr_k^2} + \frac{1}{2} \ln\left(\frac{R}{r_k}\right) + \frac{1}{4} + \pi D(U(\mathbf{x}_k; \mathbf{x}_k) - G(\mathbf{A}; \mathbf{x}_k) + G(0; \mathbf{A}) - G(0; \mathbf{x}_k))}{\frac{D}{Vr_k^2} + \frac{1}{2} \ln\left(\frac{R}{r_k}\right) + \ln\left(\frac{R}{\varepsilon}\right) + \frac{11}{8} + \pi D(U(\mathbf{x}_k; \mathbf{x}_k) - 2G(\mathbf{A}; \mathbf{x}_k))}. \quad (3.78)$$

3.5 Asymptotic formulas vs simulations

To study the influence of the killing region on the mean time and path of fastest particle escaping in the narrow absorbing window, we perform stochastic simulations where the Brownian particles are released at the origin. The domain is the origin centered disk with radius $R = 2$. We consider the absorbing boundary as the 10° arc of the disk, centered at point $A = (R, 0)$, and the rest of the boundary is reflecting. We implemented the Euler's scheme

$$\boldsymbol{x}(t + \Delta t) = \begin{cases} \boldsymbol{x}(t) + \sqrt{2D}\Delta\boldsymbol{w}(t) & \text{w.p } 1 - k(\boldsymbol{x})I_{\{\boldsymbol{x}(t) \in \text{Killing Zone}\}}\Delta t \\ \text{TERMINATED} & \text{w.p } k(\boldsymbol{x})I_{\{\boldsymbol{x}(t) \in \text{Killing Zone}\}}\Delta t, \end{cases} \quad (3.79)$$

where live particles can be destroyed at Poissonian rate V ($k(\boldsymbol{x}) = V$) with probability $V\Delta t$ at anytime inside the killing area. As now the killing area is a sub-region fully contained in the domain Ω but not the full domain itself, we believe the MFPT formula should be of the form

$$\bar{\tau} \sim \frac{R^2\beta}{4D \left(\ln \left(\frac{N_0}{2\ln(\frac{1}{\varepsilon})} \right) + \alpha \right)} \quad (3.80)$$

as suggested by formula (3.46) when the killing rate V goes to 0. The parameter β here should corrects the distance between the initial point and the absorbing boundary as now the fastest particles should not enter in the killing zone avoiding the direct path. We expect thus $\beta > 1$ and if it has a small variance for different values of V , this could indicate us that the fastest particle follows always the same path. The parameter α corrects the number of particles that are killed while going through the killing area.

3.5.1 MFPT and P_e vs killing weight V

For our first simulations, we consider the killing region as the disk of radius $r_k = 0.25$ centered in $\boldsymbol{x}_k = (1, 0)$. We considered that the uniform killing measure is given by $k(\boldsymbol{x}) = V \cdot I_{\{\boldsymbol{x} \in B_{r=0.25}(1,0)\}}(\boldsymbol{x})$. We choose the diffusion coefficient as $D = 1$ and the time step $\Delta t = 0.01$ for the Euler's scheme (3.79). The initial number of particles N_0 was fixed and we then varied the killing rate V across the range (1, 10, 25, 50, 75, 90) for 1000 runs.

We show two examples of Brownian trajectories in Fig. 3.4A: a green particle that survives and escapes through the absorbing window (blue), while the orange trajectory terminates within the killing area (in red), as a consequence of the killing measure.

The MFPT is fitted to the logarithmic formula (3.80) (Fig. 3.4B) and the additive parameter α corrects the number N_0 of initial particles that have been killed. We remark a small variance for the parameter β , meaning that regardless of the value of the killing rate V , the particle always follows a path that has a length that varies little. In Fig. 3.4C we can understand how the killing measure affects the final number of survival particles. The escape probability is thus given from the simulations as the average over the total number of runs (M) of the rate: escaping/ initial particles. That is, if e_i is the amount of escaping particles in the i -th run, then

$$P_e(N_0) = \frac{\sum_{i=1}^M e_i}{N_0 M}. \quad (3.81)$$

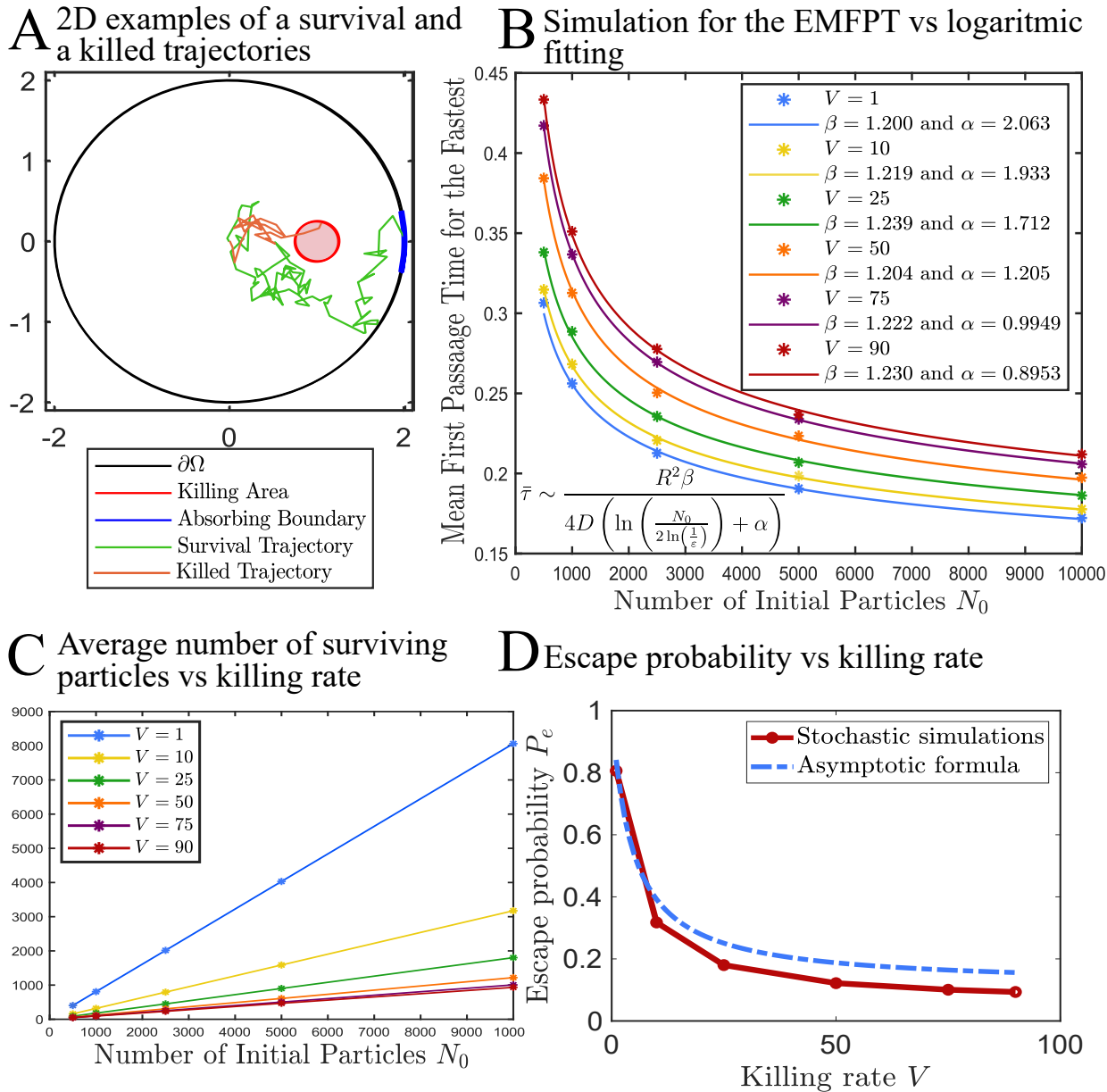


Figure 3.4: **Influence of the killing measure on the MFPT when the initial number of particles N_0 is large.** **A.** Two 2D examples of survival and killed particles for the problem in a disk. **B.** MFPT vs N_0 obtained from stochastic simulations (colored disks) and the fitting to the logarithmic decay (3.80) (continuous lines) for 1000 runs. **C.** Influence of the killing weight V on the number of surviving particles. **D.** Decay of the escape probability for different values of the killing weight V obtained from stochastic simulations (continuous line in red) and the asymptotic formula (3.78)(dashed lines in blue).

Finally, we compared the escape probabilities obtained from simulations (red) and from formula (3.78) (blue) versus the killing weight V in Fig. 3.4D.

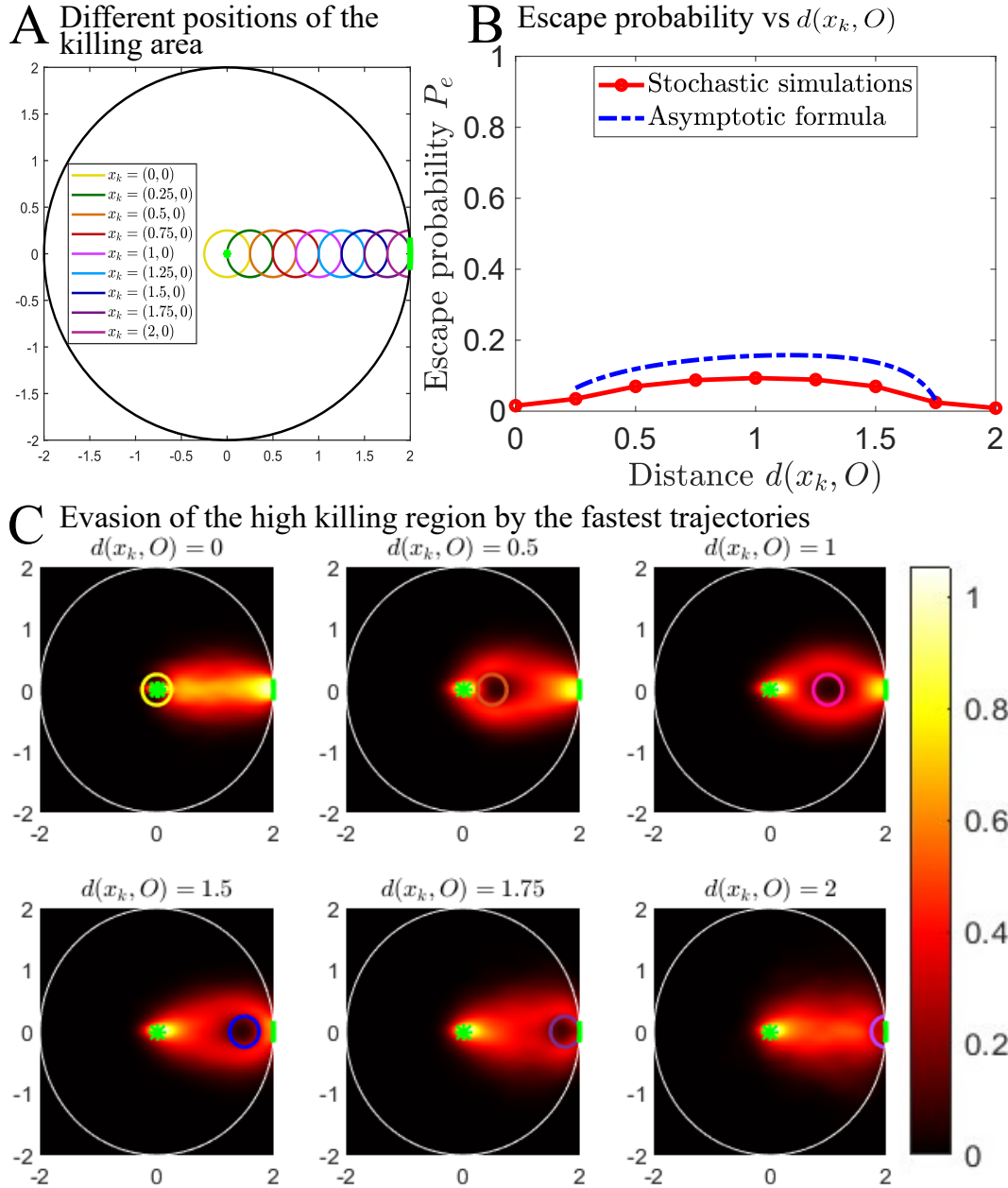


Figure 3.5: **Influence of the killing area position on the escape probability and fastest trajectory for $V = 90$, $D = 1$, $dt = 0.01$, $R = 2$, $r = 0.25$, $\mathbf{A} = (2, 0)$, $\varepsilon = 0.175$ and 1000 runs.** **A.** Schematic representation of different killing areas first located at the center and moving toward the narrow exit window. The initial position of the particles remains at the center of the external disk. **B.** Escape probability versus $d(x_k, O)$. **C.** Spatial distribution of the fastest trajectories for various locations of killing region.

3.5.2 MFPT and P_e vs the killing area position

We show here how the escape probability and the most likely path are affected by the location of the killing area. To do this, we fixed the killing rate to $V = 90$ and the radius of the killing disk to $r_k = 0.25$. The values for the distance between the origin and the center \mathbf{x}_k of the killing area, denoted by $d(x_k, O)$, are taken from the vector $(0, 0.25, 0.5, 0.75, 1, 1.25, 1.5, 1.75, 2)$, as shown

in Fig. 3.5A.

We ran 1000 simulations with $N_0 = (500, 1000, 2500, 5000, 10000)$ particles and each time we saved the amount of survival particles at the end of the run and the path of the fastest trajectory. We report here that the escape probability first increases as the narrow absorbing window and the origin are well separated from the killing area. However, this probability decreases again when the killing area approaches the initial point or the narrow window, achieving its maximum value when \mathbf{x}_k is the middle point. We analyzed the path distribution for the fastest trajectories of each simulation (Fig. 3.5C), revealing that the fastest trajectories avoid the killing zone when the killing rate is very large. We used the *ksdensity* function from Matlab to obtain the spatial distribution of the fastest particles, and we projected this distribution over the domain Ω to obtain the heat map of the fastest trajectories. When the killing area is overlapping the narrow absorbing window (last panel of Fig. 3.5C), the density of the fastest path is lower than in the other panels. But still, the fastest trajectories are moving along the straight line, meaning that depending on the position, the killing measure will not affect the fastest path but instead it will affect drastically the amount of survival particles.

3.5.3 MFPT and P_e vs the killing area radius

To investigate how the radius of the killing area r_k affects the escape dynamics, we fixed the center at $\mathbf{x}_k = (1, 0)^T$ and we varied the radius r_k in the vector $(0.01, 0.1, 0.25, 0.5)$ as shown in Fig. 3.6A.

How the escape probability decreases with respect to the radius of the killing area is shown in Fig. 3.6B. The spatial distribution of the fastest particles is shown in Fig. 3.6C. When the radius increases, the fastest particles avoid the killing area. But, in order to observe an effect on the most likely path, the killing area must intersect the straight path between the origin and the absorbing boundary. For example when the killing area is instead located at $\mathbf{x}_k = (-1, 0)^T$ and we keep the narrow absorbing boundary around $\mathbf{A} = (2, 0)^T$ the fastest trajectory would always move along the straight line connecting the initial point and absorbing window. In that case, the killing measure will not affect the first arrival time neither the most likely path.

3.6 Optimal path for the fastest particles

Numerical simulations suggested that the trajectories for the fastest among N to escape concentrates in a refined region of the space. To study the optimal path associated with the fastest survival particles to escape, we shall use the formal argument (92) based on the large deviation principle [32, 132] associated to the Brownian motion. In the present case, the stochastic equation reduces to

$$\mathbf{x}_t^\epsilon = \sqrt{2D\epsilon}\mathbf{w}(t), \quad (3.82)$$

where $\mathbf{w}(t)$ is the standard Brownian motion. The fluctuations of the diffusion process with small noise amplitude ϵ around the deterministic function ϕ_t is given by the action functional in the time interval $[t_0, T]$,

$$\Pr \{ \forall t \in [t_0, T], \mathbf{x}_t^\epsilon \approx \phi_t \} \asymp \exp \left\{ - \frac{\mathcal{S}_{[t_0, T]}, \mathbf{x}_0(\phi_t)}{\epsilon} \right\}, \quad (3.83)$$

where

$$\mathcal{S}_{[t_0, T]}, \mathbf{x}_0(\phi_t) = \frac{1}{2D} \int_{t_0}^T |\dot{\phi}_t|^2 dt. \quad (3.84)$$

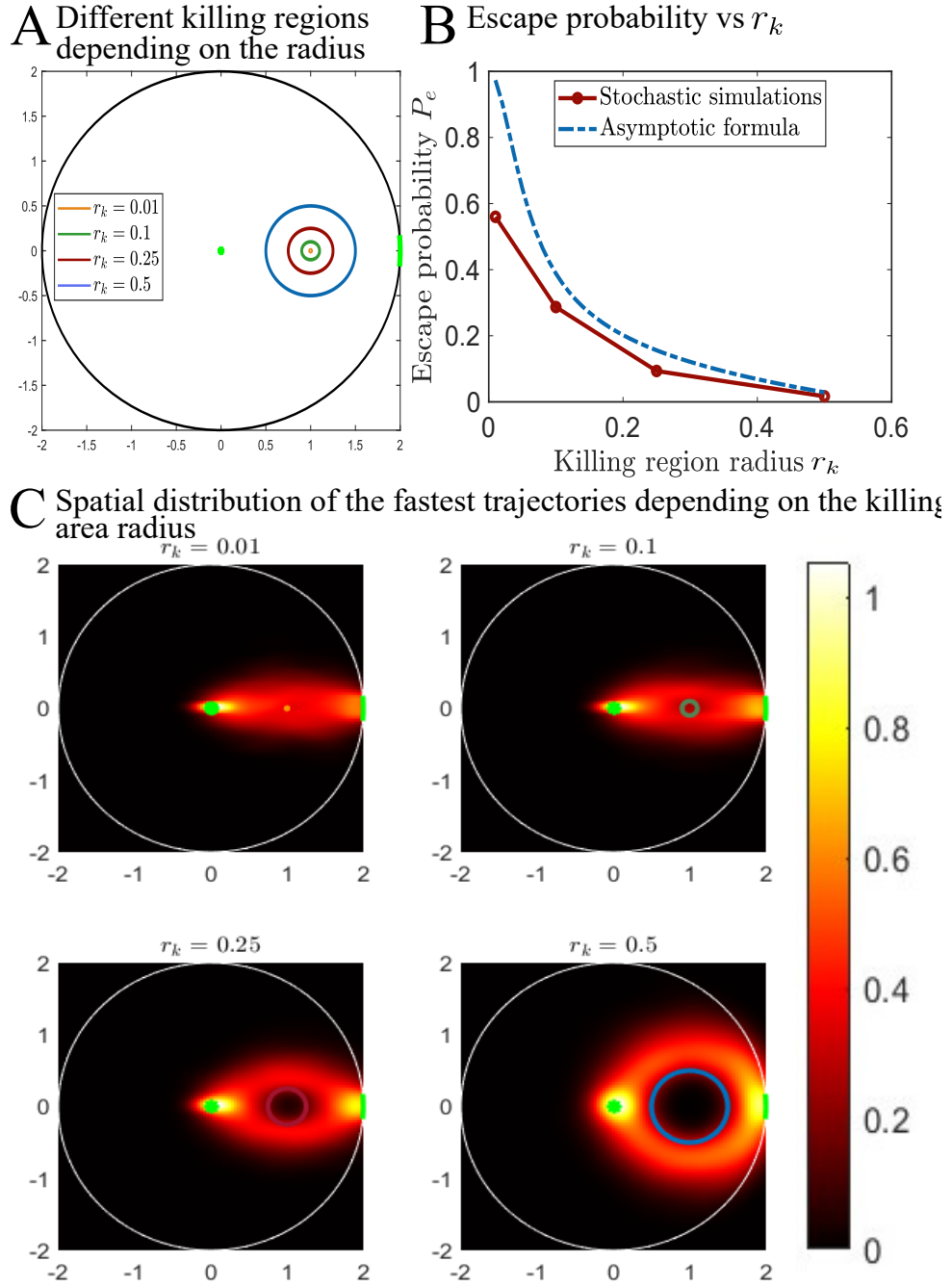


Figure 3.6: **Influence of the killing area radius on the escape probability and space distribution.** **A.** Schematic representation of different killing areas depending on the value of the radius with a fixed center at $\mathbf{x}_k = (1, 0)^T$. **B.** Effect of the killing radius on the escape probability for $V = 90$. **C.** Spatial distribution for the fastest trajectories for different values of the killing area radius, $D = 1$, $\varepsilon = 0.175$, $R = 2$ and 1000 runs.

To account for the killing measure $k(\mathbf{x})$, we use the Feynman-Kac representation (93) to express the pdf as

$$p(\mathbf{x}, T) = \mathbb{E} \left[f(\mathbf{x}_T^\epsilon) \exp \left(- \int_{t_0}^T k(\mathbf{x}_s^\epsilon) ds \right) \right], \quad (3.85)$$

where \mathbf{x}_t^ϵ is the Brownian trajectory of (3.82), starting at time $t = t_0$ at position \mathbf{x}_0 and $f(\mathbf{x}) = p(\mathbf{x}, 0)$. Integrating over the domain we obtain the survival probability given by

$$S(t) = \int_{\Omega} p(\mathbf{x}, t) d\mathbf{x} = \mathbb{E} \left[\exp \left(- \int_{t_0}^t k(\mathbf{x}_s^\epsilon) ds \right) \middle| \mathbf{x}_{t_0} = \mathbf{x}_0 \right], \quad (3.86)$$

as all particles start at point \mathbf{x}_0 . This can be written as

$$\int_{\Omega} p(\mathbf{x}, t) d\mathbf{x} = \int_{\Omega} \exp \left(- \int_{t_0}^t k(\mathbf{x}_s^\epsilon) ds \right) \Pr \{ \mathbf{x}_t^\epsilon \in [\mathbf{x}, \mathbf{x} + d\mathbf{x}] \}, \quad (3.87)$$

with $[\mathbf{x}, \mathbf{x} + d\mathbf{x}] \subset \Omega$. This last integral can be converted into the path integral

$$\begin{aligned} \int_{\Omega} p(\mathbf{x}, t) d\mathbf{x} &= \int_{\substack{\phi \text{ paths} \\ \phi_0 = \mathbf{x}_0, \phi_t \in \partial\Omega_a}} \exp \left\{ - \int_{t_0}^t k(\phi_s) ds \right\} \Pr \{ \forall t \in [t_0, t], \mathbf{x}_t^\epsilon \approx \phi_t \} \\ &= \int_{\substack{\phi \text{ paths} \\ \phi_0 = \mathbf{x}_0, \phi_t \in \partial\Omega_a}} \exp \left\{ - \frac{\mathcal{S}_{[t_0, t], \mathbf{x}_0}(\phi_s)}{\epsilon} - \int_{t_0}^t k(\phi_s) ds \right\} d\mathcal{D}(\phi) \\ &\sim \int_{\substack{\phi \text{ paths} \\ \phi_0 = \mathbf{x}_0, \phi_t \in \partial\Omega_a}} \exp \left\{ - \left(\frac{1}{4D\epsilon} \int_{t_0}^t |\dot{\phi}_s|^2 ds + \int_{t_0}^t k(\phi_s) ds \right) \right\} d\mathcal{D}(\phi), \end{aligned} \quad (3.88)$$

for ϵ small. Thus, the MFPT, denoted by $\bar{\tau}$ is given by

$$\bar{\tau} = \int_0^\infty (S(t))^N dt \sim \int_0^\infty \exp \left\{ N \ln \left(\int_{\substack{\phi \text{ paths} \\ \phi_0 = \mathbf{x}_0, \phi_t \in \partial\Omega_a}} \exp \left\{ - \int_{t_0}^t \left(\frac{1}{4D\epsilon} |\dot{\phi}_s|^2 + k(\phi_s) \right) ds \right\} d\mathcal{D}(\phi) \right) \right\} dt,$$

and, by Laplace's method [22], the contribution of the integral for large N [133] occurs at the maximum value of

$$\ln \left(\int_{\substack{\phi \text{ paths} \\ \phi_0 = \mathbf{x}_0, \phi_t \in \partial\Omega_a}} \exp \left\{ - \int_{t_0}^t \left(\frac{1}{4D\epsilon} |\dot{\phi}_s|^2 + k(\phi_s) \right) ds \right\} d\mathcal{D}(\phi) \right). \quad (3.89)$$

Since the previous path integral takes values between $(0, 1)$, and the logarithm function $\ln(x)$ is increasing, this problem reduces to find the time t that maximizes

$$\mathcal{F}(t) = \int_{\substack{\phi \text{ paths} \\ \phi_0 = \mathbf{x}_0, \phi_t \in \partial\Omega_a}} \exp \left\{ - \int_{t_0}^t \left(\frac{1}{4D\epsilon} |\dot{\phi}_s|^2 + k(\phi_s) \right) ds \right\} d\mathcal{D}(\phi). \quad (3.90)$$

Note now that the time t that maximizes this function is any time between $[\max(t_i), +\infty)$ where t_i is the arrival time of the i -th particle if the particle survived. Note that instead of a maximum

value, we have a supremum if the arrival time of at least one particle is ∞ . But in general, $\forall t > \tau$, the exponential function inside the functional (3.90), takes a larger value, since we are adding larger paths. We are adding then exponentially small terms, compared to the value of the functional at the time of first arrival, that can be ignored at the leading order approximation. Thus, we want to find now the shortest path arriving at the absorbing boundary $\partial\Omega_a$ in a minimal time τ , this is, we want to minimize of the functional

$$\min_{\substack{\phi_0 = \mathbf{x}_0 \\ \phi_\tau \in \partial\Omega_a}} \left\{ \frac{1}{4D\epsilon} \int_0^\tau |\dot{\phi}_s|^2 ds + \int_0^\tau k(\phi_s) ds \right\}, \quad (3.91)$$

with τ fixed. Applying Euler-Lagrange's principle (section 0.1.4 page 23) to the functional

$$\mathcal{Q}(\phi_s) = \int_0^\tau \left(\frac{1}{4D\epsilon} |\dot{\phi}_s|^2 + k(\phi_s) \right) ds, \quad (3.92)$$

where $L(s, \phi, \dot{\phi}) = \frac{1}{4D\epsilon} |\dot{\phi}_s|^2 + k(\phi_s)$, we obtain as stationary point, the path solution of

$$\frac{\partial L}{\partial \phi}(s, \phi_s, \dot{\phi}_s) - \frac{\partial}{\partial s} \frac{\partial L}{\partial \dot{\phi}}(s, \phi_s, \dot{\phi}_s) = 0. \quad (3.93)$$

Here, $\frac{\partial L}{\partial \phi}(s, \phi_s, \dot{\phi}_s) = \nabla k(\phi_s)$ and $\frac{\partial L}{\partial \dot{\phi}}(s, \phi_s, \dot{\phi}_s) = \frac{\dot{\phi}_s}{2D\epsilon}$, leading to the differential equation

$$-\ddot{\phi}_s + 2D\epsilon \nabla k(\phi_s) = 0. \quad (3.94)$$

We know now that equations (3.94) are the equations of motion for the fastest particle. To simulate this second order ODE, we use the regularized killing measure defined in (3.49), from which we readily compute the gradient

$$\nabla k(\mathbf{x}) = \frac{V}{2\Gamma|\mathbf{x} - \mathbf{x}_k|} \operatorname{sech}^2 \left(\frac{r_k - |\mathbf{x} - \mathbf{x}_k|}{\Gamma} \right) (x_k - x, y_k - y), \quad (3.95)$$

and then upon introducing the variables $v_1(s) \equiv x(s)$, $v_2 \equiv y(s)$, $v_3(s) \equiv \dot{x}(s)$, $v_4(s) \equiv \dot{y}(s)$, we can transform (3.94) into a system of 4 first order ODEs given by

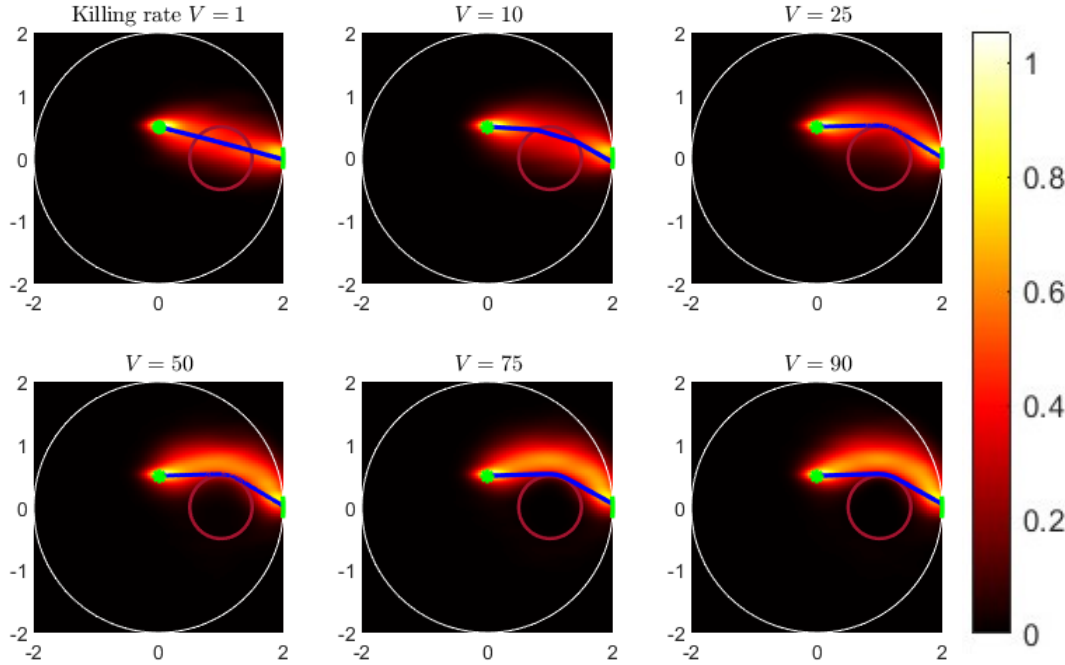
$$\begin{pmatrix} \dot{v}_1(s) \\ \dot{v}_2(s) \\ \dot{v}_3(s) \\ \dot{v}_4(s) \end{pmatrix} = \begin{pmatrix} v_3(s) \\ v_4(s) \\ 2D\epsilon \frac{\partial k}{\partial x} \Big|_{(v_1(s), v_2(s))} \\ 2D\epsilon \frac{\partial k}{\partial y} \Big|_{(v_1(s), v_2(s))} \end{pmatrix}, \quad (3.96)$$

with initial conditions

$$\begin{pmatrix} v_1(0) \\ v_2(0) \\ v_3(0) \\ v_4(0) \end{pmatrix} = \begin{pmatrix} x_0 \\ y_0 \\ \cos(\theta) \\ \sin(\theta) \end{pmatrix}, \quad (3.97)$$

where θ is a free parameter indicating the initial speed angle. In the absence of a killing measure, the solutions of (3.96) correspond to straight lines (Euclidean geodesics). With a localized killing field at some point over the straight line, the deterministic trajectories entering the killing area

A Spatial distribution of the fastest particles when the killing rate increases vs optimal trajectories



B Distribution of the first arrival time when the killing rate increases

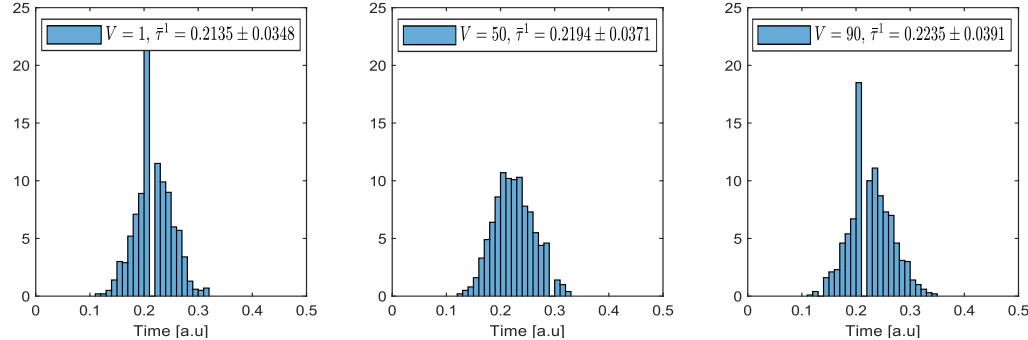


Figure 3.7: **Influence of the killing weight on the optimal path of the fastest particle.** **A.** Deviation of the most likely path when the killing weight V increases for 1000 runs and $N_0 = 10000$ initial particles. **B.** The mean escape time increases as the fastest particles deviate their trajectory to the absorbing windows.

are deviated due to the killing measure effects. After carefully choosing the initial angle θ for the trajectory to end at the center of the absorbing boundary, we obtain the shortest trajectory avoiding the killing region.

We then compared the deterministic trajectories (Fig. 3.7, blue) solution of (3.96) to the spatial distribution of the fastest trajectories obtained from stochastic simulations. In order to break the symmetry the initial coordinates are set to $x_0 = 0$ and $y_0 = 0.5$, corresponding to the green dots in Fig. 3.7A. Values for the killing weight V are chosen from the vector $(1, 10, 25, 50, 75, 90)$. Thus, with a time-step of $dt = 0.01$ on the Euler's scheme, the killing probabilities respectively become $(0.01, 0.1, 0.25, 0.5, 0.75, 0.9)$.

When V is small, the trajectories of the fastest particles concentrate along the straight line going

from the starting point to the narrow window, as shown in Fig. 3.7A (first panel). As expected the most likely path for both stochastic and deterministic cases deviates as the killing rate increases. We believe then, that the path given by the differential system (3.79) is in fact the optimal path of (3.91). Our simulations reveal that for large V the fastest trajectories avoid the killing region and the shortest path is now concentrated along the shortest geodesic inside the domain $\Omega \setminus B_{r=0.5}(1, 0)$. However this shortest geodesic still corresponds to a larger travel distance for a stochastic particle, and as a consequence longer escape times are obtained (Fig. 3.7B). The discrepancy between the most likely path and the solution of the ode system (Fig. 3.7A) is due to the fact that the noise intensity in the stochastic simulations was chosen as $\epsilon = 1$, while the solution of the ode system is obtained in the limit $\epsilon \rightarrow 0$.

Another interesting case, is the one already studied in section 3.3.2, when the killing measure is uniform in Ω . In that case, we do not need to regularize the killing measure since it is continuous over the domain, and thus, its gradient is always the null vector. The equation (3.94) shows that also in this case, regardless the value of the killing rate V the fastest trajectories will concentrate around the straight line connecting the initial point and the absorbing boundary, as shown in Fig. 3.8.

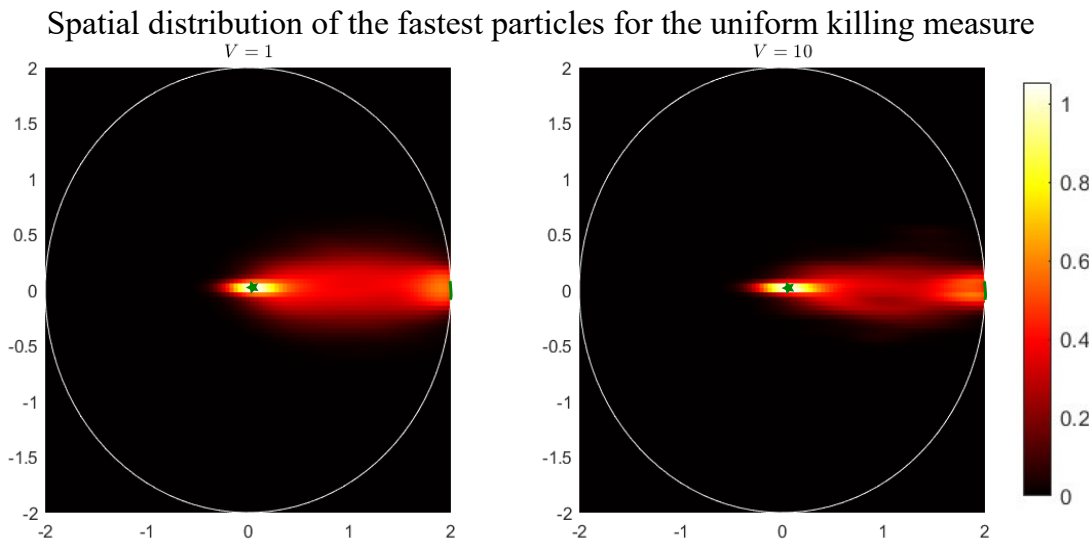


Figure 3.8: **Straight path for a killing measure uniform over the domain.** Spatial distribution for the fastest trajectories for different values of the killing rate V , with $D = 1$, $\epsilon = 0.175$, $R = 2$, $\epsilon = 1$ and 1000 runs. The initial point of the particles is marked with a green start while the small absorbing boundary is the green arc around $A = (2, 0)^T$.

3.7 Killing area tangent to the narrow absorbing boundary

In this subsection, we shall study the effect on the escape time and on the most likely path when the killing region is tangent to absorbing boundary. In that case, we expect a change in the space distribution of the fastest trajectories such that the optimal path should move along the boundary, a situation that is not accounted for in the minimization problem (3.91).

For the simulations we set now the killing area around the point $x = (1.5, 0)$ with a radius $r_k = 0.5$ (Fig. 3.9A), the killing area becomes now tangent to the absorbing boundary around

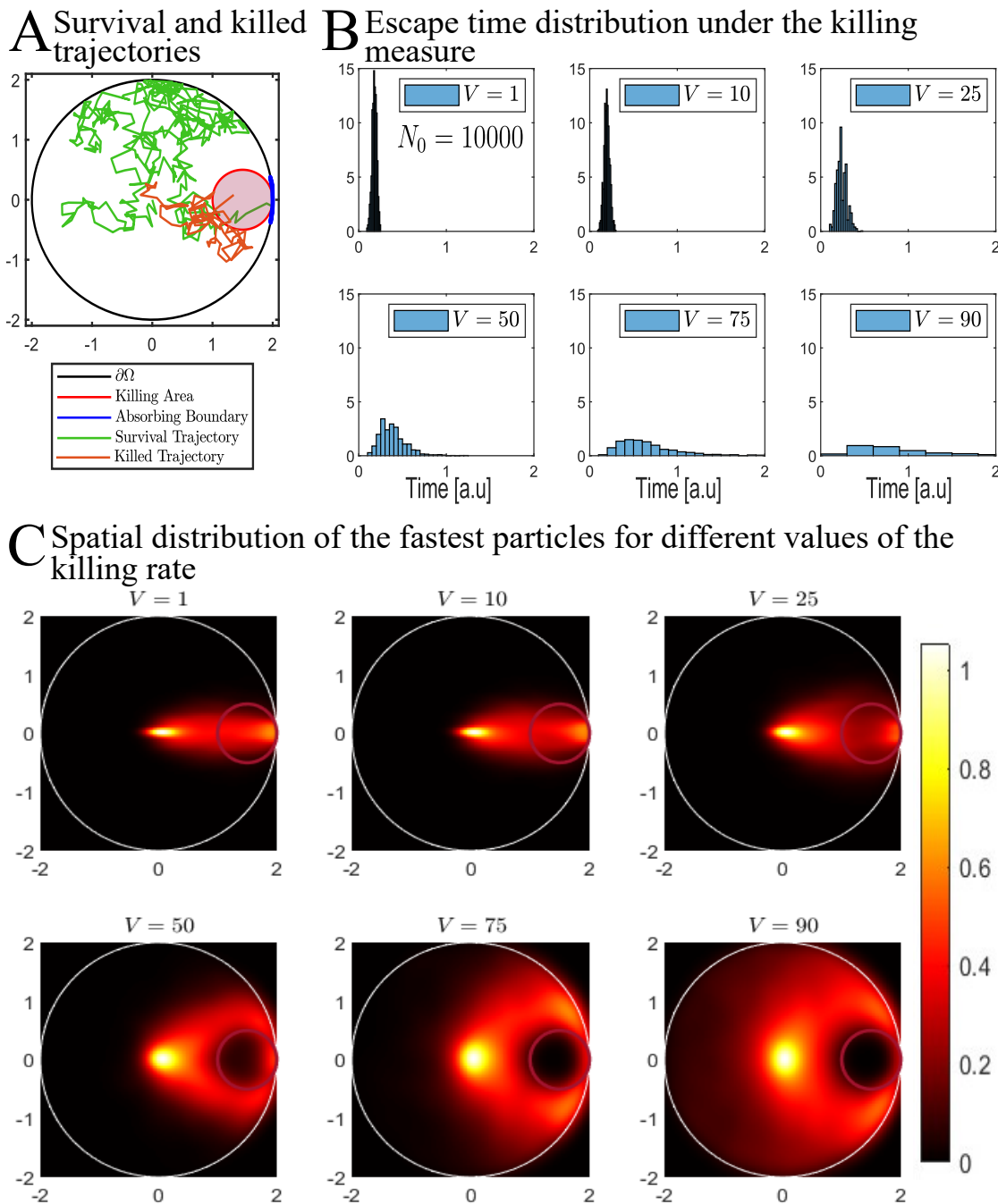


Figure 3.9: **Influence of the killing measure on the MFPT when the initial number of particles N_0 is large and the killing area overlaps locally with the absorbing boundary.** **A.** Two 2D examples of survival and killed particle in a disk with a tangent killing field. **B.** Escape time distribution of the fastest particle $\bar{\tau}^1$ when the killing increases in a disk tangent to the absorbing window. **C.** Effect of the killing measure on the spatial distribution of the fastest particle for considered $N_0 = 10000$ particles starting at the origin, $r_k = 0.5$, $x_k = (1.5, 0)^T$, $D = 1$, $R = 2$ and $k = 1000$ runs.

the point $A = (2, 0)$. This overlap between the killing area and the absorbing boundary results in a drastic flattening in the escape time distribution and an increase of the mean escape time

(Fig. 3.9B). The spatial distribution of the fastest particles when the killing weight increases, not only shows that the fastest particles avoid the killing area but they spread more in the domain before escaping. This dispersion of the fastest particles results in an increase in the mean escape time (Fig. 3.9B). Because the killing field is tangent to the absorbing windows, the particles are left with smaller safe cones (area between the killing zone and the boundary) where they can escape. Also, a large number of particles are killed before finding their way through the absorbing boundary. We remark also that the adjustments to the logarithmic law and the decay $\frac{1}{N^\alpha}$ did not work well for this problem, possibly due to the strong dependence on the way the killing area overlaps with the absorbing boundary. Interestingly, the killing measure can also influence the distribution of the exit points on the absorbing boundary as a consequence of the deformation of the safe zone (now become the safe cones), as shown in Fig. 3.10. When the killing area and the absorbing window are well separated, the distribution of exits points is uniform along the boundary (Fig. 3.10A). But, when the killing measure is tangent, a large killing weight leads to a parabolic deformation on the distribution (Fig. 3.10B). The fittings were made with respect to the respective constant $y = 0.1$ and parabolic functions ($y = a(x - b)^2 + c$) where the coefficients were chosen from a confidence interval with p-value $p = 0.05$. The sums of the square errors corresponding to each fitting are shown in the legends.

3.8 Conclusions, applications, and perspective

In this manuscript, we analyzed the effect of a killing measure on the escape of Brownian particles from a two-dimensional circular domain. In particular, we modeled the degradation of particles such as ions and molecules by some constant killing measure inside a confined space. For instance, proteins such as transcription factors are rapidly degraded inside the nucleus in order to regulate the response to external stimuli [134]. We studied here the mean time for the fastest Brownian particles to escape alive from a disk when a killing measure is uniform on the full domain and on a sub-region. We derived asymptotic formulas for the mean first passage time for the fastest particle (3.26) and (3.45), showing the role of the various parameters on the escape time. An asymptotic formula (3.78) was also obtained for the probability to escape through the a narrow absorbing window when it is well separated from the killing area.

The spatial distribution of the fastest particle revealed how the fastest particles always avoid the killing area when there is a high probability of being killed. Indeed, the most likely path for the fastest trajectories was concentrated around the shortest geodesic in a domain $\Omega \setminus B_{r_k}(\mathbf{x}_k)$ with the killing area removed. By performing stochastic simulations we explored the impact of several parameters such as the center and the radius of the killing area, and the weight of the killing measure on the mean first passage time for the fastest and on the escape probability. The radius of the killing area not only modified the escape probability (by reducing the number of survival particles) but it also impacted the shortest path to the absorbing window depending on its position. In Fig. 3.7 we noticed some discrepancies between the solution of the differential system (3.94) and the most likely path obtained from the simulations, due to the fact that the optimal path found through Euler-Lagrange equation holds when the noise intensity ϵ tends to zero. In our stochastic simulations, we have considered $\epsilon = 1$. Another possibility is that, in order to find the path, we selected the angle to end the trajectory at the center of the absorbing boundary, but in the simulations particles can escape everywhere in $\partial\Omega_a$.

The escape problem with a killing measure was already studied in [126] for a 1D domain. In the case of a 3D domain Ω and a 3D killing area Ω_k , the shortest path when the killing weight is large is

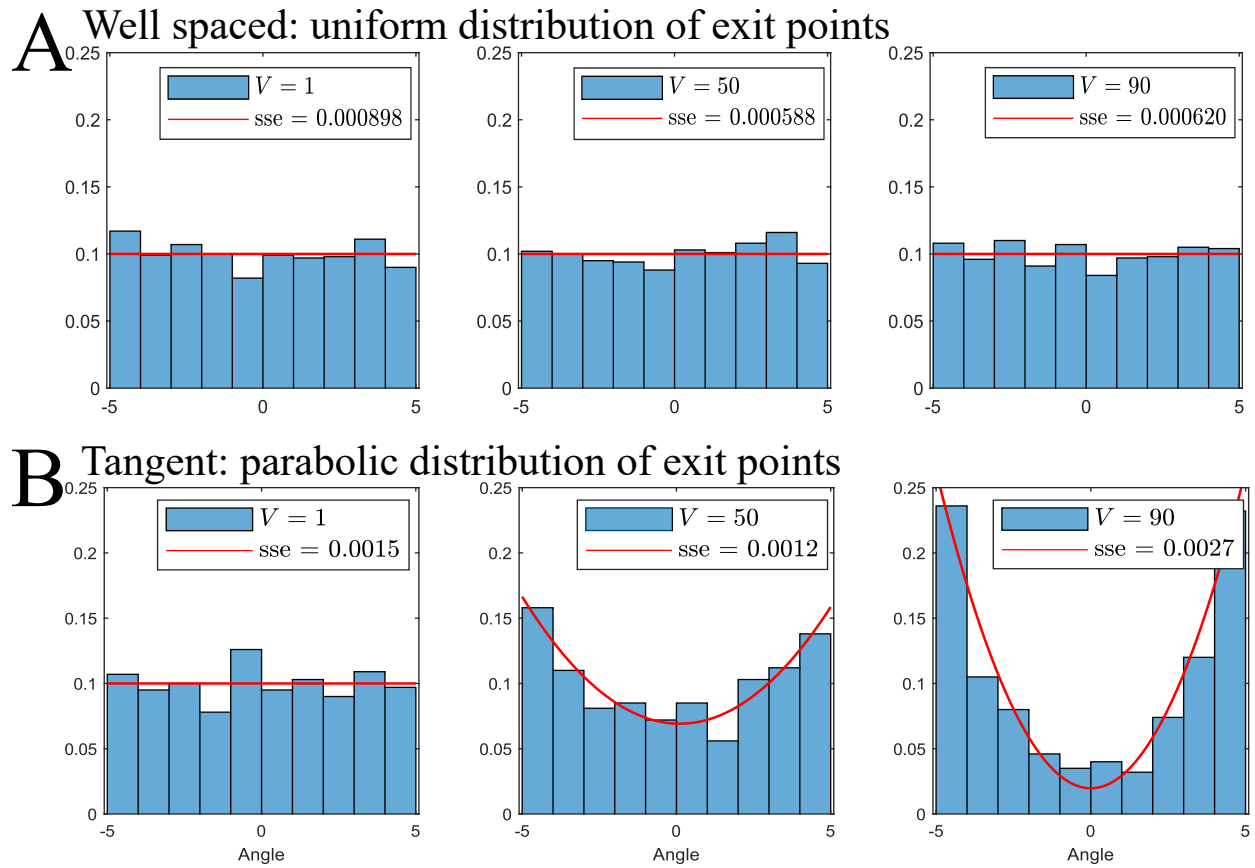


Figure 3.10: **Influence of the killing measure on the exit points of the boundary.** **A.** Uniform distribution of the exit points over the boundary when the killing area and the narrow escape windows are well separated for different values of the killing weight V . **B.** Parabolic effect of the killing measure in the distribution of the exit points over the absorbing window for different values of the killing weight V . Fitting with the parabolic function ($y = a(x - b)^2 + c$). First panel: $a = 0$, $b = 0$, $c = 0.1$. Second panel: $a = 0.003731$, $b = 0.1056$, $c = 0.06918$. Third panel: $a = 0.009735$, $b = -0.0006226$, $c = 0.01969$.

expected to be given by geodesic between the starting point and the center of the narrow absorbing window in the truncated domain where the killing field has been removed.

Part II

Asymptotic formulas for transport and synthesis of proteins

Chapter 4

Arrival time for the fastest among N switching stochastic particles

Published in TOSTE S. & HOLCMAN D., “Arrival time for the fastest among N switching stochastic particles” *The European Physical Journal B*, Volume 95, Number 113 (2022).
[arXiv:2112.12760](https://arxiv.org/abs/2112.12760) / hal:04101401

Abstract

The first arrivals among N Brownian particles is ubiquitous in the life sciences, as it often triggers cellular processes from the molecular level. We study here the case where stochastic particles, which represent proteins or molecules, can switch between two states inside the non-negative real line. The switching process is modeled as a two-state Markov chain and particles can only escape in state 1. We estimate the fastest arrival time by solving asymptotically the Fokker-Planck equation for three different initial distributions: Dirac delta, uniformly distributed and long-tail decay. The derived formulas suggest that the fastest particle avoids switching states when the switching rates are much smaller than the diffusion time scale. The formulas for the first arrival were compared with stochastic simulations in order to test the parametric region where these asymptotic results hold.

4.1 Introduction

The process of escaping for the fastest particle is often studied as an extreme statistical event [39, 59, 63, 71, 95, 101, 122, 135–137] where Brownian particles have to find a narrow window, which represents a small fraction of the explored space. The probability distribution function for the arrival time and the mean time $\bar{\tau}^N$ for the fastest particles among N , depend on: the geometry of the domain, the size and shape of the target, the boundary conditions and several other parameters. Sometimes, explicit computations can be derived [39, 64, 67, 71, 138]. Interestingly, the mean time of the fastest particle depends also on the initial distribution [67, 102, 122], leading to various decay with respect to N .

In this paper we study the extreme statistic properties for an ensemble of Brownian particles that can switch between two states characterized by two different diffusion coefficients D_1 and D_2 (Fig. 4.1A). This question has gained much attention in the recent years due to the possibility of deriving explicit formulas [114, 120, 139, 140]. The case of J possible switching states, modeled by a

Markov chain have been studied before in [16] and [140] as a discrete version of diffusing diffusivity models. In both papers, explicit formulas are derived in order to compute first arrival distributions for the non-negative real line. Extreme statistics formulas for the mean first arrival time have been derived in [139] for two-channel Markov additive diffusion in a 3-dimensional spherical domain. They proved that the first arrival behavior of a Markov additive process cannot be adequately captured by averaging quantities of the effective constants.

In this paper we compute the distribution and the mean first arrival time (MFAT) for the fastest particle to reach a target in the non-negative real line, and we clarify how they depend on the initial distribution. To study the variability of the MFAT with respect to the number of particles N , we consider four different initial distributions as shown in Fig. 4.1B. These initial distributions were already studied in chapter 1, leading to different decays in N for the MFAT, coming from the possible overlap between the initial distribution and the absorbing boundary. We assume as well in the model that particles can only escape in state 1 (Fig. 4.1A and C). If one particle touches the absorbing boundary in state 2, the particle will be reflected. This leads to two different boundary condition at the position of the target, depending on the state of the particles. The main computations for the MFAT made when N is large, rely on the short-time asymptotic formulas of the survival probability for the Fokker-Planck equation following the Laplace method.

This chapter is organized as follows: Section 4.2 presents the stochastic model and the associated mixed boundary value problem for two coupled Fokker-Planck equations. In section 4.3, we compute the asymptotic solutions for two Dirac delta initial conditions and different diffusion coefficients. In section 4.4, we study the case where particles are initially uniformly distributed in an interval. In section 4.5, we present the distribution of the arrival times for a long-tail initial distribution. Finally, in section 4.6, we discuss some possible applications of the present results to elementary signaling in cell biology. We have added as an appendix the previous computations made to obtain the survival probability in each case, in order to make the chapter more easy to read and follow.

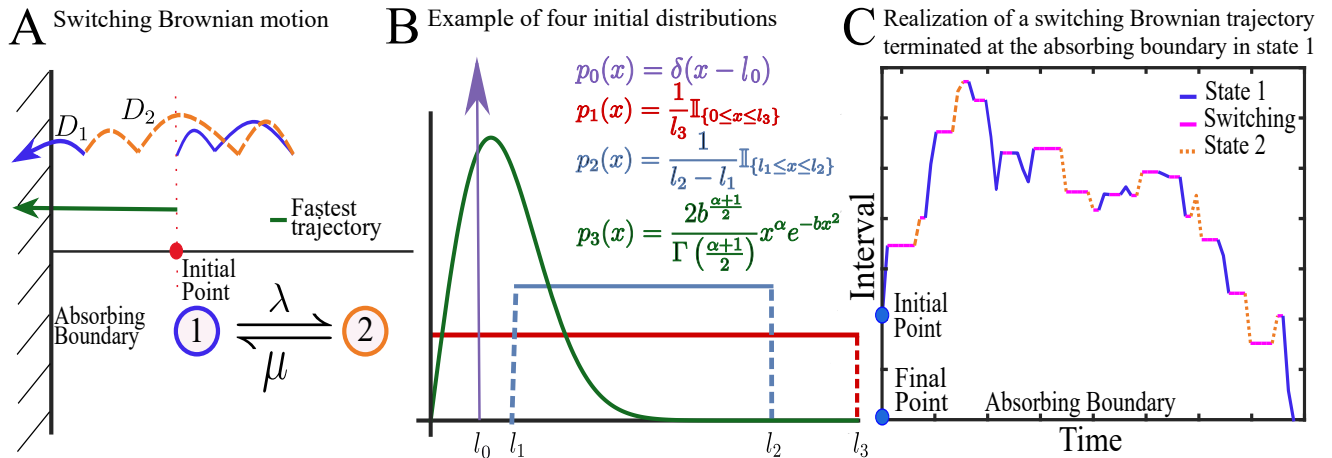


Figure 4.1: **Schematic figure for switching Brownian dynamics.** **A.** Example of two switching Brownian motions with two states in a line and an absorbing boundary. The particle can escape only in state 1 (blue). The fastest trajectory (green) should move in the shortest path and be in state 1 at the absorbing boundary to escape. **B.** Four initial distributions for the stochastic particles, notice that some of them can touch the absorbing boundary (red and green). **C.** Realization of a Brownian trajectory starting at $x = 2$ and absorbed at $x = 0$ with $dt = 0.01$.

4.2 Stochastic model

We consider here the 1D version of the switching model presented in section 0.1.3 for N identical independently distributed Brownian particles that can switch at Poissonian random times between two states

$$1 \xrightleftharpoons[k_{12}]{k_{21}} 2,$$

with rates k_{12} and k_{21} . We remark that particles can escape only in state 1. Following (59), the stochastic equation for the position $x(t, i)$ in state i of the particle is given for $i, j = 1, 2$ by

$$x(t + \Delta t, i) = \begin{cases} x(t, i) + \sqrt{2D_i} \Delta w(t) & \text{w.p } 1 - k_{ij} \Delta t + o(\Delta t) \\ x(t, j) & \text{w.p } k_{ij} \Delta t + o(\Delta t), i \neq j \end{cases}, \quad (4.1)$$

where $w(t)$ are independent standard Brownian motions, $\Delta w(t) = w(t + \Delta t) - w(t)$, and k_{ij} are the transition rates from state i to j . The transition probability density function $p(x, i, t|y, s, j)$ of the trajectory $x(t, i)$ with the initial condition $x(s, j) = x$, is the limit as $\Delta t \rightarrow 0$ of the integral equations

$$\begin{aligned} p(x, i, t + \Delta t|y, j, s) &= \frac{1 - k_{ij} \Delta t}{\sqrt{2\pi D_i \Delta t}} \int_{\Omega} p(z, i, t|y, j, s) \exp \left\{ -\frac{|x - z|^2}{2D_i \Delta t} \right\} dz \\ &\quad + k_{ji} \Delta t p(x, l, t|y, j, s) + o(\Delta t) \quad \text{for } i, j, l = 1, 2, i \neq j. \end{aligned} \quad (4.2)$$

In the present case, we will use the notation $k_{12} = \lambda$, $k_{21} = \mu$, $p(x, 1, t|y, 1, 0) = p_1(x, t)$ and $p(x, 2, t|y, 1, 0) = p_2(x, t)$, in order to simplify the equations. In the limit $\Delta t \rightarrow 0$, the forward system of Kolmogorov equations is given by [16]

$$\begin{aligned} \frac{\partial p_1}{\partial t}(x, t) &= D_1 \frac{\partial^2 p_1}{\partial x^2}(x, t) - \lambda p_1(x, t) + \mu p_2(x, t) \\ \frac{\partial p_2}{\partial t}(x, t) &= D_2 \frac{\partial^2 p_2}{\partial x^2}(x, t) - \mu p_2(x, t) + \lambda p_1(x, t). \end{aligned} \quad (4.3)$$

Our goal is to find the probability density function and the MFAT for the fastest particle escaping at point $x = 0$ in the domain $[0, +\infty)$. We start by adding to system (4.3) the boundary conditions

$$\begin{aligned} p_1(0, t) &= 0 \\ \frac{\partial p_2}{\partial x}(0, t) &= 0. \end{aligned} \quad (4.4)$$

When all particles start in state 1 at point $y > 0$, the initial conditions are given by

$$\begin{aligned} p_1(x, 0) &= \delta(x - y) \\ p_2(x, 0) &= 0. \end{aligned} \quad (4.5)$$

We impose the normalization condition

$$\int_0^\infty (p_1(x, 0) + p_2(x, 0)) dx = 1.$$

When all particles start in state 2 at point $y > 0$, the associated initial conditions are

$$\begin{aligned} p_1(x, 0) &= 0 \\ p_2(x, 0) &= \delta(x - y). \end{aligned} \quad (4.6)$$

4.3 Explicit expressions for the MFAT when the Brownian particles start in state 1

To solve the system (4.3-4.4-4.5), we use the Laplace transform in time

$$L(p_i(x, t)) = \hat{p}_i(x, q) = \int_0^\infty p_i(x, t) e^{-qt} dt \quad \text{for } i = 1, 2;$$

and we obtain the system of two ordinary differential equations

$$\begin{aligned} D_1 \frac{\partial^2 \hat{p}_1}{\partial x^2}(x, q) - (\lambda + q) \hat{p}_1(x, q) + \mu \hat{p}_2(x, q) + \delta(x - y) &= 0 \\ D_2 \frac{\partial^2 \hat{p}_2}{\partial x^2}(x, q) - (\mu + q) \hat{p}_2(x, q) + \lambda \hat{p}_1(x, q) &= 0. \end{aligned} \quad (4.7)$$

4.3.1 Prototype testing case: particles start in state 1 and $D_2 = 0$

This is the easiest case to explore. To find the Laplace transform of the survival probability we set $D_2 = 0$ in the Laplace transformed system given by (4.7). Then, we obtain the differential equation

$$\left[\frac{\partial^2}{\partial x^2} - \frac{q(q + \theta)}{D_1(q + \mu)} \right] \hat{p}_1(x, q) = -\frac{\delta(x - y)}{D_1}, \quad (4.8)$$

where $\theta = \lambda + \mu$, and whose solution is given by

$$\hat{p}_1(x, q) = \sqrt{\frac{q + \mu}{4D_1q(q + \theta)}} \exp \left\{ -\sqrt{\frac{q(q + \theta)}{D_1(q + \mu)}} |x - y| \right\}. \quad (4.9)$$

To satisfy the boundary condition $\hat{p}_1(0, q) = 0$, we finally obtain

$$\hat{p}_1(x, q) = \frac{\sqrt{q + \mu} \left(\exp \left\{ -\sqrt{\frac{q(q + \theta)}{D_1(q + \mu)}} |x - y| \right\} - \exp \left\{ -\sqrt{\frac{q(q + \theta)}{D_1(q + \mu)}} |x + y| \right\} \right)}{\sqrt{4D_1q(q + \theta)}}, \quad (4.10)$$

and

$$\hat{p}_2(x, q) = \lambda \frac{\left(\exp \left\{ -\sqrt{\frac{q(q + \theta)}{D_1(q + \mu)}} |x - y| \right\} + \exp \left\{ -\sqrt{\frac{q(q + \theta)}{D_1(q + \mu)}} |x + y| \right\} \right)}{\sqrt{4D_1q(q + \theta)(q + \mu)}}. \quad (4.11)$$

Thus, the Laplace transform of the survival probability is given by

$$\hat{S}(q) = \int_{\Omega} (\hat{p}_1(x, q) + \hat{p}_2(x, q)) dx = \frac{1}{q} - \frac{q + \mu}{q(q + \theta)} \exp \left\{ -\sqrt{\frac{q(q + \theta)}{D_1(q + \mu)}} y \right\}. \quad (4.12)$$

The expansion in large q for the survival probability (4.12) is given by

$$\hat{S}(q) = \frac{1}{q} - \frac{\exp \left\{ -\sqrt{\frac{q}{D_1}} y \right\}}{q} + \lambda y \frac{\exp \left\{ -\sqrt{\frac{q}{D_1}} y \right\}}{q\sqrt{4D_1q}} + O \left(\frac{\exp \left\{ -\sqrt{\frac{q}{D_1}} y \right\}}{q^2} \right). \quad (4.13)$$

The function $\hat{S}(q)$ has a simple zero when $q \rightarrow +\infty$ and a pole when $q = 0$, thus we can obtain the inverse Laplace transform by integrating over $\mathcal{R}(q) = \alpha$ where $\alpha > 0$. We can then recover the small t approximation

$$S(t) \approx 1 - \operatorname{erfc}\left(\frac{y}{\sqrt{4D_1 t}}\right) + \lambda \operatorname{terfc}\left(\frac{y}{\sqrt{4D_1 t}}\right) \sim 1 - \sqrt{4D_1 t} \frac{\exp\left\{-\frac{y^2}{4D_1 t}\right\}}{y\sqrt{\pi}}. \quad (4.14)$$

This leads for large N , following Laplace's method, to the asymptotic formula for the mean first arrival time

$$\bar{\tau}^N = \mathbb{E}\{\tau^1\} \sim \int_0^\infty \exp\left\{N \ln\left\{1 - \frac{\sqrt{4D_1 t}}{y\sqrt{\pi}} e^{-\frac{y^2}{4D_1 t}}\right\}\right\} dt \sim \frac{y^2}{4D_1 \ln\left(\frac{N}{\sqrt{\pi}}\right)}. \quad (4.15)$$

The formula (4.15) is the same as in the case when no switching is considered [71]. This result, gives us the idea that when the diffusion coefficient in state 2 is zero, the fastest particle does not waste time switching to a state where it cannot escape.

To study the probability density function for the first arrival time, we are going to consider the r.v. σ_s^N with distribution

$$\Pr\{\sigma_s^N \leq t\} = 1 - \exp\left\{-\frac{\sqrt{4D_1 t} N}{y\sqrt{\pi}} e^{-\frac{y^2}{4D_1 t}}\right\}. \quad (4.16)$$

Note that the pdf of σ_s^N is given by

$$\begin{aligned} \Pr\{\sigma_s^N \in [t, t+dt]\} &= -\frac{d}{dt} \left[\exp\left\{-\frac{\sqrt{4D_1 t} N}{y\sqrt{\pi}} e^{-\frac{y^2}{4D_1 t}}\right\} \right] dt \\ &= \frac{N(\sqrt{4D_1 t})}{y\sqrt{\pi}} \exp\left\{-\frac{y^2}{4D_1 t}\right\} \exp\left\{-\frac{\sqrt{4D_1 t} N}{y\sqrt{\pi}} e^{-\frac{y^2}{4D_1 t}}\right\} \left[\frac{y^2}{4D_1 t^2} + \frac{1}{2t} \right] dt, \end{aligned} \quad (4.17)$$

and note also that

$$\Pr\{\tau^1 \leq t\} = 1 - [S(t)]^N \sim \Pr\{\sigma_s^N \leq t\} \text{ when } t \text{ is small.} \quad (4.18)$$

We thus expect the density of the distribution for the arrival times to be close enough of the density (4.17) when the escape times are small. When we consider that the particle can stay a long time in the state where it can not escape, the escape time becomes large and the survival probability is thus given by the inverse of the long-time (small q) expansion of $\hat{S}(q)$. In this case we consider

$$\Pr\{\sigma_l^N \leq t\} = 1 - \exp\left\{-\frac{\sqrt{4D_1 t} N \mu^{\frac{3}{2}}}{y\theta^{\frac{3}{2}}\sqrt{\pi}} e^{-\frac{y^2\theta}{4D_1 \mu t}}\right\}, \quad (4.19)$$

where

$$\begin{aligned} \Pr\{\sigma_l^N \in [t, t+dt]\} &= -\frac{d}{dt} \left[\exp\left\{-\frac{\sqrt{4D_1 t} N \mu^{\frac{3}{2}}}{y\theta^{\frac{3}{2}}\sqrt{\pi}} e^{-\frac{y^2\theta}{4D_1 \mu t}}\right\} \right] dt \\ &= \frac{N \mu^{\frac{3}{2}} (\sqrt{4D_1 t})}{y\theta^{\frac{3}{2}}\sqrt{\pi}} \exp\left\{-\frac{y^2\theta}{4D_1 \mu t}\right\} \exp\left\{-\frac{\sqrt{4D_1 t} N \mu^{\frac{3}{2}}}{y\theta^{\frac{3}{2}}\sqrt{\pi}} e^{-\frac{y^2\theta}{4D_1 \mu t}}\right\} \left[\frac{y^2\theta}{4D_1 \mu t^2} + \frac{1}{2t} \right] dt, \end{aligned} \quad (4.20)$$

and we know

$$\Pr\{\tau^1 \leq t\} \sim \Pr\{\sigma_i^N \leq t\} \text{ when } t \text{ is large.} \quad (4.21)$$

It is important to remark here that we are able to give asymptotic formulas for the first arrival time only through the small time limit. This is due to the fact that we are approximating the integral for the expected value of τ^1 using the Laplace method, this is, we are approximating the value of this integral by the value of the integral around the maximum value of the survival probability, which occurs when $t \rightarrow 0^+$.

To evaluate the range of validity of the formula (4.15), we decided to compare the asymptotic distributions with stochastic simulations made in a finite interval, avoiding simulate particles that could go very far from the absorbing boundary leading to a high computational cost. The asymptotic formula for the MFAT of the fastest particle on the finite interval $[0, a]$ where the initial point satisfies $2y_0 \ll a$ is equivalent to the formula for the MFAT in the non-negative real line when the number N is large [71]. Indeed the formulas are depending on the minimal distance from the initial position to the absorbing boundary, and the trajectory of the fastest particle is located near the shortest line connecting the initial point with the closest absorbing boundary [66, 93]. This means that when N is large, the minimal times over the two domains are similar, result that allows us to perform the simulations in a finite interval that here we consider as $[0, 5]$.

We generated trajectories until they reach the origin in state 1 and selected the fastest one. The Fig. 4.2 shows the statistics for the simulation of the switching process, starting in state 1 at position $y = 2$ with diffusion coefficients $D_1 = 1$ and $D_2 = 0$. We use for the initial number of particles $N = (500, 1000, 2500, 5000, 10000)$ with a time step $\Delta t = 0.0001$. The switching rates are $\lambda = 100$ and $\mu = (1000, 2500, 5000, 7500, 9000)$. We obtain a good agreement between the long-time approximation for the distribution (equation (4.20)) of the arrival time and the stochastic simulations (Fig. 4.2A). This means that the time that the particle spends in the fastest state is still small compare with the escape time. Note that as μ increases, the distribution converges to the short time distribution. We further confirm the decay of the MFAT vs N . We use a shift α in formula (4.15) to correct for possible switching: indeed in the large N limit, the fastest particle arriving at the target should not switch when it starts in state 1 and $D_1 > D_2$. When $\mu = 1000$ the agreement between the simulations and the formula is not good and it cannot even be corrected by the term α in the formula, this means that in this case we are not in the regime where the asymptotic formula holds. In addition, we report here a large value for the mean number M_{swit} of switchings (Fig. 4.2C) for the fastest particles, corresponding with the large values of λ and μ . The numerical simulations suggest that this number is independent of the switching rate μ when $\mu \gg \lambda$. To clarify this property, we compute the number of switchings during time t using the probability distribution function for a given switch from 1 to 2 that occurs during a time $\tau^{1 \rightarrow 2}$ and then back from 2 to 1, during the time $\tau^{2 \rightarrow 1}$. Since the underlying processes are Poissonian with rate λ and μ respectively, the probability that a full cycle of switchings occurs at time t is given by the convolution

$$\begin{aligned} \Pr\{\tau^{\text{switch}} = t\} &= \Pr\{\tau^{1 \rightarrow 2} + \tau^{2 \rightarrow 1} = t\} = \int_0^t \lambda \exp(-\lambda(t-s)) \mu \exp(-\mu s) ds \\ &= \lambda \mu \frac{\exp(-\lambda t) - \exp(-\mu t)}{\mu - \lambda} = f(t). \end{aligned} \quad (4.22)$$

Thus, the probability of m switchings occurs in a time t is the convolution

$$\Pr\{m \text{ switchings at time } t\} = \Pr\{\tau^1 \text{ switch} + \dots + \tau^m \text{ switches} = t\} = f(t) * \dots * f(t). \quad (4.23)$$

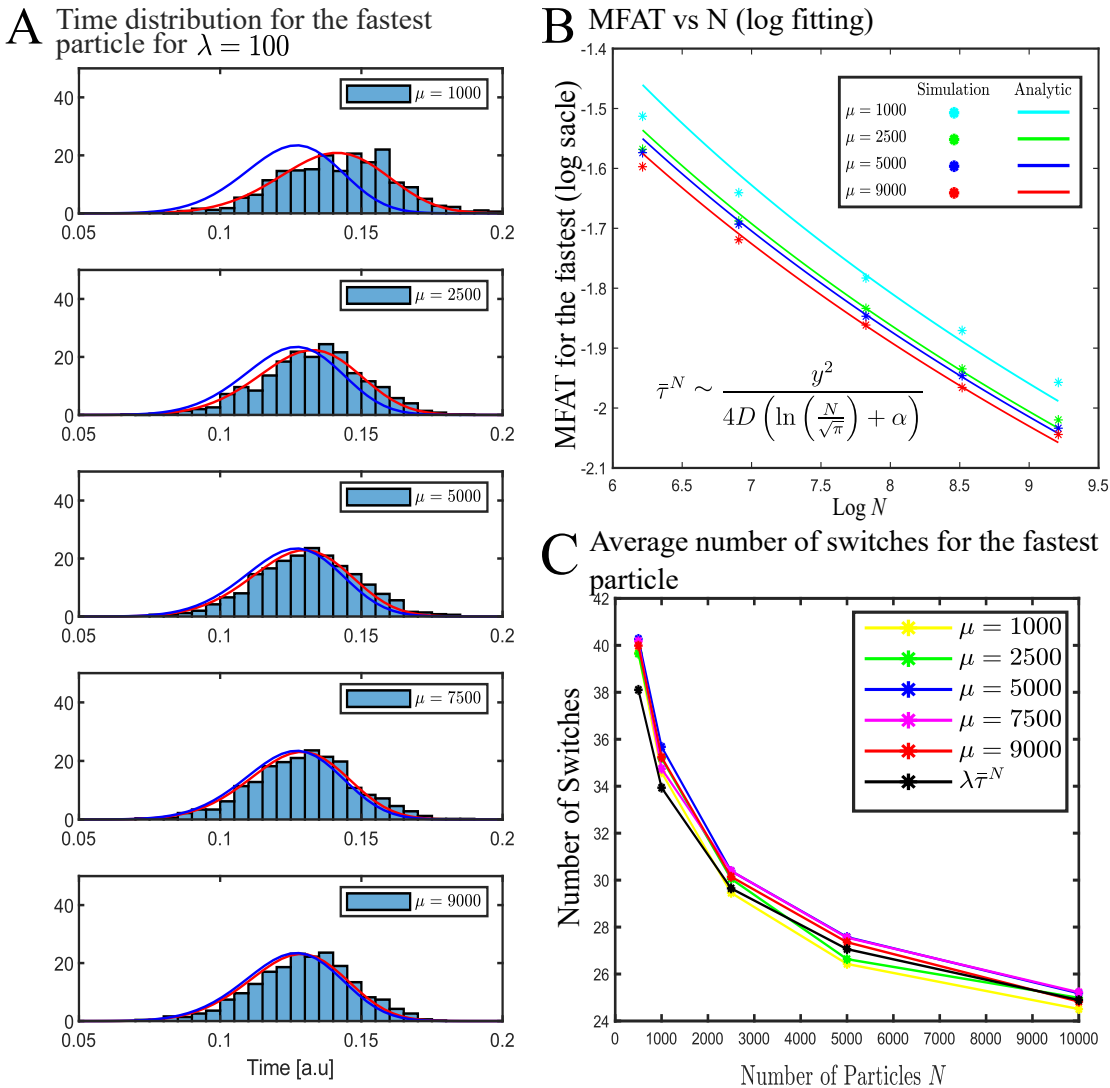


Figure 4.2: **Mean fastest arrival time vs the number of particles N .** **A.** Density function for the distribution of the arrival time $\bar{\tau}^1$: analytical short-time approximation (4.17) (blue) and analytical long-time approximation (4.20) (red) vs stochastic simulations (blue histogram) for particles starting at position $y = 2$ for $N = 10000$ with 1000 runs and $D_1 = 1$ and $D_2 = 0$ in the interval $[0, 5]$. **B.** MFAT vs N for the stochastic simulations (colored disks) and the asymptotic formulas (continuous lines) (equation 4.20) for different values of $\mu = (1000, 2500, 5000, 7500, 9000)$ and $\lambda = 100$ plotted in Log-Log scale. An optimal fit gives $\alpha = (-1.334, -0.9959, -0.9292, -0.8109)$. **C.** Mean number of switchings for the fastest particles (colored for each different value of μ) until its arrival to the target compared with the logarithmic law (black) proposed in formula (4.26) for $\lambda = 100$ and a factor of 1.09.

In a first approximation, when $\lambda \ll \mu$, formula (4.23) is the classical Poisson distribution for having m events during time t , this is:

$$\Pr\{m \text{ switchings at time } t\} = \frac{(\lambda t)^m}{m!} \exp(-\lambda t). \quad (4.24)$$

Thus, the mean number of switchings at time t is given by

$$\mathbb{E}[M(t)] = \sum_{m=0}^{\infty} m \Pr\{M(t) = m\} = \lambda t, \quad (4.25)$$

where $M(t)$ is the amount of switching occurring until time t . Thus, during the fastest arrival, the mean number of switching is given by

$$\mathbb{E}(M(\bar{\tau}^N)) = \lambda \bar{\tau}^N = \lambda \frac{y^2}{4D_1 \ln\left(\frac{N}{\sqrt{\pi}}\right)}. \quad (4.26)$$

We can now use this asymptotic behavior to fit the curve of Fig. 4.2C (black line) with $1/\ln\left(\frac{N}{\sqrt{\pi}}\right)$. Interestingly, the mean number of switchings goes to zero as $N \rightarrow \infty$. When $\lambda \bar{\tau}^N < 1$, this is

$$N > \sqrt{\pi} \exp\left(\lambda \frac{y^2}{4D_1}\right), \quad (4.27)$$

we will observe no switch with probability $\exp(-\lambda \bar{\tau}^N)$. We observe a good agreement between the mean number of switchings with the logarithmic function for $\lambda = 100$ (Fig. 4.2C) with a factor 1.09, due probably to the approximations made in (4.24).

There are, from our understanding, a few necessary comments to make suggested by the simulation results. The first one, is how the short time distribution can be seen as the limit of the long time distribution when $\mu \rightarrow +\infty$ for a fixed λ . This result can be observed from Fig. 4.2A and it is quite natural if we understand the limit $\mu \rightarrow +\infty$ as one only possible state for the particle. This is also the idea behind the MFAT formulas in Fig. 4.2B. As soon as μ increases, the time spent in state 2 decreases, meaning that the particle will mostly move in the fastest state where it can escape, and escaping faster in consequence. This is the reason why the MFAT decreases when μ increases, and this is also the reason why for μ large we obtain a better fit with our asymptotic formula. The last remark, and probably the most important one, is that the asymptotic results are not valid for every set of parameters λ, μ, D_1, D_2 and N as shown in Fig. 4.2A. In the ideal case where it is possible to have an infinite number of particles N the short time formulas are always valid, but in practice N is finite. Thus, restrictions in the set of parameters or a restriction for the number of particles N such the formula (4.27) are needed in order to keep holding the asymptotic results.

A very important detail is the meaning of short time and long time expansions here. From our understanding long time expansion is needed when the particles make a large number of switches and when particles are moving in the slower state. From here, is quite clear now that the case where $\lambda \rightarrow +\infty$ and $\mu \rightarrow +\infty$ simultaneously will not lead to an accurate agreement between the simulations and the asymptotic formula since particles will be mostly alternating, even if the condition $\frac{1}{\lambda} + \frac{1}{\mu} \ll 1$ is clearly satisfied, meaning that the switches are almost instantaneous.

So, we believe that the main criteria here, is not that the switches are instantaneous but instead, we need that the switch from the slower state to the fastest state should be, at least, faster than diffusing in the fastest state. And then, the diffusion time in the fastest state should be small than the expected time for a full switching. This last condition is implicit imposing that we are maximizing the time in the fastest state. The idea that the expected time in the slower state should be small, leaves us with a restriction in the way $\mu \rightarrow +\infty$ or $\lambda \rightarrow +\infty$ depending on which one is related to the slower state, pointing out about an inequality with the diffusion coefficients. For instance, in this case where all particles are starting at state 1, with $D_1 > D_2$, the restriction could

be

$$\frac{1}{\mu} \ll \frac{y^2}{4D_1 \log\left(\frac{N}{\sqrt{\pi}}\right)} \ll \frac{1}{\lambda} + \frac{1}{\mu}. \quad (4.28)$$

The first inequality means that the time to switch from state 2 to 1 is small than the time it takes to only move in state 1. The second part is just saying that escaping without switching is faster than the expected time for a full switching. Note that if we simultaneously consider (4.28) and $\mu \rightarrow +\infty$ as the condition to avoid the slow state, we will end up with the same constrain as in (4.27).

We believe that there is even a more simple way to compute the mean number of switchings until time T , with T fixed, given by

$$\mathbb{E}(M(T)) = \frac{T}{\frac{1}{\lambda} + \frac{1}{\mu}}. \quad (4.29)$$

Thus, in the limit $N \rightarrow \infty$, the escape time τ^N is independent of the Poissonian switching processes, and thus

$$\mathbb{E}(M(\bar{\tau}^N)) = \frac{\bar{\tau}^N}{\frac{1}{\lambda} + \frac{1}{\mu}}. \quad (4.30)$$

Note that here again, if we assume $\mathbb{E}(M(\bar{\tau}^N)) \ll 1$ we are back to the right hand restriction in equation (4.28). We thus propose a general constrain that needs to be adapted at each case depending on the initial state of particles, given by

$$\bar{\tau}^S \rightarrow f \ll \bar{\tau}^{(N|I_0)} \ll \bar{\tau}^{(I_0|1)}, \quad (4.31)$$

where $\bar{\tau}^S \rightarrow f$ is the mean time to switch from the slower state to the fastest one, $\bar{\tau}^{(N|I_0)}$ is the asymptotic formula found through the Laplace method when particles start in state I_0 and $\bar{\tau}^{(I_0|1)}$ is the mean time to be in the state 1, where escape is possible, given the initial state. In this simple case, as $D_1 > D_2$ we know that $\bar{\tau}^S \rightarrow f = \frac{1}{\mu}$, and as particles start in state 1, the mean time to be in the state 1 again is $\bar{\tau}^{(1|1)} = \frac{1}{\lambda} + \frac{1}{\mu}$.

4.3.2 Particles start in state 1 and $D_2 \neq 0$

To compute the escape time for the fastest particle when $D_2 \neq 0$, we start from system (4.7). We shall now distinguish two cases, when $D_1 = D_2$, and when they are different but strictly positive.

Particles start in state 1 and the diffusion coefficients satisfy $D_1 = D_2 = D$

The equation obtained while solving the system (4.3) for $\hat{p}_2(x, q)$ with the initial condition (4.5), is given by

$$\left[\frac{\partial^4}{\partial x^4} - \left(\frac{\lambda+q}{D_1} + \frac{\mu+q}{D_2} \right) \frac{\partial^2}{\partial x^2} + \left(\frac{(\lambda+q)(\mu+q) - \lambda\mu}{D_1 D_2} \right) \right] \hat{p}_2(x, q) = \frac{\lambda}{D_1 D_2} \delta(x - y). \quad (4.32)$$

Now, we use the boundary conditions (4.4) and we set $D_1 = D_2 = D$. In this case, the solutions are given by the expressions

$$\begin{aligned}\hat{p}_1(x, q) &= \frac{\lambda}{2\theta\sqrt{D}\sqrt{q+\theta}} \left(e^{-\sqrt{\frac{q+\theta}{D}}|x-y|} - e^{-\sqrt{\frac{q+\theta}{D}}|x+y|} \right) \\ &\quad + \frac{\mu}{2\theta\sqrt{D}\sqrt{q}} \left(e^{-\sqrt{\frac{q}{D}}|x-y|} - e^{-\sqrt{\frac{q}{D}}|x+y|} \right), \\ \hat{p}_2(x, q) &= -\frac{\lambda}{2\theta\sqrt{D}\sqrt{q+\theta}} \left(e^{-\sqrt{\frac{q+\theta}{D}}|x-y|} + e^{-\sqrt{\frac{q+\theta}{D}}|x+y|} \right) \\ &\quad + \frac{\lambda}{2\theta\sqrt{D}\sqrt{q}} \left(e^{-\sqrt{\frac{q}{D}}|x-y|} + e^{-\sqrt{\frac{q}{D}}|x+y|} \right),\end{aligned}\tag{4.33}$$

where $\theta = \lambda + \mu$. The Laplace transform of the survival probability is

$$\begin{aligned}\hat{S}(q) &= \int_{\Omega} (\hat{p}_1(x, q) + \hat{p}_2(x, q)) dx \\ &= \int_0^{\infty} \left(\frac{1}{\sqrt{4Dq}} e^{-\sqrt{\frac{q}{D}}|x-y|} + \frac{\lambda - \mu}{\theta\sqrt{4Dq}} e^{-\sqrt{\frac{q}{D}}|x+y|} - \frac{\lambda}{\theta\sqrt{D}\sqrt{q+\theta}} e^{-\sqrt{\frac{q+\theta}{D}}|x+y|} \right) dx,\end{aligned}\tag{4.34}$$

and replacing the values of the integrals

$$\int_0^{\infty} e^{-|x-y|\frac{\sqrt{q}}{\sqrt{D}}} dx = \frac{\sqrt{4D}}{\sqrt{q}} \left(2 - e^{-y\frac{\sqrt{q}}{\sqrt{D}}} \right) \text{ and } \int_0^{\infty} e^{-|x+y|\frac{\sqrt{q}}{\sqrt{D}}} dx = \frac{\sqrt{D}}{\sqrt{q}} e^{-y\frac{\sqrt{q}}{\sqrt{D}}},$$

we obtain

$$\hat{S}(q) = \frac{1}{q} - \frac{\mu}{\theta} \frac{e^{-y\frac{\sqrt{q}}{\sqrt{D}}}}{q} - \frac{\lambda}{\theta} \frac{e^{-y\frac{\sqrt{q+\theta}}{\sqrt{D}}}}{q+\theta}.\tag{4.35}$$

The large q expansion for the Laplace transform of the survival probability leads to

$$\hat{S}(q) = \frac{1}{q} - \frac{e^{-y\frac{\sqrt{q}}{\sqrt{D}}}}{q} + \lambda \frac{e^{-y\frac{\sqrt{q}}{\sqrt{D}}}}{q} \left(\frac{1}{q} + \frac{y}{\sqrt{4Dq}} \right) + O\left(\frac{e^{-y\frac{\sqrt{q}}{\sqrt{D}}}}{q^{\frac{5}{2}}}\right).\tag{4.36}$$

The inverse Laplace transform gives the approximation

$$S(t) \sim 1 - \operatorname{erfc}\left(\frac{y}{\sqrt{4Dt}}\right) \sim 1 - \frac{e^{-\frac{y^2}{4Dt}} \sqrt{4Dt}}{y\sqrt{\pi}}.\tag{4.37}$$

We obtain thus, using Laplace's method, the asymptotic value for the MFAT when N is large

$$\bar{\tau}^N = \int_0^{\infty} [S(t)]^N dt \sim \int_0^{\infty} \exp \left\{ \ln \left\{ 1 - e^{-\frac{y^2}{4Dt}} \frac{\sqrt{4Dt}}{y\sqrt{\pi}} \right\}^N \right\} dt \sim \frac{y^2}{4D \ln \left(\frac{N}{\sqrt{\pi}} \right)}.\tag{4.38}$$

We conclude that the fastest arriving particle does not switch between states, but escape in state 1, avoiding to change state. We see this clearly from the small time approximations made for the survival probability, whose leading order term comes from the diffusion process, so the fastest particle does no switch.

Particles start in state 1 and the diffusion coefficients satisfy $D_1 \neq D_2$

In Appendix 4.7.1, we present the details of the computations when the diffusion coefficients differ for each state and both are not zero: we derived an equation of order 4 that we solve using the non-homogeneous linear equation theory. We use the solution to compute asymptotically the survival probability when q is large. It is given by

$$\hat{S}(q) \approx \frac{1}{q} - \frac{e^{-y\sqrt{\frac{q}{D_1}}}}{q} - \frac{\lambda\mu D_2^3}{(D_2 - D_1)^2} \frac{e^{-y\sqrt{\frac{q}{D_2}}}}{q^3}. \quad (4.39)$$

When $D_1 > D_2$, we obtain the small t approximation, given by

$$S(t) \sim 1 - \operatorname{erfc}\left(\frac{y}{\sqrt{4D_1 t}}\right) \sim 1 - \frac{e^{-\frac{y^2}{4D_1 t}} \sqrt{4D_1 t}}{y\sqrt{\pi}}. \quad (4.40)$$

Finally, the mean arrival time of the fastest particle is given by

$$\bar{\tau}^N = \int_0^\infty [S(t)]^N dt \sim \int_0^\infty \exp\left\{\ln\left\{1 - e^{-\frac{y^2}{4D_1 t}} \frac{\sqrt{4D_1 t}}{y\sqrt{\pi}}\right\}^N\right\} dt \sim \frac{y^2}{4D_1 \ln\left(\frac{N}{\sqrt{\pi}}\right)}. \quad (4.41)$$

This result is identical to the one when the fastest particle does not switch. Thus, the fastest particle starting in state 1, with $D_1 > D_2$ does not switch to the state 2 where it moves slowly, but it keeps moving in state 1 until it reaches the absorbing boundary, under the short time regime, given by

$$\frac{1}{\mu} \ll \frac{y^2}{4D_1 \ln\left(\frac{N}{\sqrt{\pi}}\right)} \ll \frac{1}{\lambda} + \frac{1}{\mu}. \quad (4.42)$$

We shall now consider the case where $D_2 > D_1$. In this case the leading order term in the expansion of $\hat{S}(q)$ for large q is $\frac{\lambda\mu D_2^3}{(D_2 - D_1)^2} \frac{e^{-y\sqrt{\frac{q}{D_2}}}}{q^3}$. Thus, the small t approximation for the survival probability is given by

$$S(t) \sim 1 - \frac{\lambda\mu D_2^3 e^{-\frac{y^2}{4D_2 t}} \sqrt{4D_2 t} t^2}{2(D_2 - D_1)^2 y\sqrt{\pi}}, \quad (4.43)$$

leading to the mean first arrival formula when N is large

$$\bar{\tau}^N \sim \int_0^\infty \exp\left\{\ln\left\{1 - \frac{\lambda\mu D_2 e^{-\frac{y^2}{4D_2 t}} \sqrt{4D_2 t} t^2}{2y\sqrt{\pi}}\right\}^N\right\} dt \sim \frac{y^2}{4D_2 \ln\left(\frac{N\lambda\mu D_2}{2\sqrt{\pi}} \left(\frac{y^2}{4D_2}\right)^2\right)}. \quad (4.44)$$

Here, the condition for the short time formula given by (4.31) is

$$\frac{1}{\lambda} \ll \frac{y^2}{4D_2 \ln\left(\frac{N\lambda\mu D_2}{2\sqrt{\pi}} \left(\frac{y^2}{4D_2}\right)^2\right)} \ll \frac{1}{\lambda} + \frac{1}{\mu}. \quad (4.45)$$

Formulas (4.41, 4.44) reveal the role of the diffusion coefficients in the escape process. There are two different strategies for the fastest particles depending on the diffusion coefficients: Starting in state 1 (the only state where particles can escape at the absorbing boundary), with $D_1 > D_2$, the fastest particle will simply diffuse until it reaches the target (Fig. 4.3A). However, when starting in state 1 with $D_2 > D_1$, the fastest particle will switch to state 2 where it can diffuse faster, it will then diffuse to the target and then switch back to state 1 before escaping (Fig. 4.3B). Interestingly the exponent of the factor $\frac{y^2}{4D_2}$ inside the logarithm of the asymptotic formula (4.44) confirms that the fastest particle switches twice before it escapes.

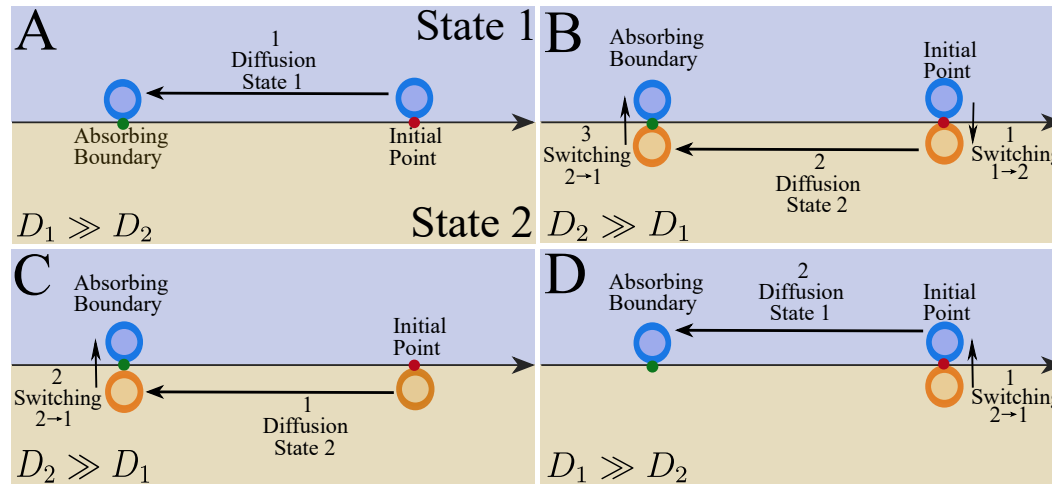


Figure 4.3: **Strategies followed by the fastest particle depending on the initial state and the diffusion coefficients.** **A.** Diffusion in state 1 onto the target (Initial state = 1 and $D_1 > D_2$). **B.** Switching from state 1 to 2. Diffusion in state 2 onto the target. Switching from state 2 to 1 (Initial state = 1 and $D_2 > D_1$). **C.** Diffusion in state 2 onto the target. Switching from state 2 to 1 (Initial state = 2 and $D_2 > D_1$). **D.** Switching from state 2 to 1. Diffusion in state 1 onto the target. (Initial state = 2 and $D_1 > D_2$).

4.3.3 Particles start in state 2

When the particles start in state 2 at position $y > 0$ we use the initial condition (4.6). To determine the distribution of arrival time, we use Laplace transform in time to get the ordinary differential equation

$$\left[\frac{\partial^4}{\partial x^4} - \left(\frac{q + \lambda}{D_1} + \frac{q + \mu}{D_2} \right) \frac{\partial^2}{\partial x^2} + \left(\frac{(q + \lambda)(q + \mu) - \lambda\mu}{D_1 D_2} \right) \right] \hat{p}_1(x, q) = \frac{\mu}{D_1 D_2} \delta_y. \quad (4.46)$$

Solution when the particles start in state 2 for $D_1 = D_2 = D$.

Similarly to the steps presented in the previous subsections, we find from the theory of non homogeneous linear equations the solution for system (4.3) with the initial condition (4.6) and boundary

conditions (4.4). This solution is given by

$$\hat{p}_1(x, q) = \frac{\mu \left(e^{-\sqrt{\frac{q}{D}}|x-y|} - e^{-\sqrt{\frac{q}{D}}|x+y|} \right)}{\theta \sqrt{4Dq}} - \frac{\mu \left(e^{-\sqrt{\frac{q+\theta}{D}}|x-y|} - e^{-\sqrt{\frac{q+\theta}{D}}|x+y|} \right)}{\theta \sqrt{4D} \sqrt{q+\theta}}, \quad (4.47)$$

$$\hat{p}_2(x, q) = \frac{\mu \left(e^{-\sqrt{\frac{q+\theta}{D}}|x-y|} + e^{-\sqrt{\frac{q+\theta}{D}}|x+y|} \right)}{\theta \sqrt{4D} \sqrt{q+\theta}} + \frac{\lambda \left(e^{-\sqrt{\frac{q}{D}}|x-y|} + e^{-\sqrt{\frac{q}{D}}|x+y|} \right)}{\theta \sqrt{4Dq}}, \quad (4.48)$$

where $\theta = \lambda + \mu$. The Laplace transform of the survival probability is thus

$$\begin{aligned} \hat{S}(q) &= \int_{\Omega} (\hat{p}_1(x, q) + \hat{p}_2(x, q)) dx \\ &= \int_0^{\infty} \left(\frac{1}{\sqrt{4Dq}} e^{-\sqrt{\frac{q}{D}}|x-y|} + \frac{\lambda - \mu}{\theta \sqrt{4Dq}} e^{-\sqrt{\frac{q}{D}}|x+y|} + \frac{2\mu}{\theta \sqrt{4D} \sqrt{q+\theta}} e^{-\sqrt{\frac{q+\theta}{D}}|x+y|} \right) dx, \\ &= \frac{1}{q} - \frac{\mu}{\lambda + \mu} \frac{e^{-y \frac{\sqrt{q}}{\sqrt{D}}}}{q} + \frac{\mu}{\lambda + \mu} \frac{e^{-y \frac{\sqrt{q+\theta}}{\sqrt{D}}}}{q + \theta}. \end{aligned} \quad (4.49)$$

The expansion in large q gives us the asymptotic expression

$$\hat{S}(q) \approx \frac{1}{q} - \mu \frac{e^{-y \frac{\sqrt{q}}{\sqrt{D}}}}{q} \left(\frac{1}{q} + \frac{y}{\sqrt{4Dq}} \right) + \frac{\mu \theta}{8Dq^3} e^{-y \frac{\sqrt{q}}{\sqrt{D}}} \left(qy^2 + D \left(8 + 5\sqrt{\frac{q}{D}}y \right) \right). \quad (4.50)$$

Applying then the inverse Laplace transform, we obtain

$$S(t) \approx 1 - \mu t \text{erfc} \left(\frac{y}{\sqrt{4Dt}} \right) \sim 1 - \mu t \frac{e^{-\frac{y^2}{4Dt}} \sqrt{4Dt}}{y \sqrt{\pi}}. \quad (4.51)$$

Considering the second order term in the expansion, we obtain

$$S(t) \sim 1 - \mu t \left(1 - \frac{(\lambda + \mu)}{2} t \right) \frac{e^{-\frac{y^2}{4Dt}} \sqrt{4Dt}}{y \sqrt{\pi}}. \quad (4.52)$$

Thus, using the asymptotic computation for the MFAT [71], we obtain

$$\bar{\tau}^N \sim \int_0^{\infty} \exp \left\{ \ln \left\{ 1 - \mu t e^{-\frac{y^2}{4Dt}} \frac{\sqrt{4Dt}}{y \sqrt{\pi}} \right\}^N \right\} dt \sim \frac{y^2}{4D \ln \left(\frac{N}{\sqrt{\pi}} \mu \frac{y^2}{4D} \right)}. \quad (4.53)$$

To conclude, this result shows that the fastest particle switches only once before it escapes.

Particles start in state 2 with $D_1 \neq D_2$

We derived in the Appendix 4.7.2 the general solution for equation (4.46) with boundary conditions (4.4) when the two diffusion coefficients are different and strictly positives. We use this solution to compute the survival probability by expanding in large q , so that when $D_2 > D_1$ we obtain

$$\hat{S}(q) \sim \frac{1}{q} - \frac{D_2 \mu}{D_2 - D_1} \frac{\exp \left\{ -\sqrt{\frac{q}{D_2}} y \right\}}{q^2}. \quad (4.54)$$

This leads to the asymptotic formula for N large

$$\bar{\tau}^N \sim \int_0^\infty \exp \left\{ \ln \left\{ 1 - \mu t \frac{e^{-\frac{y^2}{4D_2 t}} \sqrt{4D_2 t}}{y \sqrt{\pi}} \right\}^N \right\} dt \sim \frac{y^2}{4D_2 \ln \left(\frac{N}{\sqrt{\pi}} \mu \frac{y^2}{4D_2} \right)}. \quad (4.55)$$

This result shows that the fastest particle diffuses in state 2 until it reaches the target and then switches back to state 1 before escaping. This optimal strategy followed by the fastest particle is schematically represented in Fig. 4.3C. Following the restriction (4.31), the regime where this asymptotic result holds is given by

$$\frac{1}{\lambda} \ll \frac{y^2}{4D_2 \ln \left(\frac{N}{\sqrt{\pi}} \mu \frac{y^2}{4D_2} \right)} \ll \frac{1}{\mu}. \quad (4.56)$$

When $D_1 > D_2$, we have asymptotic expansion in large q for the Laplace transform of the survival probability given by

$$\hat{S}(q) \sim \frac{1}{q} - \frac{D_1 \mu}{D_1 - D_2} \frac{\exp \left\{ -\sqrt{\frac{q}{D_1}} y \right\}}{q^2}, \quad (4.57)$$

which leads to the asymptotic formula for large N

$$\bar{\tau}^N \sim \int_0^\infty \exp \left\{ \ln \left\{ 1 - \mu t \frac{e^{-\frac{y^2}{4D_1 t}} \sqrt{4D_1 t}}{y \sqrt{\pi}} \right\}^N \right\} dt \sim \frac{y^2}{4D_1 \ln \left(\frac{N}{\sqrt{\pi}} \mu \frac{y^2}{4D_1} \right)}. \quad (4.58)$$

This formula reveals that in this case, the fastest particle switches from the beginning to state 1 and then diffuses with the biggest coefficient to arrive at the absorbing boundary, as shown by Fig. 4.3D. The regime where the asymptotic formula holds is given following (4.31) as

$$\frac{1}{\mu} \ll \frac{y^2}{4D_1 \ln \left(\frac{N}{\sqrt{\pi}} \mu \frac{y^2}{4D_1} \right)} \ll \frac{1}{\lambda}. \quad (4.59)$$

To conclude this section, our results reveal how the diffusion coefficients play a role in the order of the 2 possible actions to be done by the fastest particle (switching and diffusion). The limit case, when D_1 and D_2 are close, is presented in the Appendix 4.7.2 showing the same dependency for the decay $\left(\frac{1}{\ln(N)} \right)$ in the asymptotic formula.

4.4 Particles are initially uniformly distributed in an interval

We now consider the system (4.3) in the domain $\Omega = [0, +\infty)$ with the boundary condition (4.4), and a uniform initial distribution in the interval $[0, y_0]$. When particles start in state 1, the initial condition is given by

$$\begin{aligned} p_1(x, 0) &= \frac{1}{y_0} \mathbb{I}_{\{x \in [0, y_0]\}} \\ p_2(x, 0) &= 0, \end{aligned} \quad (4.60)$$

and when the particles start in state 2 we have the initial condition given by

$$\begin{aligned} p_1(x, 0) &= 0 \\ p_2(x, 0) &= \frac{1}{y_0} \mathbb{I}_{\{x \in [0, y_0]\}}. \end{aligned} \quad (4.61)$$

4.4.1 Particles start in state 1

Applying the Laplace transform to the system (4.3) with the initial condition (4.60) we obtain the ordinary differential equation

$$\left[\frac{\partial^4}{\partial x^4} - \left(\frac{\lambda + q}{D_1} + \frac{\mu + q}{D_2} \right) \frac{\partial^2}{\partial x^2} + \left(\frac{(\lambda + q)(\mu + q) - \lambda\mu}{D_1 D_2} \right) \right] \hat{p}_2(x, q) = \frac{\lambda \mathbb{I}_{\{x \in [0, y_0]\}}}{y_0 D_1 D_2}. \quad (4.62)$$

This equation has same homogeneous part as equation (4.32) but with an indicator function as a non-homogeneous term. The solution of this equation is obtained by the convolution between the non-homogeneous function and the solution obtained with the Dirac delta function. Then, the Laplace transform of the survival probability in this case is also the convolution between the Laplace transform of the survival probability for the Dirac delta initial condition and the uniform distribution. When $D_1 = D_2 = D$, from the expansion in large q (4.36), we obtain the approximation for the Laplace transform of the survival probability

$$\hat{S}(q) \approx \frac{1}{y_0} \int_0^{y_0} \left(\frac{1}{q} - \frac{e^{-y\sqrt{\frac{q}{D}}}}{q} \right) dy \sim \frac{1}{q} - \frac{\sqrt{D}}{y_0 q^{\frac{3}{2}}}. \quad (4.63)$$

The inverse Laplace transform leads to the short-time asymptotic,

$$S(t) \sim 1 - \frac{\sqrt{4Dt}}{y_0 \sqrt{\pi}}, \quad (4.64)$$

and

$$\bar{\tau}^N = \int_0^\infty [S(t)]^N dt \sim \int_0^\infty \exp \left\{ \ln \left\{ 1 - \frac{\sqrt{4Dt}}{y_0 \sqrt{\pi}} \right\}^N \right\} dt \sim \frac{y_0^2 \pi}{2DN^2}. \quad (4.65)$$

When $D_1 \neq D_2$, we obtain the asymptotic expansion in large q for the Laplace transform of the survival probability

$$\hat{S}(q) \approx \frac{1}{q} - \frac{\sqrt{D_1}}{y_0 q^{\frac{3}{2}}} - \frac{\lambda\mu D_2^3}{(D_2 - D_1)^3} \frac{\sqrt{D_2}}{y_0 q^{\frac{7}{2}}}. \quad (4.66)$$

Since the leading order terms are not given anymore by exponential terms, then the approximation for the survival probability is given by

$$S(t) \sim 1 - \frac{\sqrt{4D_1 t}}{y_0 \sqrt{\pi}}, \quad (4.67)$$

and the asymptotic formula for the MFAT

$$\bar{\tau}^N = \int_0^\infty [S(t)]^N dt \sim \int_0^\infty \exp \left\{ \ln \left\{ 1 - \frac{\sqrt{4D_1 t}}{y_0 \sqrt{\pi}} \right\}^N \right\} dt \sim \frac{y_0^2 \pi}{2D_1 N^2}. \quad (4.68)$$

The fact that in this case the fastest particle does not switch is given by the initial distribution of the particles. In this case, for N large is always possible to find a particle that at the beginning is very close to the target, and then, the fastest particle does not need to switch states to escape faster.

4.4.2 Particles start in state 2

We have derived in the Appendix 4.7.3 the computations in order to find the Laplace transform of the survival probability for the system (4.3) with the initial condition (4.61). When $D_1 = D_2$, the expansion in large q for the Laplace transform of the survival probability is given by the formula

$$\hat{S}(q) \approx \frac{1}{y_0} \int_0^{y_0} \left(\frac{1}{q} - \frac{\mu e^{-y\sqrt{\frac{q}{D}}}}{q} \left(\frac{1}{q} + \frac{y}{\sqrt{4Dq}} \right) \right) dy \sim \frac{1}{q} - \frac{3\mu\sqrt{D}}{2y_0 q^{\frac{5}{2}}}. \quad (4.69)$$

Thus, we obtain, up to leading order the formula

$$\bar{\tau}^N \sim \int_0^\infty \exp \left\{ \ln \left\{ 1 - \frac{\mu t \sqrt{4D_1 t}}{y_0 \sqrt{\pi}} \right\}^N \right\} dt \sim \left(\frac{\sqrt{\pi} y_0}{\mu \sqrt{4DN}} \right)^{\frac{2}{3}} \Gamma \left(\frac{5}{3} \right), \quad (4.70)$$

where $\Gamma(x)$ is the Gamma function.

When $D_1 \neq D_2$, we have the asymptotic expansion in large q for the survival probability given by

$$\hat{S}(q) \approx \frac{1}{q} - \frac{\mu D_2^{\frac{3}{2}}}{y_0(D_2 - D_1)q^{\frac{5}{2}}} + \frac{\mu D_1^{\frac{3}{2}}}{y_0(D_2 - D_1)q^{\frac{5}{2}}}. \quad (4.71)$$

When $D_1 > D_2$ we have the approximation

$$\hat{S}(q) \sim \frac{1}{q} - \frac{3\mu D_1^{\frac{1}{2}}}{2y_0 q^{\frac{5}{2}}}, \quad (4.72)$$

leading to the asymptotic formula for N large

$$\bar{\tau}^N \sim \left(\frac{\sqrt{\pi} y_0}{\mu \sqrt{4D_1 N}} \right)^{\frac{2}{3}} \Gamma \left(\frac{5}{3} \right). \quad (4.73)$$

When $D_2 > D_1$ we have the approximation

$$\hat{S}(q) \sim \frac{1}{q} - \frac{3\mu D_2^{\frac{1}{2}}}{2y_0 q^{\frac{5}{2}}}, \quad (4.74)$$

leading to the asymptotic formula

$$\bar{\tau}^N \sim \left(\frac{\sqrt{\pi} y_0}{\mu \sqrt{4D_2 N}} \right)^{\frac{2}{3}} \Gamma \left(\frac{5}{3} \right). \quad (4.75)$$

With this initial condition, the fastest particles switch and diffuse depending only on the diffusion coefficients: when $D_1 > D_2$ the fastest particle switches first and diffuses to the target, but if $D_2 > D_1$ it diffuses first to the target and then switches back to the state 1 before escape.

4.4.3 Particles start in state 1 uniformly distributed in $[y_1, y_2]$ with $y_1 > 0$

For an initial condition given by $p_1(x, 0) = \frac{1}{y_2 - y_1} \mathbb{I}_{\{x \in [y_1, y_2]\}}$ with $y_1 > 0$, particles start in state 1 uniformly distributed in $[y_1, y_2]$. We apply the Laplace transform to the system (4.3) and obtain the ordinary differential equation with the same homogeneous part as in (4.46) but with the indicator function for this interval as non-homogeneous term. We derived in the Appendix 4.7.3 the computations to find the survival probability, given by the convolution between the solution for the Dirac delta case starting in state 2 and the uniform distribution in $[y_1, y_2]$. An asymptotic expansion in large q , when $D_1 > D_2$ gives the approximation

$$\hat{S}(q) \sim \frac{1}{q} - \frac{D_1^{\frac{1}{2}}}{(y_2 - y_1)q^{\frac{3}{2}}} \exp \left\{ -\sqrt{\frac{q}{D_1}} y_1 \right\}. \quad (4.76)$$

To leading order we obtain the asymptotic formula for N large

$$\bar{\tau}^N \sim \int_0^\infty \exp \left\{ \ln \left\{ 1 - \frac{(\sqrt{4D_1 t})^3}{2\sqrt{\pi}(y_2 - y_1)y_1^2} e^{-\frac{y_1^2}{4D_1 t}} \right\}^N \right\} dt \sim \frac{y_1^2}{4D_1 \ln \left(\frac{Ny_1}{2\sqrt{\pi}(y_2 - y_1)} \right)}. \quad (4.77)$$

When $D_2 > D_1$ we obtain the approximation

$$\hat{S}(q) \sim \frac{1}{q} - \frac{D_2^{\frac{3}{2}} \lambda \mu}{(y_2 - y_1)q^{\frac{7}{2}}} \exp \left\{ -\sqrt{\frac{q}{D_2}} y_1 \right\}. \quad (4.78)$$

To leading order we obtain the asymptotic formula when N is large

$$\bar{\tau}^N \sim \frac{y_1^2}{4D_2 \ln \left(\frac{N\lambda\mu D_2}{15\sqrt{\pi} \left(\frac{y_2 - y_1}{y_1} \right)} \left(\frac{y_1^2}{4D_2} \right)^2 \right)}. \quad (4.79)$$

To conclude, when the fastest particle starts in the state 1, if $D_1 > D_2$, the particle will not switch but diffuse to the target. On the contrary, if $D_2 > D_1$, the particle switches to state 2, diffuses to the target and then switches back again in order to escape.

4.4.4 Particles start in state 2 uniformly distributed in $[y_1, y_2]$

In the case where the particles follows the initial condition $p_2(x, 0) = \frac{1}{y_2 - y_1} \mathbb{I}_{\{x \in [y_1, y_2]\}}$ with $y_1 > 0$, which means that the particles start in state 2, uniformly distributed in $[y_1, y_2]$, we have from Appendix 4.7.3 that the asymptotic expansion in large q for the Laplace transform of the survival probability given by

$$\begin{aligned} \hat{S}(q) &= \frac{1}{q} - \frac{\mu D_2^{\frac{3}{2}}}{(y_2 - y_1)(D_2 - D_1)q^{\frac{5}{2}}} \left(\exp \left\{ -\sqrt{\frac{q}{D_2}} y_1 \right\} - \exp \left\{ -\sqrt{\frac{q}{D_2}} y_2 \right\} \right) \\ &\quad + \frac{\mu D_1^{\frac{3}{2}}}{(y_2 - y_1)(D_2 - D_1)q^{\frac{5}{2}}} \left(\exp \left\{ -\sqrt{\frac{q}{D_1}} y_1 \right\} - \exp \left\{ -\sqrt{\frac{q}{D_1}} y_2 \right\} \right). \end{aligned} \quad (4.80)$$

When $D_1 > D_2$ we have the approximation

$$\hat{S}(q) \sim \frac{1}{q} - \frac{\mu D_1^{\frac{1}{2}}}{(y_2 - y_1)q^{\frac{5}{2}}} \exp \left\{ -\sqrt{\frac{q}{D_1}} y_1 \right\}. \quad (4.81)$$

This leads to the asymptotic formula

$$\bar{\tau}^N \sim \int_0^\infty \exp \left\{ \ln \left\{ 1 - \frac{\mu \sqrt{4D_1} t e^{-\frac{y_1^2}{4D_1 t}}}{3\sqrt{\pi} (y_2 - y_1)} \right\}^N \right\} dt \sim \frac{y_1^2}{4D_1 \ln \left(\frac{N\mu}{3\sqrt{\pi} \left(\frac{y_2 - y_1}{y_1} \right)} \left(\frac{y_1^2}{4D_1} \right) \right)}. \quad (4.82)$$

This means that the fastest particle first switches to state 1 and diffuses in this state until it reaches the target.

When $D_2 > D_1$ we have the approximation

$$\hat{S}(q) \sim \frac{1}{q} - \frac{\mu D_2^{\frac{1}{2}}}{(y_2 - y_1) q^{\frac{5}{2}}} \exp \left\{ -\sqrt{\frac{q}{D_2}} y_1 \right\}. \quad (4.83)$$

This leads to the asymptotic formula

$$\bar{\tau}^N \sim \int_0^\infty \exp \left\{ \ln \left\{ 1 - \frac{\mu \sqrt{4D_2} t e^{-\frac{y_1^2}{4D_2 t}}}{3\sqrt{\pi} (y_2 - y_1)} \right\}^N \right\} dt \sim \frac{y_1^2}{4D_2 \ln \left(\frac{N\mu}{3\sqrt{\pi} \left(\frac{y_2 - y_1}{y_1} \right)} \left(\frac{y_1^2}{4D_2} \right) \right)}. \quad (4.84)$$

In this case, since $D_2 > D_1$, the fastest particle diffuses to the target and then it switches to state 1 to escape.

4.5 Initial distribution with a long tail

4.5.1 Particles start in state 1

We shall study the MFAT when the initial distribution of particles is given by

$$\begin{aligned} p_1(x, 0) &= \frac{2b^{\frac{1+\alpha}{2}}}{\Gamma(\frac{1+\alpha}{2})} x^\alpha \exp \{-bx^2\} \\ p_2(x, 0) &= 0. \end{aligned} \quad (4.85)$$

For this new initial condition, we can find the solution as the convolution between this initial distribution and the solution for the Dirac delta case starting in state 1. Then, the Laplace transform of the survival probability is given by the formula

$$\begin{aligned} \hat{S}(q) &= \frac{2b^{\frac{1+\alpha}{2}}}{\Gamma(\frac{1+\alpha}{2})} \int_0^\infty \left[\frac{1}{q} + \frac{(\mu + q - D_2 w_+^2)e^{w+y}}{D_1 D_2 w_+^2 (w_+^2 - w_-^2)} - \frac{(\mu + q - D_2 w_-^2)e^{w-y}}{D_1 D_2 w_-^2 (w_+^2 - w_-^2)} \right] y^\alpha \exp \{-by^2\} dy \\ &= \frac{1}{q} - \frac{\Gamma(1+\alpha)(\mu + q - D_2 w_+^2)}{\Gamma(\frac{1+\alpha}{2}) 2^{1+\alpha} b^{\frac{1}{2}} D_1 D_2 w_+ (w_+^2 - w_-^2)} U \left(1 + \frac{\alpha}{2}, \frac{3}{2}, \frac{w_+^2}{4b} \right) \\ &\quad + \frac{\Gamma(1+\alpha)(\mu + q - D_2 w_-^2)}{\Gamma(\frac{1+\alpha}{2}) 2^{1+\alpha} b^{\frac{1}{2}} D_1 D_2 w_- (w_+^2 - w_-^2)} U \left(1 + \frac{\alpha}{2}, \frac{3}{2}, \frac{w_-^2}{4b} \right), \end{aligned} \quad (4.86)$$

where, $U(a, b, z)$ is the confluent hypergeometric function, w_+ and w_- are given by the formula (4.101). Using the large q expansion of the survival probability given by formula (4.86), we obtain

$$\hat{S}(q) \approx \frac{1}{q} - \frac{\Gamma(1+\alpha) 2b^{\frac{\alpha+1}{2}}}{\Gamma(\frac{1+\alpha}{2})} \left[\frac{D_1^{\frac{1+\alpha}{2}}}{q^{\frac{3+\alpha}{2}}} + \frac{\lambda \mu D_2^{\frac{1+\alpha}{2}}}{q^{\frac{7+\alpha}{2}}} \right]. \quad (4.87)$$

In both cases, when $D_1 > D_2$ or $D_2 > D_1$, we obtain the leading order approximation

$$\hat{S}(q) \sim \frac{1}{q} - \frac{2b^{\frac{\alpha+1}{2}}\Gamma(1+\alpha)D_1^{\frac{1+\alpha}{2}}}{\Gamma(\frac{1+\alpha}{2})q^{\frac{3+\alpha}{2}}}. \quad (4.88)$$

Thus the inverse Laplace transform leads to

$$S(t) \sim 1 - \frac{2b^{\frac{\alpha+1}{2}}\Gamma(1+\alpha)D_1^{\frac{1+\alpha}{2}}}{\Gamma(\frac{1+\alpha}{2})\Gamma(\frac{3+\alpha}{2})}t^{\frac{1+\alpha}{2}}. \quad (4.89)$$

Following the steps described in the previous section, we obtain that the mean arrival time for the fastest particle is given by

$$\begin{aligned} \bar{\tau}^N &= \int_0^\infty [S(t)]^N dt \sim \int_0^\infty \exp \left\{ \ln \left\{ 1 - \frac{2b^{\frac{\alpha+1}{2}}\Gamma(1+\alpha)D_1^{\frac{1+\alpha}{2}}}{\Gamma(\frac{1+\alpha}{2})\Gamma(\frac{3+\alpha}{2})}t^{\frac{1+\alpha}{2}} \right\}^N \right\} dt \\ &\sim \left[\frac{\Gamma(\frac{1+\alpha}{2})\Gamma(\frac{3+\alpha}{2})}{2\Gamma(1+\alpha)} \right]^{\frac{2}{1+\alpha}} \frac{\Gamma(\frac{\alpha+3}{\alpha+1})}{bD_1} \frac{1}{N^{\frac{2}{1+\alpha}}}. \end{aligned} \quad (4.90)$$

This means that the fastest particle never switches to state 2, even when $D_2 > D_1$. This is due to the initial distribution of the particles. As in the case where the particles were initially distributed in $[0, y_0]$, it is always possible to find a particle very close to the absorbing boundary that only needs to escape.

4.5.2 Particles start in state 2

When the particles are initially distributed in state 2 according to

$$\begin{aligned} p_1(x, 0) &= 0 \\ p_2(x, 0) &= \frac{2b^{\frac{1+\alpha}{2}}}{\Gamma(\frac{1+\alpha}{2})}x^\alpha \exp\{-bx^2\}, \end{aligned} \quad (4.91)$$

we have derived the computations to find the survival probability in Appendix 4.7.4. When $D_1 = D_2 = D$, an asymptotic expansion in large q give us the approximation

$$\hat{S}(q) \sim \frac{1}{q} - \frac{(bD)^{\frac{1+\alpha}{2}}\mu(3+\alpha)\Gamma(1+\alpha)}{\Gamma(\frac{1+\alpha}{2})q^{\frac{5+\alpha}{2}}}, \quad (4.92)$$

leading to the short-time asymptotic

$$S(t) \sim 1 - \frac{(bD)^{\frac{1+\alpha}{2}}\mu(3+\alpha)\Gamma(1+\alpha)}{\Gamma(\frac{1+\alpha}{2})\Gamma(\frac{5+\alpha}{2})}t^{\frac{3+\alpha}{2}}, \quad (4.93)$$

and the mean first arrival time

$$\begin{aligned} \bar{\tau}^N &\sim \int_0^\infty \exp \left\{ \ln \left\{ 1 - \frac{(bD)^{\frac{1+\alpha}{2}}\mu(3+\alpha)\Gamma(1+\alpha)}{\Gamma(\frac{1+\alpha}{2})\Gamma(\frac{5+\alpha}{2})}t^{\frac{3+\alpha}{2}} \right\}^N \right\} dt \\ &\sim \left[\frac{\Gamma(\frac{1+\alpha}{2})\Gamma(\frac{5+\alpha}{2})}{\mu(3+\alpha)\Gamma(1+\alpha)N} \right]^{\frac{2}{3+\alpha}} \frac{\Gamma(\frac{5+\alpha}{3+\alpha})}{(bD)^{\frac{1+\alpha}{3+\alpha}}}. \end{aligned} \quad (4.94)$$

This decay for the mean first arrival time of the fastest particle for large N , shows a single switch before escapes. When $D_1 \neq D_2$, we can have the approximation for the survival probability in the large q expansion given by

$$\hat{S}(q) \sim \frac{1}{q} - \frac{2b^{\frac{1+\alpha}{2}}\mu\Gamma(1+\alpha)}{\Gamma(\frac{1+\alpha}{2})(D_2 - D_1)q^{\frac{5+\alpha}{2}}} \left[D_2^{\frac{3+\alpha}{2}} - D_1^{\frac{3+\alpha}{2}} \right]. \quad (4.95)$$

When $D_1 > D_2$, we have then the approximation

$$\hat{S}(q) \sim \frac{1}{q} - \frac{2b^{\frac{1+\alpha}{2}}\mu\Gamma(1+\alpha)}{\Gamma(\frac{1+\alpha}{2})q^{\frac{5+\alpha}{2}}} D_1^{\frac{1+\alpha}{2}}, \quad (4.96)$$

leading to the asymptotic formula

$$\begin{aligned} \bar{\tau}^N &\sim \int_0^\infty \exp \left\{ \ln \left\{ 1 - \frac{2(bD_1)^{\frac{1+\alpha}{2}}\mu\Gamma(1+\alpha)}{\Gamma(\frac{1+\alpha}{2})\Gamma(\frac{5+\alpha}{2})} t^{\frac{3+\alpha}{2}} \right\}^N \right\} dt \\ &\sim \left[\frac{\Gamma(\frac{1+\alpha}{2})\Gamma(\frac{5+\alpha}{2})}{2\mu b^{\frac{1+\alpha}{2}}D_1^{\frac{1+\alpha}{2}}\Gamma(1+\alpha)} \right]^{\frac{2}{3+\alpha}} \frac{\Gamma(\frac{5+\alpha}{3+\alpha})}{N^{\frac{2}{3+\alpha}}}. \end{aligned} \quad (4.97)$$

When $D_2 > D_1$, we have the approximation in large q

$$\hat{S}(q) \sim \frac{1}{q} - \frac{2b^{\frac{1+\alpha}{2}}\mu\Gamma(1+\alpha)}{\Gamma(\frac{1+\alpha}{2})q^{\frac{5+\alpha}{2}}} D_2^{\frac{1+\alpha}{2}}. \quad (4.98)$$

This, leads to

$$\begin{aligned} \bar{\tau}^N &\sim \int_0^\infty \exp \left\{ \ln \left\{ 1 - \frac{2(bD_2)^{\frac{1+\alpha}{2}}\mu\Gamma(1+\alpha)}{\Gamma(\frac{1+\alpha}{2})\Gamma(\frac{5+\alpha}{2})} t^{\frac{3+\alpha}{2}} \right\}^N \right\} dt \\ &\sim \left[\frac{\Gamma(\frac{1+\alpha}{2})\Gamma(\frac{5+\alpha}{2})}{2\mu b^{\frac{1+\alpha}{2}}D_2^{\frac{1+\alpha}{2}}\Gamma(1+\alpha)} \right]^{\frac{2}{3+\alpha}} \frac{\Gamma(\frac{5+\alpha}{3+\alpha})}{N^{\frac{2}{3+\alpha}}}. \end{aligned} \quad (4.99)$$

To conclude, in this case the fastest particle switches to state 1 only once, but depending if $D_1 > D_2$ it switches at the very beginning before diffuses, or in the opposite case, if $D_2 > D_1$ it diffuses and then it switches at the very end once the particle is at the absorbing boundary.

4.6 Discussion and concluding remarks

In the present manuscript, we obtained several asymptotic formulas (4.15, 4.41, 4.44, 4.55, 4.58, 4.53, 4.65, 4.70, 4.90, 4.94) for the mean time of the fastest Brownian particles arriving at the absorbing target. These particles can switch between two states and escape from the non-negative real line only in state 1. Resulting formulas are associated with different initial distributions and whether all the particles start in state 1 or 2. We found a decay in $\frac{1}{\ln N}$ when the initial distribution does not intersect the target location. However, when the initial distribution $p_0(x)$ intersects the absorbing boundary, we obtain an algebraic decay for N , e.g. $\frac{1}{N^\alpha}$, as already suspected from [102].

When the initial distribution of particles is given as Dirac delta function at a given position y in state 1, where escape is possible, the escapes time strategy depends on the diffusion coefficients: when $D_1 > D_2$ the fastest particle does not switch before escaping. However, when $D_2 > D_1$ the fastest particle switches twice. When particles start in state 2, depending on the value for the largest diffusion coefficient, the fastest particles will either switch from the beginning and then diffuses or it can diffuses and then switch near the absorbing target. We remark that the number of switchings is given by the exponent of the factor $\frac{y^2}{4D}$ inside the logarithm of formulas (4.41, 4.44, 4.55, 4.58). These extreme statistics formulas are relevant in the context of fast molecular signaling in cell biology. The activation is a MFAT and depends on the main parameters, involving the geometrical organization of the domain, the initial distribution of the molecules as well as the initial number of them, and the specific dynamics of the particles (diffusion, switching and/or other stochastic dynamics). This approach can be used to compute the time of activation by diffusing molecules crossing a region where switching is possible. Indeed, the behavior of the fastest particle described in this paper can be extended to the case of a finite interval [71]. The analytical computations presented here provide a quantitative description of switching associated to transcription factors (TF) moving in the nucleus cell toward their promoter site. If a large number of switching states are considered, the computations and formulas would rapidly become impractical and unwieldy. However, we believe that the present work could be generalized for the problem in 2d or 3d, but in these domains the size of the target ε becomes a relevant parameter that needs to be integrated in the analytical formulas. For a narrow target, we predict a term of the type $\frac{1}{\ln(\frac{1}{\varepsilon})}$ in the leading order term of the survival probability, as previously derived for the non-switching case in [71]. From the second inequality in general restriction here proposed to model the region of parameters where the asymptotic results holds

$$\bar{\tau}^S \rightarrow f \ll \bar{\tau}^{(N|I_0)} \ll \bar{\tau}^{(I_0|1)}, \quad (4.100)$$

we could always obtain the restriction for N large where the minimal amount of switchings is expected with a large probability.

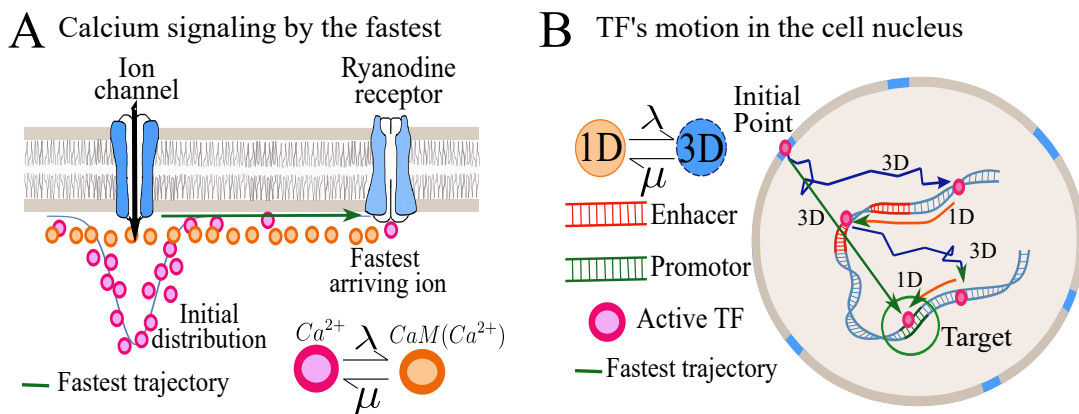


Figure 4.4: **Application of the MFAT.** **A.** Example of Calcium ions entering through a ionic Channel. These ions can switch states between free Ca^{2+} or bound to calmodulin CaM , occurring diffusion. This binding interferes with the fast activation of the Ryanodine receptor [66]. **B.** Example of a TF moving randomly inside a cell nucleus, alternating between 1d and 3d diffusion. The time for the first TF to activate an enhancer falls into the class of MFAT.

Key chemical reactions occurring in cells depend on the arrival of the first molecules to small

targets [69]. This is the case for a large class of agonist molecules arriving to a gated channel [141] located on the cell membrane, triggering signaling cascades [16, 142, 143]. Upon arrival of the first molecules, channels open and thus it is not necessary to track the rest of the agonist population in the process of cellular activation [52, 144]. This shows that the statistics of the fastest arrival time is a key event in revealing the time scale of sub-cellular processes triggered by single channel activation.

In the field of cellular signaling transduction, the time of the first signaling protein to reach a target in various states of phosphorylation and location (inside the cytoplasm or the nucleus) can be used to characterize the response of the reaction network [120].

Distinguishing between single- and multi-state dynamics at molecular level remains difficult [145], there are ubiquitous examples where particles such as molecules and *TF* have to switch between different states before reaching a small target site [52]. For example, when particles are injected slowly in a domain, an extended initial distribution can build up, leading to a long-tail distribution. This distribution could be approximated by a Gaussian or any other related distribution with even an algebraic decay, especially when the motion can be modeled as anomalous diffusion [146]. To cover this case, we studied here different initial distributions such as the exponential families. For example, calcium ions enter in less than a few milliseconds inside a dendrite or neuronal synapses through few channels located on the membrane, as shown in Fig. 4.4A. When channels are closed again, the calcium concentration has already spread over the entire domain. These calcium ions can also change their state due to possible chemical reactions. One classical example is the interaction between calcium ions and calmodulin molecules *CaM* [147]. Calcium signaling in dendritic spines, is often mediated by the fastest arriving calcium ion to Ryanodine receptors. During this fast process, the fastest calcium ions do not bind to a *CaM* molecule, as it would lead to a much longer arrival time compared to the one observed experimentally [40]. This result can be explained by the present theory, showing that the fast particle does not switch to a state were it diffuses slower. Another example is the case of a *TF*, the motion of which can be described as Brownian inside the nucleus. The *TFs* can alternate motion between a 1D sliding along the DNA and a 3D motion inside the nucleus (Fig. 4.4B), with diffusion coefficients $D_1 \neq D_2$ and switching at Poissonian rates λ and μ . Although a lot of the literature was dedicated to the case of a single *TF* [148], it is possible that the fastest *TF* arrives to the promoter site directly without switching, a scenario that should be further studied.

4.7 Appendix

In this appendix, we summarized the main computations involving the Laplace transform of the survival probability taking into account the different initial conditions (spatial and state). We also added numerical simulations that emphasize a deviation with the asymptotic formulas for the Dirac delta initial condition, under some specific values of the parameters.

4.7.1 Survival probability for particles starting at position $y > 0$ in state 1 with $D_1 \neq D_2$

In the general case, when $D_1 \neq D_2$ and both are strictly positive, we can derive from system (4.7) the differential equation of order 4

$$\left[\frac{\partial^4}{\partial x^4} - \left(\frac{\lambda+q}{D_1} + \frac{\mu+q}{D_2} \right) \frac{\partial^2}{\partial x^2} + \left(\frac{(\lambda+q)(\mu+q) - \lambda\mu}{D_1 D_2} \right) \right] \hat{p}_2(x, q) = \frac{\lambda}{D_1 D_2} \delta_y.$$

We are going to solve these equation with the boundary conditions (4.4) and the initial condition given for $p_2(x, q)$ in (4.5). Using the ensemble of smooth compact support $f(x)$ in \mathbb{R} such that

$$\frac{\partial^4 \varphi}{\partial x^4}(x) - a \frac{\partial^2 \varphi}{\partial x^2}(x) + b\varphi(x) = f(x),$$

we shall compute $\int_{\mathbb{R}} G(x)f(x)dx$, where $G(x)$ is the solution of the homogeneous equation and $a = \frac{\lambda+q}{D_1} + \frac{\mu+q}{D_2}$ and $b = \frac{(\lambda+q)(\mu+q) - \lambda\mu}{D_1 D_2}$. Integrating by parts and using the fact that the derivatives of $G(x)$ until order 2 are continuous in \mathbb{R} , we get

$$\begin{aligned} \int_{\mathbb{R}} G(x)f(x)dx &= \int_{\mathbb{R}} G(x) \left(\frac{\partial^4 \varphi}{\partial x^4}(x) - a \frac{\partial^2 \varphi}{\partial x^2}(x) + b\varphi(x) \right) dx = \varphi(y) \left(\frac{d^3 G_+}{dx^3}(y) - \frac{d^3 G_-}{dx^3}(y) \right) \\ &= \varphi(y)(2Aw_1^3 + 2Bw_+^3 + 2Cw_3^3 + 2Dw_-^3). \end{aligned}$$

If we choose A, B, C and D such that $2Aw_1^3 + 2Bw_+^3 + 2Cw_3^3 + 2Dw_-^3 = \frac{\lambda}{D_1 D_2}$, we get

$$\begin{aligned} \int_{\mathbb{R}} G(x)f(x)dx &= \langle G(x), \frac{\partial^4 \varphi}{\partial x^4}(x) - a \frac{\partial^2 \varphi}{\partial x^2}(x) + b\varphi(x) \rangle = \langle \frac{\partial^4 G}{\partial x^4}(x) - a \frac{\partial^2 G}{\partial x^2}(x) + bG(x), \varphi(x) \rangle \\ &= \frac{\lambda}{D_1 D_2} \varphi(y) = \langle \frac{\lambda}{D_1 D_2} \delta(x-y), \varphi(x) \rangle. \end{aligned}$$

Then,

$$\frac{\partial^4 G}{\partial x^4}(x) - a \frac{\partial^2 G}{\partial x^2}(x) + bG(x) = \frac{\lambda}{D_1 D_2} \delta(x-y).$$

Using the previous condition for $G(x)$ be a solution in the sense of Distributions

$$2Aw_1^3 + 2Bw_+^3 + 2Cw_3^3 + 2Dw_-^3 = \frac{\lambda}{D_1 D_2},$$

and the condition coming from the fact that all derivatives until order 2 are continuous

$$2Aw_1 + 2Bw_+ + 2Cw_3 + 2Dw_- = 0,$$

we can write the solution under the following form

$$\begin{aligned} G(x, q) &= - \left(\frac{Bw_+ + Cw_3 + Dw_-}{w_1} \right) e^{w_1|x-y|} + Be^{w_+|x-y|} \\ &\quad + \left(\frac{\lambda}{2D_1 D_2 w_3 (w_3^2 - w_1^2)} - \frac{2Bw_+(w_+^2 - w_1^2)}{2w_3(w_3^2 - w_1^2)} - \frac{2Dw_-(w_-^2 - w_1^2)}{2w_3(w_3^2 - w_1^2)} \right) e^{w_3|x-y|} \\ &\quad + De^{-|x-y|}. \end{aligned}$$

Since the solution is bounded, we obtain that $A = C = 0$, and this leads to

$$B = \frac{\lambda}{2D_1 D_2 w_+ (w_+^2 - w_-^2)}, \quad D = \frac{\lambda}{2D_1 D_2 w_- (w_-^2 - w_+^2)},$$

and the solution is

$$\hat{p}_2(x, q) = \frac{\lambda}{2D_1 D_2 w_+ (w_+^2 - w_-^2)} e^{w_+ |x-y|} + \frac{\lambda}{2D_1 D_2 w_- (w_-^2 - w_+^2)} e^{w_- |x-y|}.$$

Finally, the boundary conditions leads to

$$\begin{aligned} \hat{p}_2(x, q) &= \frac{\lambda}{2D_1 D_2 w_+ (w_+^2 - w_-^2)} (e^{w_+ |x-y|} + e^{w_+ |x+y|}) \\ &\quad + \frac{\lambda}{2D_1 D_2 w_- (w_-^2 - w_+^2)} (e^{w_- |x-y|} + e^{w_- |x+y|}). \end{aligned}$$

Using the relation between $p_1(x, q)$ and $p_2(x, q)$ given in (4.7), we find that

$$\hat{p}_1(x, q) = \frac{(\mu + q - D_2 w_+^2)}{2D_1 D_2 w_+ (w_+^2 - w_-^2)} e^{w_+ |x-y|} + \frac{(\mu + q - D_2 w_-^2)}{2D_1 D_2 w_- (w_-^2 - w_+^2)} e^{w_- |x-y|},$$

and using the boundary conditions $\hat{p}_1(0, q) = 0$, we get

$$\begin{aligned} \hat{p}_1(x, q) &= \frac{(\mu + q - D_2 w_+^2)}{2D_1 D_2 w_+ (w_+^2 - w_-^2)} (e^{w_+ |x-y|} - e^{w_+ |x+y|}) \\ &\quad + \frac{(\mu + q - D_2 w_-^2)}{2D_1 D_2 w_- (w_-^2 - w_+^2)} (e^{w_- |x-y|} - e^{w_- |x+y|}), \end{aligned}$$

where

$$w_{\pm} = \frac{\sqrt{\frac{\lambda+q}{D_1} + \frac{\mu+q}{D_2}} \pm \sqrt{q^2 \left(\frac{1}{D_1} - \frac{1}{D_2}\right)^2 + 2q \left(\frac{1}{D_1} - \frac{1}{D_2}\right) \left(\frac{\lambda}{D_1} - \frac{\mu}{D_2}\right) + \left(\frac{\lambda}{D_1} + \frac{\mu}{D_2}\right)^2}}{-\sqrt{2}}. \quad (4.101)$$

To compute the Laplace transform of the survival probability, we start with

$$\begin{aligned} \hat{S}(q) &= \int_0^\infty (\hat{p}_1(x, q) + \hat{p}_2(x, q)) dx \\ &= \frac{(\mu + q - D_2 w_+^2)}{2D_1 D_2 w_+ (w_+^2 - w_-^2)} \int_0^\infty (e^{w_+ |x-y|} - e^{w_+ |x+y|}) dx \\ &\quad + \frac{(\mu + q - D_2 w_-^2)}{2D_1 D_2 w_- (w_-^2 - w_+^2)} \int_0^\infty (e^{w_- |x-y|} - e^{w_- |x+y|}) dx \\ &\quad + \frac{\lambda}{2D_1 D_2 w_+ (w_+^2 - w_-^2)} \int_0^\infty (e^{w_+ |x-y|} + e^{w_+ |x+y|}) dx \\ &\quad + \frac{\lambda}{2D_1 D_2 w_- (w_-^2 - w_+^2)} \int_0^\infty (e^{w_- |x-y|} + e^{w_- |x+y|}) dx \\ &= -\frac{(\mu + q - D_2 w_+^2)}{D_1 D_2 w_+^2 (w_+^2 - w_-^2)} (1 - e^{w_+ y}) - \frac{(\mu + q - D_2 w_-^2)}{D_1 D_2 w_-^2 (w_-^2 - w_+^2)} (1 - e^{w_- y}) \\ &\quad - \frac{\lambda}{D_1 D_2 w_+^2 (w_+^2 - w_-^2)} - \frac{\lambda}{D_1 D_2 w_-^2 (w_-^2 - w_+^2)} \\ &= \frac{1}{q} + T_1(q) + T_2(q), \end{aligned}$$

where w_+ and w_- are given by formula (4.101) and using

$$T_1(q) = \frac{\mu + q - D_2 w_+^2}{D_1 D_2 w_+^2 (w_+^2 - w_-^2)} e^{w_+ y}, \quad T_2(q) = -\frac{\mu + q - D_2 w_-^2}{D_1 D_2 w_-^2 (w_+^2 - w_-^2)} e^{w_- y}.$$

Using the notations $\alpha = \frac{\lambda}{D_1} + \frac{\mu}{D_2}$, $\beta = \frac{1}{D_1} - \frac{1}{D_2}$, $\gamma = \frac{\lambda}{D_1} - \frac{\mu}{D_2}$ and $\eta = \frac{1}{D_1} + \frac{1}{D_2}$, we can rewrite $T_1(q)$ and $T_2(q)$ as

$$\begin{aligned} T_1(q) &= \exp \left\{ -\sqrt{\frac{\alpha + \eta q + \sqrt{\beta^2 q^2 + 2\beta\gamma q + \alpha^2}}{2}} y \right. \\ &\quad + \ln \left(2q + 2\mu - D_2 \left(\alpha + \eta q + \sqrt{\beta^2 q^2 + 2\beta\gamma q + \alpha^2} \right) \right) \\ &\quad \left. - \ln \left(D_1 D_2 \left(\alpha + \eta q + \sqrt{\beta^2 q^2 + 2\beta\gamma q + \alpha^2} \right) \sqrt{\beta^2 q^2 + 2\beta\gamma q + \alpha^2} \right) \right\}, \\ T_2(q) &= -\exp \left\{ -\sqrt{\frac{\alpha + \eta q - \sqrt{\beta^2 q^2 + 2\beta\gamma q + \alpha^2}}{2}} y \right. \\ &\quad + \ln \left(2q + 2\mu - D_2 \left(\alpha + \eta q - \sqrt{\beta^2 q^2 + 2\beta\gamma q + \alpha^2} \right) \right) \\ &\quad \left. - \ln \left(D_1 D_2 \left(\alpha + \eta q - \sqrt{\beta^2 q^2 + 2\beta\gamma q + \alpha^2} \right) \sqrt{\beta^2 q^2 + 2\beta\gamma q + \alpha^2} \right) \right\}. \end{aligned}$$

Expanding $T_1(q)$ and $T_2(q)$ for q large, we have the approximation for the survival probability

$$\hat{S}(q) \sim \frac{1}{q} - \frac{e^{-y\sqrt{\frac{q}{D_1}}}}{q} - \frac{\lambda\mu D_2^3}{(D_2 - D_1)^2} \frac{e^{-y\sqrt{\frac{q}{D_2}}}}{q^3}.$$

4.7.2 Particles start in state 2 with $D_1 \neq D_2$

] When the particles start in state 2 at position $y > 0$ we have the Laplace transform of the Kolmogorov master system (4.3) given by the ordinary differential equation (4.46)

$$\frac{\partial^4 \hat{p}_1}{\partial x^4}(x, q) - \left[\frac{q + \lambda}{D_1} + \frac{q + \mu}{D_2} \right] \frac{\partial^2 \hat{p}_1}{\partial x^2}(x, q) + \left[\frac{(q + \lambda)(q + \mu) - \lambda\mu}{D_1 D_2} \right] \hat{p}_1(x, q) = \frac{\mu}{D_1 D_2} \delta_y,$$

and this leads to a solution under the form

$$\hat{p}_1(x, q) = \frac{\mu}{2D_1 D_2 w_+(w_+^2 - w_-^2)} e^{w_+|x-y|} + \frac{\mu}{2D_1 D_2 w_-(w_-^2 - w_+^2)} e^{w_-|x-y|},$$

as in the above computations. Finally, the boundary conditions impose that

$$\hat{p}_1(x, q) = \frac{\mu}{2D_1 D_2 w_+(w_+^2 - w_-^2)} (e^{w_+|x-y|} - e^{w_+|x+y|}) + \frac{\mu}{2D_1 D_2 w_-(w_-^2 - w_+^2)} (e^{w_-|x-y|} - e^{w_-|x+y|}).$$

Then, we obtain

$$\hat{p}_2(x, q) = \frac{(\lambda + q - D_1 w_+^2)}{2D_1 D_2 w_+(w_+^2 - w_-^2)} e^{w_+|x-y|} + \frac{(\lambda + q - D_1 w_-^2)}{2D_1 D_2 w_-(w_-^2 - w_+^2)} e^{w_-|x-y|},$$

and from the boundary condition, $\frac{\partial \hat{p}_2}{\partial x}(0, q) = 0$, we get

$$\hat{p}_2(x, q) = \frac{(\lambda + q - D_1 w_+^2)}{2D_1 D_2 w_+(w_+^2 - w_-^2)} (e^{w_+|x-y|} + e^{w_+|x+y|}) + \frac{(\lambda + q - D_1 w_-^2)}{2D_1 D_2 w_-(w_-^2 - w_+^2)} (e^{w_-|x-y|} + e^{w_-|x+y|}).$$

The Laplace transform of the survival probability leads to

$$\begin{aligned} \hat{S}(q) &= \int_0^\infty (\hat{p}_1(x, q) + \hat{p}_2(x, q)) dx \\ &= \frac{\mu}{2D_1 D_2 w_+(w_+^2 - w_-^2)} \int_0^\infty (e^{w_+|x-y|} - e^{w_+|x+y|}) dx \\ &+ \frac{\mu}{2D_1 D_2 w_-(w_-^2 - w_+^2)} \int_0^\infty (e^{w_-|x-y|} - e^{w_-|x+y|}) dx \\ &+ \frac{\lambda + q - D_1 w_+^2}{2D_1 D_2 w_+(w_+^2 - w_-^2)} \int_0^\infty (e^{w_+|x-y|} + e^{w_+|x+y|}) dx \\ &+ \frac{\lambda + q - D_1 w_-^2}{2D_1 D_2 w_-(w_-^2 - w_+^2)} \int_0^\infty (e^{w_-|x-y|} + e^{w_-|x+y|}) dx \\ &= -\frac{\mu}{D_1 D_2 w_+^2 (w_+^2 - w_-^2)} (1 - e^{w_+y}) - \frac{\mu}{D_1 D_2 w_-^2 (w_-^2 - w_+^2)} (1 - e^{w_-y}) \\ &- \frac{\lambda + q - D_1 w_+^2}{D_1 D_2 w_+^2 (w_+^2 - w_-^2)} - \frac{\lambda + q - D_1 w_-^2}{D_1 D_2 w_-^2 (w_-^2 - w_+^2)} \\ &= \frac{1}{q} + T_3(q) - T_4(q), \end{aligned}$$

where w_+ and w_- are given by the formula (4.101), and

$$T_3(q) = \frac{\mu}{D_1 D_2 w_+^2 (w_+^2 - w_-^2)} e^{w_+y}, \quad T_4(q) = \frac{\mu}{D_1 D_2 w_-^2 (w_-^2 - w_+^2)} e^{w_-y}.$$

Rewriting $\alpha = \frac{\lambda}{D_1} + \frac{\mu}{D_2}$, $\beta = \frac{1}{D_1} - \frac{1}{D_2}$, $\gamma = \frac{\lambda}{D_1} - \frac{\mu}{D_2}$ and $\eta = \frac{1}{D_1} + \frac{1}{D_2}$, and working in $T_3(q)$ and $T_4(q)$, we obtain

$$\begin{aligned} T_3(q) &= \frac{2\mu}{D_1 D_2} \exp \left\{ -\sqrt{\frac{\alpha + \eta q + \sqrt{\beta^2 q^2 + 2\gamma\beta q + \alpha^2}}{2}} y \right. \\ &\quad \left. - \ln \left(\alpha + \eta q + \sqrt{\beta^2 q^2 + 2\gamma\beta q + \alpha^2} \right) - \ln \left(\sqrt{\beta^2 q^2 + 2\gamma\beta q + \alpha^2} \right) \right\}, \\ T_4(q) &= \frac{2\mu}{D_1 D_2} \exp \left\{ -\sqrt{\frac{\alpha + \eta q - \sqrt{\beta^2 q^2 + 2\gamma\beta q + \alpha^2}}{2}} y \right. \\ &\quad \left. - \ln \left(\alpha + \eta q - \sqrt{\beta^2 q^2 + 2\gamma\beta q + \alpha^2} \right) - \ln \left(\sqrt{\beta^2 q^2 + 2\gamma\beta q + \alpha^2} \right) \right\}. \end{aligned}$$

Expanding $T_3(q)$ and $T_4(q)$ for q large, we obtain an expansion for the survival probability given by the expression

$$\begin{aligned}\hat{S}(q) &= \frac{1}{q} - \frac{D_2\mu}{D_2 - D_1} \frac{\exp\left\{-\sqrt{\frac{q}{D_2}}y\right\}}{q^2} + \frac{D_1\mu}{D_2 - D_1} \frac{\exp\left\{-\sqrt{\frac{q}{D_1}}y\right\}}{q^2} \\ &+ O\left(\frac{\exp\left\{-\sqrt{\frac{q}{D_1}}y\right\}}{q^{\frac{5}{2}}} + \frac{\exp\left\{-\sqrt{\frac{q}{D_2}}y\right\}}{q^{\frac{5}{2}}}\right).\end{aligned}$$

The expression above contains two exponentially small terms. In the limit D_1 close to D_2 when $D_2 > D_1$, we use the expansion $D_2 = D_1(1+\varepsilon)$ and studying the limit when ε goes to zero, we have

$$\hat{S}_\varepsilon(q) \sim \frac{1}{q} - \frac{\mu \exp\left\{-\sqrt{\frac{q}{D_1(1+\varepsilon)}}y\right\}}{q^2} \left[1 + \frac{\exp\left\{-\sqrt{\frac{q}{D_1(1+\varepsilon)}}y\right\} - \exp\left\{-\sqrt{\frac{q}{D_1}}y\right\}}{\varepsilon \exp\left\{-\sqrt{\frac{q}{D_1(1+\varepsilon)}}y\right\}} \right].$$

The expansion in ε and εq leads to

$$\hat{S}_\varepsilon(q) = \frac{1}{q} - \frac{\mu}{q^2} \exp\left\{-\sqrt{\frac{q}{D_1}}y\right\} \left[1 + \sqrt{\frac{q}{4D_1}}y \right] + O(\varepsilon) + O(\varepsilon q).$$

When $\varepsilon \rightarrow 0$, the survival probability $\hat{S}_\varepsilon(q)$ converges to $\hat{S}_0(q)$ corresponding to the solution for $D_1 = D_2$, defined by equation (4.51). However, the convergence is not uniform in t in the interval $[0, \infty[$, preventing us to use this expansion to estimate the MFAT for this case. Thus to leading order, using that

$$\lim_{D_2 \rightarrow D_1} \Pr\{t_1 > t\} \sim 1 - \mu t \frac{e^{-\frac{y^2}{4D_1 t}} \sqrt{4D_1 t}}{y \sqrt{\pi}},$$

we obtain the asymptotic formula for N large

$$\bar{\tau}_\varepsilon^N \sim \int_0^\infty \exp\left\{\ln\left\{1 - \mu t \frac{e^{-\frac{y^2}{4D_1 t}} \sqrt{4D_1 t}}{y \sqrt{\pi}}\right\}\right\} dt \sim \frac{y^2}{4D_1 \ln\left(\frac{N}{\sqrt{\pi}} \mu \frac{y^2}{4D_1} + A_\varepsilon\right)},$$

where $A_\varepsilon = A_0 + \varepsilon A_1 + \dots$, and A_k are constants. To conclude, to leading order in ε , the MFAT for the case when $D_1 \neq D_2$ is similar to the case $D_1 = D_2$.

When $D_1 > D_2$, we study the limit case by making the expansion $D_1 = D_2(1+\varepsilon)$ and studying the limit when ε goes to zero. In that case, we have

$$\hat{S}(q) \sim \frac{1}{q} - \frac{\mu}{q^2} \left[\exp\left\{-\sqrt{\frac{q}{D_2(1+\varepsilon)}}y\right\} + \frac{\exp\left\{-\sqrt{\frac{q}{D_2(1+\varepsilon)}}y\right\} - \exp\left\{-\sqrt{\frac{q}{D_2}}y\right\}}{\epsilon} \right].$$

The expansion in ε and εq leads to

$$\hat{S}_\varepsilon(q) = \frac{1}{q} - \frac{\mu}{q^2} \exp\left\{-\sqrt{\frac{q}{D_2}}y\right\} \left[1 + \sqrt{\frac{q}{4D_2}}y \right] + O(\varepsilon) + O(\varepsilon q).$$

When $\varepsilon \rightarrow 0$, the survival probability $\hat{S}_\varepsilon(q)$ converges to $\hat{S}_0(q)$ (equation (4.51)) corresponding to the solution for $D_1 = D_2$. Working as we did before, we have the limit

$$\lim_{D_1 \rightarrow D_2} \Pr \{t_1 > t\} \sim 1 - \mu \frac{e^{-\frac{y^2}{4D_2 t}} \sqrt{4D_2 t}}{y \sqrt{\pi}}.$$

Thus to leading order, we obtain the asymptotic formula when the number of particle is large N

$$\bar{\tau}_\varepsilon^N \sim \int_0^\infty \exp \left\{ \ln \left\{ 1 - \mu t \frac{e^{-\frac{y^2}{4D_2 t}} \sqrt{4D_2 t}}{y \sqrt{\pi}} \right\}^N \right\} dt \sim \frac{y^2}{4D_2 \ln \left(\frac{N}{\sqrt{\pi}} \mu \frac{y^2}{4D_2} \right) + A_\varepsilon},$$

where we have used the expansion $A_\varepsilon = A_0 + \varepsilon A_1 + \dots$, and A_k are constants. To conclude, we remark that still in the limit case is possible to find an asymptotic formula which decay with the same law, $\frac{1}{\ln N}$.

4.7.3 Particles start uniformly distributed in an interval

Particles start in state 2 with $D_1 \neq D_2$ uniformly distributed in $[0, y_0]$

When the particles start in state 2 uniformly distributed, the Laplace transform applied to the survival probability is given by the convolution

$$\begin{aligned} \hat{S}(q) &= \frac{1}{y_0} \int_0^{y_0} \left[\frac{1}{q} + \frac{\mu e^{w+y}}{D_1 D_2 w_+^2 (w_+^2 - w_-^2)} - \frac{\mu e^{w-y}}{D_1 D_2 w_-^2 (w_+^2 - w_-^2)} \right] dy \\ &\approx \frac{1}{q} - \frac{\mu}{y_0 D_1 D_2 w_+^3 (w_+^2 - w_-^2)} + \frac{\mu}{y_0 D_1 D_2 w_-^3 (w_+^2 - w_-^2)} \\ &\approx \frac{1}{q} + T_7(q) + T_8(q), \end{aligned}$$

where $T_7(q) = -\frac{\mu}{y_0 D_1 D_2 w_+^3 (w_+^2 - w_-^2)}$ and $T_8(q) = \frac{\mu}{y_0 D_1 D_2 w_-^3 (w_+^2 - w_-^2)}$. Using the expansion in q large for $T_7(q)$ and $T_8(q)$, we obtain

$$T_7(q) \sim \frac{\mu D_1^{\frac{3}{2}}}{y_0 (D_2 - D_1) q^{\frac{5}{2}}} \text{ and } T_8(q) \sim -\frac{\mu D_2^{\frac{3}{2}}}{y_0 (D_2 - D_1) q^{\frac{5}{2}}}.$$

In the limit $D_2 = D_1(1 + \varepsilon)$, when $D_2 > D_1$, an expansion in ε leads to

$$\hat{S}_\varepsilon(q) \sim \frac{1}{q} - \frac{\mu}{y_0 q^{\frac{5}{2}}} \frac{D_1^{\frac{3}{2}} (1 + \varepsilon)^{\frac{3}{2}} - D_1^{\frac{3}{2}}}{D_1 \varepsilon} \sim \frac{1}{q} - \frac{3\mu \sqrt{D_1}}{2y_0 q^{\frac{5}{2}}} - \frac{\mu \sqrt{D_1}}{y_0 q^{\frac{5}{2}}} \left(\sum_{n=1}^{\infty} \binom{\frac{3}{2}}{n+1} \varepsilon^n \right).$$

When $\varepsilon \rightarrow 0$, the survival probability $\hat{S}_\varepsilon(q)$ converges to $\hat{S}_0(q)$ corresponding to the solution when $D_1 = D_2$, given by equation (4.69). Thus to leading order, using that

$$\lim_{D_2 \rightarrow D_1} \Pr \{t_1 > t\} \sim 1 - \mu t \frac{\sqrt{4D_1 t}}{y_0 \sqrt{\pi}},$$

we obtain the asymptotic formula for N large

$$\bar{\tau}_\varepsilon^N \sim \int_0^\infty \exp \left\{ \ln \left\{ 1 - \frac{\mu t \sqrt{4D_1 t}}{y_0 \sqrt{\pi}} \right\}^N \right\} dt \sim \Gamma \left(\frac{5}{3} \right) \left(\frac{y_0 \sqrt{\pi}}{\mu \sqrt{4D_1}} \right)^{\frac{2}{3}} \frac{1}{N^{\frac{2}{3}} + A_\varepsilon},$$

where $A_\varepsilon = A_0 + \varepsilon A_1 + \dots$, and A_k are constants as before. When $D_1 > D_2$, we have then,

$$\hat{S}(q) \sim \frac{1}{q} - \frac{\mu D_1^{\frac{3}{2}}}{y_0(D_1 - D_2)q^{\frac{5}{2}}} + \frac{\mu D_2^{\frac{3}{2}}}{y_0(D_1 - D_2)q^{\frac{5}{2}}}.$$

Making now, $D_1 = D_2(1 + \varepsilon)$ and expanding in ε , we have

$$\hat{S}_\varepsilon(q) \sim \frac{1}{q} - \frac{\mu}{y_0 q^{\frac{5}{2}}} \frac{D_2^{\frac{3}{2}} (1 + \varepsilon)^{\frac{3}{2}} - D_2^{\frac{3}{2}}}{D_2 \varepsilon} \sim \frac{1}{q} - \frac{3\mu \sqrt{D_2}}{2y_0 q^{\frac{5}{2}}} - \frac{\mu \sqrt{D_2}}{y_0 q^{\frac{5}{2}}} \left(\sum_{n=1}^{\infty} \binom{\frac{3}{2}}{n+1} \varepsilon^n \right).$$

When $\varepsilon \rightarrow 0$, the survival probability $\hat{S}_\varepsilon(q)$ converges to $\hat{S}_0(q)$, corresponding to the solution when $D_1 = D_2$, given by the equation (4.69). For the same reasons as above, to leading order, using that

$$\lim_{D_1 \rightarrow D_2} \Pr \{t_1 > t\} \sim 1 - \mu t \frac{\sqrt{4D_2 t}}{y_0 \sqrt{\pi}},$$

we obtain the asymptotic formula for N large

$$\bar{\tau}_\varepsilon^N \sim \int_0^\infty \exp \left\{ \ln \left\{ 1 - \frac{\mu t \sqrt{4D_2 t}}{y_0 \sqrt{\pi}} \right\}^N \right\} dt \sim \Gamma \left(\frac{5}{3} \right) \left(\frac{y_0 \sqrt{\pi}}{\mu \sqrt{4D_2}} \right)^{\frac{2}{3}} \frac{1}{N^{\frac{2}{3}} + A_\varepsilon},$$

where $A_\varepsilon = A_0 + \varepsilon A_1 + \dots$, and A_k are constants. To conclude, to leading order, we obtain a formula for the MFAT when D_1 and D_2 are closed and the initial condition is uniformly distributed in $[0, y_0]$ with the same law $\frac{1}{N^{\frac{2}{3}}}$ when they are different.

Particles start in state 1 uniformly distributed in $[y_1, y_2]$ with $y_1 > 0$

Considering now the initial condition $p_1(x, 0) = \frac{1}{y_2 - y_1} \mathbb{I}_{\{x \in [y_1, y_2]\}}$, when the particles start in state 1, we obtain the Laplace transform of the survival probability given by the convolution

$$\begin{aligned} \hat{S}(q) &= \frac{1}{q} + \frac{(q + \mu - D_2 w_+^2)(e^{w+y_2} - e^{w+y_1})}{(y_2 - y_1) D_1 D_2 w_+^3 (w_+^2 - w_-^2)} - \frac{(q + \mu - D_2 w_-^2)(e^{w-y_2} - e^{w-y_1})}{(y_2 - y_1) D_1 D_2 w_-^3 (w_+^2 - w_-^2)} \\ &= \frac{1}{q} + T_9(q) + T_{10}(q), \end{aligned}$$

where $T_9(q) = \frac{(q + \mu - D_2 w_+^2)(e^{w+y_2} - e^{w+y_1})}{(y_2 - y_1) D_1 D_2 w_+^3 (w_+^2 - w_-^2)}$ and $T_{10}(q) = -\frac{(q + \mu - D_2 w_-^2)(e^{w-y_2} - e^{w-y_1})}{(y_2 - y_1) D_1 D_2 w_-^3 (w_+^2 - w_-^2)}$. And using the expansion in q large we get

$$T_9(q) \sim \frac{D_1^{\frac{3}{2}}}{2^{\frac{3}{2}} q^{\frac{3}{2}}} \frac{\left(\exp \left\{ -\sqrt{\frac{q}{D_1}} y_2 \right\} - \exp \left\{ -\sqrt{\frac{q}{D_1}} y_1 \right\} \right)}{y_2 - y_1},$$

$$T_{10}(q) \sim \frac{\lambda \mu D_2^{\frac{5}{2}}}{2^{\frac{3}{2}} (D_1 - D_2)^2 q^{\frac{7}{2}}} \frac{\left(\exp \left\{ -\sqrt{\frac{q}{D_2}} y_2 \right\} - \exp \left\{ -\sqrt{\frac{q}{D_2}} y_1 \right\} \right)}{y_2 - y_1}.$$

This leads to

$$\begin{aligned}\hat{S}(q) &\sim \frac{1}{q} - \frac{D_1^{\frac{3}{2}}}{2^{\frac{3}{2}}(y_2 - y_1)q^{\frac{3}{2}}} \left(\exp \left\{ -\sqrt{\frac{q}{D_1}}y_1 \right\} - \exp \left\{ -\sqrt{\frac{q}{D_1}}y_2 \right\} \right) \\ &- \frac{\lambda\mu D_2^{\frac{5}{2}}}{2^{\frac{3}{2}}(y_2 - y_1)(D_1 - D_2)^2 q^{\frac{7}{2}}} \left(\exp \left\{ -\sqrt{\frac{q}{D_2}}y_2 \right\} - \exp \left\{ -\sqrt{\frac{q}{D_2}}y_1 \right\} \right).\end{aligned}$$

Particles start in state 2 uniformly distributed in $[y_1, y_2]$

In the case where the particles follows the initial condition $p_2(x, 0) = \frac{1}{y_2 - y_1} \mathbb{I}_{\{x \in [y_1, y_2]\}}$, meaning that the particles start in state 2 uniformly distributed in $[y_1, y_2]$, the Laplace transform of the survival probability given by the convolution

$$\begin{aligned}\hat{S}(q) &= \frac{1}{(y_2 - y_1)} \int_{y_1}^{y_2} \left(\frac{1}{q} + \frac{\mu e^{w+y}}{D_1 D_2 w_+^2 (w_+^2 - w_-^2)} - \frac{\mu e^{w-y}}{D_1 D_2 w_-^2 (w_+^2 - w_-^2)} \right) dy \\ &= \frac{1}{q} + \frac{\mu (e^{w+y_2} - e^{w+y_1})}{D_1 D_2 w_+^3 (w_+^2 - w_-^2)} - \frac{\mu (e^{w-y_2} - e^{w-y_1})}{D_1 D_2 w_-^3 (w_+^2 - w_-^2)} \\ &= \frac{1}{q} + T_{11}(q) + T_{12}(q),\end{aligned}$$

where $T_{11}(q) = \frac{\mu(e^{w+y_2} - e^{w+y_1})}{D_1 D_2 w_+^3 (w_+^2 - w_-^2)}$ and $T_{12}(q) = -\frac{\mu(e^{w-y_2} - e^{w-y_1})}{D_1 D_2 w_-^3 (w_+^2 - w_-^2)}$, and making the Taylor expansion in q large for $T_{11}(q)$ and $T_{12}(q)$ we get

$$\begin{aligned}T_{11}(q) &\sim -\frac{D_1^{\frac{3}{2}} \mu}{(D_2 - D_1) q^{\frac{5}{2}}} \frac{\left(\exp \left\{ -\sqrt{\frac{q}{D_1}}y_2 \right\} - \exp \left\{ -\sqrt{\frac{q}{D_1}}y_1 \right\} \right)}{y_2 - y_1}, \\ T_{12}(q) &\sim \frac{D_2^{\frac{3}{2}} \mu}{(D_2 - D_1) q^{\frac{5}{2}}} \frac{\left(\exp \left\{ -\sqrt{\frac{q}{D_2}}y_2 \right\} - \exp \left\{ -\sqrt{\frac{q}{D_2}}y_1 \right\} \right)}{y_2 - y_1}.\end{aligned}$$

We can have the approximation for the Laplace transform of the survival probability given by

$$\begin{aligned}\hat{S}(q) &\sim \frac{1}{q} - \frac{\mu D_2^{\frac{3}{2}}}{(y_2 - y_1)(D_2 - D_1) q^{\frac{5}{2}}} \left(\exp \left\{ -\sqrt{\frac{q}{D_2}}y_1 \right\} - \exp \left\{ -\sqrt{\frac{q}{D_2}}y_2 \right\} \right) \\ &+ \frac{\mu D_1^{\frac{3}{2}}}{(y_2 - y_1)(D_2 - D_1) q^{\frac{5}{2}}} \left(\exp \left\{ -\sqrt{\frac{q}{D_1}}y_1 \right\} - \exp \left\{ -\sqrt{\frac{q}{D_1}}y_2 \right\} \right),\end{aligned}$$

and making $y_2 = y_1(1 + \varepsilon)$, we have

$$\begin{aligned}\hat{S}_\varepsilon(q) &= \frac{1}{q} - \frac{\mu D_2^{\frac{3}{2}}}{y_1 \varepsilon (D_2 - D_1) q^{\frac{5}{2}}} \exp \left\{ -\sqrt{\frac{q}{D_2}}y_1 \right\} \left(1 - \exp \left\{ -\sqrt{\frac{q}{D_2}}y_1 \varepsilon \right\} \right) \\ &+ \frac{\mu D_1^{\frac{3}{2}}}{y_1 \varepsilon (D_2 - D_1) q^{\frac{5}{2}}} \exp \left\{ -\sqrt{\frac{q}{D_1}}y_1 \right\} \left(1 - \exp \left\{ -\sqrt{\frac{q}{D_1}}y_1 \varepsilon \right\} \right).\end{aligned}$$

Using the expansion for the exponential function we have

$$\begin{aligned}\hat{S}_\varepsilon(q) &= \frac{1}{q} - \frac{\mu D_2 \exp\left\{-\sqrt{\frac{q}{D_2}}y_1\right\}}{(D_2 - D_1)q^2} + \frac{\mu D_2 \exp\left\{-\sqrt{\frac{q}{D_2}}y_1\right\}}{(D_2 - D_1)q^2} \sum_{n=1}^{\infty} \left(-\sqrt{\frac{q}{D_2}}y_1\varepsilon\right)^n \\ &\quad + \frac{\mu D_1 \exp\left\{-\sqrt{\frac{q}{D_1}}y_1\right\}}{(D_2 - D_1)q^2} - \frac{\mu D_1 \exp\left\{-\sqrt{\frac{q}{D_1}}y_1\right\}}{(D_2 - D_1)q^2} \sum_{n=1}^{\infty} \left(-\sqrt{\frac{q}{D_1}}y_1\varepsilon\right)^n.\end{aligned}$$

When $\varepsilon \rightarrow 0$, the survival probability $S_\varepsilon(t)$ converges to $S_0(t)$ corresponding to an initial condition for the Dirac delta function at position y_1 for $D_1 \neq D_2$. Thus to leading order, using that

$$\lim_{\substack{y_2 \rightarrow y_1, \\ D_2 \rightarrow D_1}} \Pr\{t_1 > t\} \sim 1 - \frac{\mu t \sqrt{4D_1 t}}{\sqrt{\pi}} \left[\frac{e^{-\frac{y_1^2}{4D_1 t}}}{y_1} \right],$$

we obtain the asymptotic formula for N large

$$\bar{\tau}_\varepsilon^N \sim \int_0^\infty \exp \left\{ \ln \left\{ 1 - \frac{\mu t \sqrt{4D_1 t}}{\sqrt{\pi}} \left[\frac{e^{-\frac{y_1^2}{4D_1 t}}}{y_1} \right] \right\}^N \right\} dt \sim \frac{y_1^2}{4D_1 \ln \left(\frac{N}{\sqrt{\pi}} \mu \frac{y_1^2}{4D_1} \right) + A_\varepsilon},$$

where $A_\varepsilon = A_0 + \varepsilon A_1 + \dots$, where A_k are constants. When $D_1 > D_2$, we have the expansion for the Laplace transform of the survival probability

$$\begin{aligned}\hat{S}(q) &= \frac{1}{q} - \frac{\mu D_1^{\frac{3}{2}}}{(y_2 - y_1)(D_1 - D_2)q^{\frac{5}{2}}} \left(\exp\left\{-\sqrt{\frac{q}{D_1}}y_1\right\} - \exp\left\{-\sqrt{\frac{q}{D_1}}y_2\right\} \right) \\ &\quad + \frac{\mu D_2^{\frac{3}{2}}}{(y_2 - y_1)(D_1 - D_2)q^{\frac{5}{2}}} \left(\exp\left\{-\sqrt{\frac{q}{D_2}}y_1\right\} - \exp\left\{-\sqrt{\frac{q}{D_2}}y_2\right\} \right),\end{aligned}$$

and making $y_2 = y_1(1 + \varepsilon)$, we have

$$\begin{aligned}\hat{S}_\varepsilon(q) &= \frac{1}{q} - \frac{\mu D_1^{\frac{3}{2}}}{y_1 \varepsilon (D_1 - D_2) q^{\frac{5}{2}}} \exp\left\{-\sqrt{\frac{q}{D_1}}y_1\right\} \left(1 - \exp\left\{-\sqrt{\frac{q}{D_1}}y_1\varepsilon\right\} \right) \\ &\quad + \frac{\mu D_2^{\frac{3}{2}}}{y_1 \varepsilon (D_1 - D_2) q^{\frac{5}{2}}} \exp\left\{-\sqrt{\frac{q}{D_2}}y_1\right\} \left(1 - \exp\left\{-\sqrt{\frac{q}{D_2}}y_1\varepsilon\right\} \right).\end{aligned}$$

Then, using the Taylor expansion of the exponential functions we have

$$\begin{aligned}\hat{S}_\varepsilon(q) &= \frac{1}{q} - \frac{\mu D_1 \exp\left\{-\sqrt{\frac{q}{D_1}}y_1\right\}}{(D_1 - D_2)q^2} + \frac{\mu D_1 \exp\left\{-\sqrt{\frac{q}{D_1}}y_1\right\}}{(D_1 - D_2)q^2} \sum_{n=1}^{\infty} \left(-\sqrt{\frac{q}{D_1}}y_1\varepsilon\right)^n \\ &\quad + \frac{\mu D_2 \exp\left\{-\sqrt{\frac{q}{D_2}}y_1\right\}}{(D_1 - D_2)q^2} - \frac{\mu D_2 \exp\left\{-\sqrt{\frac{q}{D_2}}y_1\right\}}{(D_1 - D_2)q^2} \sum_{n=1}^{\infty} \left(-\sqrt{\frac{q}{D_2}}y_1\varepsilon\right)^n.\end{aligned}$$

When $\varepsilon \rightarrow 0$, the survival probability $S_\varepsilon(t)$ converges to $S_0(t)$ corresponding to an initial condition for the Dirac delta function at position y_1 for $D_1 \neq D_2$. Using the same reasoning as above, to

leading order, using that

$$\lim_{\substack{y_2 \rightarrow y_1, \\ D_1 \rightarrow D_2}} \Pr \{t_1 > t\} \sim 1 - \frac{\mu t \sqrt{4D_2 t}}{\sqrt{\pi}} \left[\frac{e^{-\frac{y_1^2}{4D_2 t}}}{y_1} \right],$$

we obtain the asymptotic formula for N large

$$\bar{\tau}_\varepsilon^N \sim \int_0^\infty \exp \left\{ \ln \left\{ 1 - \frac{\mu t \sqrt{4D_2 t}}{\sqrt{\pi}} \left[\frac{e^{-\frac{y_1^2}{4D_2 t}}}{y_1} \right] \right\}^N \right\} dt \sim \frac{y_1^2}{4D_2 \ln \left(\frac{N}{\sqrt{\pi}} \mu \frac{y_1^2}{4D_2} \right) + A_\varepsilon},$$

where $A_\varepsilon = A_0 + \varepsilon A_1 + \dots$, where A_k are constants.

4.7.4 The initial distribution has a long tail and particles start in state 2

The Laplace transform of the survival probability when $D_1 = D_2 = D$ and the initial condition is given by (4.91), is the convolution

$$\begin{aligned} \hat{S}(q) &= \frac{2b^{\frac{1+\alpha}{2}}}{\Gamma(\frac{1+\alpha}{2})} \int_0^\infty \left[\frac{1}{q} - \frac{\mu e^{-y} \sqrt{\frac{q}{D}}}{\theta q} + \frac{\mu e^{-y} \sqrt{\frac{q+\theta}{D}}}{\theta(q+\theta)} \right] y^\alpha \exp \{-bx^2\} \\ &= \frac{1}{q} - \frac{2^{-(1+\alpha)} b^{-\frac{1}{2}} \mu \Gamma(1+\alpha)}{\Gamma(\frac{1+\alpha}{2}) \sqrt{D}} \left[\frac{1}{\sqrt{q}} U \left(1 + \frac{\alpha}{2}, \frac{3}{2}, \frac{q}{4bD} \right) \right. \\ &\quad \left. - \frac{1}{\sqrt{q+\theta}} U \left(1 + \frac{\alpha}{2}, \frac{3}{2}, \frac{q+\theta}{4bD} \right) \right], \end{aligned}$$

where $U(a, b, z)$ is the confluent hyper geometric function and $\theta = \lambda + \mu$. When $D_1 \neq D_2$, the Laplace transform of the survival probability gives

$$\begin{aligned} \hat{S}(q) &= \frac{2b^{\frac{1+\alpha}{2}}}{\Gamma(\frac{1+\alpha}{2})} \int_0^\infty \left[\frac{1}{q} + \frac{\mu e^{w+y}}{D_1 D_2 w_+^2 (w_+^2 - w_-^2)} - \frac{\mu e^{w-y}}{D_1 D_2 w_-^2 (w_+^2 - w_-^2)} \right] y^\alpha \exp \{-bx^2\} \\ &= \frac{1}{q} + \frac{2^{-(1+\alpha)} b^{-\frac{1}{2}} \mu \Gamma(1+\alpha)}{\Gamma(\frac{1+\alpha}{2}) D_1 D_2 (w_+^2 - w_-^2)} \left[\frac{U \left(1 + \frac{\alpha}{2}, \frac{3}{2}, \frac{w_-^2}{4b} \right)}{w_-} - \frac{U \left(1 + \frac{\alpha}{2}, \frac{3}{2}, \frac{w_+^2}{4b} \right)}{w_+} \right], \end{aligned}$$

where $U(a, b, z)$ is the confluent hyper geometric function. We can have the approximation for the survival probability for q large

$$\hat{S}(q) \sim \frac{1}{q} - \frac{2\mu\Gamma(1+\alpha)}{b^{-\frac{1+\alpha}{2}} \Gamma(\frac{1+\alpha}{2}) (D_2 - D_1) q^{\frac{5+\alpha}{2}}} \left[D_2^{\frac{3+\alpha}{2}} - D_1^{\frac{3+\alpha}{2}} \right].$$

For $D_2 = D_1 (1 + \varepsilon)$, we have

$$\hat{S}_\varepsilon(q) \sim \frac{1}{q} - \frac{2\mu\Gamma(1+\alpha) b^{\frac{1+\alpha}{2}} D_1^{\frac{3+\alpha}{2}}}{\Gamma(\frac{1+\alpha}{2}) D_1 \varepsilon q^{\frac{5+\alpha}{2}}} \left[(1 + \varepsilon)^{\frac{3+\alpha}{2}} - 1 \right],$$

and expanding the above expression in ε , we have

$$\hat{S}_\varepsilon(q) \sim \frac{1}{q} - \frac{\mu(3+\alpha)\Gamma(1+\alpha)b^{\frac{1+\alpha}{2}}D_1^{\frac{1+\alpha}{2}}}{\Gamma(\frac{1+\alpha}{2})q^{\frac{5+\alpha}{2}}} - \frac{2\mu\Gamma(1+\alpha)b^{\frac{1+\alpha}{2}}D_1^{\frac{1+\alpha}{2}}}{\Gamma(\frac{1+\alpha}{2})q^{\frac{5+\alpha}{2}}} \sum_{n=1}^{\infty} \binom{\frac{3+\alpha}{2}}{n+1} \varepsilon^n.$$

When $\varepsilon \rightarrow 0$, the survival probability $S_\varepsilon(t)$ converges to $S_0(t)$ corresponding to an initial condition with a long tail for $D_1 = D_2$. Using the same reasoning as we did before, to leading order, using that

$$\lim_{D_2 \rightarrow D_1,} \Pr\{t_1 > t\} \sim 1 - \frac{(bD_1)^{\frac{1+\alpha}{2}}\mu(3+\alpha)\Gamma(1+\alpha)}{\Gamma(\frac{1+\alpha}{2})\Gamma(\frac{5+\alpha}{2})} t^{\frac{3+\alpha}{2}},$$

we obtain the asymptotic formula for N large

$$\begin{aligned} \bar{\tau}_\varepsilon^N &= \int_0^\infty [S(t)]^N dt \sim \int_0^\infty \exp \left\{ \ln \left\{ 1 - \frac{(bD_1)^{\frac{1+\alpha}{2}}\mu(3+\alpha)\Gamma(1+\alpha)}{\Gamma(\frac{1+\alpha}{2})\Gamma(\frac{5+\alpha}{2})} t^{\frac{3+\alpha}{2}} \right\} \right\} dt \\ &\sim \left[\frac{\Gamma(\frac{1+\alpha}{2})\Gamma(\frac{5+\alpha}{2})}{\mu(3+\alpha)\Gamma(1+\alpha)} \right]^{\frac{2}{3+\alpha}} \frac{\Gamma(\frac{5+\alpha}{3+\alpha})}{(bD_1)^{\frac{1+\alpha}{3+\alpha}}} \frac{1}{N^{\frac{2}{3+\alpha}} + A_\varepsilon}, \end{aligned}$$

where $A_\varepsilon = A_0 + \varepsilon A_1 + \dots$, where A_k are constants. To conclude, to leading order in ε , the MFAT when we have the initial distribution with a long tail and different diffusion coefficients starting in state 2 is similar to the case $D_1 = D_2$. When $D_1 \geq D_2$ we have the expression for the survival probability written as

$$\hat{S}(q) \sim \frac{1}{q} - \frac{2\mu\Gamma(1+\alpha)}{b^{-\frac{1+\alpha}{2}}\Gamma(\frac{1+\alpha}{2})(D_1 - D_2)q^{\frac{5+\alpha}{2}}} \left[D_1^{\frac{3+\alpha}{2}} - D_2^{\frac{3+\alpha}{2}} \right].$$

Making $D_1 = D_2(1 + \varepsilon)$, we have

$$\hat{S}_\varepsilon(q) \sim \frac{1}{q} - \frac{2\mu\Gamma(1+\alpha)b^{\frac{1+\alpha}{2}}D_2^{\frac{3+\alpha}{2}}}{\Gamma(\frac{1+\alpha}{2})D_2\varepsilon q^{\frac{5+\alpha}{2}}} \left[(1 + \varepsilon)^{\frac{3+\alpha}{2}} - 1 \right],$$

and expanding the above expression in ε , we have

$$\hat{S}_\varepsilon(q) \sim \frac{1}{q} - \frac{\mu(3+\alpha)\Gamma(1+\alpha)b^{\frac{1+\alpha}{2}}D_2^{\frac{1+\alpha}{2}}}{\Gamma(\frac{1+\alpha}{2})q^{\frac{5+\alpha}{2}}} - \frac{2\mu\Gamma(1+\alpha)b^{\frac{1+\alpha}{2}}D_2^{\frac{1+\alpha}{2}}}{\Gamma(\frac{1+\alpha}{2})q^{\frac{5+\alpha}{2}}} \sum_{n=1}^{\infty} \binom{\frac{3+\alpha}{2}}{n+1} \varepsilon^n.$$

When $\varepsilon \rightarrow 0$, the survival probability $S_\varepsilon(t)$ converges to $S_0(t)$ corresponding to an initial condition with a long tail for $D_1 = D_2$. Thus to leading order, using that

$$\lim_{D_1 \rightarrow D_2,} \Pr\{t_1 > t\} \sim 1 - \frac{(bD_2)^{\frac{1+\alpha}{2}}\mu(3+\alpha)\Gamma(1+\alpha)}{\Gamma(\frac{1+\alpha}{2})\Gamma(\frac{5+\alpha}{2})} t^{\frac{3+\alpha}{2}},$$

we obtain for N large

$$\begin{aligned} \bar{\tau}_\varepsilon^N &= \int_0^\infty [S(t)]^N dt \sim \int_0^\infty \exp \left\{ \ln \left\{ 1 - \frac{(bD_2)^{\frac{1+\alpha}{2}}\mu(3+\alpha)\Gamma(1+\alpha)}{\Gamma(\frac{1+\alpha}{2})\Gamma(\frac{5+\alpha}{2})} t^{\frac{3+\alpha}{2}} \right\} \right\} dt \\ &\sim \left[\frac{\Gamma(\frac{1+\alpha}{2})\Gamma(\frac{5+\alpha}{2})}{\mu(3+\alpha)\Gamma(1+\alpha)} \right]^{\frac{2}{3+\alpha}} \frac{\Gamma(\frac{5+\alpha}{3+\alpha})}{(bD_2)^{\frac{1+\alpha}{3+\alpha}}} \frac{1}{N^{\frac{2}{3+\alpha}} + A_\varepsilon}, \end{aligned}$$

where $A_\varepsilon = A_0 + \varepsilon A_1 + \dots$, where A_k are constants. To conclude, the MFAT for an initial distribution with a long tail and different diffusion coefficients starting in state 2 is similar to the case $D_1 = D_2$.

Discussion and perspectives

Many friend recommend not to write conclusions since we already have a small conclusion at the end of each chapter, but what is the meaning of a large work without one final general vision on what we have done and most important, the motivating future ideas that came from it. Then, instead of repeating everything again, we will summarize the main important ideas and results supporting this investigation and right away we will present you the future directions of this investigation.

We devoted this PhD thesis to the study of molecular processes whose activation time scales are given as the mean first passage time for the fastest particle among N (i.i.d) from the initial position to the target. We obtained specific formulas for each dynamic here considered when N is large using the Laplace method.

We have started this research in chapter 1 studying the effect in the MFAT of considering that the N particles are initially distributed following a distribution that resembles a Gaussian but with a long tail, leading to an algebraic decay in N (faster than the logarithmic formulas), never studied before. This initial distribution can be useful when the injection of particles is slow, thus, at the final moment of the injection the first particles going through the source have spread a bit. We have also analyzed the effect of a positive oriented constant drift in the diffusion equation leading to a decreasing on the MFAT. In chapter 2 and 3 we have also studied the effect of introducing a killing term in the diffusion model, related with the degradation of particles, and we have obtained the formulas for the MFAT conditioned on that at least one particle escapes and conditioned on that a large number of particles escape for dimension 1 and 2. The most important results coming from the analytical formulas is the increasing behavior of the MFAT while conditioning to at least one particle escapes and the decreasing behavior of the MFAT when large number of particles escape. From the simulations results for the 2D case where particles can avoid the killing area, we found the equation of motion for the fastest particles and we showed that this path never intersects the killing area. In the other hand, when the killing is uniform, no deviation from the straight line is expected.

We have used the obtained formulas to understand better various calcium signaling mechanism leaded by a few transient calcium ions inside the dendrites, specifically CICR where buffers and SERCA pumps can capture calcium ions.

Almost in parallel, in chapter 4, we obtained from the study of the first arriving particles the extreme strategy followed for the fastest particle when the particles alternate states. The MFAT formulas were depending on the initial state of the particle, the Poissonian rates for the switching process and the diffusion coefficients for each state. This analysis was useful to learn about the motion of transcription factors inside the nucleus starting the transcription of the DNA.

There are still at least 3 more projects that we would like to have the time to accomplished during this investigation, and they were appearing naturally from the previous projects here addressed.

7.1 The fastest arrival distribution

We have model all these processes previously discussed using the Fokker-Planck equation as the supporting dynamic for the particles and we were adding others, depending on the process that we wanted to studied. Thus, the density of particles satisfies the heat equation with homogeneous Dirichlet boundary condition at the target site and homogeneous Neumann boundary conditions in the rest of the boundary for a bounded domain Ω . From the beginning of the introduction we pointed out that MFAT was computed following

$$\bar{\tau}^N = \mathbb{E}[\tau^1] = \int_0^\infty \Pr\{\tau^1 > t\} dt = \int_0^\infty [\Pr\{t_1 > t\}]^N dt = \int_0^\infty [e^{\ln(\Pr\{t_1 > t\})}]^N dt = \int_0^\infty e^{\ln(S(t))} dt, \quad (7.1)$$

and through all the manuscript we solved this integral using the Laplace method, and approximating the integral above in a neighborhood of the supremum value of $\ln(S(t))$. We used then the short-time regime since

$$\sup_{t \in (0, +\infty)} \ln(S(t)) = \ln \left(\sup_{t \in (0, +\infty)} S(t) \right) = 0 = \lim_{t \rightarrow 0^+} \ln(S(t)) \quad (7.2)$$

where

$$\sup_{t \in (0, +\infty)} S(t) = 1. \quad (7.3)$$

This means that the main contribution to the MFAT always comes from the short-time expansion of the survival probability. Depending on the dynamics of the particles we obtained different approximations for the survival probability. For instance, when only diffusion is modeled, as it is the case for transient calcium ions in the dendritic spine when no SERCA pumps are taken into account, the survival probability is given at leading order by $S(t) \sim 1 - \sqrt{4Dt} \frac{e^{-\frac{y^2}{4Dt}}}{y\sqrt{\pi}}$ for small t , leading to

$$\Pr\{\tau^1 > t\} \sim e^{-N\sqrt{4Dt} \frac{e^{-\frac{y^2}{4Dt}}}{y\sqrt{\pi}}} \text{ for } t \text{ small.} \quad (7.4)$$

For the case of transcription factors, where they can switch states between active and idle when considering that all the particles start at position y with the target at position $x = 0$ for the 1D model, if the fastest state is 1 ($D_1 > D_2$) and particles start in state 1, the survival probability has the shape

$$S(t) \sim 1 - \frac{\sqrt{4D_1 t} e^{-\frac{y^2}{4D_1 t}}}{y\sqrt{\pi}}, \quad (7.5)$$

meaning that the fastest particle is not switching states but only diffusing to the target. But, when the fastest state is 2 ($D_2 > D_1$), the survival probability is given by

$$S(t) \sim 1 - \frac{\lambda \mu D_2^3 \sqrt{4D_2 t} t^2 e^{-\frac{y^2}{4D_2 t}}}{2(D_2 - D_1)^2 y\sqrt{\pi}}, \quad (7.6)$$

leading to

$$\Pr\{\tau^1 > t\} \sim e^{-N \frac{\lambda \mu D_2 \sqrt{4D_2 t} t^2 e^{-\frac{y^2}{4D_2 t}}}{2y\sqrt{\pi}}} \text{ for } t \text{ small.} \quad (7.7)$$

One remark from this two examples is that the survival probability for the fastest arrival under the small time regime can be always written as

$$\Pr \{ \tau^1 > t \} = e^{-Nt^k e^{-\frac{1}{t^\alpha}}}, \quad (7.8)$$

for some parameters N , k , and α . We propose then to study the general distribution (called as FAD in the introduction) associated with the first arrivals since everywhere in this manuscript we were approximating the density for the first arrival distribution as the density of a r.v. with distribution

$$F(x, N, k, \alpha) = F(x) = 1 - e^{-Nx^k e^{-\frac{1}{x^\alpha}}}, \quad (7.9)$$

for $x > 0$, $N > 0$, $k > 0$ and $\alpha > 0$.

7.2 Target competition

One interesting project in the study of proteins transport is the study of the splitting probability between two targets defined as the probability to reach one target prior the other one. This splitting probability can help us to understand which target will be accomplished first with a certain probability. Considering the transcription of the DNA as the molecular process to study we would like to understand where is most probably the escape of the mRNA. This process is started by the first transcription factors arriving at the enhancer site of the DNA and binding with the DNA strand, as we already explained in chapter 4. After the binding, the RNA polymerase is thus recruited to start the synthesis of a mRNA molecule which will be released inside the nucleus. This molecule needs to exit the nucleus compartment through a tiny pore to find one ribosome in the cytoplasm and start the synthesis of the encoded protein, as shown in Fig. 7.1A.

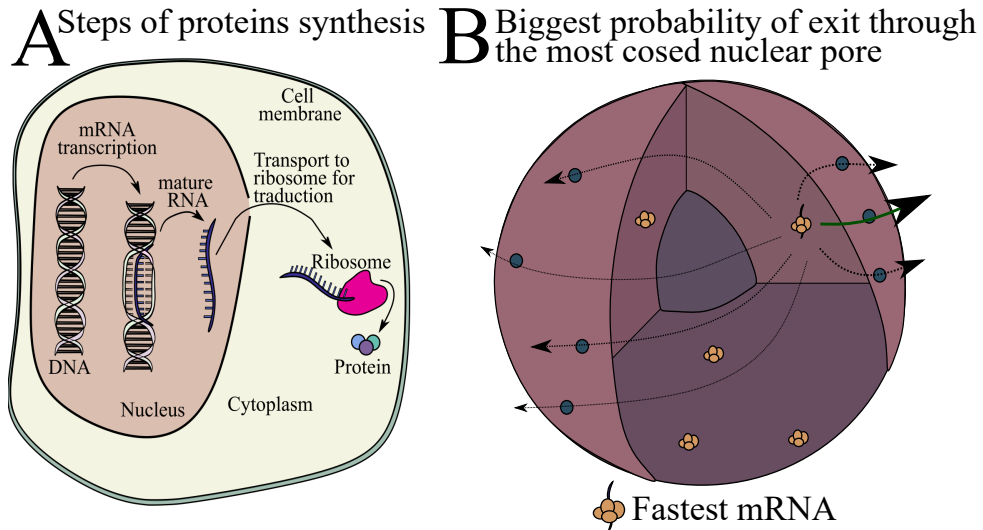


Figure 7.1: **A.** Schematic steps of protein synthesis with DNA transcription as a first step. **B.** Probability of escape through each nuclear pore quantified in the size of the arrow.

Because many mRNA copies (even from the same gene as the release of the RNA is almost immediate) can be made in a very short period of time [149], we could use the Laplace method to obtain the asymptotic formulas predicting the probability for the fastest mRNA leaving the nucleus through the i -th pore among M . We expected the pore (target) most close to the initial position to have the higher escape probability.

7.3 Tracking proteins in the ER

The final project that could be derived from this computations is the understanding of proteins motion inside the cell. In this field, all the formulas here derived can be used for the different dynamics of the proteins. The process of protein folding leads to the consideration of a model with different states for the classification of proteins: folded and unfolded (or misfolded) as we derive in chapter 4. During the conformational folding of a large number of proteins, these are chaperoned by other molecules that assist them in the process. Chaperon molecules assist the proteins by binding to and stabilizing folding intermediates that avoid the segregation of other unfolded proteins. This binding process could lead to a slower diffusion coefficient in the misfolded state. We could also use the formulas that will come from the target competition to simulate the exit probabilities of the proteins for a fixed exit windows of the ER. Finally, the degradation dynamic studied in chapters 2 and 3 should be also taken in account in the general model since it is an essential process that allows to remove damaged proteins. The only missing part here, that should be taken in account as well, is the transportation of proteins by vesicles, that could be understood as a package of a few number of proteins that moves with a different diffusion coefficient once it is full.

To continue this project, the arrival formula for the first arriving package needs to be derived and

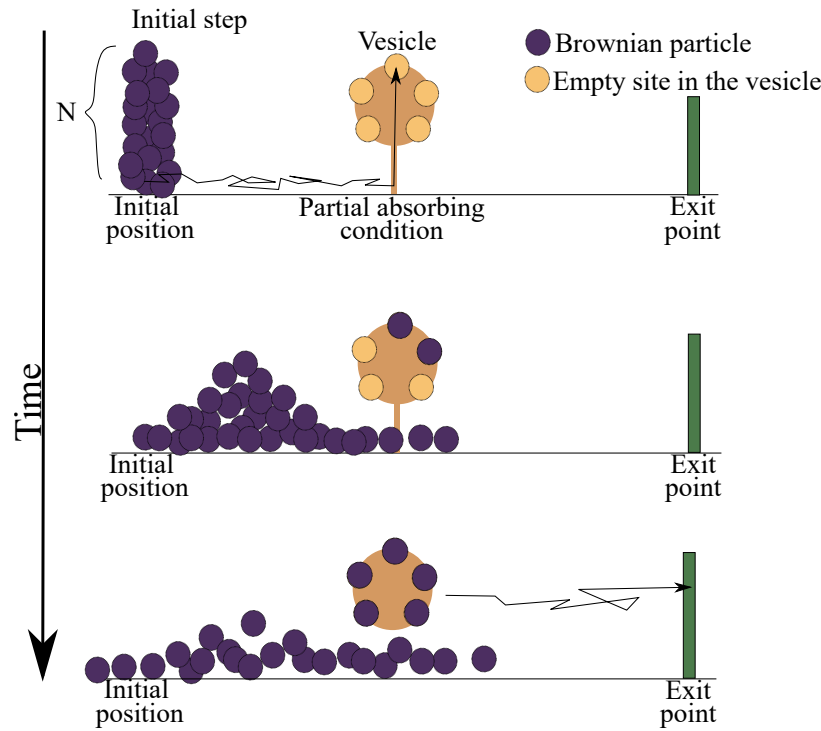


Figure 7.2: Schematic representation in time of Brownian motions filling a vesicle under certain probability law that depends on the initial state of the particles.

the simulations could be made in a structure obtained by segmentation of a real image of ER. In Fig. 7.2 we propose a schematic representation of the motion by packages. In the first state we have all the Brownian particles started at the initial position, and we place an empty vesicle between the initial position and the exit point. The partial absorbing boundary condition associated to the vesicle could modeled the transportation of proteins that are properly folded. After some time,

when the vesicle is filled, it will move as one complex with a different diffusion coefficient. The amount of vesicles to take in account in the model could be discussed with experimentalists based in their real observations.

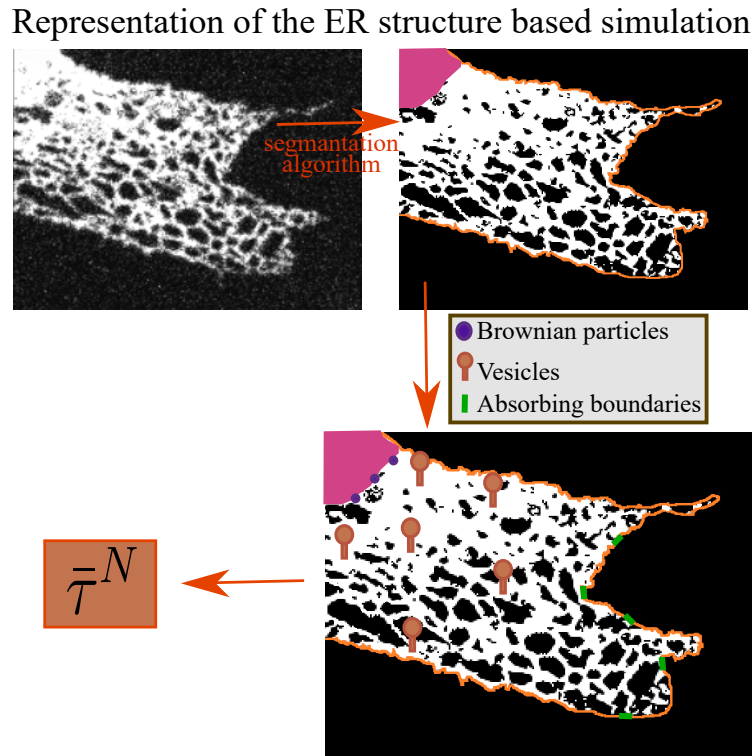


Figure 7.3: General representation of a simulation that takes in account the real structure of the ER for protein transport.

Finally, for the entire process, we shall derive the formula for the arriving package splitting the process as follows. We could first derive an asymptotic formula for the time it take to the m first Brownian particles to arrive at the vesicle with the partial absorbing boundary condition that will depends on the state of the particles. Then, the mean time for the general process is the mean filling time in addition with the arrival time of the vesicle that is the usual diffusive formula (for 1 particle) that depends on the diffusion coefficient of the vesicle and the distance between the vesicle and the exit point. The diffusion coefficient should be large enough to justify the motion by packages. Once we have the main parameters interfering in the filling process we could perform simulations in domains based on real ER structure, as we propose in Fig. 7.3. To do so, we could start with real ER images and extract the cell structure with a segmentation algorithm as represented in the first part of Fig. 7.3. This segmentation algorithm is supposed to delimit the ER structure from the nucleus and other organelles. Then, the second part will be to decide with the experimentalists, the initial configuration of the simulations, as the initial distribution of the Brownian particles, the initial distribution and amount of vesicles to consider, and the position of the exit windows. One first approximation could be just start the particles in a few points on the boundary of the nucleus (represented in pink Fig. 7.3), distribute the vesicles uniformly in the ER, and uniformly distribute the exit windows in the region close to the Golgi apparatus. This initial simulation could help us to understand which are the most important parameters in the model. We expect a strong dependency with the distance between the initial position of the fastest vesicle and the exit window where the

escape occurs.

Bibliography

- [1] D. Holcman and Z. Schuss, “The narrow escape problem,” *siam REVIEW*, vol. 56, no. 2, pp. 213–257, 2014.
- [2] Z. Schuss, A. Singer, and D. Holcman, “The narrow escape problem for diffusion in cellular microdomains,” *Proceedings of the National Academy of Sciences*, vol. 104, no. 41, pp. 16098–16103, 2007.
- [3] T. Calandre, O. Bénichou, D. Grebenkov, and R. Voituriez, “Splitting probabilities and interfacial territory covered by two-dimensional and three-dimensional surface-mediated diffusion,” *Physical Review E*, vol. 89, no. 1, p. 012149, 2014.
- [4] Y. A. Melnikov, *Green’s functions and infinite products: bridging the divide*. Springer Science & Business Media, 2011.
- [5] I. Stakgold and M. J. Holst, *Green’s functions and boundary value problems*. John Wiley & Sons, 2011.
- [6] L. C. Evans, *Partial differential equations*, vol. 19. American Mathematical Society, 2022.
- [7] J. L. Schiff, *The Laplace transform: theory and applications*. Springer Science & Business Media, 1999.
- [8] D. Holcman, A. Marchewka, and Z. Schuss, “The survival probability of diffusion with killing,” *arXiv preprint math-ph/0502035*, 2005.
- [9] T. Lagache, E. Dauty, and D. Holcman, “Quantitative analysis of virus and plasmid trafficking in cells,” *Physical Review E*, vol. 79, no. 1, p. 011921, 2009.
- [10] Z. Schuss, *Theory and Applications of Stochastic Processes: An Analytical Approach*. Springer New York, 2010.
- [11] D. Holcman and Z. Schuss, *Stochastic Narrow Escape in Molecular and Cellular Biology: Analysis and Applications*. Springer, 2015.
- [12] T. Lagache, E. Dauty, and D. Holcman, “Physical principles and models describing intracellular virus particle dynamics,” *Current opinion in microbiology*, vol. 12, no. 4, pp. 439–445, 2009.
- [13] D. Holcman, “Modeling viral and dna trafficking in the cytoplasm of a cell,” *J. Stat. Phys.*, vol. 127, no. 3, pp. 471–494, 2007.
- [14] S. Toste and D. Holcman, “Extreme diffusion with point-sink killing field,” 2022.

- [15] R. G. Gallager and R. G. Gallager, *Poisson processes*. Springer, 1996.
- [16] J. Reingruber and D. Holcman, “Gated narrow escape time for molecular signaling,” *Physical review letters*, vol. 103, no. 14, p. 148102, 2009.
- [17] K. Basnayake, Z. Schuss, and D. Holcman, “Asymptotic formulas for extreme statistics of escape times in 1, 2 and 3-dimensions,” *Journal of Nonlinear Science*, pp. 1–39, 2018.
- [18] D. V. Widder, *Laplace transform (PMS-6)*, vol. 64. Princeton university press, 2015.
- [19] J. D. Murray, *Asymptotic analysis*, vol. 48. Springer Science & Business Media, 2012.
- [20] P. D. Miller, *Applied asymptotic analysis*, vol. 75. American Mathematical Soc., 2006.
- [21] G. F. Carrier, M. Krook, and C. E. Pearson, *Functions of a complex variable: theory and technique*. SIAM, 2005.
- [22] N. Bleistein and R. A. Handelsman, *Asymptotic expansions of integrals*. Ardent Media, 1975.
- [23] K. Cooray, “Generalized gumbel distribution,” *Journal of Applied Statistics*, vol. 37, no. 1, pp. 171–179, 2010.
- [24] S. Nadarajah and S. Kotz, “The beta gumbel distribution,” *Mathematical Problems in engineering*, vol. 2004, no. 4, pp. 323–332, 2004.
- [25] S. Adeyemi and M. O. Ojo, “A generalization of the gumbel distribution,” *Kragujevac Journal of Mathematics*, vol. 25, no. 25, pp. 19–29, 2003.
- [26] E. Bertin, “Global fluctuations and gumbel statistics,” *Physical review letters*, vol. 95, no. 17, p. 170601, 2005.
- [27] S. Nadarajah, “The exponentiated gumbel distribution with climate application,” *Environmetrics: The official journal of the International Environmetrics Society*, vol. 17, no. 1, pp. 13–23, 2006.
- [28] T. Andrade, H. Rodrigues, M. Bourguignon, and G. Cordeiro, “The exponentiated generalized gumbel distribution,” *Revista Colombiana de Estadística*, vol. 38, no. 1, pp. 123–143, 2015.
- [29] R. L. Smith, “Extreme value theory,” *Handbook of applicable mathematics*, vol. 7, no. 437-471, p. 18, 1990.
- [30] E. Castillo, *Extreme value theory in engineering*. Elsevier, 2012.
- [31] L. Haan and A. Ferreira, *Extreme value theory: an introduction*, vol. 3. Springer, 2006.
- [32] M. I. Freidlin and A. D. Wentzell, “Random perturbations,” in *Random perturbations of dynamical systems*, pp. 15–43, Springer, 1998.
- [33] S. Peszat, “Large deviation principle for stochastic evolution equations,” *Probability Theory and Related Fields*, vol. 98, pp. 113–136, 1994.
- [34] I. Karatzas and S. Shreve, *Brownian motion and stochastic calculus*, vol. 113. Springer Science & Business Media, 1991.

- [35] P. Del Moral, *Feynman-kac formulae*. Springer, 2004.
- [36] B. Dacorogna, *Introduction to the Calculus of Variations*. World Scientific Publishing Company, 2014.
- [37] I. M. Gelfand, R. A. Silverman, *et al.*, *Calculus of variations*. Courier Corporation, 2000.
- [38] B. Alberts, D. Bray, K. Hopkin, A. D. Johnson, J. Lewis, M. Raff, K. Roberts, and P. Walter, *Essential cell biology*. Garland Science, 2013.
- [39] G. Schehr and S. N. Majumdar, “Exact record and order statistics of random walks via first-passage ideas,” in *First-Passage Phenomena and Their Applications*, pp. 226–251, World Scientific, 2014.
- [40] K. Basnayake, D. Mazaud, A. Bemelmans, N. Rouach, E. Korkotian, and D. Holcman, “Fast calcium transients in dendritic spines driven by extreme statistics,” *PLoS biology*, vol. 17, no. 6, 2019.
- [41] D. E. Clapham, “Calcium signaling,” *Cell*, vol. 131, no. 6, pp. 1047–1058, 2007.
- [42] A. N. Dodd, J. Kudla, and D. Sanders, “The language of calcium signaling,” *Annual review of plant biology*, vol. 61, pp. 593–620, 2010.
- [43] J. Kudla, D. Becker, E. Grill, R. Hedrich, M. Hippler, U. Kummer, M. Parniske, T. Romeis, and K. Schumacher, “Advances and current challenges in calcium signaling,” *New Phytologist*, vol. 218, no. 2, pp. 414–431, 2018.
- [44] G. J. Augustine, F. Santamaria, and K. Tanaka, “Local calcium signaling in neurons,” *Neuron*, vol. 40, no. 2, pp. 331–346, 2003.
- [45] A. P. Thomas, G. S. J. Bird, G. Hajnóczky, L. D. Robb-Gaspers, and J. W. Putney Jr, “Spatial and temporal aspects of cellular calcium signaling,” *The FASEB Journal*, vol. 10, no. 13, pp. 1505–1517, 1996.
- [46] M. D. Bootman and M. J. Berridge, “The elemental principles of calcium signaling,” *Cell*, vol. 83, no. 5, pp. 675–678, 1995.
- [47] M. J. Berridge, “Neuronal calcium signaling,” *Neuron*, vol. 21, no. 1, pp. 13–26, 1998.
- [48] A. Kornberg, T. A. Baker, *et al.*, *DNA replication*, vol. 3. Wh Freeman New York, 1992.
- [49] R. A. Bradshaw and E. A. Dennis, *Handbook of cell signaling*. Academic press, 2009.
- [50] J. A. Papin, T. Hunter, B. O. Palsson, and S. Subramaniam, “Reconstruction of cellular signalling networks and analysis of their properties,” *Nature reviews Molecular cell biology*, vol. 6, no. 2, pp. 99–111, 2005.
- [51] G. Dupont, M. Falcke, V. Kirk, and J. Sneyd, “Models of calcium signalling,” 2016.
- [52] D. A. Potoyan and P. G. Wolynes, “Stochastic dynamics of genetic broadcasting networks,” *Physical Review E*, vol. 96, no. 5, p. 052305, 2017.

- [53] W. K. Purves, D. E. Sadava, G. H. Orians, and H. C. Heller, *Life: The Science of Biology Seventh Edition 7th Edition*. Sinauer Associates and W. H. Freeman, 2004.
- [54] K. Basnayake, D. Mazaud, A. Bemelmans, N. Rouach, E. Korkotian, and D. Holcman, “Fast calcium transients in dendritic spines driven by extreme statistics,” *PLOS Biology*, vol. 17, pp. 1–26, 06 2019.
- [55] G. L. Fain, *Sensory transduction*. Oxford University Press, 2019.
- [56] D. Holcman and Z. Schuss, *Asymptotics of Elliptic and Parabolic PDEs: and their Applications in Statistical Physics, Computational Neuroscience, and Biophysics*, vol. 199. Springer, 2018.
- [57] D. Coombs, “First among equals: Comment on “redundancy principle and the role of extreme statistics in molecular and cellular biology” by Z. Schuss, K. Basnayake and D. Holcman,” *Physics of life reviews*, 2019.
- [58] S. Redner and B. Meerson, “Redundancy, extreme statistics and geometrical optics of brownian motion: Comment on “redundancy principle and the role of extreme statistics in molecular and cellular biology” by z. schuss et al.,” *Physics of life reviews*, 2019.
- [59] C. Mej  a-Monasterio, G. Oshanin, and G. Schehr, “First passages for a search by a swarm of independent random searchers,” *Journal of Statistical Mechanics: Theory and Experiment*, vol. 2011, no. 06, p. P06022, 2011.
- [60] B. Besga, F. Faisant, A. Petrosyan, S. Ciliberto, and S. N. Majumdar, “Dynamical phase transition in the first-passage probability of a brownian motion,” *arXiv preprint arXiv:2102.07232*, 2021.
- [61] R. Metzler and J. Klafter, “The random walk’s guide to anomalous diffusion: a fractional dynamics approach,” *Physics reports*, vol. 339, no. 1, pp. 1–77, 2000.
- [62] B. E. Herring and R. A. Nicoll, “Long-term potentiation: from camkii to ampa receptor trafficking,” *Annual review of physiology*, vol. 78, pp. 351–365, 2016.
- [63] G. H. Weiss, K. E. Shuler, and K. Lindenberg, “Order statistics for first passage times in diffusion processes,” *Journal of Statistical Physics*, vol. 31, no. 2, pp. 255–278, 1983.
- [64] S. N. Majumdar, A. Pal, and G. Schehr, “Extreme value statistics of correlated random variables: a pedagogical review,” *Physics Reports*, vol. 840, pp. 1–32, 2020.
- [65] S. Redner, *A guide to first-passage processes*. Cambridge University Press, 2001.
- [66] K. Basnayake and D. Holcman, “Fastest among equals: a novel paradigm in biology. reply to comments: Redundancy principle and the role of extreme statistics in molecular and cellular biology,” *PhLRv*, vol. 28, pp. 96–99, 2019.
- [67] D. Grebenkov, R. Metzler, and G. Oshanin, “From single-particle stochastic kinetics to macroscopic reaction rates: fastest first-passage time of n random walkers,” *New Journal of Physics*, 2020.
- [68] J. Yang, I. Kupka, Z. Schuss, and D. Holcman, “Search for a small egg by spermatozoa in restricted geometries,” *Journal of mathematical biology*, vol. 73, no. 2, pp. 423–446, 2016.

- [69] B. Alberts, D. Bray, K. Hopkin, A. D. Johnson, J. Lewis, M. Raff, K. Roberts, and P. Walter, *Essential cell biology*. Garland Science, 2015.
- [70] T. Riedl and J.-M. Egly, “Phosphorylation in transcription: the ctd and more,” *Gene Expression The Journal of Liver Research*, vol. 9, no. 1-2, pp. 3–13, 2001.
- [71] K. Basnayake, Z. Schuss, and D. Holcman, “Asymptotic formulas for extreme statistics of escape times in 1, 2 and 3-dimensions,” *Journal of Nonlinear Science*, Sep 2018.
- [72] K. Basnayake, A. Hubl, Z. Schuss, and D. Holcman, “Extreme narrow escape: Shortest paths for the first particles among n to reach a target window,” *Physics Letters A*, 2018.
- [73] K. Basnayake and D. Holcman, “Extreme escape from a cusp: When does geometry matter for the fastest brownian particles moving in crowded cellular environments?,” *The Journal of Chemical Physics*, vol. 152, no. 13, p. 134104, 2020.
- [74] F. Beukers, “Gauss’ hypergeometric function,” *Arithmetic and Geometry Around Hypergeometric Functions: Lecture Notes of a CIMPA Summer School held at Galatasaray University, Istanbul, 2005*, pp. 23–42, 2007.
- [75] W. Gautschi and W. F. Cahill, “Exponential integral and related functions,” *Handbook of mathematical functions with formulas, graphs, and mathematical tables*, p. 272, 1964.
- [76] G. Jameson, “The incomplete gamma functions,” *The Mathematical Gazette*, vol. 100, no. 548, pp. 298–306, 2016.
- [77] S. N. Majumdar, S. Sabhapandit, and G. Schehr, “Exact distributions of cover times for n independent random walkers in one dimension,” *Physical Review E*, vol. 94, no. 6, p. 062131, 2016.
- [78] K. Basnayake and D. Holcman, “Fastest among equals: a novel paradigm in biology. reply to comments: Redundancy principle and the role of extreme statistics in molecular and cellular biology,” *Physics of life reviews*, vol. 28, pp. 96–99, 2019.
- [79] I. M. Sokolov, “Extreme fluctuation dominance in biology: On the usefulness of wastefulness: Comment on “redundancy principle and the role of extreme statistics in molecular and cellular biology” by Z. Schuss, K. Basnayake and D. Holcman,” *Physics of life reviews*, 2019.
- [80] D. A. Rusakov and L. P. Savtchenko, “Extreme statistics may govern avalanche-type biological reactions: Comment on “redundancy principle and the role of extreme statistics in molecular and cellular biology” by z. schuss, k. basnayakey, d. holcman.,” *Physics of life reviews*, 2019.
- [81] E. Korkotian, E. Oni-Biton, and M. Segal, “The role of the store-operated calcium entry channel orai1 in cultured rat hippocampal synapse formation and plasticity,” *The Journal of physiology*, vol. 595, no. 1, pp. 125–140, 2017.
- [82] E. Korkotian, M. Frotscher, and M. Segal, “Synaptopodin regulates spine plasticity: mediation by calcium stores,” *Journal of Neuroscience*, vol. 34, no. 35, pp. 11641–11651, 2014.
- [83] E. Korkotian and M. Segal, “Release of calcium from stores alters the morphology of dendritic spines in cultured hippocampal neurons,” *Proceedings of the National Academy of Sciences*, vol. 96, no. 21, pp. 12068–12072, 1999.

- [84] K. Basnayake, D. Mazaud, A. Bemelmans, N. Rouach, E. Korkotian, and D. Holcman, “Fast calcium transients in dendritic spines driven by extreme statistics,” *PLoS biology*, vol. 17, no. 6, p. e2006202, 2019.
- [85] N. Rouach, J. Glowinski, and C. Giaume, “Activity-dependent neuronal control of gap-junctional communication in astrocytes,” *The Journal of cell biology*, vol. 149, no. 7, pp. 1513–1526, 2000.
- [86] M. Dora and D. Holcman, “Active unidirectional network flow generates a packet molecular transport in cells,” *arXiv preprint arXiv:1810.07272*, 2018.
- [87] R. Weber, M. Genovese, A. Louli, S. Hames, C. Martin, I. G. Hill, and J. Dahn, “Long cycle life and dendrite-free lithium morphology in anode-free lithium pouch cells enabled by a dual-salt liquid electrolyte,” *Nature Energy*, vol. 4, no. 8, pp. 683–689, 2019.
- [88] Z. Schuss, *Brownian dynamics at boundaries and interfaces*. Springer, 2015.
- [89] S. Chandrasekhar, “Stochastic problems in physics and astronomy,” *Reviews of modern physics*, vol. 15, no. 1, p. 1, 1943.
- [90] C. Gardiner, *Handbook of Stochastic Methods for Physics, Chemistry, and the Natural Sciences*. Proceedings in Life Sciences, Springer-Verlag, 1985.
- [91] H. Risken, “Fokker-planck equation,” in *The Fokker-Planck Equation*, pp. 63–95, Springer, 1996.
- [92] K. Basnayake, Z. Schuss, and D. Holcman, “Asymptotic formulas for extreme statistics of escape times in 1, 2 and 3-dimensions,” *Journal of Nonlinear Science*, vol. 29, no. 2, pp. 461–499, 2019.
- [93] Z. Schuss, K. Basnayake, and D. Holcman, “Redundancy principle and the role of extreme statistics in molecular and cellular biology,” *Physics of life reviews*, 2019.
- [94] L. Martyushev, “Minimal time, weibull distribution and maximum entropy production principle: Comment on “redundancy principle and the role of extreme statistics in molecular and cellular biology” by Z. Schuss et al.,” *Physics of life reviews*, 2019.
- [95] R. Metzler, S. Redner, and G. Oshanin, *First-passage phenomena and their applications*, vol. 35. World Scientific, 2014.
- [96] M. Tamm, “Importance of extreme value statistics in biophysical contexts: Comment on “redundancy principle and the role of extreme statistics in molecular and cellular biology”,” *Physics of life reviews*, 2019.
- [97] J. Ma, M. Do, M. A. Le Gros, C. S. Peskin, C. A. Larabell, Y. Mori, and S. A. Isaacson, “Strong intracellular signal inactivation produces sharper and more robust signaling from cell membrane to nucleus,” *PLoS computational biology*, vol. 16, no. 11, p. e1008356, 2020.
- [98] G. H. Weiss, “A perturbation analysis of the wilemski-fixman approximation for diffusion-controlled reactions,” *The Journal of chemical physics*, vol. 80, no. 6, pp. 2880–2887, 1984.
- [99] S. B. Yuste and K. Lindenberg, “Order statistics for first passage times in one-dimensional diffusion processes,” *J. Stat. Phys.*, vol. 85, pp. 501–512, 1996.

- [100] S. D. Lawley, “Distribution of extreme first passage times of diffusion,” *J. Math. Biol.*, vol. 80, no. 7, pp. 2301–2325, 2020.
- [101] S. D. Lawley, “Extreme first-passage times for random walks on networks,” *Phys. Rev. E*, vol. 102, no. 6, pp. 062118, 14, 2020.
- [102] S. Toste and D. Holcman, “Asymptotics for the fastest among n stochastic particles: role of an extended initial distribution and an additional drift component,” *Journal of Physics A: Mathematical and Theoretical*, 2021.
- [103] S. Linn and S. D. Lawley, “Extreme hitting probabilities for diffusion,” *Journal of Physics A: Mathematical and Theoretical*, vol. 55, no. 34, p. 345002, 2022.
- [104] K. Reynaud, Z. Schuss, N. Rouach, and D. Holcman, “Why so many sperm cells?,” *Communicative & integrative biology*, vol. 8, no. 3, p. e1017156, 2015.
- [105] B. Meerson and S. Redner, “Mortality, redundancy, and diversity in stochastic search,” *Physical review letters*, vol. 114, no. 19, p. 198101, 2015.
- [106] J. Lee, X. Chen, and R. A. Nicoll, “Synaptic memory survives molecular turnover,” *Proceedings of the National Academy of Sciences*, vol. 119, no. 42, p. e2211572119, 2022.
- [107] S. Karlin and S. Tavaré, “A diffusion process with killing: the time to formation of recurrent deleterious mutant genes,” *Stochastic Processes and their Applications*, vol. 13, no. 3, pp. 249–261, 1982.
- [108] S. Karlin and S. Tavaré, “A class of diffusion processes with killing arising in population genetics,” *SIAM Journal on Applied Mathematics*, vol. 43, no. 1, pp. 31–41, 1983.
- [109] S. M. Berman and F. Halina, “Distributions associated with markov processes with killing,” *Stochastic Models*, vol. 12, no. 3, pp. 367–388, 1996.
- [110] A. Mazzolo and C. Monthus, “Conditioning diffusion processes with killing rates,” *arXiv preprint arXiv:2204.05607*, 2022.
- [111] D. Holcman and Z. Schuss, “Stochastic narrow escape in molecular and cellular biology,” *Analysis and Applications. Springer, New York*, 2015.
- [112] R. Yuste, *Dendritic spines*. MIT press, 2010.
- [113] R. Erban and S. J. Chapman, *Stochastic modelling of reaction-diffusion processes*, vol. 60. Cambridge University Press, 2019.
- [114] K. Lindenberg, R. Metzler, and G. Oshanin, *Chemical Kinetics: Beyond the Textbook*. World Scientific Publishing Europe Ltd, 2019.
- [115] J. Sneyd, J. Keizer, and M. J. Sanderson, “Mechanisms of calcium oscillations and waves: a quantitative analysis,” *The FASEB Journal*, vol. 9, no. 14, pp. 1463–1472, 1995.
- [116] G. Dupont and J. Sneyd, “Recent developments in models of calcium signalling,” *Current opinion in systems biology*, vol. 3, pp. 15–22, 2017.

- [117] G. L. Smith and D. A. Eisner, “Calcium buffering in the heart in health and disease,” *Circulation*, vol. 139, no. 20, pp. 2358–2371, 2019.
- [118] D. Holcman and Z. Schuss, “Modeling calcium dynamics in dendritic spines,” *Siam Journal on Applied Mathematics*, vol. 65, no. 3, pp. 1006–1026, 2005.
- [119] D. Holcman, Z. Schuss, and E. Korkotian, “Calcium dynamics in dendritic spines and spine motility,” *Biophysical journal*, vol. 87, no. 1, pp. 81–91, 2004.
- [120] T. Lu, T. Shen, C. Zong, J. Hasty, and P. G. Wolynes, “Statistics of cellular signal transduction as a race to the nucleus by multiple random walkers in compartment/phosphorylation space,” *Proceedings of the National Academy of Sciences*, vol. 103, no. 45, pp. 16752–16757, 2006.
- [121] G. Malherbe and D. Holcman, “The search for a dna target in the nucleus,” *Physics Letters A*, vol. 374, no. 3, pp. 466–471, 2010.
- [122] J. B. Madrid and S. D. Lawley, “Competition between slow and fast regimes for extreme first passage times of diffusion,” *J. Phys. A*, vol. 53, no. 33, pp. 335002, 32, 2020.
- [123] N. Hoze, D. Nair, E. Hosy, C. Sieben, S. Manley, A. Herrmann, J.-B. Sibarita, D. Choquet, and D. Holcman, “Heterogeneity of ampa receptor trafficking and molecular interactions revealed by superresolution analysis of live cell imaging,” *Proceedings of the National Academy of Sciences*, vol. 109, no. 42, pp. 17052–17057, 2012.
- [124] Y. C. Tsai and A. M. Weissman, “The unfolded protein response, degradation from the endoplasmic reticulum, and cancer,” *Genes & cancer*, vol. 1, no. 7, pp. 764–778, 2010.
- [125] I. X. Zhang, M. Raghavan, and L. S. Satin, “The endoplasmic reticulum and calcium homeostasis in pancreatic beta cells,” *Endocrinology*, vol. 161, no. 2, 2020.
- [126] S. Toste and D. Holcman, “Extreme escape with killing for diffusing particles in one dimension,” *arXiv preprint arXiv:2201.05915*, 2022.
- [127] Z. Schuss, *Diffusion and Stochastic Processes. An Analytical Approach*. Springer-Verlag, New York, NY, 2009.
- [128] B. G. Korenev, *Bessel functions and their applications*. CRC Press, 2002.
- [129] M. Abramowitz, I. A. Stegun, and R. H. Romer, “Handbook of mathematical functions with formulas, graphs, and mathematical tables,” 1988.
- [130] W. Chen and M. J. Ward, “The stability and dynamics of localized spot patterns in the two-dimensional gray-scott model,” *SIAM Journal on Applied Dynamical Systems*, vol. 10, no. 2, pp. 582–666, 2011.
- [131] T. Kolokolnikov, M. S. Titcombe, and M. J. Ward, “Optimizing the fundamental Neumann eigenvalue for the Laplacian in a domain with small traps,” *Eur. J. Appl. Math.*, vol. 16, no. 2, pp. 161–200, 2005.
- [132] F. Bouchet and J. Reyner, “Generalisation of the Eyring-Kramers transition rate formula to irreversible diffusion processes,” *Ann. Henri Poincaré*, vol. 17, no. 12, pp. 3499–3532, 2016.

- [133] H. Touchette, “A basic introduction to large deviations: Theory, applications, simulations,” *arXiv preprint arXiv:1106.4146*, 2011.
- [134] G. M. Cooper, R. E. Hausman, and R. E. Hausman, *The cell: a molecular approach*, vol. 4. ASM press Washington, DC, 2007.
- [135] A. Godec and R. Metzler, “First passage time distribution in heterogeneity controlled kinetics: going beyond the mean first passage time,” *Scientific reports*, vol. 6, no. 1, pp. 1–11, 2016.
- [136] A. J. Bray, S. N. Majumdar, and G. Schehr, “Persistence and first-passage properties in nonequilibrium systems,” *Advances in Physics*, vol. 62, no. 3, pp. 225–361, 2013.
- [137] S. D. Lawley, “Distribution of extreme first passage times of diffusion,” *J. Math. Biol.*, vol. 80, no. 7, pp. 2301–2325, 2020.
- [138] S. D. Lawley and J. B. Madrid, “A probabilistic approach to extreme statistics of brownian escape times in dimensions 1, 2, and 3,” *Journal of Nonlinear Science*, vol. 30, no. 3, pp. 1207–1227, 2020.
- [139] A. Godec and R. Metzler, “First passage time statistics for two-channel diffusion,” *Journal of Physics A: Mathematical and Theoretical*, vol. 50, no. 8, p. 084001, 2017.
- [140] D. S. Grebenkov, “A unifying approach to first-passage time distributions in diffusing diffusivity and switching diffusion models,” *Journal of Physics A: Mathematical and Theoretical*, vol. 52, no. 17, p. 174001, 2019.
- [141] B. Hille, “Ionic channels in excitable membranes. current problems and biophysical approaches,” *Biophysical Journal*, vol. 22, no. 2, pp. 283–294, 1978.
- [142] Y. A. Makhnovskii, A. M. Berezhkovskii, S.-Y. Sheu, D.-Y. Yang, J. Kuo, and S. H. Lin, “Stochastic gating influence on the kinetics of diffusion-limited reactions,” *The Journal of chemical physics*, vol. 108, no. 3, pp. 971–983, 1998.
- [143] K. Roberts, B. Alberts, A. Johnson, P. Walter, and T. Hunt, “Molecular biology of the cell,” *New York: Garland Science*, vol. 32, no. 2, 2002.
- [144] A. Szabo, D. Shoup, S. H. Northrup, and J. A. McCammon, “Stochastically gated diffusion-influenced reactions,” *The Journal of Chemical Physics*, vol. 77, no. 9, pp. 4484–4493, 1982.
- [145] C. Dieball, D. Krapf, M. Weiss, and A. Godec, “Scattering fingerprints of two-state dynamics,” *New Journal of Physics*, 2022.
- [146] R. Metzler and J. Klafter, “The random walk’s guide to anomalous diffusion: a fractional dynamics approach,” *Phys. Rep.*, vol. 339, no. 1, pp. 1 – 77, 2000.
- [147] D. X. Keller, K. M. Franks, T. M. Bartol Jr, and T. J. Sejnowski, “Calmodulin activation by calcium transients in the postsynaptic density of dendritic spines,” *PLoS One*, vol. 3, no. 4, p. e2045, 2008.
- [148] J. Reingruber and D. Holcman, “Transcription factor search for a dna promoter in a three-state model.,” *Phys Rev E*, vol. 84, p. 020901, 2011.
- [149] N. Chaffey, “Alberts, b., johnson, a., lewis, j., raff, m., roberts, k. and walter, p. molecular biology of the cell. 4th edn.,” 2003.

RÉSUMÉ

Dans cette thèse, nous étudions le temps d'arrivée moyen de la particule la plus rapide (TAMPR) d'un ensemble de N particules browniennes sous différentes dynamiques. Ce temps d'arrivée définit le temps d'activation de nombreux processus moléculaires qui se produisent au niveau cellulaire et déclenchent des cascades de signalisation, lorsque les premières particules atteignent une cible. Dans une première partie nous étudions la TMAPR en fonction du chevauchement entre la cible et de la distribution initiale des particules, conduisant à une nouvelle loi de décroissance algébrique pour le TMAPR. Par la suite, nous étudions l'influence d'un terme d'élimination dans le modèle de diffusion unidimensionnel, en considérant que l'élimination des particules peut se produire lors de la traversée d'un point fixé du domaine ou uniformément dans un intervalle. Ce terme d'élimination conduit à une réduction du TMAPR lorsqu'un grand nombre de particules survivent ou à un incrément du TMAPR lorsque le nombre initial de particules est fixé. Nous avons prolongé cette étude à un disque borné en 2D, considérant que l'élimination peut être uniforme dans tout le domaine ou dans une sous-région de celui-ci. Dans une deuxième partie, nous avons obtenu des formules pour le TMAPR lorsque des particules alternent entre deux états et n'échappent qu'à l'un d'entre eux, révélant que la stratégie la plus rapide est toujours de se déplacer dans l'état avec le coefficient de diffusion le plus élevé. Toutes ces formules ont été obtenues par la méthode de Laplace avec N comme paramètre long et peuvent être utilisées pour comprendre des processus plus complexes, tels que le trafic de protéines dans les cellules.

MOTS CLÉS

Particules browniennes, dynamiques d'élimination, dynamiques d'alternance, diffusion, temps d'arrivée, méthode de Laplace.

ABSTRACT

In this PhD, we study the mean first arrival time (MFAT) for the fastest particle among an ensemble of N Brownian particles under different dynamics. These arrival times define the activation time of many molecular processes that occur at the cellular level and trigger signaling cascades, when the first particles reach the target. In the first part we study the MFAT depending on the overlapping between the target and the initial distribution of the particles, leading to a new algebraic decay law in the MFAT. Subsequently, we study the influence of an elimination term in the diffusion model, considering that the elimination of particles can occur when crossing a point of the domain or uniformly in an interval. This elimination term leads to a reduction in the MFAT for the fastest particle when a large number of particles survive or an increase when the initial number of particles is fixed. We extend this study to a 2D bounded disk, considering that the degradation of particles can occurs everywhere in the domain or in a sub-region of it. In the second part we study the MFAT when particles can alternate between two states and only escape in one of them, revealing that the fastest strategy is always to move in the state with the largest diffusion coefficient. All these formulas were obtained by the Laplace method with N as large parameter and can be used to understand more complex processes, such as protein trafficking in cells.

KEYWORDS

Brownian particles, killing dynamics, switching dynamics, diffusion, arrival time, Laplace method.